STUDIES ON MARINE NATURAL PRODUCTS

A thesis

submitted in partial fulfilment

of the requirements for the Degree

of

Doctor of Philosophy in Chemistry

in the

University of Canterbury

by

Joanne B. Hart

University of Canterbury
Christchurch
New Zealand
1995

CONTENTS

ABSTRACT

The halichondrins are a series of polyether macrolides displaying potent *in vitro* and *in vivo* antitumour activities and, as such, represent important leads as anticancer drugs. These compounds had previously been isolated from a number of unrelated marine sponges, such as *Lissodendoryx* sp., a high yielding deep-water sponge located off the Kaikoura coast of New Zealand.

Structure-activity relationships in the halichondrin series have now been investigated. Hemi-synthetic modifications of selected naturally-occurring halichondrins have produced over fourteen new analogues. The biological activities of twelve of these analogues have been assessed in an in-house P388 *in vitro* assay and in the National Cancer Institute's (USA) *in vitro* sixty cell-line human tumour panel. An analysis of these data has shown that the lactone ring (C1-C30), the olefinic functionalities (C19 and C26), the natural C38 stereochemistry and the tricyclo ring system (C-E rings) are essential structural features of the halichondrins.

The characterisation of the hemi-synthetic derivatives has been facilitated by the full NMR spectroscopic assignments of halichondrin B and homohalichondrin B.

The future progress of the halichondrins as anticancer drugs will have been assisted by the development of an understanding of the general chemistry of the halichondrins.

CHAPTER 1

Introduction

1.1 Marine Natural Products

1.1.1 Introduction- Natural Products as Potential Drug Sources

For thousands of years mankind has sought to conquer and control diseases arising in humans, domesticated animals and food crops. Nature, in particular terrestrial flora and fauna, has traditionally provided the source for the treatment of many such diseases. However, the use of crude preparations from plants and animals can have several disadvantages including seasonal and geographical variations in the quantities of the active constituent(s). Other drawbacks include the possible co-occurrence of undesirable components with detrimental side effects and the loss of biological activity in the preparation or storage of the crude material. It is therefore desirable to isolate the individual natural products giving rise to the observed biological activity.

Williams *et al*[1] define a natural product as an organic compound that has "no explicit role in the internal economy of the organism that produces it". These authors argue that the existence of natural products in an organism serves to increase its survival fitness and hence gain a competitive edge in its environment. They further suggest that all natural products have evolved under the pressure of natural selection to interact with specific receptors of the competitor.

Biologically active natural products associated with an organism may be synthesised *de novo* by the organism itself or they may be sequestered from a dietary source. It is also possible that a symbiotic organism in close association synthesises the bioactive natural product.

Bioactive natural products can be seen as having a protective role in the organism: protection from predation, protection from competition for space, light and nutrients, and protection from infection by micro-organisms. This is supported by the observation that many organisms will only produce natural products while under some kind of stress.[2] Williams *et al*[1] note that natural products are common in organisms lacking an immune system and are sparse in those possessing an immune system. This implies that natural products play an important role in the chemical defences of organisms lacking immune systems such as plants, fungi, micro-organisms and invertebrate animals. Indeed, the very survival of such organisms may, in part, be a function of the chemical "warfare" available to it. Natural compounds isolated from species which are lacking an immune system are therefore a rich source of biologically active compounds.

Screening of extracts for a particular biological activity, for example antiviral activity, from plant, animal, microbial or fungal sources with a disease-specific biological assay provides an invaluable guide for the separation and isolation of bioactive natural products. In this way important leads in drug discovery and development can be revealed for the potential treatment of specific diseases.

1.1.1.1 Cancer

"Cancer" describes more than two hundred different diseases, each characterised by unrestrained cell growth.[3] Cancer is caused, in most instances, by mutation or abnormal activation of cellular genes that control cell growth and mitosis. Only a minute fraction of cells that mutate actually lead to cancer. This is because most of the mutated cells have a decreased survival capacity, due to the mutation, and only a few mutated cells actually lose the feedback mechanism that prevents excessive cell

growth. The immune system also serves to destroy most mutated cells before they can develop into a cancer.[4]

A cancer cell has many characteristics that distinguish it from a normal cell and gives rise to its invasive nature. A cancer cell does not respect usual cellular growth limits, resulting in unrestrained growth. The cells are less adhesive to each other and can therefore move through tissues and be freely circulated by the bloodstream resulting in numerous new growths. Some cancers produce angiogenic factors *ie* causing the growth of new blood vessels, to supply the nutrients to the cells that are required for cancer growth. As cancer cells undergo indefinite proliferation they have an increasingly high nutrient demand resulting in the gradual nutritive death of normal cells and ultimately death for the patient.[4]

Cancer cells are continuously dividing, though this process is inefficient. Normal cells divide more rapidly than cancer cells but fewer are in a state of active division at any one moment. Therefore drugs which can specifically target the continuously dividing cancer cells will be relatively selective as anticancer compounds. A "good" anticancer drug will be able to differentiate between the normal, healthy cells and cancerous cells (*ie* the drug should be "selective") and it should also be able to destroy the cancer cells (*ie* the drug should be cytotoxic). It is important to note that cytotoxicity alone is not sufficient for antitumour activity in a therapeutic sense, since the compound must also be selectively toxic. However, cytotoxicity is consistent with most observations of antitumour activity. "Cytotoxicity" is therefore described as an *in vitro* observation of biological activity and "antitumour activity" is described as an *in vivo* activity.

1.1.1.2 Marine Natural Products

The seas and oceans of the world cover a vast area of the earth and contain a huge diversity of relatively unexplored flora and fauna. It has been estimated that four-fifths of the Earth's animal life live in or on the water.[5] Coupled with the growing accessibility of the marine environment, such as by SCUBA diving, marine organisms now represent a valuable resource for the discovery of novel bioactive natural products with pharmaceutical potential.

Data from the National Cancer Institute (NCI) in the USA, compiled by Dr. Peter Murphy of the Australian Institute of Marine Sciences (AIMS) in 1992,[6] further illustrates the utility of screening marine natural products as potential drug sources. **Figure 1.1.1** displays the number of anticancer leads from various sources in the NCI *in vitro* preclinical antitumour drug screen. It can be seen that although, relative to terrestrial sources, a low number compounds of marine origin have been screened, there are a high proportion of anticancer leads originating from marine animal sources.

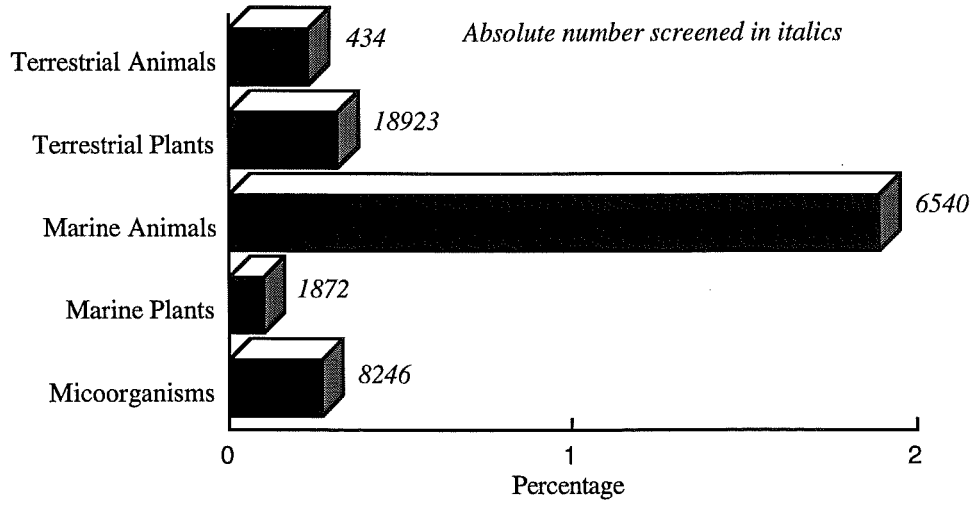

Figure 1.1.1 Anticancer Leads with Significant Selective Cytotoxic Activity in the NCI Preclinical Antitumour Drug Discovery Screen.[6]

Australian results from AIMS[6] indicate that more specifically, the marine invertebrate phylum Porifera (sponges) provides a rich source of cytotoxic marine natural products, with over 11% of specimens in this phylum displaying significant cytotoxicity (*viz* IC_{50} <4 μg/mL).

1.1.1.3 Sponges[7]

Sponges are classed in a subkingdom of their own called Parazoa as they appear to have travelled a unique evolutionary route relative to other animals.[8] They are classed in the phylum Porifera (meaning "pore bearing"). In the adult stage they are sessile and largely plant-like in appearance. There are about five thousand species of sponges divided into four classes based on their skeletal structure.[8] Their habitat generally consists of attachment to the ocean floors of shallow coastal areas although some sponges are located at great depths. A few sponges are found in fresh water.

Sponges are essentially an aggregation of cells, with no specialised organs or tissues, although there is some degree of coordination between different cell types, and cellular recognition within the aggregation. Sponges are filter-feeders, drawing in water through oscules (pores) dotting the external surface of the sponge body into one or more internal chambers by the combined effect of the current across the osculum (the cavity at the top of the chamber) and flagella lining the cavity protruding from numerous collar cells (choanocytes).[8] The choanocytes trap and absorb passing nutrients. As sponges lack an immune system and are filter-feeders, it is probable that the presence of bioactive compounds provides a defence against potentially harmful filtered bacteria.

1.1.2 The Marine Chemistry Group

The Marine Chemistry Group at the University of Canterbury was formed in 1975 with the main objective being to isolate and identify the structures of new classes of biologically active compounds derived from marine sources.

A wide range of extracts are screened in the Marine Chemistry Group's in-house *in vitro* antimicrobial, antiviral (Appendix I) and antitumour assays. Those samples producing extracts with a pertinent biological response are re-extracted on a larger scale in a bioassay-directed chromatographic separation of the active constituents. Once isolated, the active components are identified. The P388 antitumour assay is discussed in detail (Section 1.1.2.1) and examples of bioassay-directed "hits" (*ie* the isolation of biologically active compounds) are described in Section 1.1.2.2 which serves to highlight the success of the Marine Chemistry Group's approach.

1.1.2.1 The P388 Antitumour Assay

The *in vitro* "antitumour" assay uses the P388 cell line (murine leukemia cells) and it is up to a hundred times more sensitive to cytotoxicity effects than the antiviral BSC-1 cell line. The P388 assay is therefore a cytotoxicity-based assay against a specific leukemia cell type. The IC_{50} result obtained from this assay represents the concentration of the test compound at which the number of viable cells is reduced by fifty per cent relative to the control.

A two-fold dilution series of the sample of interest is incubated with P388 cells and MTT, a yellow tetrazolium salt, in small plastic wells. After seventy-two hours of incubation the concentration of the sample required to reduce the number of viable

cells by fifty per cent relative to a control (P388 cells, MTT, media and solvent) is calculated. The mitochondria of *viable* leukemia cells reduce the yellow dye MTT to a purple formazan derivative.[9] By measuring the light absorbance at 540 nm in each well, a direct quantification of formazan formation and therefore the number of viable cells is able to be determined. The absorbance is expressed as a percentage cell viability relative to the control, and is plotted against the logarithm of the sample concentration in the well to generate a sample concentration *vs* cell viability curve. The antilogarithm of the concentration producing a fifty per cent reduction in the number of viable cells gives the IC_{50} result, which is usually expressed in units of ng/mL.

The P388 cell line represents a rapidly dividing cell type, thus its efficacy in finding products with activity in the predominantly occurring slow growing solid tumours of humans such as lung, colon, breast, skin and kidney cancers is strictly limited.[10] However, it is important to consider that a P388-active compound may still display a selective activity against these types of tumour.

1.1.2.2 Bioassay-Directed Isolations

The antiviral and antitumour compounds mycalamide A (**1.1.1**) and mycalamide B (**1.1.2**) were isolated in an antiviral-directed extraction of a New Zealand species of *Mycale* found in the Otago Harbour.[11,12]

R = H mycalamide A (**1.1.1**)
R = CH_3 mycalamide B (**1.1.2**)

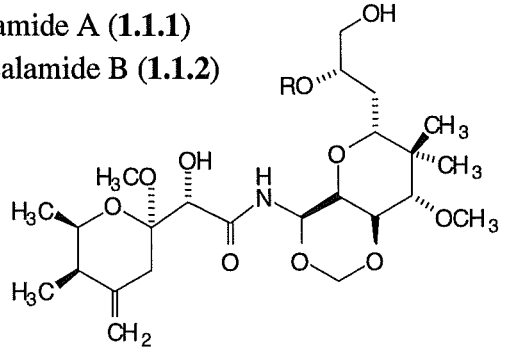

The mycalamides later proved to be too cytotoxic to be effective as antiviral agents but at present they represent important anticancer leads.

A bioassay-directed analysis of bulk New Zealand *Latrunculia* sp. sponge extracts led to the isolation of the structurally related iminoquinones, discorhabdins A, B and C as the major cytotoxic components.[12] Discorhabdins A, B and C (**1.1.3**) displayed strong antiviral activity *in vitro*; high activity in the *in vitro* P388 assay and selected antimicrobial activity.[13] Discorhabdin C, like the mycalamides, currently represents an important anticancer lead.

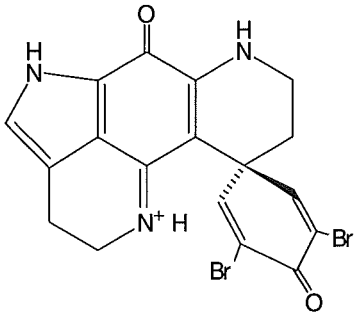

discorhabdin C (**1.1.3**)

Bioassay-directed separation of the active constituents from a small sample of a deep-water Kaikoura sponge (*Lissodendoryx* sp.) yielded several novel members of the halichondrin series of antitumour compounds. The isolation of halichondrins at high levels compared to other sponges allowed the bioassay-directed, bulk extraction and separation of relatively "large" quantities of halichondrins.[14] Some of this material provided the basis for the investigations described in this thesis (Section 1.4). The halichondrins are discussed in greater detail in Section 1.2.

1.1.3 Anticancer Drug Development- the NCI

Since 1955, the National Cancer Institute (NCI) of the National Institutes of Health in the USA has operated a major program to coordinate anticancer drug development at a national and international level. Screening of synthetic and naturally occurring compounds has been undertaken at the NCI to ascertain the antitumour and other biological properties of these compounds. In fact, mass screening of synthetic or naturally occurring products as well as complex extracts of natural products has proved to be the most effective means of discovering new chemotypes with antitumour or other biological properties.[15] The discovery of novel active compounds has, in some cases, lead directly to candidates for new drug development or these compounds have served as the starting point for analogue synthesis directed at producing analogues with more potent and/or selective biological activities.

From 1975 to 1985, the primary screen used by the NCI was the *in vivo* P388 mouse leukemia assay. An increasing emphasis on solid tumour models and disease-specific screening saw, in 1985, the introduction of an *in vitro* disease-oriented panel of (predominantly) human tumour cell lines as the primary screen and the phasing out of the *in vivo* P388 murine leukemia screen used previously. **Figure 1.1.1** displays the NCI screening and drug development strategy operational in 1990. Decisions and actions regarding the pathway of potential anticancer drugs in this strategy are controlled by the Decision Network Committee (DNC) of the NCI. Compounds that prove sensitive in the *in vitro* primary screen are selected for secondary *in vivo* xenograft testing with selected, sensitive human tumour cell lines.

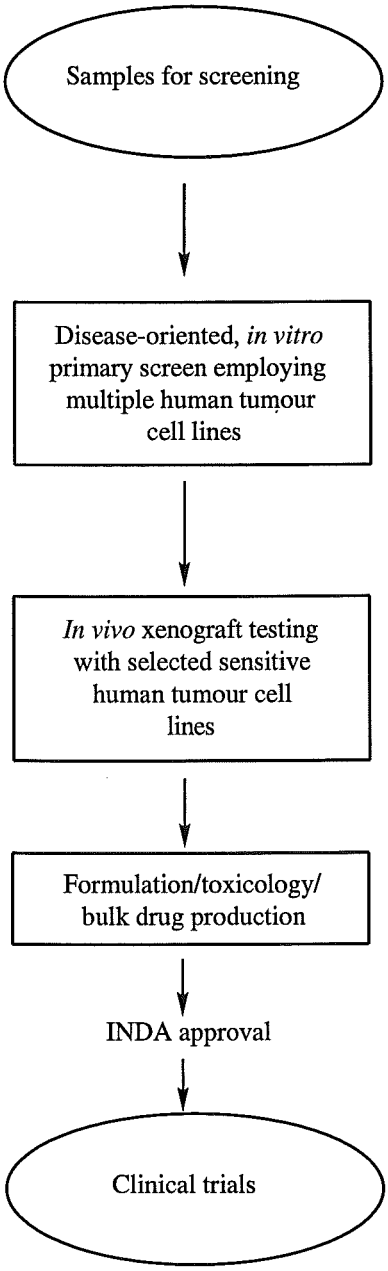

Figure 1.1.1 Schematic Representation of NCI Preclinical Screening and Drug Development Operational in 1990.[15]

Stages "IA" and "IB" of the DNC strategy involve, among other actions, the *in vitro* testing of selected compounds in the primary screening system. Approximately two hundred compounds that possess suitable bioactivities pass this point each year. At

the IIA stage in preclinical development, isolation and/or synthesis of the drug is optimised and the studies on the feasibility and cost of scale-up are carried out. The qualitative and quantitative analytical methods for the drug are set up, and tests of oral bioavailability are conducted. *In vivo* activity is tested for in appropriate models. The DNC allows approximately ten compounds per year past this point. Stage IIB involves bulk drug production and purity monitoring, while route and schedule dependency studies are undertaken *in vivo*. At this stage pharmacokinetic studies are carried out and toxicological evaluations in rodents and dogs are also undertaken. At stage III level, INDA (Investigational New Drug Application) approval is sought, then clinical trials may commence.

Currently (as of May 31 1994), the primary *in vitro* screen comprises sixty human tumour cell lines in nine histological subpanels *viz* leukemias, non-small cell lung cancers, colon cancers, CNS cancers, melanomas, ovarian cancers, renal cancers, prostate cancers and breast cancers.

Each compound is tested in quadruplicate at each of three different concentration ranges (10^{-7}, 10^{-8}, 10^{-9} M as the upper limits with five $\log_{10}$ dilutions) against the sixty tumour cell lines in the panel.[15] Three different target responses may be chosen to quantitate the data: by the GI_{50}, LC_{50} or TGI response. The GI_{50} represents the drug concentration producing an apparent fifty per cent decrease in the number of tumour cells relative to an appropriate non-drug control at the end of the drug incubation.[15] The LC_{50} is defined as the concentration of drug producing an apparent fifty percent reduction in the number of tumour cells in reference to an appropriate non-drug control at the start of the incubation. The TGI is the concentration at which the number of tumour cells remaining at the end of the incubation is the same as at the beginning of the incubation.

A mean-graph format can be constructed to display the data. This graph displays horizontal bars for individual cell line for any of the desired target responses (for example, the negative $\log_{10}$TGI results) relative to the averaged response (negative $\log_{10}$TGI) over all cell lines. The mean graph therefore provides a characteristic "fingerprint" for a given compound, depicting individual cell lines that are proportionally more sensitive than average (bars to the right of the average response) or less sensitive than the average (bars to the left of the average response). Mean graphs from the testing of halichondrin B in the NCI primary screen are displayed in Appendix II (at 1×10^{-8} M, average of quadruplicate).

Compounds may be classified as having non-specific cytotoxicity (*eg* a general cell poison) by showing no cell line or panel-specific differential cytototoxicity. Other compounds may show differential cytotoxicity for specific cell lines or panels in the screen; these compounds are of most interest as they may represent a new class of disease-specific compounds and/or a new mechanism of action. The observation of such selective cytotoxicity "implicitly suggests the presence of a cell-specific receptor that differentiates one tumour from another".[16] These compounds will serve as important tools for probing tumour-specific anticancer agents and could be useful in the treatment of specific cancer types.[16]

The distinctive mean-graph "fingerprint" can also give an indication of the mechanism of action of a particular class of compounds. Boyd[9] states that:

> *a medicinal chemist might wish to prepare new derivatives of a known prototype drug that might have improved physiochemical properties, or lower toxicity or otherwise potentially improved features, yet that retained the desired highly characteristic cellular response "fingerprint" produced by the prototype.*

1.2 The Halichondrins

1.2.1 Background

A novel series of structurally related polyether macrolides with remarkable antitumour activities were first reported in 1985 by Uemura *et al*[17] followed up by a related paper in 1986 by Hirata and Uemura.[18] These compounds were named the halichondrins after the sponge they were extracted from, *Halichondria okadai* Kadota, located off the Pacific coast of Japan. Eight halichondrins were isolated and identified: halichondrins B (**1.2.1**) and C; norhalichondrins B (**1.2.2**), A and C; and homohalichondrins B (**1.2.2**), A and C. The unique members of the halichondrin series (*eg* norhalichondrin or homohalichondrin) differ in structure beyond the C45 position. The families A (**1.2.4**), B (**1.2.5**) and C (**1.2.6**) designate the degree of oxygenation at the C12 and C13 positions.

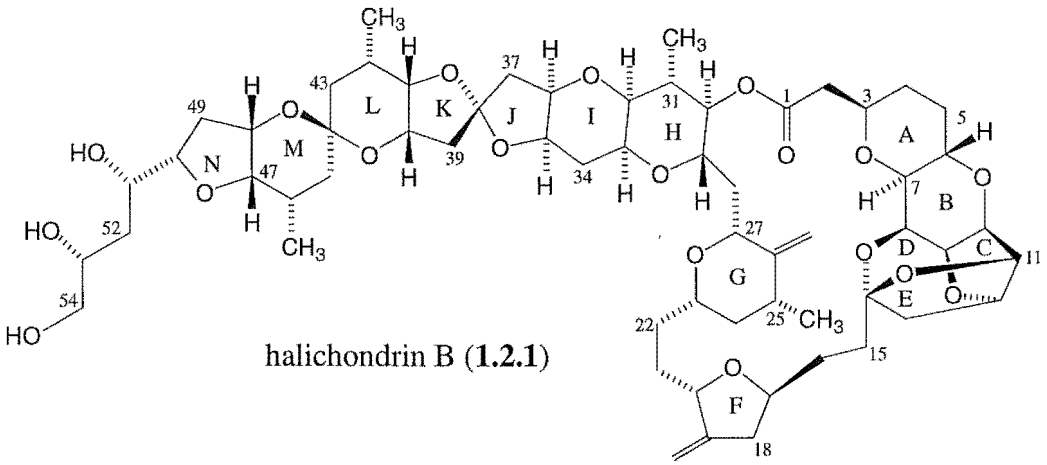

halichondrin B (**1.2.1**)

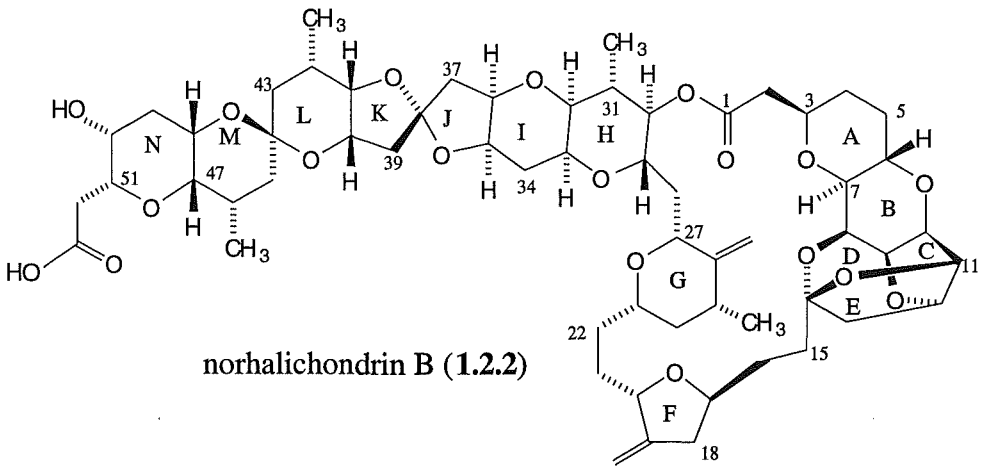

norhalichondrin B (**1.2.2**)

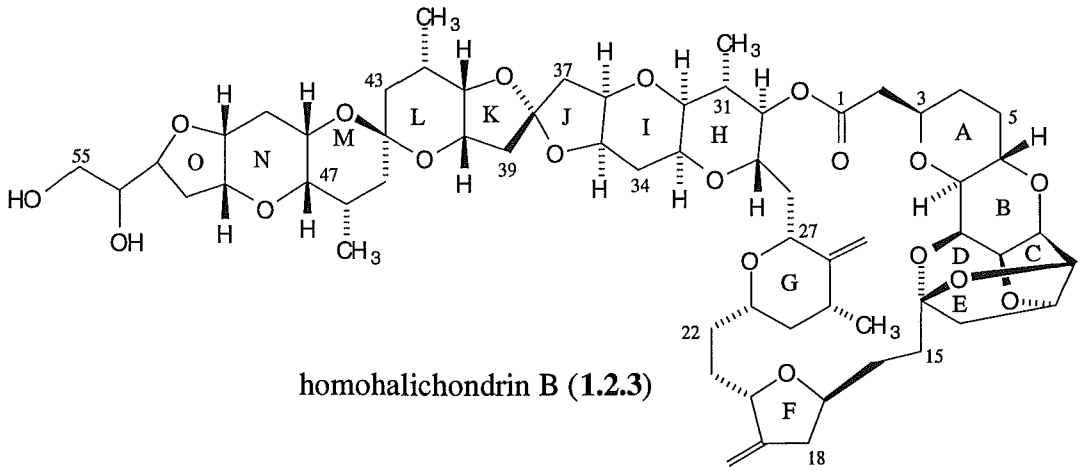

homohalichondrin B (**1.2.3**)

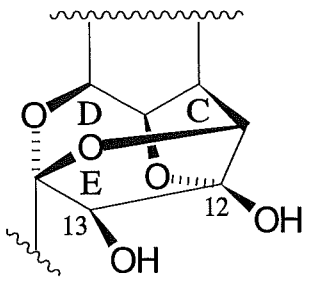

A family (**1.2.4**)

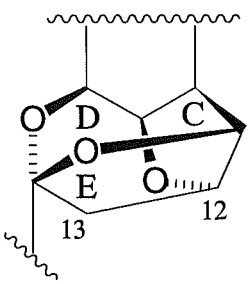

B family (**1.2.5**)

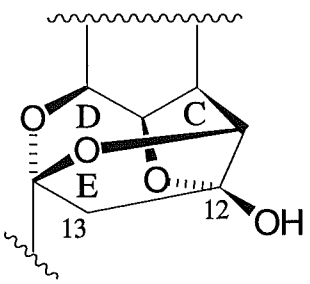

C family (**1.2.6**)

The halichondrin series of compounds are characterised by a large 22-membered lactone ring (C1-C30), two exocyclic olefinic groups at C19 and C26, an unusual tricyclo ring system (the C to E rings) and numerous furanose and pyranose ring systems such as the A to L rings common to all halichondrins isolated thus far.

In terms of cytotoxicity and antitumour activity, Uemura *et al* reported halichondrin B (**1.2.1**) as the most cytotoxic of the halichondrins they isolated. The *in vitro* cytotoxicity results for the compounds tested against the B-16 melanoma cell line are given in **Table 1.2.1**.[18]

Table 1.2.1 IC_{50} values against B-16 melanoma cells (ng/mL)

Halichondrin series	Halichondrin family		
	A family	B family	C family
norhalichondrin	5.2	NR[a]	NR[a]
halichondrin		0.09	0.35
homohalichondrin	0.26	0.10	NR[a]

[a] Data not reported (NR) but result less than for halichondrin B.

From the cytotoxicity results shown in **Table 1.2.1**, it can be seen that halichondrin B and homohalichondrin B present higher activities relative to the other halichondrins.

The antitumour activities of halichondrin B (**1.2.1**) and homohalichondrin B (**1.2.3**) were also investigated by *in vivo* testing on mice with B-16 melanoma, P388 leukemia and L-1210 leukemia tumours. A three hundred per cent increase in the

life expectancy of the P388 leukemia afflicted mice was reported relative to the control group (no halichondrin administered) for halichondrin B.[18] Similar results were observed for the other two cell lines and for homohalichondrin B.[18]

In 1993, Pettit *et al* reported the isolation and characterisation of two new halichondrin compounds, halistatin 1 (**1.2.7**)[19] and halistatin 2 (**1.2.8**).[20] Halistatin 1 is essentially 10α-hydroxy substituted halichondrin B and halistatin 2 is 10α-hydroxy substituted homohalichondrin B. Halistatin 1 was initially isolated from the East Indian Ocean sponge *Phakellia carteri*, a sponge located in the coastal areas of the Republic of Cormoros. Halichondrin B (**1.2.1**) and homohalichondrin B (**1.2.3**) were also isolated from this sponge. This sponge yielded <0.1 mg of these halichondrins per kg (wet sponge). Halistatin 2 was isolated from *Axinella* cf. *carteri* (Dendy), also a Cormoros sponge, along with halistatin 1, halichondrin B and homohalichondrin B. *Axinella* cf. *carteri* yielded *ca* 0.1 mg of these halichondrins per kg wet sponge.

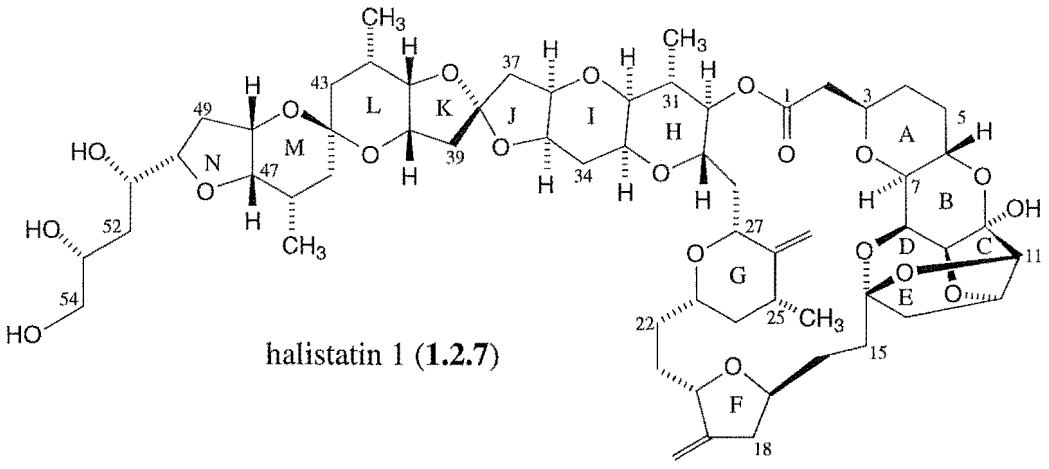

halistatin 1 (**1.2.7**)

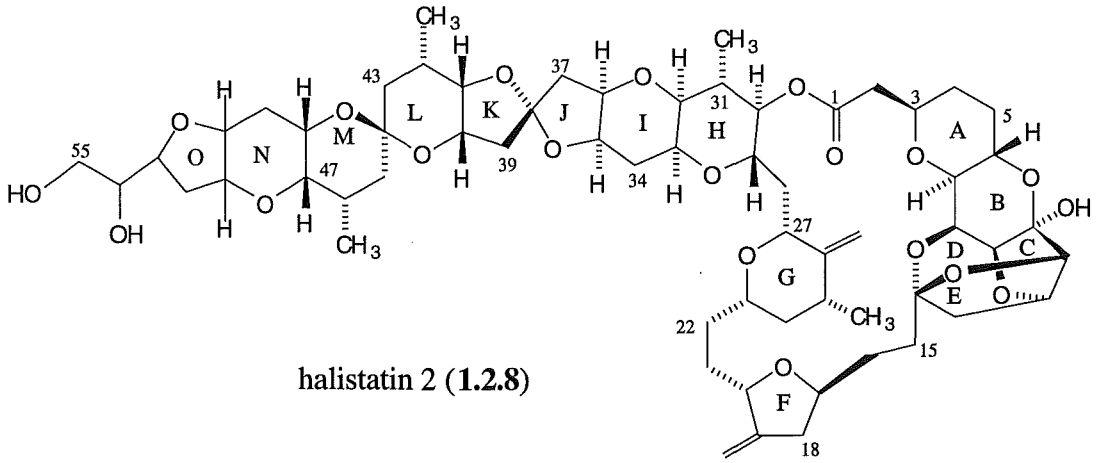

halistatin 2 (**1.2.8**)

The cytotoxicities of halistatin 1 and halistatin 2 were tested in the NCI's human tumour, disease-oriented *in vitro* primary screen. The overall GI_{50} results were reported at 7.1×10^{-10} M and 6.8×10^{-10} M respectively.[20] Halichondrin B (**1.2.1**) was reported by Pettit to be more active with a GI_{50} of 2.3×10^{-10} M.

1.2.2 Halichondrins- Marine Chemistry Group Involvement

In 1987, halichondrin-type compounds were first identified by Dr. Robin Lake from two unrelated sponges. One of these sponges was identified as one or more new species of the genus *Lissodendoryx* Topsent (class Demospongiae, subclass Ceractinomorphia, order Poecilosclerida, family Myxillidae).[21] This bright yellow sponge (**Figure 1.2.1**) was collected by dredging deep waters (*ca* 100m) off the Kaikoura coast.

Dr. Lake also detected halichondrins in a cytotoxic extract from another sponge, *Raspailia agminata* (order Axinellida, family Raspailiidae), a black, shallow water

sponge from the Leigh area of the North Island.[22] The halichondrins were present at low levels (<0.5 mg total halichondrins/kg wet sponge) relative to the high yielding *Lissodendoryx* sp. sponge (*ca* 1.6 mg/kg).

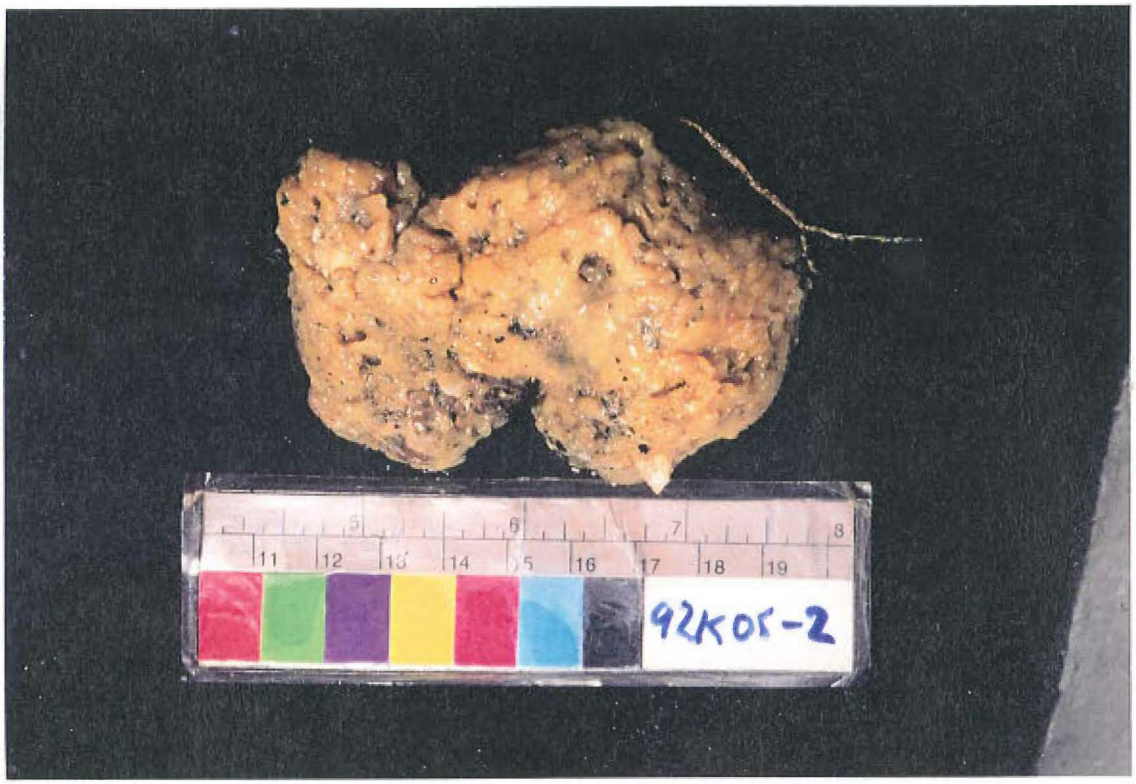

Figure 1.2.1 *Lissodendoryx* sp.

From a small sample of *Lissodendoryx* sp. sponge a new halichondrin-type compound was identified, by Dr. Lake, as one of the major cytotoxic components, although at that stage a full characterisation was not achieved.[22] It was observed that this compound transformed cleanly to another compound in CD_3OD. Two other major cytotoxic compounds were identified as a mixture of halichondrin B (**1.2.1**) and homohalichondrin B (**1.2.3**).

A later extraction of *Lissodendoryx* sp. by Dr. Marc Litaudon reisolated 4.5 mg of the new halichondrin, which was then able to be structurally characterised by MS and NMR spectroscopy. This novel halichondrin was given the name isohomohalichondrin B (**1.2.9**)[14] as it is isobaric with homohalichondrin B (**1.2.3**). It has an obvious similarity to the structure of norhalichondrin B (**1.2.2**), except at C53 there is an aliphatic ketone rather than a carboxylate and a -CH_2CH_2OH terminus attached to C53.

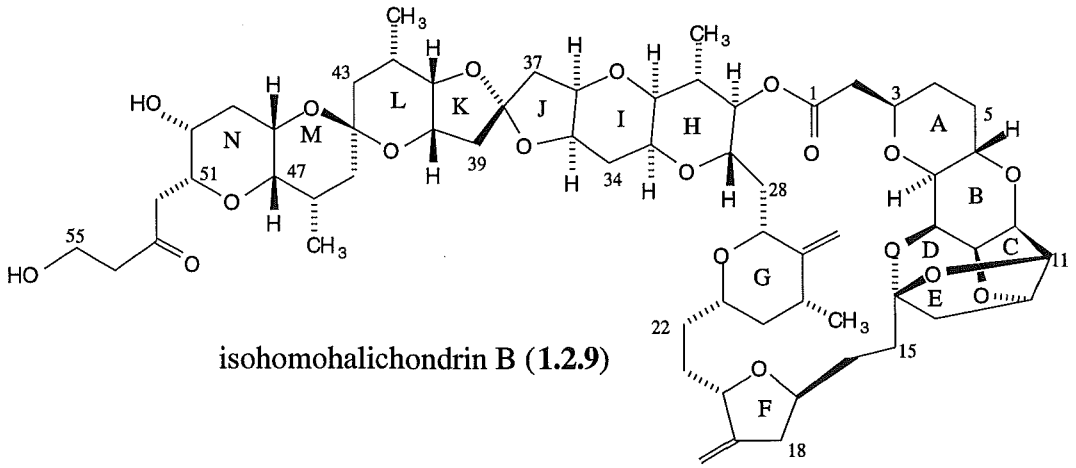

isohomohalichondrin B (**1.2.9**)

A bulk extraction of *ca* 100 kg of *Lissodendoryx* sp. sponge produced 52.8 mg halichondrin B, 53.5 mg of homohalichondrin B, 65.8 mg of isohomohalichondrin B and several novel, minor, halichondrin compounds.[23] Five of these minor compounds have been isolated and their structures established: 3 mg of Me-isohomohalichondrin B-a (**1.2.10**), 7 mg of neohomohalichondrin B (**1.2.11**), 0.7 mg of Me-isohomohalichondrin B-b (**1.2.12**), 0.9 mg of isonorhalichondrin B (**1.2.13**) and 0.7 mg of the previously identified norhalichondrin B (**1.2.2**).[23]

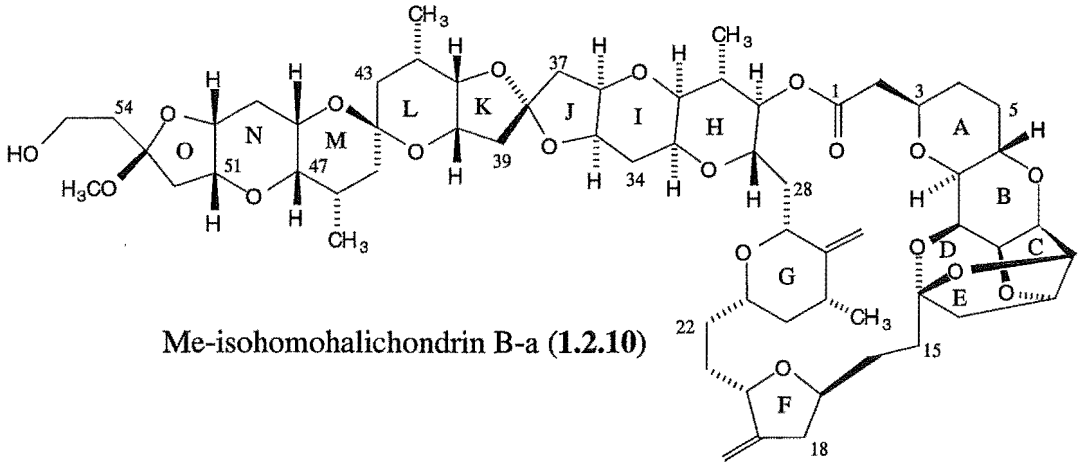

Me-isohomohalichondrin B-a (**1.2.10**)

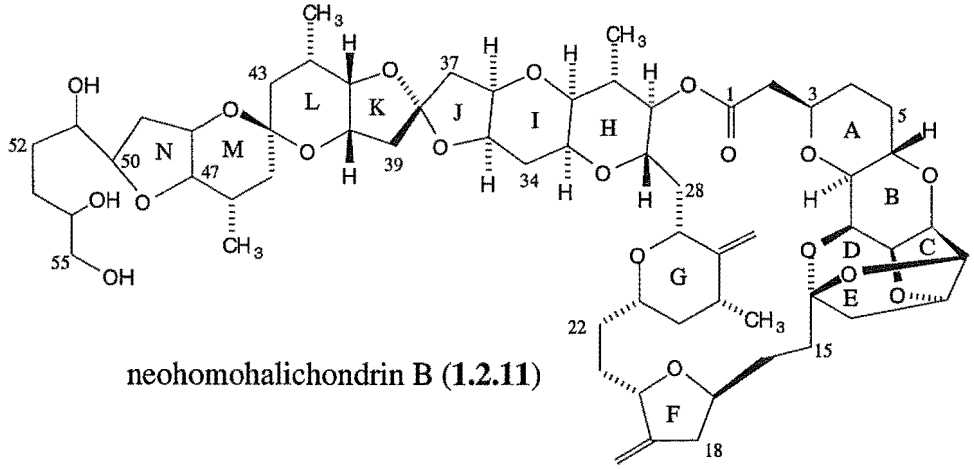

neohomohalichondrin B (**1.2.11**)

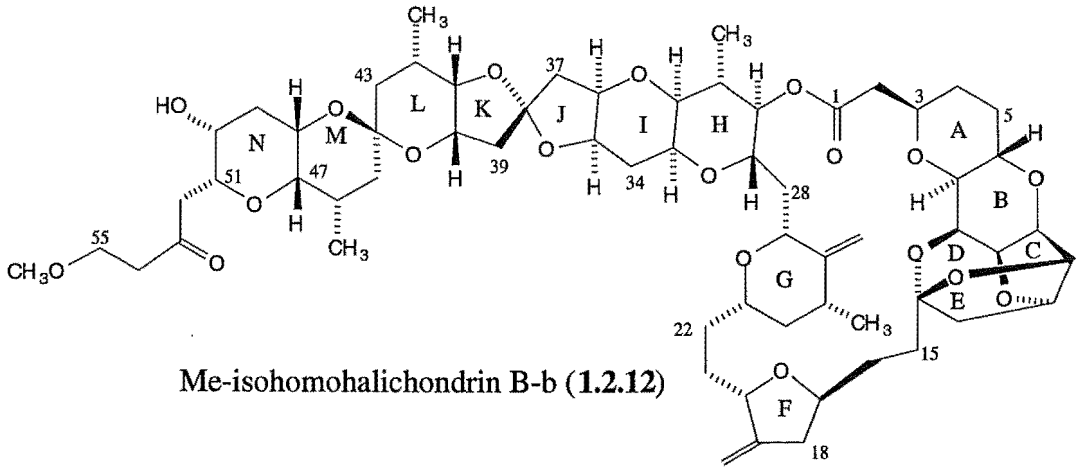

Me-isohomohalichondrin B-b (**1.2.12**)

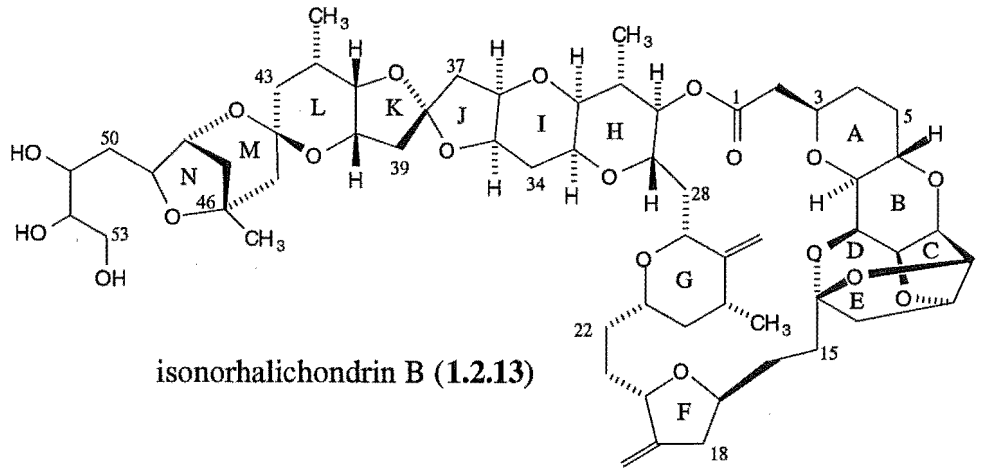

isonorhalichondrin B (**1.2.13**)

Me-isohomohalichondrin B-a (**1.2.10**) was observed to transform to isohomohalichondrin B (**1.2.9**) in an NMR tube, presumably *via* acetal hydrolysis. The reverse reaction, although much slower, was realised on a sample of isohomohalichondrin B in CD_3OD.[23] It is still unclear as to which compound is the natural component and which is a product of the extraction and purification procedure. A small amount of the C53 ketal diastereoisomer of Me-isohomohalichondrin B-a was also isolated, and this material was also observed to transform rapidly to isohomohalichondrin B (**1.2.9**).

Me-isohomohalichondrin B-b (**1.2.12**) is the C55 methoxyl derivative of isohomohalichondrin B. Neohomohalichondrin B (**1.2.11**) has a structure similar to halichondrin B (**1.2.1**) except for an additional methylene group inserted between the two secondary alcohol groups in the terminal moiety. Finally, isonorhalichondrin B (**1.2.13**) displays a unique terminal M and N ring fusion.

The cytotoxicities of the halichondrins isolated in the bulk *Lissodendoryx* sp. extraction were tested in our in-house *in vitro* P388 murine leukemia assay and in the

NCI's *in vitro* antitumour primary screening system (the GI_{50} data).[23] These results are summarised in **Table 1.2.2**. It is apparent that isohomohalichondrin B (**1.2.9**) and Me-isohomohalichondrin B-a (**1.2.10**) possess cytotoxicities in the order of halichondrin B (**1.2.1**) and homohalichondrin B (**1.2.3**). Neohomohalichondrin B (**1.2.11**) and Me-isohomohalichondrin B-b (**1.2.12**) appear to be very slightly less active in the NCI screen. The P388 cell line appears to be relatively insensitive to Me-isohomohalichondrin B-b. Both isonorhalichondrin B (**1.2.13**) and norhalichondrin B (**1.2.2**) appear to be less cytotoxic relative to the other halichondrins in the NCI screen, although the P388 assay appears to be more sensitive to isonorhalichondrin B than the cytotoxicity result from the NCI GI_{50} result tends to suggest. A further analysis of these results in terms of their relationship to structure is found in Chapter 9.

Table 1.2.2 *In Vitro* Cytotoxicities of Halichondrins From *Lissodendoryx* sp.

Compound	P388 IC_{50} (ng/mL)	GI_{50} ($\times 10^{-10}$ M)
halichondrin B (1.2.1)	0.78	1.38
norhalichondrin B (1.2.2)		29.50
homohalichondrin B (1.2.3)	0.22	3.16
isohomohalichondrin B (1.2.9)	0.18	1.15
Me-isohomohalichondrin B-a (1.2.10)	0.1	1.23
neohomohalichondrin B (1.2.11)	0.8	3.39
Me-isohomohalichondrin B-b (1.2.12)	10.0	2.00
isonorhalichondrin B (1.2.13)	0.4	12.30

Halichondrin B (**1.2.1**) was later chosen for *in vivo* evaluation against selected tumours. Halichondrin B was found to be active *in vivo* against selected sensitive melanoma, colon, ovarian, lung and breast cancer cell line xenograft implantations in athymic nude mice.

Currently, halichondrin B (**1.2.1**) has NCI Decision Network Committee "IIA status", awaiting further supplies for preclinical development and the implementation of an effective, sensitive method of analysis for halichondrin B in body fluids.

1.2.3 Halichondrin Mechanism of Action

An analysis of the halichondrin B (**1.2.1**, Appendix II) and homohalichondrin B (**1.2.3**) mean-graph "fingerprints" by the COMPARE pattern recognition algorithm showed that their profiles were most highly correlated to the structurally unrelated, tubulin-binding standards vincristine and taxol.[24]

Tubulin is a globular protein that normally undergoes polymerisation to form microtubules which, in turn, play an important role in moving chromosomes together and apart during the process of mitosis (cellular replication). Most antimitotic agents are known to interfere with the *in vitro* polymerisation of tubulin *via* specific interaction. One notable exception is the anticancer compound taxol, a complex terpene, that acts to stabilise microtubules, thus acting as a depolymerisation inhibitor of tubulin.

The alkaloid colchicine binds specifically and reversibly with tubulin, resulting in the blocking of mitosis at metaphase by arresting the formation of the mitotic spindle. The *Vinca rosea* alkaloids vincristine and vinblastine inhibit mitosis in metaphase by tubulin binding, but at a site distinct from the colchicine binding site.[25] The "vinca site" represents the region of tubulin where the vinca alkaloids and their competitive inhibitors (*eg* maytansine) bind. The peptide antimitotics dolastatin 10 and phomopsin A are non-competitive inhibitors of the vinca alkaloid binding to tubulin. Classically, this is interpreted as binding in a region, physically near to, but distinct from the vinca site and this site is termed the "vinca domain".

Investigations by Bai *et al*[24] noted the accumulation of cells arrested in mitosis at cytotoxic concentrations of either halichondrin B (**1.2.1**) or homohalichondrin B (**1.2.3**) for L1210 murine leukemia cells *in vitro*. These compounds were found to inhibit the polymerisation of purified tubulin and microtubule assembly dependent on microtubule associated proteins. Halichondrin B was found to be a relatively weak inhibitor of tubulin polymerisation, despite its potent cytotoxicity. Bai *et al*[24] speculated that this was a reflection of either the highly efficient uptake of the drug or its intracellular metabolism to more potent compounds. Halichondrin B did not interfere with colchicine binding to tubulin, but was found to be a non-competitive inhibitor of the vinca alkaloid vinblastine. This suggested that halichondrin B was binding in the vinca domain of tubulin. Vinca domain drugs inhibit tubulin-dependent GTP hydrolysis and also inhibit GTP/GDP exchange at the exchangeable nucleotide site of tubulin. Halichondrin B was found to inhibit net GTP hydrolysis and nucleotide exchange on tubulin. These observations verified the earlier COMPARE differential cytotoxicity analysis that the mode of action for halichondrin B and homohalichondrin B was as antimitotic agents.

1.3 Halichondrin Supply

As indicated in Section 1.1.3, the bulk supply of a potential anticancer drug is an essential requirement for entry into the clinical trial stage. There are several options for obtaining large amounts (gram quantities) of a material such as the halichondrins: collection, aquaculture, microbial or tissue culture, genome transfer or the total synthesis of the compound. These options are briefly discussed.

1.3.1 Collection

Bulk extraction of sponges producing the halichondrins has provided the major source of the halichondrins isolated to date. *Lissodendoryx* sp. provides a rich source of halichondrins relative to the other sponges[14] (refer Sections 1.2.1 and 1.2.2). Initial investigations established that the only known source of *Lissodendoryx* sp. was in deep water off the Kaikoura peninsula. Before large quantities of sponge can be collected, it is essential to gauge the size of the existing sponge field, the impact of collection on the environment and the regrowth of the sponge in the harvested area. A major survey of the sponge field has been undertaken to establish the population size and density of sponge and the efficiency and impact of trawling on the sponge field.[26]

A video on board a Remote Operated Vehicle (ROV) was used to establish the preferred habitat and population density over a 5.3 km^2 area of the sea bed. It was found that *Lissodendoryx* sp. was the dominant sponge in this area with an average

density of 5.4 ± 2.7 g/m^2 with only 43% of the habitat being available to it.[26] Controlled trawls within the sponge field were backed up by the use of the ROV. Trawling was estimated to be 73% efficient[26] at harvesting the *Lissodendoryx* sponge. Re-examination of the trawled areas after 12 months will establish the regrowth pattern in the trawled areas.

1.3.2 Aquaculture

The aquaculture of explanted *Lissodendoryx* sp. into a more accessible environment may provide the quantities necessary for bulk halichondrin extraction. However, it is possible that the explanted sponge may not survive or produce halichondrins in a new environment. Alterations in salinity, pressure, temperature, sunlight, oxygen levels, available nutrients, associated microorganisms, competition and other forms of stress may all contribute to decrease the chances of survival of the sponge or limit the production of halichondrins.

Initial explants of *Lissodendoryx* sp. were taken from deep water off Kaikoura to a more accessible shallow water site in Wellington Harbour by Dr. Chris Battershill of the New Zealand Oceanographic Institute. These sponge samples were found to double in size over the four months at the new site and it was also observed that small samples had broken off the main explants and had recruited neighbouring sites.[26] It appears that the sponge can survive and is rapidly growing under these conditions. Investigations on samples of the Wellington Harbour sponges indicate that high levels of cytotoxicity are still produced in the sponge. Efforts are currently

focused on identifying the cytotoxic components to determine the quantities and relative proportions of halichondrins being produced in the explanted sponge.

1.3.3 Microbial or Tissue Culture

Given that halichondrins have been found in several unrelated species of sponge, it would evidently appear more likely that the halichondrins are produced by a symbiotic, microbial source rather than *de novo* by the sponge cells. Therefore the isolation and culture of the microorganisms responsible for producing the halichondrins could provide an efficient method for bulk halichondrin production. Alternatively, the location of the sponge cell type producing the halichondrins and its subsequent culture could efficiently provide the quantities of halichondrin required.

Some preliminary investigations to determine the location of the halichondrins within the sponge were carried out by Dr. Mary Garson while in the Marine Chemistry Group. Sponge cell dissociation and separation into different cell types by a Ficoll gradient[27] was carried out as well as membrane fractionation, and a combined Ficoll gradient-membrane fractionation experiment. These experiments were followed up with P388 bioassays and electron microscopy. The results of these experiments suggested that the activity associated with *Lissodendoryx* sp. was associated with the sponge cells themselves rather than a symbiont source.[28] There appeared to be little in the way of bacterial cells associated with the sponge, from electron micrographs of tissue preparations and the fractions from the dissociation experiments.[29] The results furthermore suggested that the activity was membrane-associated. Antibiotic experiments on *Lissodendoryx* sp. to kill any sponge-

associated extracellular and intracellular bacterial cells may help to confirm that the sponge cells are producing the halichondrins *de novo*.

1.3.4 Genome Transfer

The transfer of the genome from a halichondrin producing cell to a vector amenable to fermentation is becoming increasingly viable, particularly for compounds of polyketide biosynthetic origins.[26]

1.3.5 Synthesis

The total synthesis of the halichondrins provides another option in supplying a large amount of halichondrin material. This is by no means a trivial task. Kishi and co-workers first reported the total synthesis of halichondrin B (**1.2.1**) and norhalichondrin B (**1.2.2**) in 1992.[29] Although the starting points for the synthesis relied upon inexpensive compounds of known absolute stereochemistry, the synthesis encompassed over a hundred reaction steps. A review of the Kishi synthesis (Appendix III) was undertaken in order to examine some of the chemistry that might be pertinent to this project, and it gives the overall synthetic strategy in the total synthesis of halichondrin B. For the bulk total synthesis of halichondrins to be cost competitive relative to the bulk extraction methods, a great deal of synthetic refinement will be required.

1.4 Project Aims

The objectives of this project fell into four main areas:

i) A prime objective of this project was to develop an understanding of the relationship between structure and the expression of biological activity in the halichondrin series of antitumour compounds.

The chemical modification of selected members of the halichondrin family would give some insight into the essential structural and conformational features for the expression of biological activity. Evidence from the pharmaceutical industry has shown that the most effective drug may not be the natural compound, but rather an analogue of it. Therefore, it was also possible that the analogues produced may have improved biological properties relative to the naturally-occurring compounds, and thus provide additional leads as potential antitumour drugs.

ii) The structural assignment of the derivatives produced during the course of this project relied upon the full assignment of the NMR spectral data of the parent compounds, to be used for reference purposes. The initial objective to be accomplished, prior to the production of halichondrin analogues, was therefore the full spectroscopic assignment of selected naturally-occurring halichondrins.

iii) Another objective of this work was to gain an understanding of the important solution conformation(s) of the halichondrins and selected derivatives.

It is likely that the conformation(s) of the halichondrins is an important factor in the expression of antitumour activity. It was envisaged that computer modelling would

provide essential information as to the important solution conformation(s). This data could then be related to the NMR data collected for verification.

iv) The final objective of this project was the development of the general chemistry of the halichondrins. Along with a knowledge of the relative reactivities of the various functional groups in the molecule gained in the structure/activity studies this would allow for the future design of specific derivatives, such as orally bioavailable derivatives.

For example, an important consideration in the development and evaluation of any potential pharmaceutical is a study of pharmacokinetics which is defined by Albert as "the study of the kinetics of drug absorption, distribution, metabolism, and excretion".[30] The detection and/or quantification of small quantities of halichondrins for *in vivo* pharmacokinetic studies in drug development trials requires specific "labelling" of the molecule and therefore a knowledge of the chemistry of the halichondrins. Potentially, this could involve hapten binding for enzyme linked immunoassay (ELISA), fluorescent labelling or isotopic labelling.

CHAPTER 2

NMR Spectroscopic Assignment of Selected Halichondrins

2.1 Introduction

One of the goals of this research was to produce semi-synthetic derivatives of the naturally-occurring halichondrins. To facilitate the NMR spectroscopic characterisation of these derivatives it was initially necessary to fully assign the NMR spectra of selected, naturally-occurring halichondrins. This information was then used as a reference for future chemical modifications, allowing the NMR spectra to be assigned in terms of differences relative to the parent compound.

Initially, the 75 MHz ^{13}C and 300 MHz ^{1}H NMR spectra of halichondrin B (**1.2.1**) were completely assigned in $CDCl_3$/ 0.1% pyridine-d_5. Later, a full assignment of homohalichondrin B (**1.2.3**) was also achieved. Hirata and Uemura had previously achieved only a partial assignment of the ^{13}C and ^{1}H NMR spectra of halichondrin B and homohalichondrin B in CD_3OD.[18] Dr. Marc Litaudon, in the Marine Chemistry Group, subsequently attained a partial assignment of the ^{1}H NMR spectrum of halichondrin B in CD_3OD from material isolated from *Lissodendoryx* sp. Pettit *et al* have since published NMR data (also in CD_3OD) on the related halichondrins halistatin 1 (**1.2.7**) and halistatin 2 (**1.2.8**) (10α-hydroxyhalichondrin B and 10α-hyroxyhomohalichondrin B respectively).[19,20] Their assignments are also incomplete.

The absolute stereochemistry of the halichondrins was determined by Uemura *et al* from the X-ray crystal structure of the *p*-bromophenacyl ester of norhalichondrin A.[17] The relative stereochemistry of halichondrin B was examined to ensure that it was consistent with that proposed by Uemura *et al.* It was also important to consider whether the conformation of the X-ray crystal structure accurately represented the major solution conformations of the basic halichondrin, B series, subunit.

The relative stereochemistry of halichondrin B (**1.2.1**) was determined at certain points in the molecule using selective 1D and 2D NMR spectroscopic techniques. Some insight was also gained, from these experiments, as to the overall folding conformation of halichondrin B in solution. Coupling constants were collected for halichondrin B and related to the X-ray crystal structure of norhalichondrin A. It was necessary to model the solution conformations of the C1 to C14 subunit as there was a discrepancy between the experimental and X-ray crystal structure-derived coupling constants for H11-H12. The terminal moiety of halichondrin B (C44-C54) was also modelled to determine possible solution conformations of this area in the molecule to give coupling constants and dihedral angles that were related to the experimental NMR data collected.

The solution conformations of the terminal bicyclic ring system of isohomohalichondrin B (**1.2.9**) were investigated by selected NMR experiments and computer modelling. The optical rotation of isohomohalichondrin B was measured to aid in the evaluation of the absolute stereochemistry.

2.2 NMR Spectroscopic Assignment of Halichondrin B

The ^{1}H NMR spectrum of halichondrin B (**1.2.1**) shows considerable overlap in the methylene and methine regions (**Figure 2.2.1**). There are however some distinct and isolated signals such as the olefinic protons 19=CH_2 and 26=CH_2; the methine protons H11, H32 and H7; the methylene protons H18' and H2', and the methyl protons Me-25 and Me-42. Similarly, the ^{13}C NMR spectrum of halichondrin B (**1.2.1**) is also very complex (**Figure 2.2.2**). To fully assign the ^{1}H and ^{13}C NMR spectra of halichondrin B it was therefore necessary to perform a range of selective 1D and 2D NMR experiments which allowed individual signals to be isolated and thus assigned.

The NMR experiments used to carry out these assignments are illustrated with specific examples. **Figures 2.2.3** and **2.2.4** display the important correlations from these experiments which enabled the full assignment of the ^{1}H and ^{13}C NMR spectra of halichondrin B (**1.2.1**) to be achieved. **Table 2.2.1** and **Table 2.2.2** list the chemical shifts of the protons and carbons of halichondrin B respectively. All NMR experiments were performed for *ca.* 10 mg of halichondrin B in $CDCl_3$/ 0.1% pyridine-d_5. Hirata and Uemura have stated that the decomposition of halichondrins occurs in acidic solution[18] and Cooper *et al* claim a specific mode of decomposition for the tricyclo ring system (C, D and E rings) under acidic conditions in a related synthetic C1-C21 B series fragment.[31] To eliminate the risk of acid-catalysed decomposition, pyridine-d_5 was added to all $CDCl_3$ solutions.

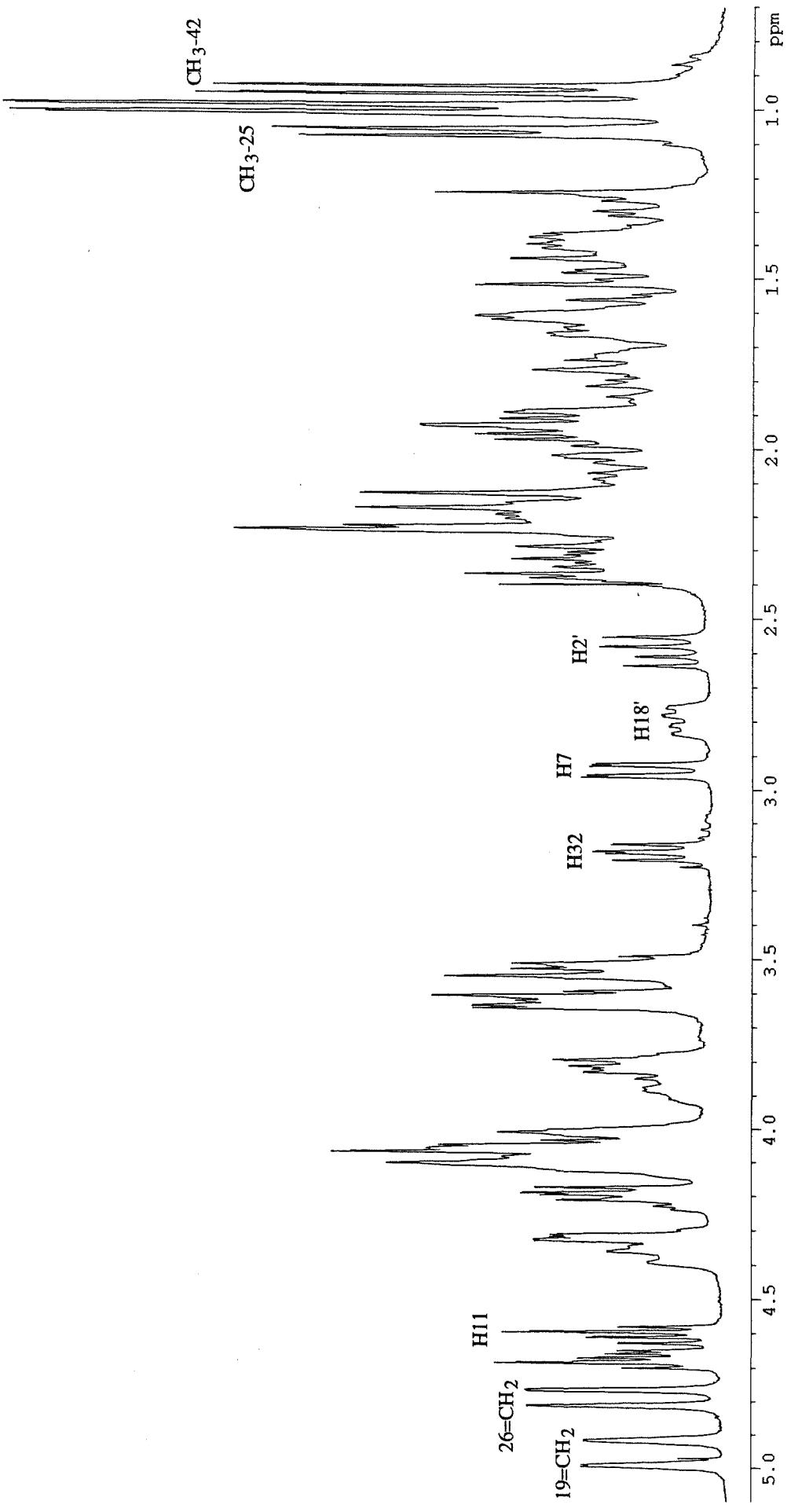

Figure 2.2.1 ^{1}H NMR Spectrum of Halichondrin B

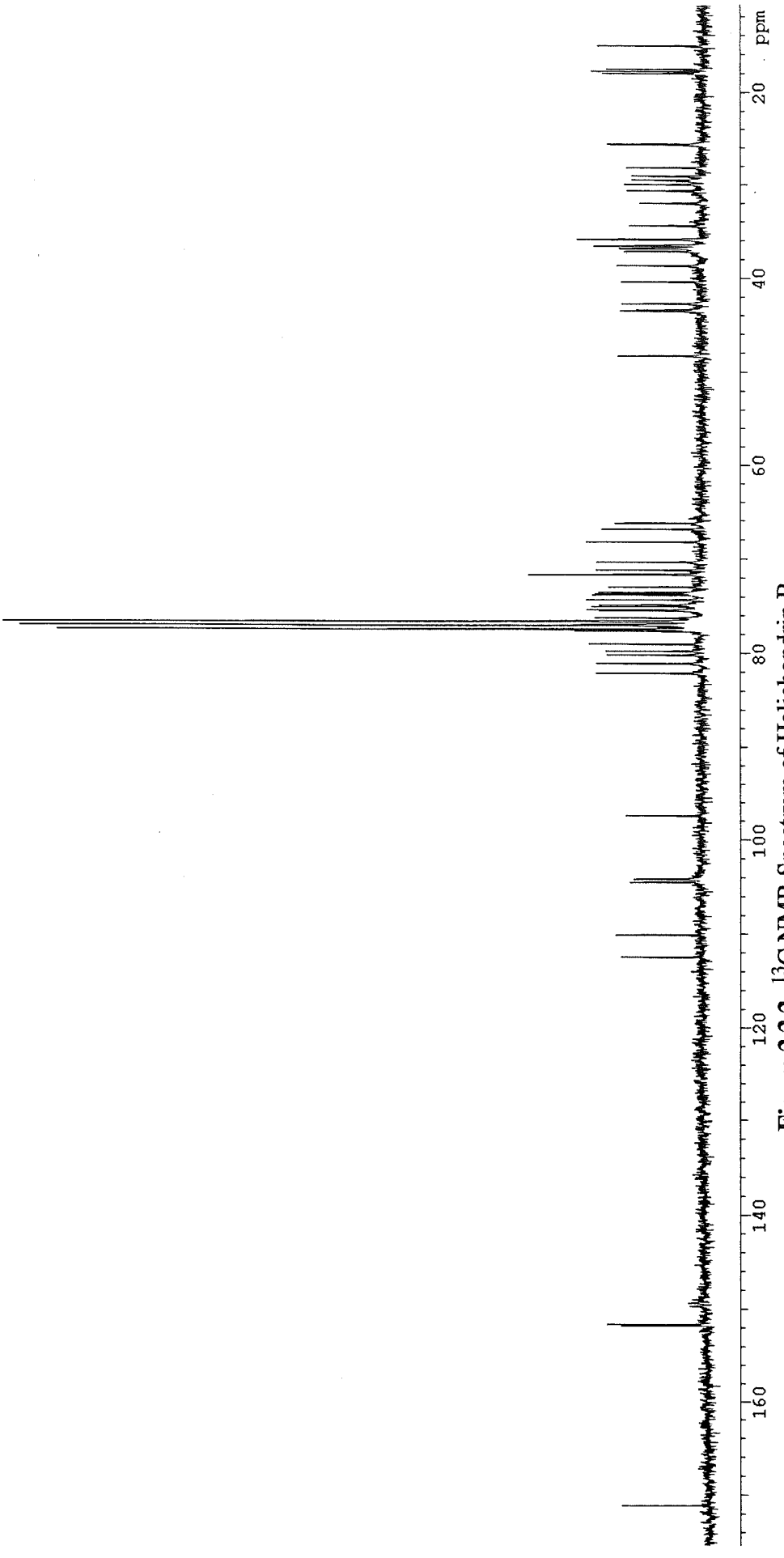

Figure 2.2.2 ^{13}C NMR Spectrum of Halichondrin B

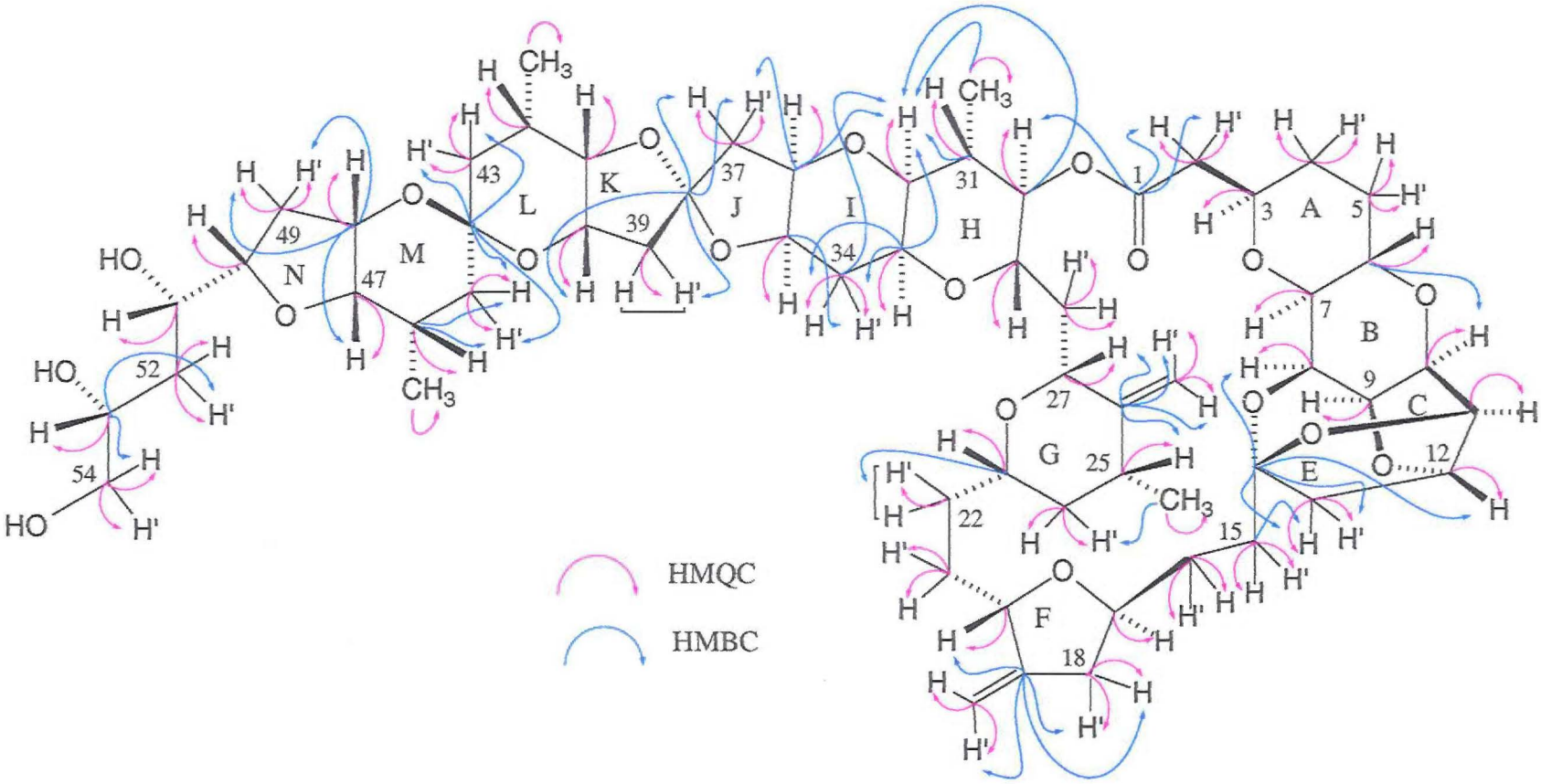

Figure 2.2.3 Halichondrin B- Important HMQC and HMBC Correlations

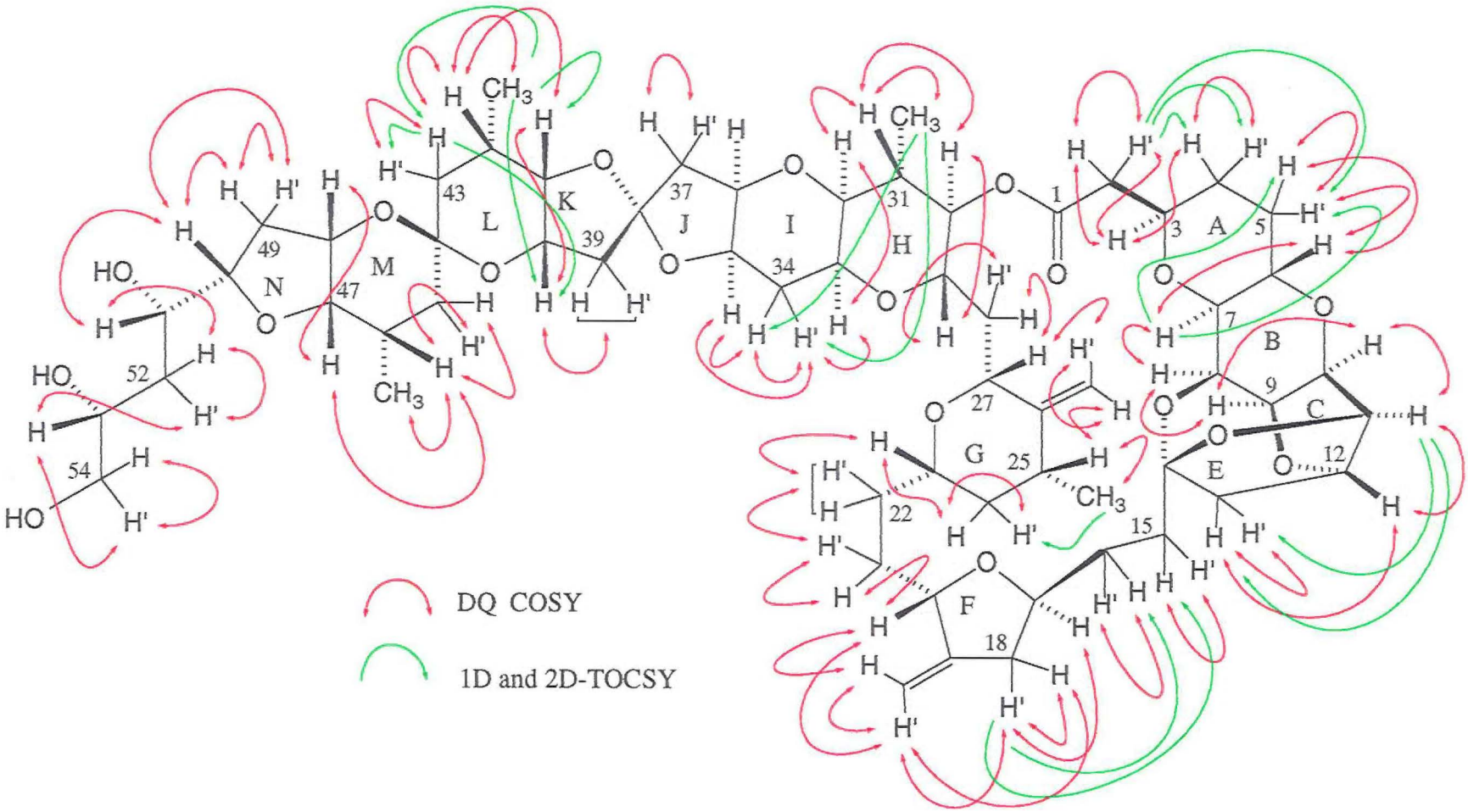

Figure 2.2.4 Halichondrin B- Important COSY and TOCSY Correlations

Table 2.2.1 ^{1}H NMR Data for Halichondrin B (**1.2.1**)

Proton[a]	Literature δ ppm[18,b]	$CDCl_3$ δ ppm[c]	**Proton**[a]	Literature δ ppm[18,b]	$CDCl_3$ δ ppm[c]
H2	2.44	2.35	**H28**		1.94
H2'	2.57	2.60	**H28'**		2.02
H3	3.88	3.86	**H29**	4.25	4.21
H4		1.35	**H30**	4.63	4.63
H4'		1.74	**H31**		2.04
H5		1.40	**CH_3-31**	1.07	0.99
H5'		2.08	**H32**	3.22	3.18
H6	4.33	4.34	**H33**	3.87	3.80
H7	2.98	2.94	**H34**		1.79
H8	4.31	4.33	**H34'**		2.13
H9	4.13	4.04	**H35**	4.12	4.10
H10	4.18	4.20	**H36**	4.10	4.10
H11	4.60	4.60	**H37**		1.92
H12	4.71	4.68	**H37'**		2.37
H13	1.98	1.94	**H39**		2.24
H13'	2.09	2.15	**H39'**		2.24
H15		1.62	**H40**	4.05	4.00
H15'		2.18	**H41**	3.69	3.63
H16		1.42	**H42**		2.23
H16'		2.16	**CH_3-42**	0.94	0.94
H17	4.08	4.10	**H43**		1.29
H18	2.32	2.26	**H43'**		1.52
H18'	2.80	2.80	**H45**		1.42
19 =CH	5.02	4.92	**H45'**		1.50
19' =CH	5.07	4.98	**H46**		2.35
H20	4.46	4.37	**CH_3-46**	1.01	0.99
H21		1.40	**H47**	3.56	3.61
H21'		1.88	**H48**	4.10	4.05
H22		1.60	**H49**	1.83	1.90
H22'		1.60	**H49'**	2.27	2.32
H23	3.71	3.53	**H50**	4.00	4.08
H24		1.04	**H51**	3.78	3.80
H24'		1.70	**H52**	1.61	1.62
H25		2.20	**H52'**	1.75	1.79
CH_3-25	1.10	1.07	**H53**	3.87	4.02
26=CH	4.82	4.77	**H54**	3.46	3.54
26'=CH	4.88	4.81	**H54'**	3.53	3.61
H27	3.62	3.54			

[a] The symbol ' represents the less shielded proton of a geminal pair.

[b] Literature data recorded in CD_3OD at 360 MHz.

[c] Data recorded at 23°C in $CDCl_3$ at 300 MHz with chemical shifts in ppm and referenced to $CHCl_3$, δ_H 7.25 ppm.

Table 2.2.2 ^{13}C NMR Data for Halichondrin B (**1.2.1**)

Carbon	Literature δ ppm[18,a]	$CDCl_3$ δ ppm[b]	Carbon	Literature δ ppm[18,a]	$CDCl_3$ δ ppm[b]
C1	171.8	171.2	**C28**		36.9
C2	41.2	40.4	**C29**	73.8	71.2
C3	74.9	73.7	**C30**	77.3	76.9
C4		30.7	**$\underline{C}$-CH_3-31**	37.5	36.6
C5		30.0	**C-$\underline{C}H_3$-31**	15.9	15.1
C6	69.6	68.2	**C32**	78.0	77.2
C7	79.1	77.4	**C33**	65.5	66.3
C8	75.8	74.3	**C34**		29.1
C9	73.3	73.8	**C35**	77.3	75.0
C10	78.0	76.5	**C36**	78.0	76.2
C11	83.8	82.1	**C37**	45.6	43.5
C12	82.5	81.1	**C38**	114.8	112.5
C13	49.4	48.3	**C39**	45.0	42.7
C14	111.3	110.1	**C40**	73.0	71.7
C15		34.4	**C41**	80.8	79.0
C16		28.2	**$\underline{C}$-CH_3-42**	27.1	25.6
C17	76.3	75.4	**C-$\underline{C}H_3$-42**	18.2	17.5
C18	39.7	38.7	**C43**		36.5
19$\underline{C}$=CH_2	153.2	151.8	**C44**	98.4	97.4
19C=$\underline{C}H_2$	105.8	104.5	**C45**		36.9
C20	76.1	75.5	**$\underline{C}$-CH_3-46**	27.1	25.7
C21		28.2	**C-$\underline{C}H_3$-46**	18.3	17.8
C22		32.0	**C47**	81.3	80.2
C23	75.3	74.9	**C48**	75.1	71.7
C24		43.4	**C49**		35.9
$\underline{C}$-CH_3-25	37.5	35.9	**C50**	81.3	79.0
C-$\underline{C}H_3$-25	18.4	18.0	**C51**	73.1	73.0
26$\underline{C}$=CH_2	153.2	151.6	**C52**		37.2
26C=$\underline{C}H_2$	104.8	104.2	**C53**	71.6	70.1
C27	75.1	73.5	**C54**	67.1	66.9

[a] Literature data recorded in CD_3OD at 75.4 MHz.

[b] Data recorded at 23° C in $CDCl_3$ at 75 MHz with chemical shifts in ppm and referenced to $CDCl_3$, δ_C 77.0 ppm.

2.2.1 The COSY Experiment

The initial assignment of protons in the ^{1}H NMR spectrum of halichondrin B (**1.2.1**) began with the double quantum filtered COSY (*C Orrelation Spectroscop Y*) experiment (**Figure 2.2.5**). From this experiment, correlations between adjacent (geminal and vicinal) protons can be observed. The strength of the observed correlation is a function of the coupling constant between the protons; the larger the coupling constant, the stronger the correlation. An example of how the COSY spectrum was used in the assignment of the ^{1}H NMR spectrum of halichondrin B will be illustrated by focusing on the C1-C14 spin system.

The isolated protons H2', H7 and H11 in the ^{1}H NMR spectrum of halichondrin B (**1.2.1**) provided the lead-in to the C1-C14 spin system. The correlations discussed are indicated in **Figure 2.2.5**. A strong correlation was observed between H2' (δ_H 2.60 ppm) and its geminal partner H2 (δ_H 2.34 ppm). Both of these protons were correlated to only one methine proton, H3, at δ_H 3.86 ppm. From H3, the only correlation to protons on C4 was to H4 (δ_H 1.35 ppm), with H4' being assigned by a geminal correlation to δ_H 1.74 ppm. Correlations to the methylene protons on C5 from H4/H4' were not able to be isolated as they were obscured by other correlations in this area of the COSY spectrum. From H7 (δ_H 2.94 ppm), it was possible to see only one correlation to an adjacent methine proton at δ_H 4.34 ppm. From this correlation, there were observed correlations to methylene protons (H5', δ_H 2.08 ppm and H5, δ_H 1.40 ppm) and a methine proton (H9, δ_H 4.04 ppm). This indicated that the chemical shifts of H6 and H8 were very similar and therefore appearing as one correlation to H7. From the H9 proton a clear correlation to H10 at δ_H 4.20 ppm was observed and also a strong correlation was apparent from H10 to the isolated H11 proton at δ_H 4.60 ppm. The H11 proton also showed one other correlation to H12 at

δ_H 4.68 ppm, and this proton was correlated, in turn, to one of the C13 methylene protons, H13 at δ_H 1.94 ppm. Finally, the H13' proton (at δ_H 2.15 ppm) was located by the appearance of a strong geminal correlation to H13.

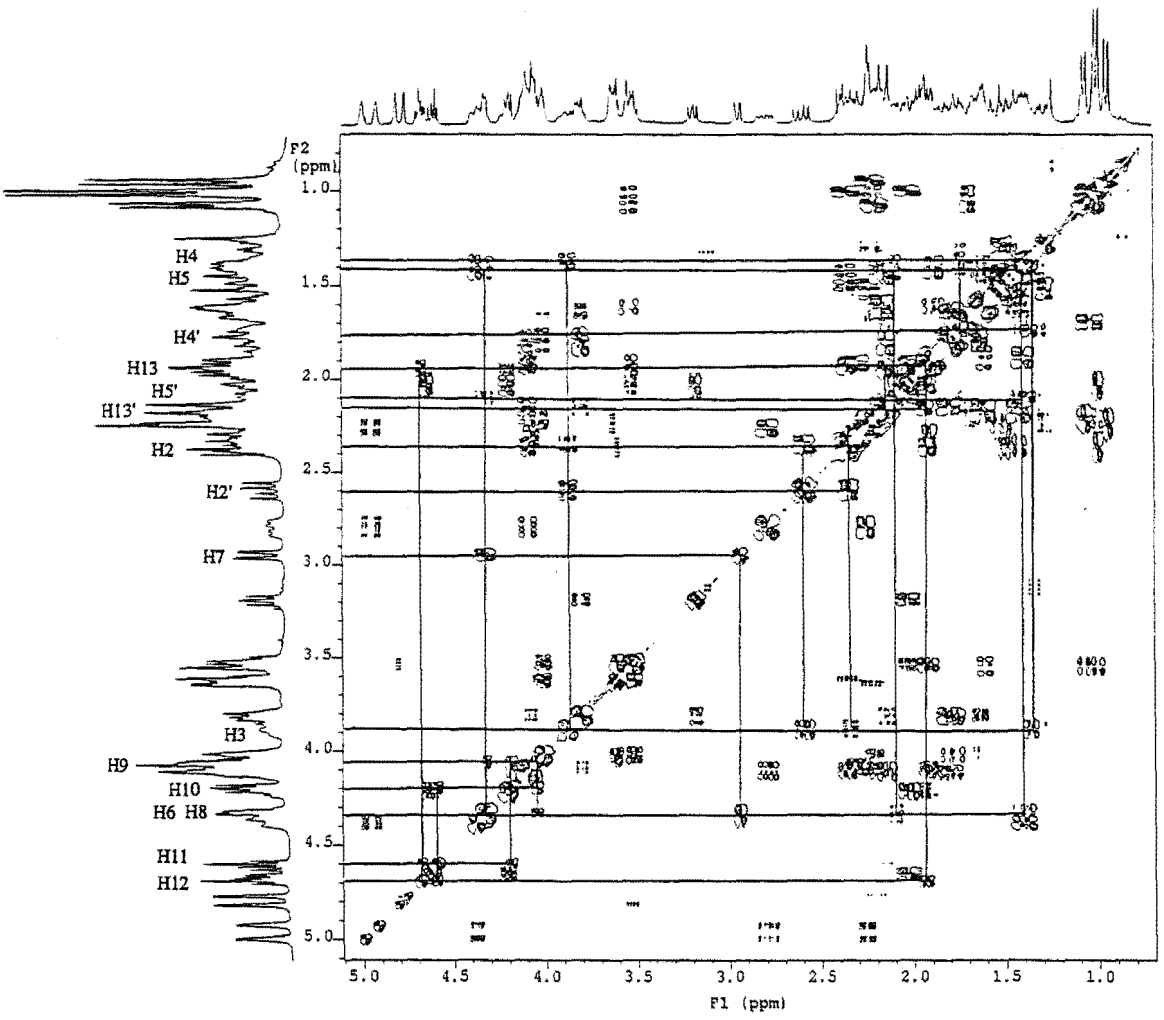

Figure 2.2.5 COSY Spectrum of Halichondrin B

2.2.2 The TOCSY Experiment

The TOCSY experiment (*TO*tal *C*orrelation *S*pectroscop*Y*) reveals the connectivity of protons through a spin system. The 2D-TOCSY spectrum of halichondrin B (**1.2.1**) is shown in **Figure 2.2.6**. Again, the example of the C1-C14 spin system will be used to illustrate the utility of this experiment and its application to the assignment of the ^{1}H NMR spectrum of halichondrin B.

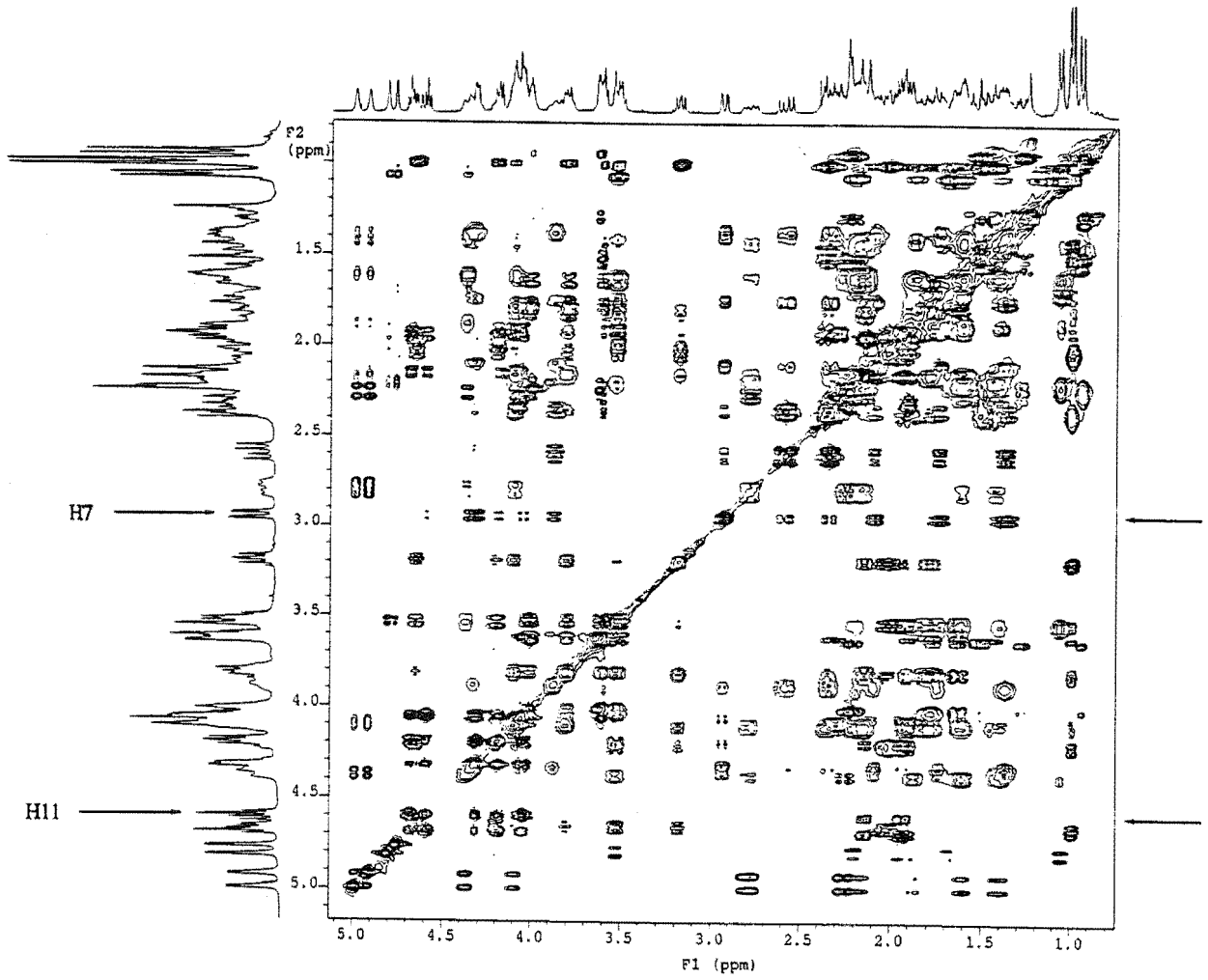

Figure 2.2.6 2D-TOCSY Spectrum of Halichondrin B

A cross-section through the H11 proton in the 2D-TOCSY spectrum is displayed as a 1D trace in **Figure 2.2.7**. From this cross-section, through-bond correlations were seen from H11 to H12, H13 and H13' in one direction and to H10, H9, H8 and H7 (weak) in the other direction. The appearance of a TOCSY signal is dependent on the magnitude of the coupling constant for the transmission of magnetisation through the spin system and also on the length of the spin-lock (the mixing time) in the pulse sequence of the experiment. For this experiment, a mixing time of 100 ms was used. A small coupling constant between H7 and H8 explains the observation of a weak signal for the H7 proton and is amplified by the losses in the transfer of magnetisation through the spin system as the proton concerned was further removed from the irradiated proton.

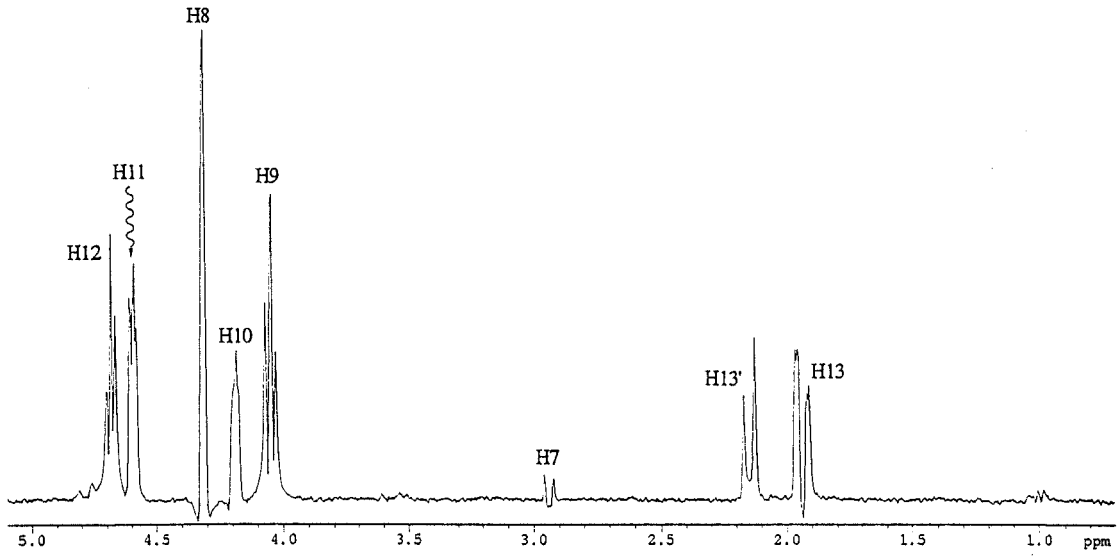

Figure 2.2.7 Cross-Section Through H11 From 2D-TOCSY Spectrum

A cross-section through H7 (**Figure 2.2.8**) from the 2D-TOCSY spectrum showed correlations to H8, H9, H10 and H11 in one direction and to H6, H5', H5 and H4, H4', H3, H2' and H2 in the other direction. Similar cross-sections can be obtained through H2' (at δ_H 2.60 ppm) showing correlations through to H6.

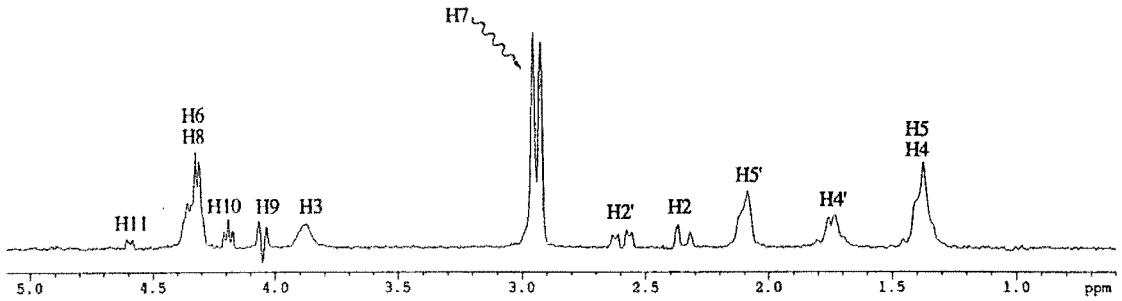

Figure 2.2.8 Cross-Section Through H7 From 2D-TOCSY Spectrum

A "time-economic" alternative to acquiring a 2D-TOCSY spectrum is to perform a 1D-TOCSY experiment. The 1D experiment is performed by selectively irradiating isolated signals in the ^1H NMR spectrum. The pulse sequence of the 1D-TOCSY experiment differs from that of the 2D-TOCSY experiment in that it initially has a selective 90° irradiation pulse rather than a non-selective 90° pulse (**Figure 2.2.9**). The 1D-TOCSY experiment can be used to probe specific spin systems providing they have a sufficiently isolated (in terms of chemical shift) proton.

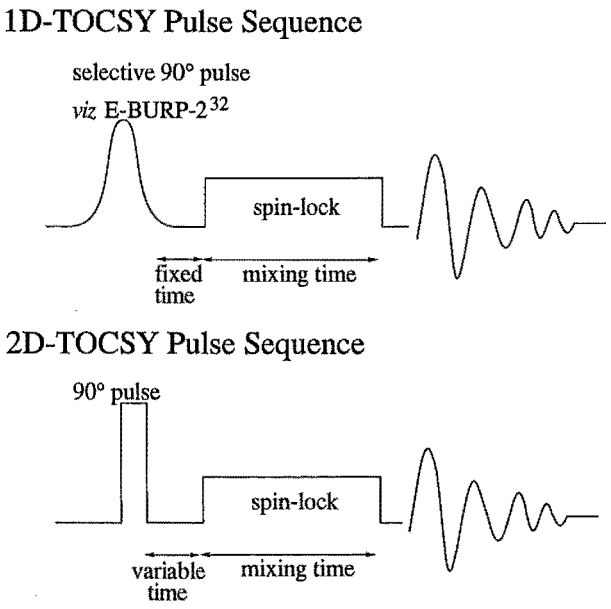

Figure 2.2.9 Pulse Sequences for 1D and 2D-TOCSY Experiments

The 1D-TOCSY experiment from selective irradiation of the H11 proton in the ^1H NMR spectrum of halichondrin B (**Figure 2.2.10**, bottom spectrum) gave the spectrum shown in **Figure 2.2.10** (top spectrum). Essentially, the 1D-TOCSY experiment gives the same information as can be obtained from a cross-section through the 2D-TOCSY experiment (**Figure 2.2.10**, middle spectrum).

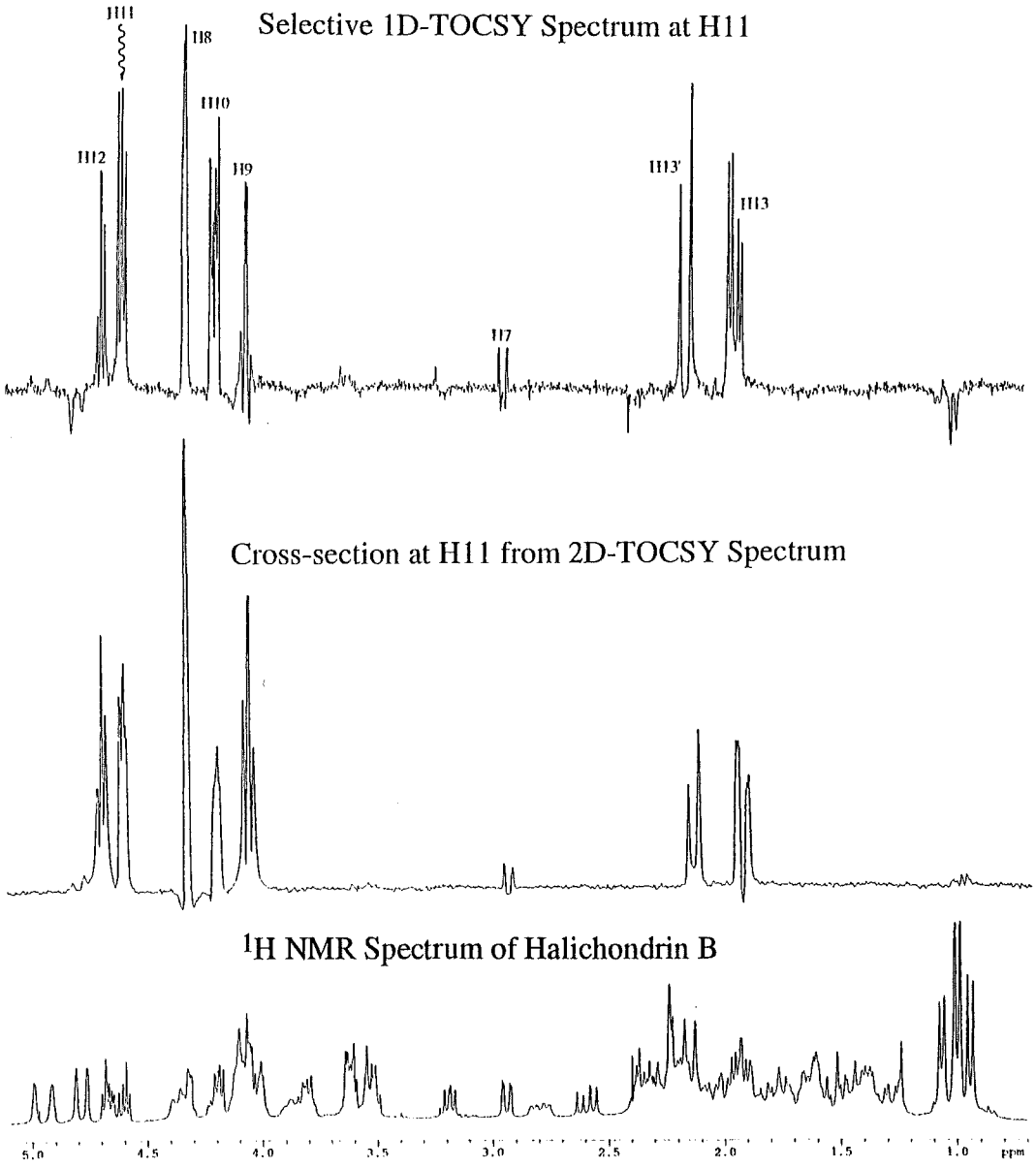

Figure 2.2.10 1D-TOCSY *vs* 2D-TOCSY Spectra for H11

The advantages of performing a 1D-TOCSY over the 2D analogue are the enhanced resolution obtained, and the reduction in the time required to obtain a given signal to noise ratio. Another advantage, related to the time saving, is that the duration of the spin lock (the mixing time) in the pulse sequence (**Figure 2.2.9**) can be varied, for a given irradiated proton, to give a range of 1D spectra on a reasonable time scale. This enables connectivity, relative to the irradiated proton, to be established.

An example of varied mixing times for the 1D-TOCSY experiment is shown in **Figure 2.2.11** for irradiation of the H11 proton. For a 10 ms mixing time, correlations were seen to H12 and H10. As the mixing time was increased to 25 ms, contributions from H9 were clearly observed; and at 50 ms, H13' and H13 and H8 were seen. Finally, with a 120 ms mixing time, contributions were observed from the H7 proton.

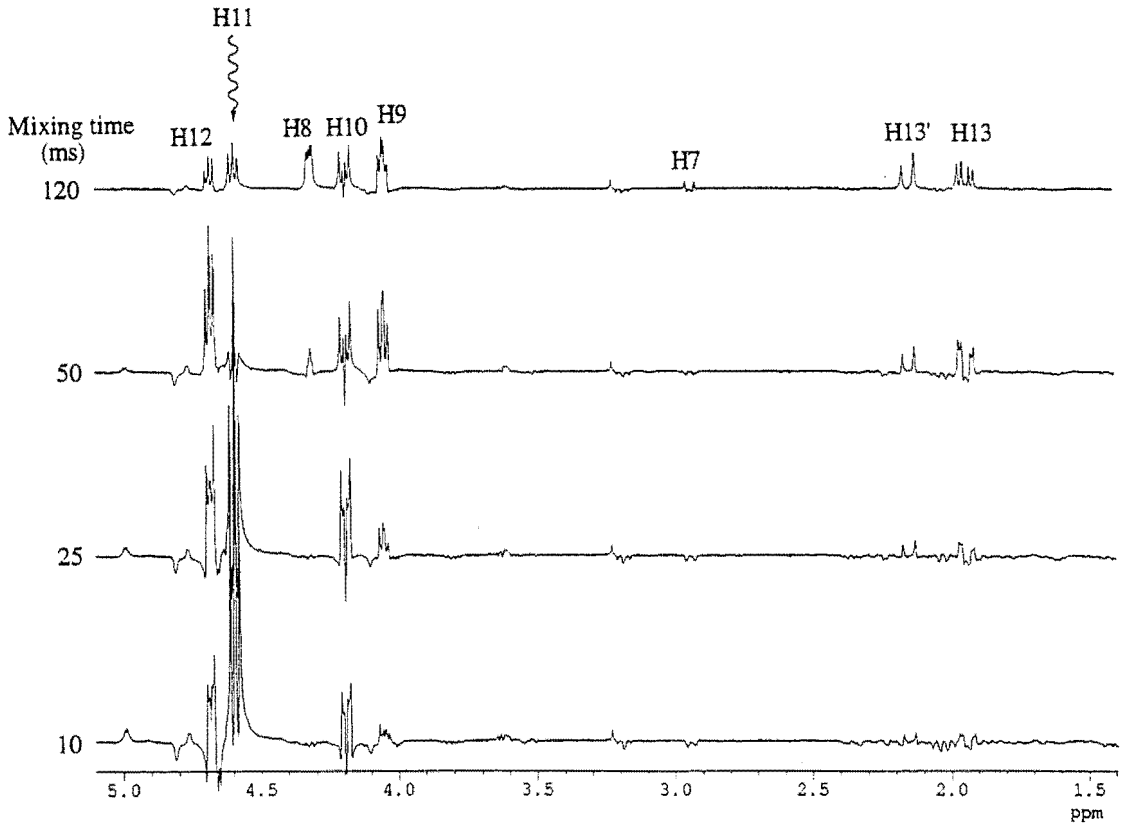

Figure 2.2.11 Varied Mixing Times for 1D-TOCSY Spectra Through H11

As the mixing time is increased, the time for the transmission of magnetisation through the spin system is also increased. There is however, a trade-off between the sensitivity of the signal and the duration of the mixing time. This effect can be seen in **Figure 2.2.11** above. As the spectra are plotted on the same vertical scale, it is apparent that the sensitivity of the spectrum acquired with a mixing time of 120 ms is much reduced relative to the spectrum obtained using a 10 ms mixing time. Two main reasons for this observation are that the magnetisation becomes spread over an increased number of signals as the mixing time is increased, and there is also a greater chance for relaxation losses occurring during this increased mixing time.

2.2.3 The HMQC Experiment

The HMQC experiment (*H*eteronuclear *M*ultiple *Q*uantum *C*oherence) shows ^{13}C-^{1}H single bond correlations. As a ^{1}H detected experiment, it is much more sensitive relative to the ^{13}C detected HETCOR experiment which gives the same information.

The HMQC experiment (and the HMBC experiment, Section 2.2.4) is particularly useful when there is no ^{13}C NMR spectrum available, for example if there is not enough material to acquire a good spectrum. The HMQC (and HMBC) experiment can therefore be used to effectively obtain and indirectly assign the ^{13}C NMR spectrum. The HMQC and HMBC experiments were therefore crucial in the ^{13}C NMR spectroscopic assignment of halichondrin derivatives produced in small quantities during the structure-activity investigations.

The HMQC spectrum of halichondrin B (**Figure 2.2.12**) was especially useful in the assignment of methylene protons that were obscured or unclear in the COSY spectrum. The spectrum was acquired with a narrowed ^{13}C NMR spectral window (δ_C 10 to δ_C 90 ppm), and therefore the olefinic ^{13}C-^{1}H correlations appeared as foldbacks into this window. All correlations discussed are indicated on the HMQC spectrum.

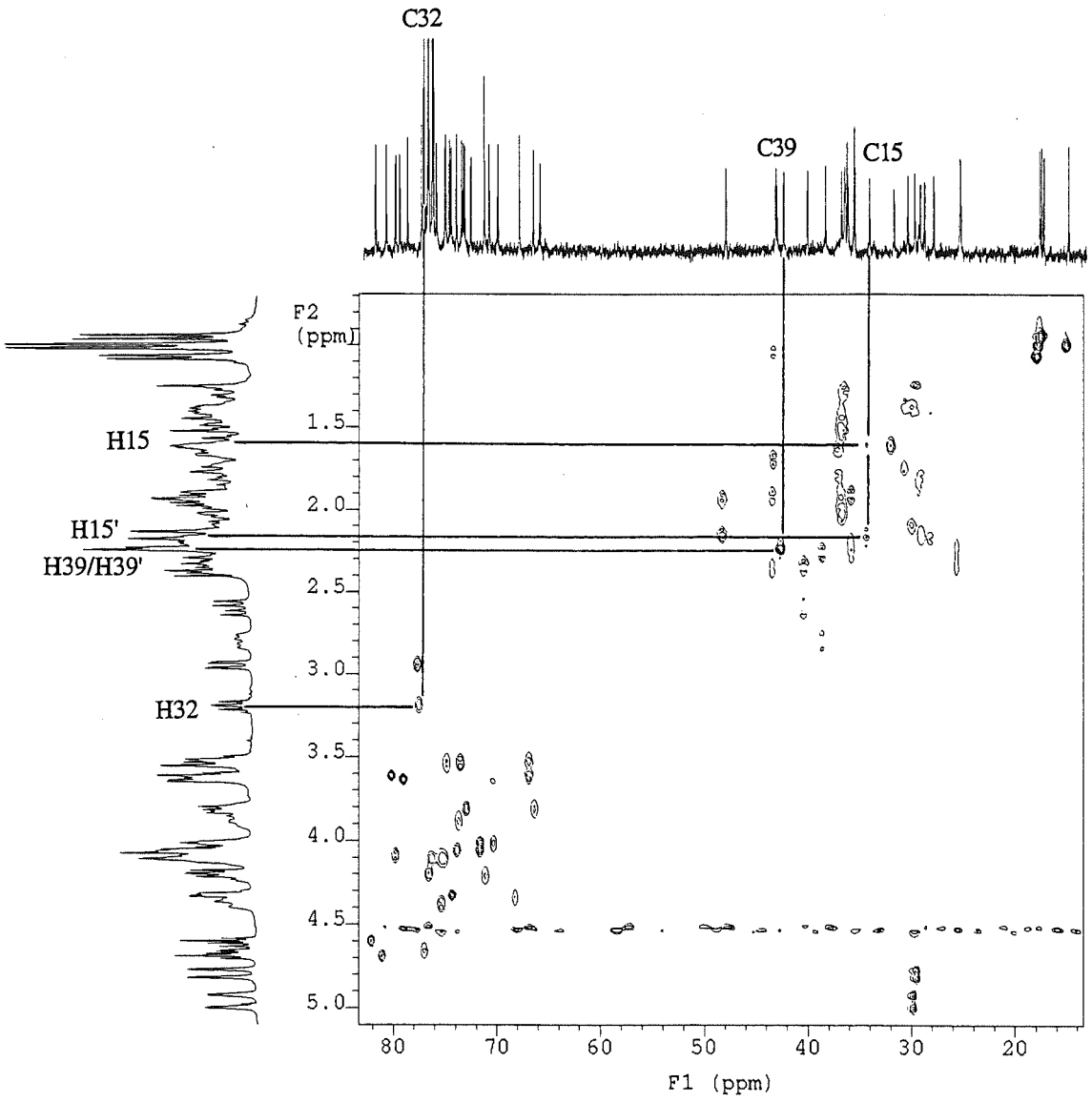

Figure 2.2.12 HMQC Spectrum of Halichondrin B

It was possible in many cases to determine where geminal partners of methylene protons were situated, either as chemical-shift equivalent protons appearing as one correlation to one carbon or as a pair of correlations into one carbon in the case of chemical-shift distinct protons. For example, only one COSY and TOCSY correlation was observed between H40 (δ_H 4.00 ppm) and H39 (δ_H 2.24 ppm). The HMQC spectrum of halichondrin B showed one intense correlation from a proton at δ_H 2.24 ppm to a carbon at δ_C 42.7 ppm, implying the H39 protons were chemically-shift equivalent. The C15 carbon resonance was able to be assigned from the chemical shifts of the attached methylene protons.

Assignment of the carbons with attached methine protons was relatively straight forward as in many cases the ^{1}H NMR chemical shift of the proton was relatively isolated or the ^{13}C NMR chemical shift could be estimated. The H32 proton, for example, was relatively isolated in the ^{1}H NMR spectrum of halichondrin B at δ_H 3.18 ppm, so a single correlation in the HMQC spectrum from H32 at δ_H 3.18 ppm into a carbon at δ_C 77.2 ppm allowed C32 to be assigned.

2.2.4 The HMBC Experiment

The HMBC experiment (*H*eteronuclear *M*ulti*B*ond *C*oherence), like the HMQC experiment, is also a reverse (^{1}H) detected experiment. The HMBC experiment shows correlations to carbons from protons on carbons two to three (and sometimes four) bonds removed. The HMBC spectrum of halichondrin B (**Figure 2.2.13**) was useful in the assignment of the ^{13}C NMR chemical shifts of carbons without attached protons such as the spiro carbon centres: C14, C38 and C44 and the carbon of the

lactone, C1. For example, correlations were observed from a foldback carbon at δ_C 31.6 ppm in the spectrum, corresponding to a real carbon at δ_C 97.4 ppm, to the previously identified H45 (δ_H 1.42 ppm), H45' (δ_H 1.50 ppm), H43 (δ_H 1.29 ppm) and H43' (δ_H 1.52 ppm). This identified the carbon signal as belonging to C44.

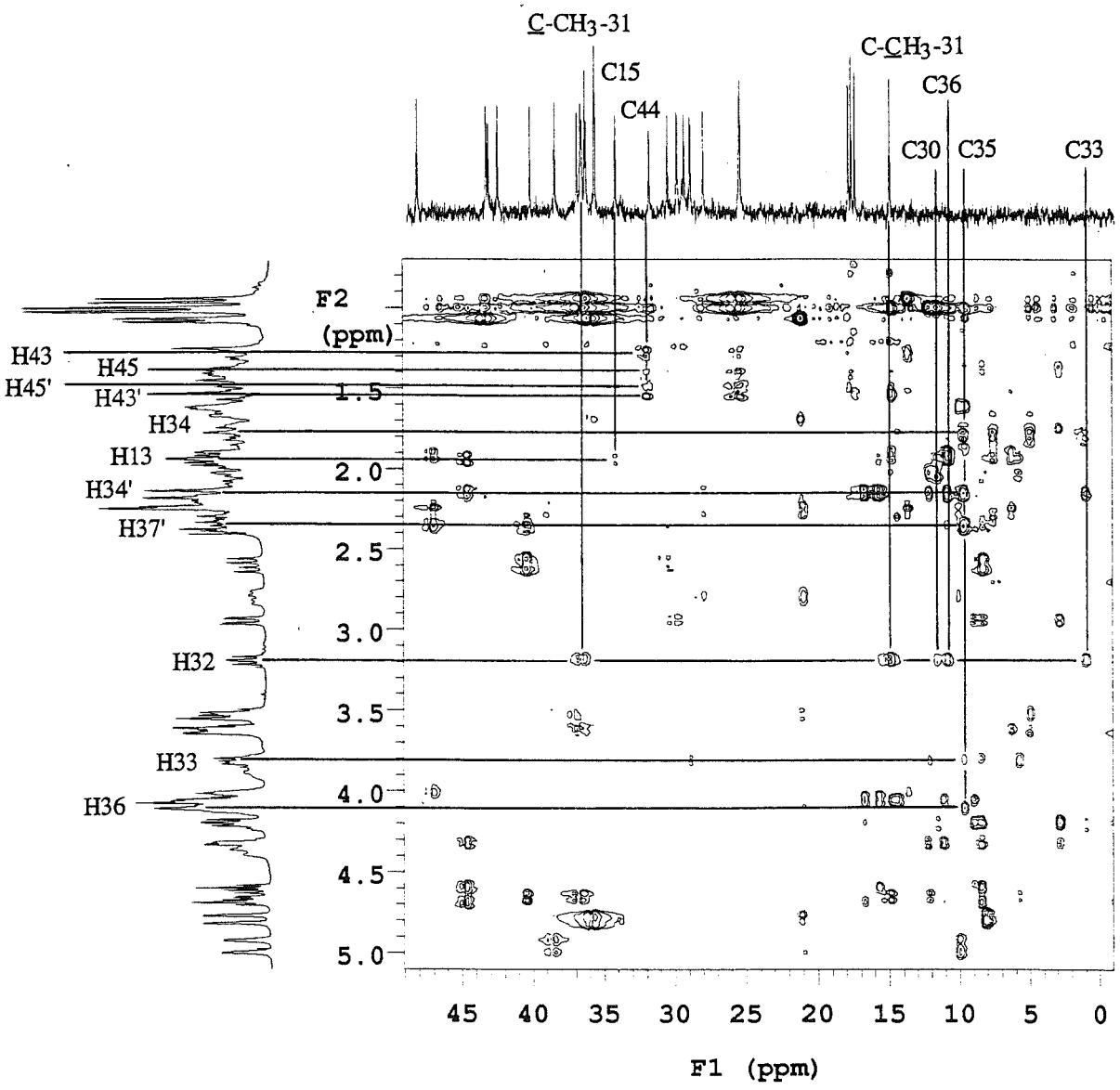

Figure 2.2.13 HMBC Spectrum of Halichondrin B

In conjunction with the closely related HMQC experiment, assignments of ^{1}H NMR chemical shifts of some unidentified methylene protons were also made. A real

carbon at δ_C 34.4 ppm showed a weak HMBC correlation to a proton at δ_H 1.94 ppm. This proton was identified as H13 as it was the only proton of this approximate chemical shift within three bonds of a methylene carbon. In the HMQC spectrum of halichondrin B, the carbon at δ_C 34.4 ppm was correlated to a methylene pair of protons at δ_H 1.62 ppm and δ_H 2.18 ppm (indicated in **Figure 2.2.12**). The carbon at δ_C 34.4 ppm was therefore identified as C15 and the methylene protons on this carbon as H15 (δ_H 1.62 ppm) and H15' (δ_H 2.18 ppm). Unfortunately no HMBC correlations were observed from the C14 carbon to the H15/H15' protons.

The assignments of the C17, C35 and C36 ^{13}C NMR chemical shifts from the HMQC experiment were ambiguous as they were correlated to protons at δ_H 4.10 ppm attached to carbons with very similar ^{13}C NMR chemical shifts. The HMBC spectrum showed that the carbon at δ_C 75.0 ppm (appearing as a foldback to δ_C 9.2 ppm) was correlated to protons at δ_H 2.35 ppm (H37'), δ_H 2.13 ppm (H34'), δ_H 1.79 ppm (H34), δ_H 3.80 ppm (H33), δ_H 3.18 ppm (H32, weak) and to δ_H 4.10 ppm (H35 or H36). Given that relatively strong correlations were observed to H33 it was more likely that the carbon at δ_C 75.0 ppm was C35 as this represented a three bond HMBC correlation. There remained two unassigned ^{13}C NMR signals at δ_C 75.4 ppm and δ_C 76.2 ppm. A cross-section through H32 (δ_H 3.18 ppm) in the HMBC spectrum showed correlations to the previously identified carbons C33 (δ_C 66.3 ppm, appearing as a foldback to δ_C 0.4 ppm), C34 (δ_C 29.1, weak), $\underline{C}$-CH_3-31(δ_C 36.6 ppm) and C-$\underline{C}H_3$-31 (δ_C 15.1 ppm). Another correlation was observed to a carbon at δ_C 76.9 ppm (appearing as a foldback to δ_C 10.4 ppm) which had previously been assigned as C30, and a strong correlation slightly upfield appearing at δ_C 11.1 ppm in the spectrum was unidentified. This carbon signal at δ_C 76.2 ppm (folded back to δ_C 11.1 ppm in the HMBC spectrum) was assigned as C36. The remaining ^{13}C NMR signal at δ_C 75.4 ppm was therefore assigned as C17.

2.3 Conformation and Stereochemistry Studies on Halichondrin B

2.3.1 Solution Conformation and Relative Stereochemistry From NMR Experiments

Assignment of the relative stereochemistry of some centres in halichondrin B (**1.2.1**) was achieved by consideration of vicinal coupling constants and the observation of correlations in the NOESY spectrum of halichondrin B. In particular, it allowed the relative stereochemistry of some of the methylene protons to be inferred. This information also gave some insight into the average solution conformation of halichondrin B in $CDCl_3$. This data was subsequently related to the X-ray crystal structure of the Uemura *et al* norhalichondrin A derivative.

2.3.1.1 The NOESY Experiment

The NOESY (*N*uclear *O*verhauser and *E*xchange *S*pectroscop*Y*) experiment shows correlations between protons situated close in space and is a direct result of the nuclear Overhauser effect. The NOESY spectrum of halichondrin B (**1.2.1**) is shown in **Figure 2.3.1**. The important correlations that were observed are indicated in **Figure 2.3.2**, showing the inferred stereochemistry at specified points in the molecule. All correlations discussed below are indicated on the NOESY spectrum, **Figure 2.3.1**.

The methylene protons that were assigned a relative stereochemistry solely from the NOESY spectrum are indicated in **Figure 2.3.2** as those displaying a specified orientation. For example, the H4 and H4' methylene protons were able to be

assigned a relative stereochemistry as NOESY correlations were observed between H6 (δ_H 4.34 ppm) and H4 (δ_H 1.35 ppm). This indicated a *cis* 1,3-diaxial relationship for H4 relative to H6. Additionally, a NOESY correlation from H3 at δ_H 3.86 ppm to H4' at δ_H 1.74 ppm implied a *trans* stereochemistry for the H4' proton relative to H6.

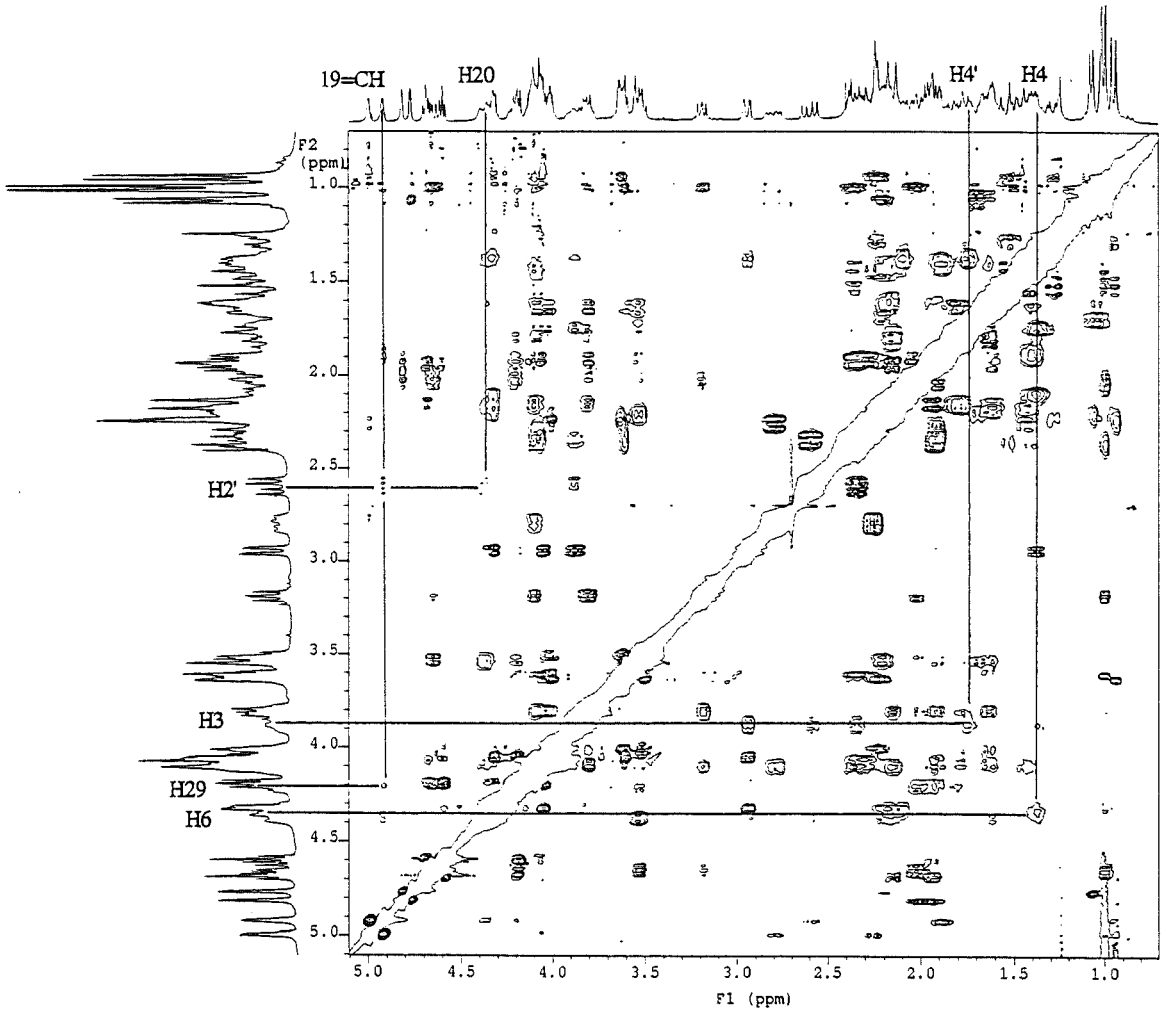

Figure 2.3.1 NOESY Spectrum of Halichondrin B

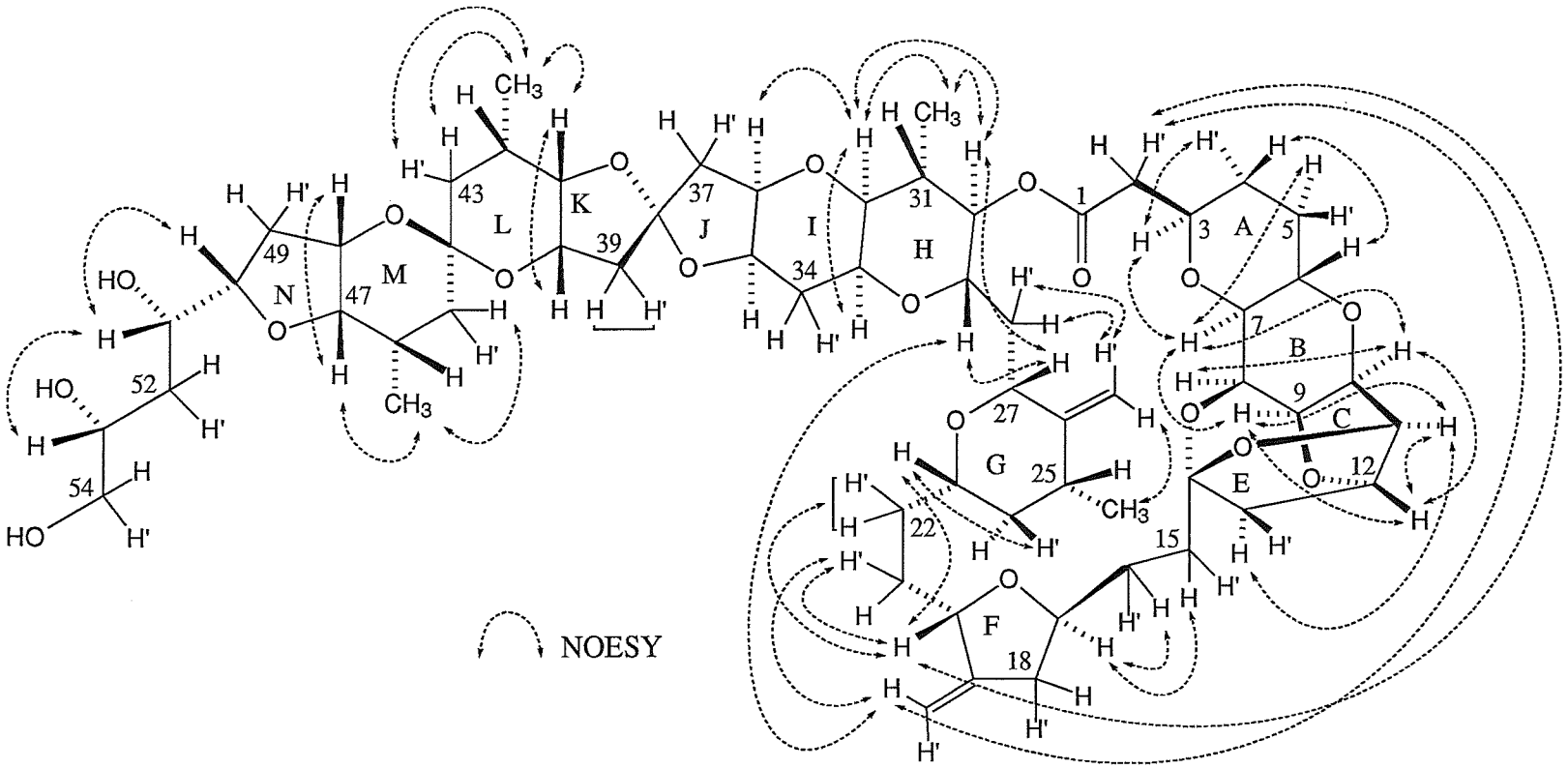

Figure 2.3.2 Halichondrin B- Important NOESY Correlations

The NOESY spectrum of halichondrin B also showed three interesting correlations that gave an indication of the overall folding conformation of the molecule in $CDCl_3$ solution. NOESY correlations were observed between the following protons: H2' (δ_H 2.60 ppm) and H20 (δ_H 4.37 ppm), H2' and 19=CH (δ_H 4.92 ppm), and between H29 (δ_H 4.21 ppm) and 19=CH. These correlations indicated that the F ring of halichondrin B (C17-C20) was orientated with 19=CH directed "into" the lactone ring and in close proximity to H2' and H29 which must also be inward facing. A model was constructed of the C1-C33 region of halichondrin B indicating that this was a feasible conformation providing that the G ring (C23-C27) was orientated with 26=CH_2 and CH_3-25 pointing "outwards" with respect to the lactone ring.

Inspection of the Uemura *et al* X-ray crystal structure of the norhalichondrin A derivative, which was imported from the Cambridge Crystallographic Database, indicated that the average folding conformation in solution postulated for halichondrin B from the NOESY spectrum was also the conformation existing in the crystal structure. This X-ray crystal structure is shown in Appendix V. Interatomic distances were collected from the X-ray crystal structure for the three NOESY correlations discussed above. These distances are given in **Table 2.3.1**. The experimentally observed NOESY correlations were therefore acceptable in terms of interatomic distance, as these values were within the distance that a NOE interaction may be observed.

Table 2.3.1 X-ray Crystal Structure Distances Between Protons

NOESY interaction	Interatomic distance (Å)
19=CH - H29	2.8
19=CH - H2'	2.6
H20 - H2'	2.9

2.3.1.2 Coupling Constants

Coupling constants were collected for halichondrin B (**1.2.1**) from the ^{1}H NMR spectrum and 1D and 2D-TOCSY experiments. These data are listed in **Table 2.3.2** (H2-H21) and **Table 2.3.3** (H22-H54). The vicinal coupling constants ($^{3}J_{HH}$) were converted to possible dihedral angles *via* a computer application of the Karplus equation.[33] Also listed in **Tables 2.3.2** and **2.3.3** are the norhalichondrin A derivative X-ray crystal structure derived vicinal coupling constants. These values were obtained using the Karplus relationship in the program MacroModel V4.0 which calculates $^{3}J_{HH}$ from the observed vicinal (H-C-C-H) dihedral angles.

The Karplus equation relates the vicinal coupling constant ($^{3}J_{HH}$) to the dihedral angle between two vicinal protons. This is a function of the identity and orientation of the attached alpha and beta substituents. The computer program generates a plot of the vicinal coupling constant as a function of the dihedral angle between the two protons and thus allows possible orientations of the vicinal protons to be obtained from experimental coupling constants.

The dihedral angles that were obtained from the NMR data were related to the X-ray crystal structure of the *p*-bromophenacyl ester of norhalichondrin A[17] where applicable *ie* H2-H43. This was carried out to compare the average solution conformation to the conformation of the crystal structure, and allowed the relative stereochemistry of some vicinal protons to be inferred. The calculated dihedral angles generally correlated well with the X-ray crystal structure conformation, although there was the suggestion of some minor twisting in the ring systems in the C29 to C44 region relative to the X-ray crystal structure, as demonstrated by the construction of Dreiding molecular models.

Table 2.3.2 Coupling Constants for H2-H21 of Halichondrin B

Proton	Mult.	J_{HH} (Hz)[a]	X-ray $^3J_{HH}$[b]	**Proton**	Mult.	J_{HH} (Hz)[a]	X-ray $^3J_{HH}$[b]
H2	dd	3.3, 16.2	1.1[c]	**H13**	dd	4.7, 13.3	5.9
H2'	dd	8.4, 16.2	10.6[c]	**H13'**	d	13.3	1.3
H3	dd	8.4, 12.6	1.1, 2.8, 10.6, 11.7	**H15**	m		6.7, 13.5[d]
H4	m		4.2, 11.7, 13.6	**H15'**	m		4.8, 13.6[d]
H4'	m		2.5, 2.8, 3.8	**H16**	m		1.5, 4.8, 13.5[d]
H5	m		3.8, 11.4, 13.6	**H16'**	m		0.7, 11.4, 13.6[d]
H5'	m		2.5, 2.8, 3.8	**H17**	m		1.1, 1.5, 7.6, 11.4
H6	ddd	4.2,9.5,9.5	4.3, 9.2, 11.4	**H18**	d	16.2	1.1[c]
H7	dd	2.1, 9.5	3.4, 9.4	**H18'**	dd	7.6,16.2	7.6[c]
H8	dd	2.1, 4.1	3.4, 4.2	**19 =CH**	d	1.4	
H9	dd	4.1, 6.6	4.2, 5.8	**19' =CH**	d	1.4	
H10	dd	4.7, 6.6	4.6, 5.8	**H20**	dd	1.4,10.9	1.4, 11.3
H11	dd	4.7, 4.7	4.6, 7.0	**H21**	m		1.4, 1.5, 13.7[d]
H12	d	4.7, 4.7	1.3, 5.9, 7.0	**H21'**	m		1.4, 5.9, 11.3[d]

a Experimental data recorded in $CDCl_3$ at 300 MHz. b Units in Hz

c Assignment of stereochemistry by comparison to experimental $^3J_{HH}$ and NOESY data.

d X-ray crystal structure assignment of $^3J_{HH}$ to specific chemical shifts of methylene protons are interchangeable.

Table 2.3.3 Coupling Constants for H22-H54 of Halichondrin B

Proton	Mult.	J_{HH} (Hz)[a]	X-ray $^3J_{HH}$[b]	**Proton**	Mult.	J_{HH} (Hz)[a]	X-ray $^3J_{HH}$[b]
H22	m		1.4, 1.7, 13.7[d]	**H39**			6.0[d]
H22'	m		1.7, 2.3,[d] 11.5,11.6	**H39'**			1.4[d]
H23	m		1.7, 2.3, 11.5, 11.6	**H40**	dd	2.2, 4.4	1.4, 2.6, 5.2
H24			11.6, 12.4	**H41**	dd	2.2, 2.2	2.6, 3.0
H24'			2.3, 3.2	**H42**	m		3.0, 3.5, 7.0, 12.3
H25	m		3.2, 7.0, 12.4	**CH_3-42**	d	7.1	7.0
CH_3-25	d	7.0	7.0	**H43**	dd	4.3, 13.0	3.8[c]
26=CH	s			**H43'**	dd	13.0, 13.0	12.3[c]
26'=CH	d	1.5		**H45**	dd	12.6, 12.6	
H27	d	12.5	1.4, 11.2	**H45'**	dd	4.2, 12.6	
H28	m		1.4, 11.2[d]	**H46**	m		
H28'	m		1.3, 11.2[d]	**CH_3-46**	d	6.9	
H29	m		1.3, 2.5, 10.7	**H47**			
H30	dd	6.5, 9.3	2.5, 9.7	**H48**			
H31	m		7.0, 9.7, 10.7	**H49**			
CH_3-31	d	6.9	7.0	**H49'**			
H32	dd	5.9, 8.0	7.5, 10.7	**H50**			
H33	ddd	5.9, 5.9, 11.0	4.7, 7.5, 11.3	**H51**			
H34	ddd	11.0, 11.0, 11.0	10.9,11.3[c]	**H52**	dd	4.3,13.7	
H34'	ddd	5.9, 5.9, 11.0	4.7, 5.4[c]	**H52'**			
H35	m		5.4, 7.1, 10.9	**H53**			
H36	dd	1.4, 11.2	7.1, 8.0, 8.8	**H54**	dd	6.6,11.3	
H37			8.0[d]	**H54'**	dd	2.7,11.3	
H37'			8.8[d]				

[a] Experimental data recorded in $CDCl_3$ at 300 MHz. [b] Units in Hz.

[c] Assignment of stereochemistry by comparison to experimental $^3J_{HH}$ and NOESY data.

[d] X-ray crystal structure assignments of $^3J_{HH}$ to specific chemical shifts of methylene protons are interchangeable.

There was a major anomaly with the experimental H11-H12 coupling constant relative to the X-ray crystal structure coupling constant calculated from the dihedral angle using the Karplus equation in MacroModel. The "A series" halichondrins are characterised by a hydroxyl groups at C12 and C13. The X-ray crystal structure was therefore modified to a "B series" halichondrin *ie* norhalichondrin B which has hydrogens at C12 and C13, to gather the H11-H12, H12-H13' and coupling constants. The experimentally observed $^{3}J_{HH}$of 4.7 Hz for H11-H12 compared well to the value of 4.5 Hz quoted by Uemura *et al* in CD_3OD.[18] However, the coupling constant of 7.0 Hz calculated from the dihedral angle in the modified X-ray crystal structure suggested several possibilities.

There could be a weakness in the model used to calculate the coupling constant in this situation, or the presence of unaccounted for coupling mechanisms. There is a lack of data in the 5.5-7.0 Hz range[34] which may lead to incorrect data extrapolations for this region. Another problem with the Karplus model is the absence of norbornene type structures and derivatives from the data set;[34] the C8-C14 tricyclo system could perhaps be loosely considered such a derivative.

Bonds which are in close proximity to the coupled nuclei, as in the cage structure of C8-C14 may provide important, alternative coupling mechanisms for the transmission of the coupling.[35] This may result in a reduced value for the observed H11-H12 coupling constant relative to the Karplus derived value which does not take this into account.

Another possible explanation for this anomaly could be that the geometry of the C1-C14 subunit observed in the X-ray crystal structure, and in particular the conformation around the constrained tricyclo ring system, may be different due to the presence of the hydroxyl groups at position C12 and C13. A conformational

search of the C2-C15 subunit was undertaken on the B series halichondrin to assess whether this would alter the conformational distribution and therefore the observed coupling constant for the H11-H12 protons. This modelling is described in Section 2.3.2.

The X-ray crystal structure coupling constant data from the norhalichondrin A crystal could only be compared for the C1-C44 region as the structure of halichondrin B differs beyond C44. The C44-C54 subunit was therefore conformationally searched in MacroModel to gain some insight into possible solution conformations of this area in the molecule. This work also enabled Boltzmann-weighted vicinal coupling constants to be extracted for the H45-H54 subunit conformers. These were then compared to the experimental vicinal coupling constants in this region. These modelling investigations are also described in Section 2.3.2.

Some methylene protons were assigned a relative stereochemistry by comparing experimental coupling constants to the X-ray crystal structure derived values and interpreting relevant NOESY observations. In some cases this allowed an evaluation of the predominant conformation of specific rings in the molecule. These methylene protons are depicted in **Figure 2.3.3** as protons in bold type and are denoted with a 'c' in **Tables 2.3.2** and **2.3.3**. For example, the "I" ring of halichondrin B was determined as being in a boat conformation from the H34/H34' coupling constants and NOESY data. The H34 and H34' protons were assigned a relative stereochemistry based on the experimental vicinal coupling constants to H33 and H35. There was a NOESY correlation observed between H32 and H36. This implied a *cis*, diaxial relationship for these two protons. The "I" ring could either be in a chair or in a boat (or twist- boat) conformation. A chair conformation would imply relatively small vicinal coupling constants for H33-H34, H33-H34', H35-H34

and H35-H34' as the dihedral angles for all four pairs would be ± *ca* 60°. However, a true boat conformation would result in one large coupling constant (dihedral angle of *ca* 180°), and one smaller coupling constant (dihedral angle *ca* 50-60°) for the *cis* proton. The vicinal coupling constants actually observed between H34 and H33, and H34 and H35 were 11.0 Hz for both couplings. The vicinal couplings between H34' and H33, and H34' and H35 were both observed at 5.9 Hz. These observations best describe a true boat conformation for the "I" ring. The H34' proton must therefore have been *cis* with respect to H33 and H35 with two small coupling constants to H33 and H35. The large coupling constants observed to H33 and H35 from H34 implied an axial position and therefore the opposite relative stereochemistry to H34'. In the X-ray crystal structure of the norhalichondrin A derivative the "I" ring is in a true boat conformation, and the coupling constants for H34 and H34' were close to those observed experimentally (see **Table 2.3.3**).

The "L" ring of halichondrin B was determined as being in a chair conformation. It was assumed that the methyl group CH_3-42 was in an equatorial position. A boat conformation would result in a small dihedral angle (*ca* 0°) between H40 and H41 giving rise to a large coupling constant. The fact that the observed coupling constant was 2.2 Hz implied a chair conformation for the "L" ring. The H43 and H43' coupling constants to the axial H42 proton would give rise to one small coupling constant to the *cis* equatorial proton and one large coupling constant to the *trans*, axial proton. Experimentally, the large coupling constant was observed between H43' and H42 ($^3J_{HH}$ 13.0 Hz) and the small coupling constant between H43 and H42 ($^3J_{HH}$ 4.3 Hz). The H43 proton was therefore assigned as *cis* with respect to H42, and H43' was assigned as the axial proton. The X-ray crystal structure of the "L" ring was also in a chair conformation and the coupling constants for H41 to H40 and H43 and H43' compared well (refer **Table 2.3.3**) with the experimental results.

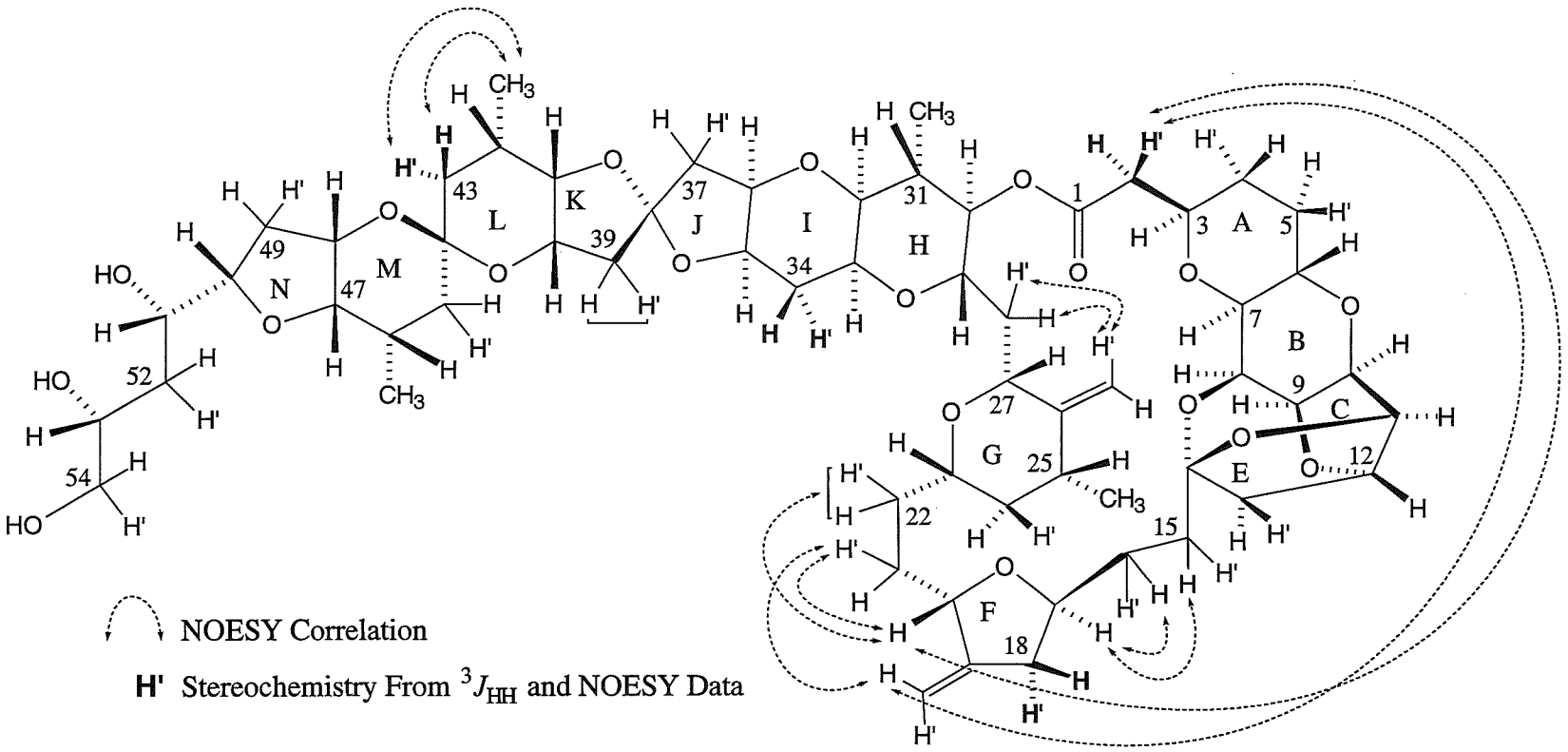

Figure 2.3.3 Halichondrin B- Relative Stereochemistry Assignments

The H18 and H18' protons were assigned a relative stereochemistry based on similar coupling constant arguments.

Assignment of the relative stereochemistry of the H2 and H2' protons was a little more ambiguous and this assignment remains tentative. The NOESY spectrum of halichondrin B showed correlations from H2' to H20 and H2' to CH=19. The H2' proton had a vicinal coupling constant of 8.4 Hz to H3. This implied that the dihedral angle between H2' and H3 was either around 0° or 180°. From the NOESY spectrum we knew that H2' pointed inwards towards H20 and was therefore *ca* 180° (*ie anti*) with respect to H3. The vicinal coupling constant for the H2 proton to H3 was observed at 3.3 Hz. This meant that the H2 dihedral angle was either +90° (clockwise rotation) or -90° (anti-clockwise rotation) relative to H3. There was not sufficient experimental data to conclude which orientation the H2 and therefore the H2' protons had. However, by examining the X-ray crystal structure conformation the proton that was within NOE interaction distance to H20 and CH=19 was *anti* with respect to H3, as predicted, so this was assigned as the H2' proton. The other proton on C2 had a dihedral angle of -90° to H3 and was 4.7 Å from H20 and 3.7 Å from CH=19. This proton was therefore assigned as H2. The X-ray crystal structure coupling constants for H2' and H2 compared relatively well to the experimental values (refer **Table 2.3.2**).

Overall, the average solution conformation of the C1-C44 portion of halichondrin B (**1.2.1**) in $CDCl_3$ appeared to be remarkably consistent with that of the X-ray crystal structure of the norhalichondrin A derivative, both in terms of the overall folding conformation of the molecule and also in terms of the conformation of the individual A to L rings.

2.3.2 Computer Modelling of Halichondrin B

The computer modelling described in this thesis involved using the program MacroModel V4.0 with the associated auxiliary computational chemistry program BatchMin. BatchMin carries out all of the energetic tasks associated with a conformational search and structure minimisations while MacroModel can be used to monitor the progress and results of BatchMin tasks so that numerical and structural information can be viewed and analysed. BatchMin jobs can be initiated independently of MacroModel by submitting jobs as command files (a "COM" file) in non-interactive batch mode. This significantly speeds up the processing time.

The molecular mechanics force field that was used in MacroModel/BatchMin for carrying out energy calculations from a specific molecular geometry was the MM2* force field.[36,37] This force field was tested on each structure submitted for energy calculations to ensure there were no low quality parameters present which would produce unreliable results.

The NMR experiments for the spectroscopic studies of the halichondrins were carried out in chloroform. The solvent medium can play an important role in determining the conformations and relative energies for a particular structure. Therefore all energetic tasks were carried out using the implicit solvent model "GB/SA" with chloroform parameters.[38] The implicit model treats the solvent as a continuum with the loss of specific solvent-solute interactions that are part of an explicit solvent model.

Conformational searching was carried out using the Monte Carlo method in MacroModel/BatchMin.[39,40] This method modifies an input structure by randomly

changing specified torsion angles. Torsional angles to be varied must be specified along with ring closure atoms if a ring is present. This allows the ring to be broken, the torsional angles to be varied, and the ring to be reformed at the specified ring closure atoms. The stereochemistry at chiral centres must also be specified to avoid inversion of stereochemistry during conformational searches.

The Monte Carlo searches performed were "usage-directed" structure selections. This means that the least used structures were used as starting geometries for Monte Carlo steps. This ensured that conformational space was efficiently searched.

Energy minimisations were carried out using the PR (Polak-Ribiere) conjugate gradient (PRCG) minimisation algorithm.[41] This enables a rapid convergence to a low energy gradient and is the best general minimisation method.[42] For Monte Carlo searches, energy minimisations are carried out for every Monte Carlo step.

2.3.2.1 The C2-C15 Subunit

A conformational search was carried out on the C2-C15 fragment of the "B" halichondrin series. Initially, the C2-C15 subunit was excised from the X-ray crystal structure and modified to give a CH_3 group at C3 and C14. This structure was then used as one starting conformation for a Monte Carlo conformational search in MacroModel. Two other searches were initiated from slightly different starting geometries.

The resulting output was identical for all three searches and resulted in only two unique, minimised conformations. The global minimum was lower in energy by 30.4 kJ/mol relative to the other conformer. This meant that for a Boltzmann-weighted distribution at 23°C there would be greater than 99.99% of the structures in

the lower energy conformation at any one time. Therefore the "average" solution geometry would essentially be represented by the lower energy conformation only. The two conformers are displayed in **Figure 2.3.4** along with their MM2* energies. The lower energy conformer (CONFORMER ONE, MM2* Energy -195.6 kJ/mol) has the A and B rings in the more stable chair/chair conformation. The higher energy conformer exists in a chair (B ring)/twist-boat (A ring) conformation.

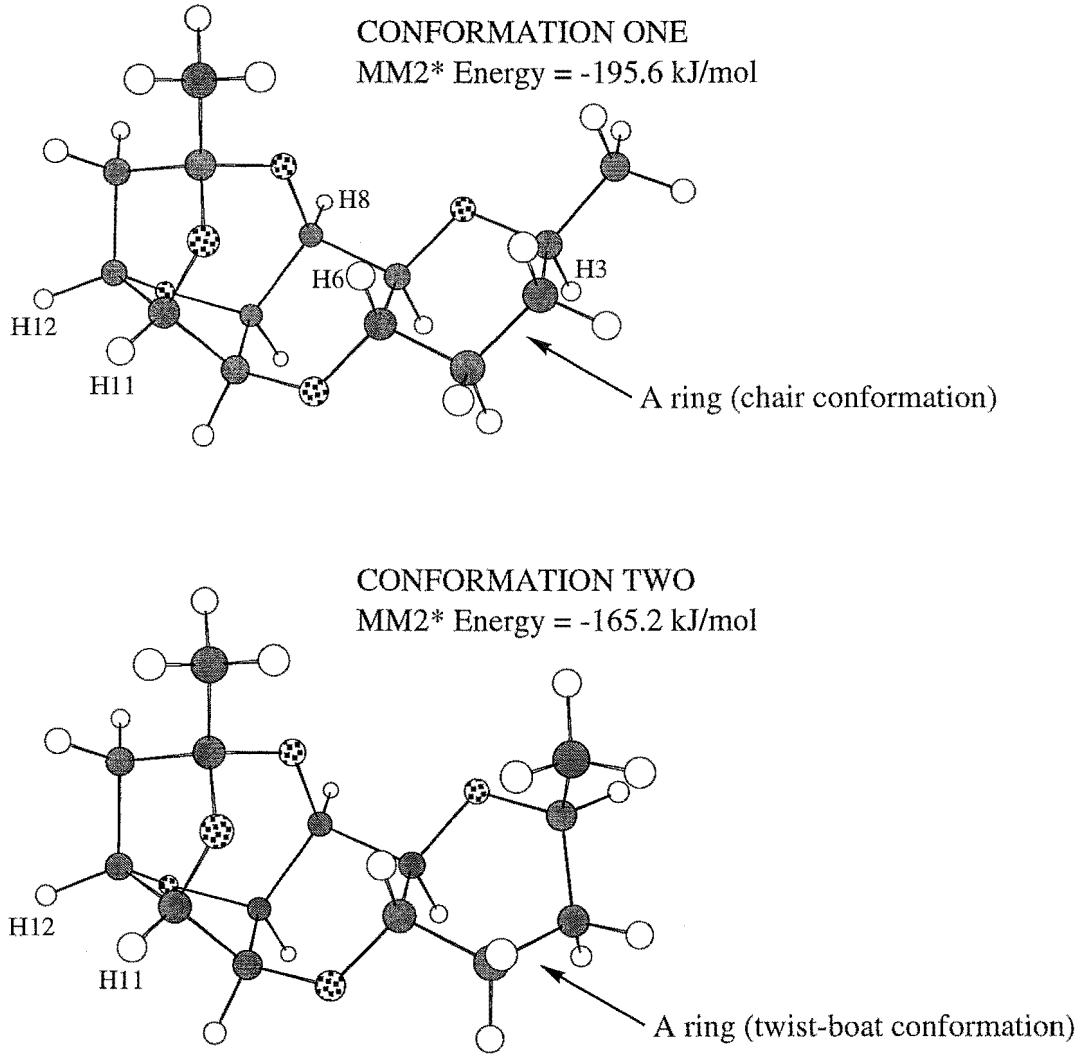

Figure 2.3.4 C2-C15 Conformational Search Output

Vicinal coupling constants were collected in MacroModel for the lower energy conformer. These values are given in **Table 2.3.4** relative to the X-ray crystal structure coupling constants and the experimental data for the H6-H13 protons.

Table 2.3.4 Modelling-Derived Coupling Constants for H6-H13

Coupled protons	CONFORMER ONE $^3J_{HH}$ (Hz)	X-ray $^3J_{HH}$ (Hz)	Experimental $^3J_{HH}$ (Hz)
H6-H7	9.3	9.2	9.5
H7-H8	2.5	3.4	2.1
H8-H9	3.3	4.2	4.1
H9-H10	6.0	5.8	6.6
H10-H11	4.6	4.6	4.7
H11-H12	6.4	7.0	4.7
H12-H13	5.5	5.9	4.7
H12-H13'	1.2	1.3	

From **Table 2.3.4**, it can be seen that the computer modelling-derived vicinal coupling constants of the C6-C13 area correlated well with the experimental results, except for H11-H12 which had a coupling constant of 6.4 Hz relative to the experimental value of 4.7 Hz. There were only relatively minor changes in terms of dihedral angles and therefore conformation from the X-ray crystal structure conformation to CONFORMER ONE. It is interesting to note that the adjacent H10-H11 and H12-H13 coupling constants compared well between CONFORMER ONE and the experimentally observed coupling constants. This suggested that the dihedral angles for H10-H11 and H12-H13 were similar between CONFORMER ONE and the experimental solution conformation. By implication, the H11-H12 dihedral angles were also similar between CONFORMER ONE and the solution conformation. This indicated that there was a problem with the Karplus derivation

of coupling constants from dihedral angles for this type of system rather than any significant conformational difference between the X-ray crystal structure and the experimental solution conformation. Possible problems with the Karplus model were highlighted in Section 2.3.1.2.

2.3.2.2 The C44-C54 Subunit- The Terminal Moiety

The Monte Carlo method of conformational searching is able to find all populated minima for up to 10-12 rotatable torsional angles.[37] It was decided to divide the C44-C54 subunit into two searches to reduce the number of rotatable torsional angles and thus increase the efficiency of the search. For this reason, only the M and N rings of halichondrin B were conformationally searched using MacroModel before the C51-C54 "tail" portion was added. A further conformational search on the lowest energy conformer(s) for the C44-C54 subunit was then undertaken.

The M ring and N rings of halichondrin B were generated in the computer program Chem3D Plus, with the M ring in a chair conformation, and a primary hydroxyl group at C51 and a methyl and a hydroxyl group on C44. This structure was searched with four different starting geometries. The same set of low energy conformers was produced in each search (**Figure 2.3.5**). A Boltzmann-weighted distribution was calculated at 23°C for the conformers produced. The lowest energy conformer (CONFORMATION ONE) and the next lowest conformer (CONFORMATION TWO) totalled 97.2% of the populated conformations. A closer examination of these two conformers indicated that the only difference between them was the orientation of the C51 hydroxyl group. The conformation of the M and N rings were the only concern at this stage as the tail portion was to be added for the next conformational search.

The C52-C54 "tail" was added to both conformers and they were both used as starting points for a Monte Carlo conformational search of the C51-C54 region.

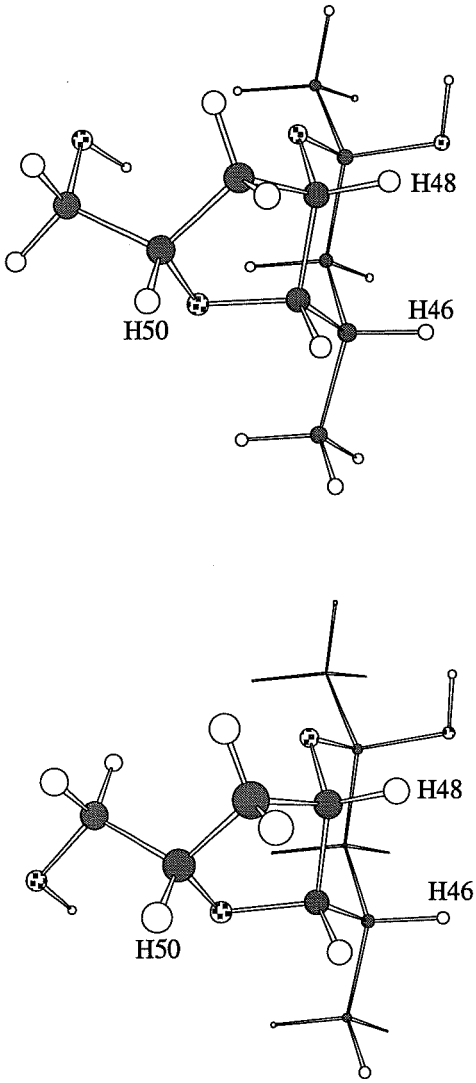

Figure 2.3.5 Conformational Search Output C44-C51

Five searches were initiated from different starting orientations of the C51-C54 tail for the C44-C54 subunit. The global minimum and low energy conformers were identical for all searches. Each conformer was tested to ensure that it was in fact a true minima using a BatchMin minima test command on each conformer in the output structure file generated from the conformational search. The Boltzmann-

weighted distribution of the each conformer was calculated at 23°C; there were six conformers contributing greater then 5% to this distribution. These conformations contributed to *ca* 94% of the total population of conformers and they are depicted in **Figure 2.3.6** with their MM2* energies and Boltzmann-weighted populations.

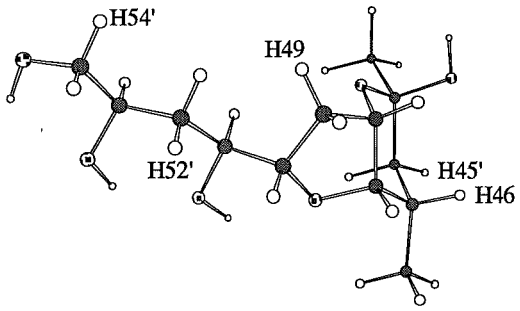

CONFORMATION ONE (29.7%)
MM2* Energy = -173.0 kJ/mol

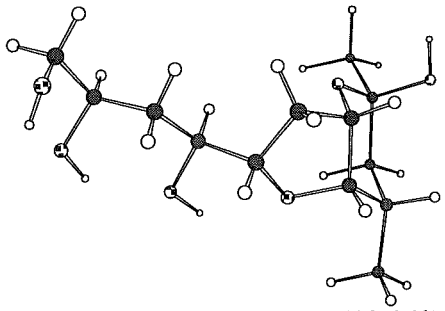

CONFORMATION TWO (19.2%)
MM2* Energy = -171.9 kJ/mol

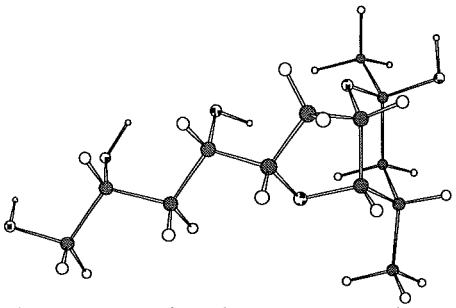

CONFORMATION THREE (18.9%)
MM2* Energy = -171.8 kJ/mol

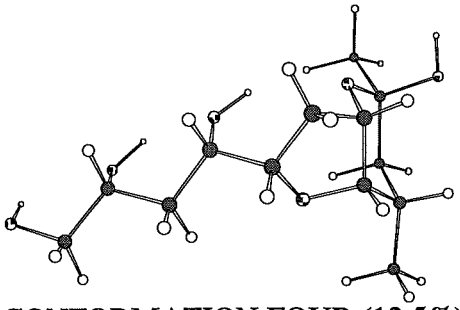

CONFORMATION FOUR (12.5%)
MM2* Energy = -170.8 kJ/mol

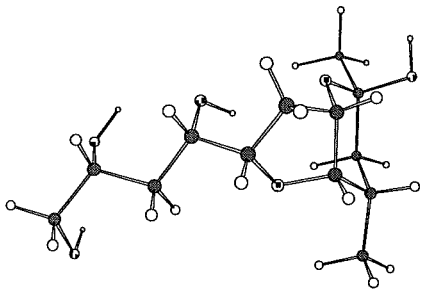

CONFORMATION FIVE (8.5%)
MM2* Energy = -169.8 kJ/mol

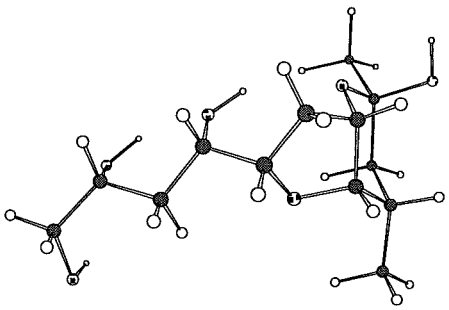

CONFORMATION SIX (5.7%)
MM2* Energy = -168.9 kJ/mol

Figure 2.3.6 Conformational Search Output C43-C54

Coupling constants were collected from MacroModel for each conformer for each dihedral angle (H-C-C-H). A Boltzmann-weighted coupling constant was calculated over all conformers for each dihedral angle. These results are given in **Table 2.3.5**. Also included in **Table 2.3.5** are the range of coupling constants generated from the conformational search for each dihedral angle.

Table 2.3.5 Modelling-Derived Coupling Constants for H45-H54

Coupled protons	Boltzmann -weighted $^3J_{HH}$ (Hz)	Experimental $^3J_{HH}$ (Hz)	Range of $^3J_{HH}$ from modelling
H45-H46	12.2	12.5	12.2-12.2
H45'-H46	3.9	3.7	3.8-4.0
H46-H47	2.3	3.0	2.2-2.3
H47-H48	1.9	2.5	1.9-2.0
H48-H49	1.3		1.2-1.4
H48-H49'	5.8		5.4-6.2
H49-H50	9.6	9.5	9.5-9.6
H49'-H50	4.2	4.8	3.7-4.9
H50-H51	4.7	5.4	0.3-9.6
H51-H52	2.3	4.3	1.0-9.1
H51-H52'	11.2	9.3	1.3-11.3
H52-H53	1.1		1.0-10.5
H52'-H53	10.6	10.5	1.1-11.7
H53-H54	7.0	6.6	0.5-10.7
H53-H54'	3.3	2.7	2.0-4.4

Further to the coupling constant data collected from the ^{1}H NMR spectrum, and 1D and 2D-TOCSY experiments, additional coupling constant data were collected from the active couplings in the phase sensitive COSY experiment. "Active" couplings in a COSY correlation arise due to a direct coupling between the protons giving rise to the cross-correlation and can be identified as those where the phase of the peak in the correlation changes phase.[43] These data are displayed in **Table 2.3.5** for comparison with the modelling results.

There were a large range of modelling-derived coupling constants for each specified dihedral angle between the different conformers in the H51-H54 region. For example, the H50-H51 coupling constant has a range from 0.3 Hz to 9.3 Hz for the first fifteen low energy conformers. Given this, the Boltzmann-weighted coupling constant of 4.7 Hz compared well with the experimentally observed value of 5.4 Hz. Generally, there was a good correlation between the modelling derived coupling constants and the experimental values.

However, it is important to note that the MM2* energies calculated represent enthalpies at 0°K, so it was important to calculate the effect of entropy on the overall distribution of conformers. It is possible that "more ordered" conformations with low enthalpies relative to the global minimum may have a higher Gibb's Free Energy and therefore a decreased relative importance. For example, the relative populations can change in a system with a high degree of intra-molecular hydrogen bonding (such as in the solvent chloroform) which would have an associated entropic cost.[44]

The conformations stored from the C44-C54 conformational search were used as the input file in a BatchMin command file to calculate the entropies from a rigid rotor, harmonic oscillator analysis (the "RRHO" command). The entropy values at 296°K

that were produced for each conformer were used as a correction to the enthalpy values from the conformational search. The relative order of the conformational search output conformers with a greater than 5% Boltzmann weighted population did not change. There were only minor changes in the relative populations of these conformations.

2.4 NMR Spectroscopic Assignment of Homohalichondrin B

The complete assignment of the ^{1}H and ^{13}C NMR spectra of homohalichondrin B (**1.2.3**) has been achieved. This enabled the characterisation of homohalichondrin B derivatives to be made in terms of differences relative to the homohalichondrin B NMR spectra. Hirata and Uemura[18] have previously assigned the ^{1}H NMR spectrum homohalichondrin B in CD_3OD but their assignments were incomplete and there were no ^{13}C NMR data given.

The 300 MHz ^{1}H NMR spectrum of homohalichondrin B (**Figure 2.4.1**) in $CDCl_3$/ 0.1% pyridine-d_5 showed some key differences to the halichondrin B ^{1}H NMR spectrum (**Figure 2.2.1**). The most obvious difference was seen in the H47 proton signal which appeared as an isolated narrow doublet at δ_H 3.06 ppm in the ^{1}H NMR spectrum of homohalichondrin B but was obscured in the halichondrin B spectrum at δ_H 3.61 ppm. Other apparent differences in the ^{1}H NMR spectrum of homohalichondrin B were a clearly visible doublet signal at δ_H 3.69 ppm (H55/H55') and a change in the relative position of the four methyl doublet resonances relative to halichondrin B.

A range of 1D and 2D NMR experiments were run on 9.1 mg of homohalichondrin B (**1.2.3**) in $CDCl_3$/0.1% pyridine-d_5 and all protons (non-exchangeable) and carbons were assigned. The 75 MHz ^{13}C NMR spectrum of homohalichondrin B is displayed in **Figure 2.4.2**.

The important HMQC and HMBC correlations in the NMR spectroscopic assignment of homohalichondrin B are depicted in **Figure 2.4.3** and the 2D-TOCSY

(100 ms mixing time), Phase Sensitive COSY (PS COSY) and NOESY correlations are displayed in **Figure 2.4.4**. The ^{1}H NMR and ^{13}C NMR chemical shifts for homohalichondrin B are given in **Table 2.4.1** and **Table 2.4.2** respectively.

As expected, the ^{13}C and ^{1}H NMR chemical shifts for the C1-C43 subunit were very similar to those of halichondrin B (**1.2.1**). Hirata and Uemura[18] did not publish ^{13}C NMR data for homohalichondrin B so the literature reference data for comparison, which is displayed in **Table 2.4.2**, are for those of homohalichondrin A (essentially the C12 and C13 hydroxyl substituted homohalichondrin B).

The ^{13}C and ^{1}H NMR assignment for the C44-C55 subunit of homohalichondrin B is discussed in more detail.

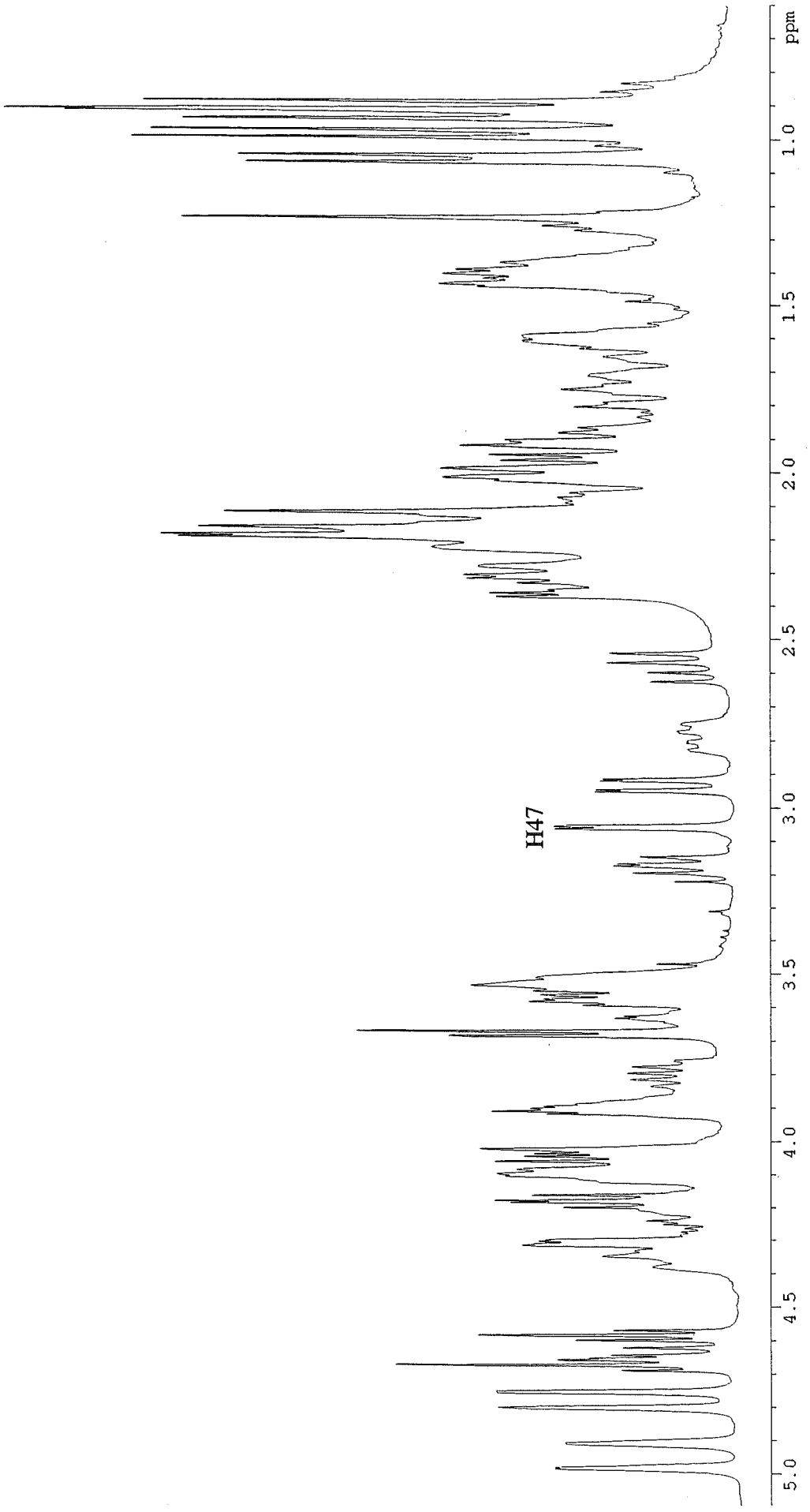

Figure 2.4.1 ^{1}H NMR Spectrum Homohalichondrin B

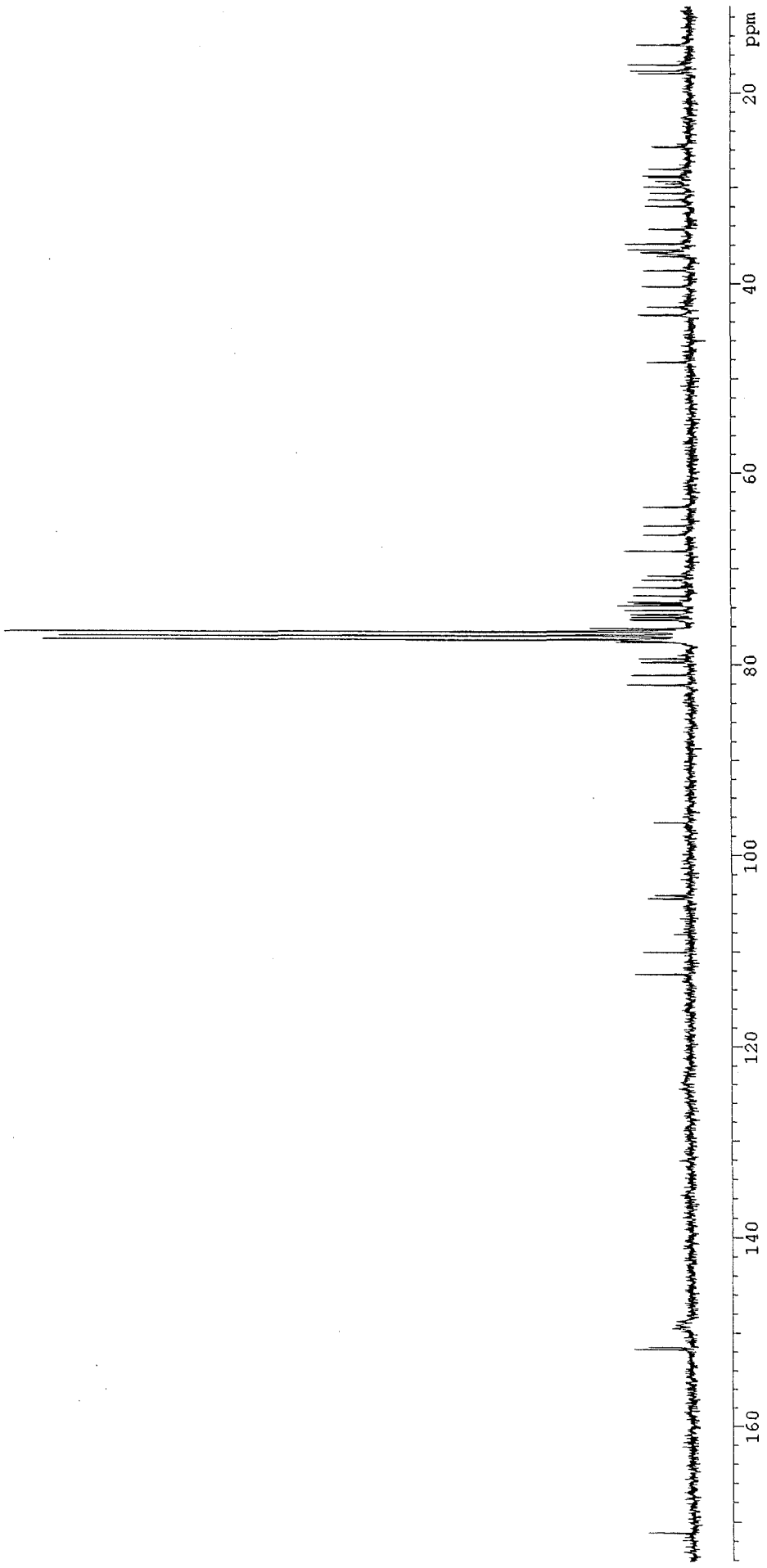

Figure 2.4.2 ^{13}C NMR Spectrum of Homohalichondrin B

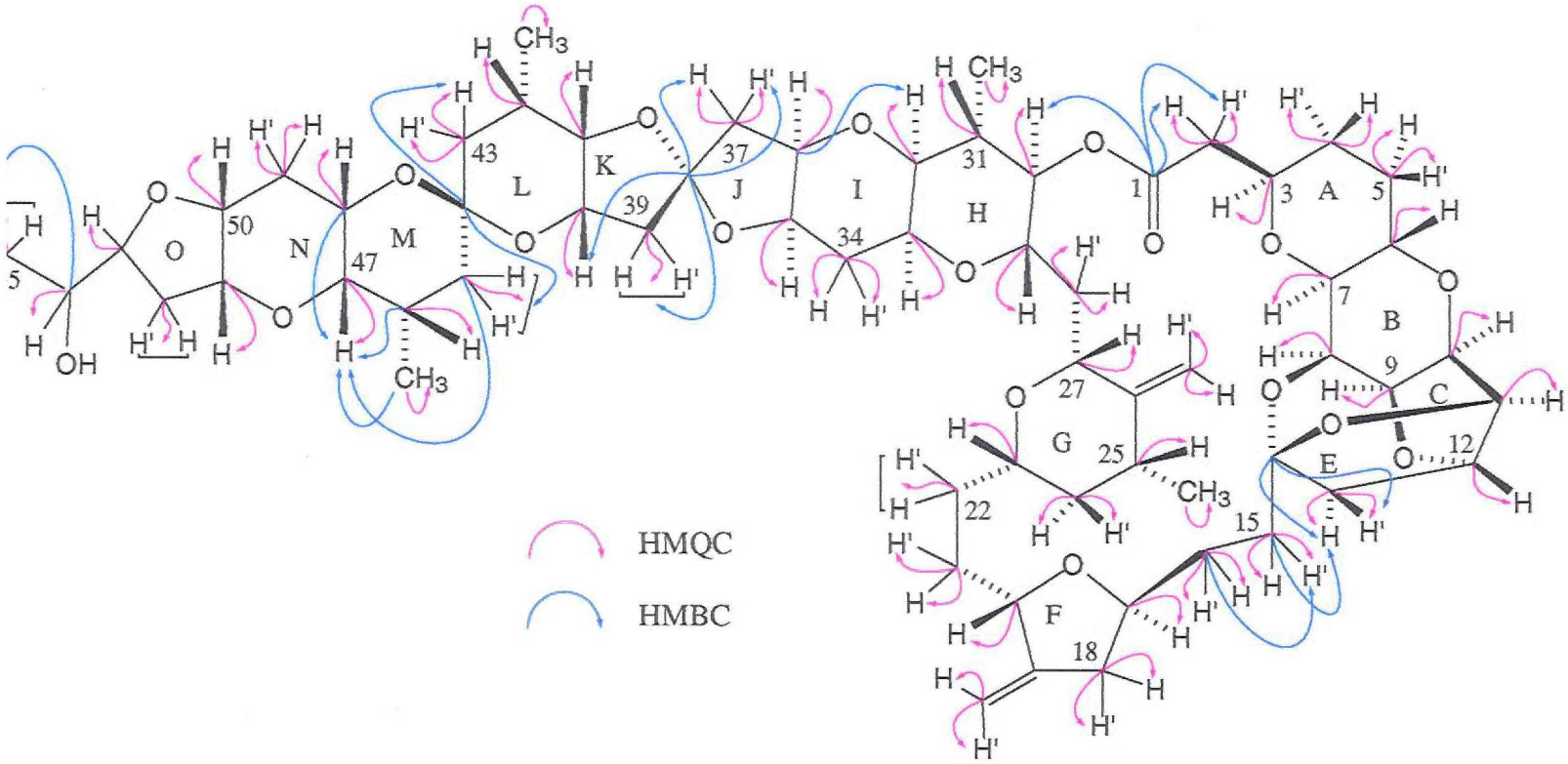

Figure 2.4.3 Homohalichondrin B- Important HMQC and HMBC Correlations

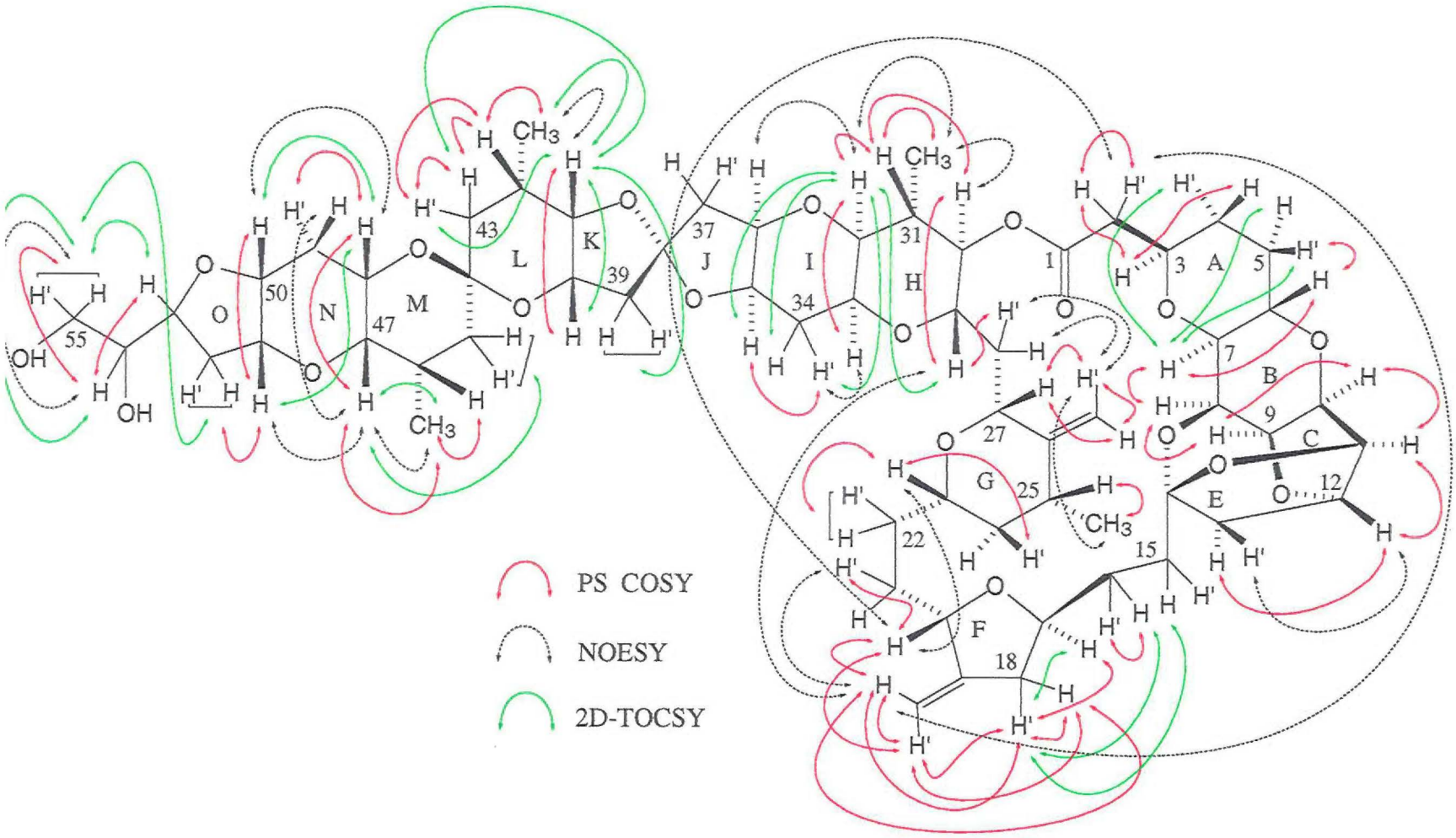

Figure 2.4.4 Homohalichondrin B- Important COSY, TOCSY and NOESY Correlations

Table 2.4.1 ^{1}H NMR Data for Homohalichondrin B (**1.2.3**)

Proton[a]	Literature δ ppm[18,b]	$CDCl_3$ δ ppm[c]	**Proton**[a]	Literature δ ppm[18,b]	$CDCl_3$ δ ppm[c]
H2	2.44	2.34	**H28**		1.94
H2'	2.56	2.58	**H28'**		2.02
H3	3.88	3.88	**H29**	4.25	4.20
H4		1.34	**H30**	4.63	4.65
H4'		1.72	**H31**		2.04
H5		1.38	**CH_3-31**	1.05	0.99
H5'		2.08	**H32**	3.22	3.17
H6	4.33	4.34	**H33**	3.87	3.78
H7	2.98	2.94	**H34**		1.80
H8	4.30	4.32	**H34'**		2.14
H9	4.10	4.04	**H35**	4.10	4.10
H10	4.18	4.20	**H36**	4.10	4.10
H11	4.60	4.58	**H37**		1.90
H12	4.70	4.68	**H37'**		2.35
H13	2.00	1.94	**H39**		2.21
H13'	2.08	2.16	**H39'**		2.21
H15		1.60	**H40**	3.95	3.92
H15'		2.16	**H41**	3.66	3.60
H16		1.40	**H42**		2.32
H16'		2.16	**CH_3-42**	0.94	0.93
H17	4.10	4.10	**H43**		1.29
H18	2.32	2.26	**H43'**		1.45
H18'	2.80	2.79	**H45**		1.42
19 =CH	5.02	4.91	**H45'**		1.42
19' =CH	5.06	4.98	**H46**		2.18
H20	4.45	4.38	**CH_3-46**	0.93	0.90
H21		1.44	**H47**	3.12	3.06
H21'		1.88	**H48**	3.58	3.53
H22		1.60	**H49**	1.90	1.79
H22'		1.60	**H49'**	2.16	2.15
H23	3.70	3.52	**H50**	3.90	3.90
H24		1.05	**H51**	4.02	4.04
H24'		1.70	**H52**	2.00	2.02
H25		2.20	**H52'**	2.00	2.02
CH_3-25	1.08	1.06	**H53**	4.23	4.25
26=CH	4.82	4.75	**H54**	3.50	3.57
26'=CH	4.87	4.80	**H55**	3.58	3.69
H27	3.61	3.54	**H55'**	3.59	3.69

[a] The symbol ' represents the less shielded proton of a geminal pair.

[b] Literature data recorded in CD_3OD at 360 MHz.

[c] Data recorded at 23°C in $CDCl_3$ at 300 MHz with chemical shifts in ppm and referenced to $CHCl_3$, δ_H 7.25 ppm.

Table 2.4.2 ^{13}C NMR Data for Homohalichondrin B (**1.2.3**)

Carbon	Literature δ ppm[18,a]	$CDCl_3$ δ ppm[b]	**Carbon**	Literature δ ppm[18,a]	$CDCl_3$ δ ppm[b]
C1	171.8	171.2	**C29**	73.8	71.2
C2	41.1	40.4	**C30**	77.3	76.6
C3	75.1	73.6	**C-CH_3-31**	37.4	36.8
C4		30.7	**C-CH_3-31**	15.8	15.0
C5		30.0	**C32**	77.9	77.5
C6	69.6	68.2	**C33**	65.6	66.5
C7	79.0	77.7	**C34**		29.4
C8	75.9	74.3	**C35**	77.6	75.3
C9	73.8	73.8	**C36**	78.0	76.3
C10	85.5	76.5	**C37**	45.6	43.4
C11	75.5	82.1	**C38**	114.8	112.4
C12	113.3	81.1	**C39**	44.9	42.5
C13	82.3	48.3	**C40**	72.3	70.8
C14	111.3	110.1	**C41**	81.0	79.4
C15		34.4	**C-CH_3-42**	27.1	25.8
C16		28.1	**C-CH_3-42**	18.2	17.7
C17	76.3	75.4	**C43**		36.5
C18	39.8	38.7	**C44**	98.1	96.6
19C=CH_2	153.0	151.8	**C45**		36.8
19C=CH_2	105.8	104.5	**C-CH_3-46**	30.1	28.9
C20	75.9	75.0	**C-CH_3-46**	17.6	17.1
C21		29.0	**C47**	74.5	72.8
C22		32.0	**C48**	65.2	63.6
C23	75.2	74.8	**C49**		31.4
C24		43.4	**C50**	75.4	74.7
C-CH_3-25	37.2	35.9	**C51**	78.4	76.3
C-CH_3-25	18.4	18.0	**C52**		37.2
26C=CH_2	153.2	151.5	**C53**	79.8	79.8
26C=CH_2	104.8	104.2	**C54**	75.0	72.0
C27	75.0	73.5	**C55**	65.1	65.6
C28		36.9			

[a] Literature data for homohalichondrin A recorded in CD_3OD at 75.4 MHz.

[b] Data recorded at 23°C in $CDCl_3$ at 75 MHz with chemical shifts in ppm and referenced to $CDCl_3$, δ_C 77.0 ppm.

The remaining unassigned methyl doublet in the ^1H NMR spectrum after the assignment of the C1-C44 subunit was CH_3-46. The HMQC spectrum showed a correlation for this doublet at δ_H 0.90 ppm to a carbon at δ_C 17.1 ppm ($\underline{C}H_3$-46). The CH_3-46 protons showed a COSY correlation to a proton at δ_H 2.18 ppm (H46). The H46 proton gave an HMQC correlation to the $\underline{C}$-CH_3-46 carbon at δ_C 28.9 ppm. A 2D-TOCSY correlation from the CH_3-46 protons to δ_H 1.42 ppm and an HMBC correlation from the previously assigned C44 also to δ_H 1.42 ppm allowed the H45 and H45' protons to be assigned. The isolated doublet at δ_H 3.06 ppm in the ^1H NMR spectrum of homohalichondrin B gave a COSY correlation to the proton at δ_H 2.18 ppm (H46). This doublet resonance was attributed to the H47 proton. An HMQC correlation between the H47 proton and a carbon at δ_C 72.8 ppm assigned the directly attached carbon, C47. A COSY correlation was observed from the H47 resonance to another methine proton resonating at δ_H 3.53 ppm which was assigned as H48. An HMQC correlation from H48 to a directly attached carbon resonance at δ_C 63.6 ppm assigned C48. The C45 carbon was assigned from an HMBC correlation from H47 to a previously unidentified carbon at δ_C 36.8 ppm. A COSY correlation from H48 to a methylene proton at δ_H 2.15 ppm allowed H49' to be assigned. The geminal partner to H49' (*ie* H49) was able to be assigned from an HMQC correlation to the C49 carbon at δ_C 31.4 ppm and a NOESY correlation from H47.

A COSY correlation was observed between two methine protons at δ_H 3.90 ppm and δ_H 4.04 ppm. The proton at δ_H 4.04 ppm showed a COSY correlation to δ_H 2.02 ppm. H51 was therefore assigned a chemical shift of δ_H 4.04 ppm, H50 at δ_H 3.90 ppm. Carbon C50 was assigned a chemical shift of δ_C 74.7 ppm from the correlation to H50 in the HMQC spectrum, and C51 at δ_C 76.3 ppm from an HMQC correlation to H51.

Two COSY correlations were observed from a central proton at δ_H 3.57 ppm to δ_H 4.25 ppm and to one in the other direction at δ_H 3.69 ppm. The central proton was therefore assigned as H54. The intensity of the δ_H 3.69 ppm HMQC correlation to a carbon at δ_C 65.6 ppm suggested that there were two protons contributing to the signal, and the proton and carbon chemical shifts were consistent with those expected for a terminal methylene group such as H55/H55' and C55. The H53 proton was therefore assigned a chemical shift of δ_H 4.25 ppm and the C53 carbon a chemical shift of δ_C 79.8 ppm from an observed HMQC correlation. Finally, the C52 carbon was assigned a chemical shift from the observance of HMQC correlations to H52 and H52'.

The relative stereochemistry at C50, C51, C53 and C54 in homohalichondrin B (**1.2.3**) was not settled by Hirata and Uemura.[18] From the NOESY spectrum of homohalichondrin B it was possible to assign a relative stereochemistry to the C51 centre and the relative orientation of the C49 methylene protons and also a likely solution conformation for the terminal M and N rings. NOESY correlations were observed from H47 to H49, from H47 to H51 and from H48 to H50. Based on the relative stereochemistry at the C47 and C48 centres as determined by Hirata and Uemura, H50, H51 and H49 must be on the same face of the N ring as H47. For NOESY correlations to be observed from H47 to H49 and H51 implied a chair/ chair conformation for the M and N rings. However, nothing could be said about the relative stereochemistry at the C53, C54 or C55 centres.

The overall folding conformation of the lactone ring appeared to be the same as that of halichondrin B (described in Section 2.3.1), with NOESY correlations observed across the ring from H2' to H20, H2' to 19=CH, and also from 19=CH to H29.

2.5 Conformational and Stereochemical Studies on Isohomohalichondrin B

2.5.1 Introduction

Isohomohalichondrin B (**1.2.9**) was first isolated by Dr. Rob Lake and identified by Dr. Marc Litaudon in the Marine Chemistry Group from a *Lissodendoryx* sp. extraction.[14] The solution conformation(s) of the terminal M and N rings had not been fully investigated.

It is important to note that the norhalichondrin A structure has identical M and N pyranose rings to those of isohomohalichondrin B. The X-ray crystal structure conformation of the M and N rings of the *p*-bromophenacyl ester of norhalichondrin A obtained by Uemura *et al*[17] is a chair and a twist-boat ring system respectively. This is shown in **Figure 2.5.1** from Uemura *et al*[17] with the terminal *p*-bromophenacyl ester group removed for simplicity.

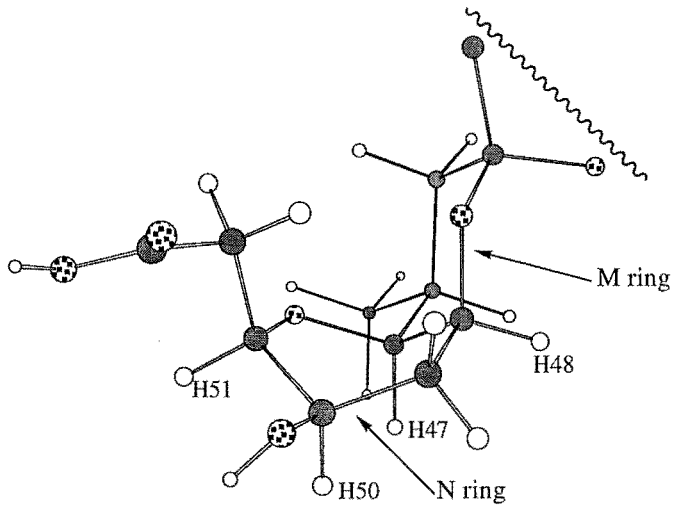

Figure 2.5.1 X-ray Crystal Structure Conformation of Norhalichondrin A

The average solution conformation of the terminal M and N rings of isohomohalichondrin B (**1.2.9**) was determined by selective NOE NMR experiments and vicinal coupling constants obtained from the ^{1}H NMR spectrum and a 2D-TOCSY experiment. The conformation suggested from these experiments was then modelled using the computer program MacroModel. The resulting vicinal coupling constants and interatomic distances between protons were compared to the experimentally obtained coupling constants and NOE observations respectively to look for possible anomalies.

The absolute stereochemistry of isohomohalichondrin B (**1.2.9**) was also assigned, based on the defined stereochemistry of the X-ray crystal structure of the norhalichondrin A derivative[17] and the measured optical rotation of isohomohalichondrin B relative to norhalichondrin A and the other known halichondrins.

2.5.2 Isohomohalichondrin B NMR Experiments

A 2D-TOCSY experiment (100 ms mixing time) and selected difference NOE experiments were recorded for *ca* 2.5 mg of pure isohomohalichondrin B (**1.2.9**). The coupling constants in the terminal region of isohomohalichondrin B were extracted from the isolated signals in the ^{1}H NMR spectrum (*viz* CH_3-46, H47, H48, H52', H52, H54/H54' and H55/H55') and from cross-sections through these protons in the 2D-TOCSY spectrum. The coupling constants (and multiplicity data) extracted are given in **Table 2.5.1.** The NOE irradiation of the CH_3-46, H48 and

H47 protons in separate experiments gave some crucial correlations. These correlations are also given in **Table 2.5.1**.

Strong H47 to H48 and H48 to H47 NOE correlations confirmed a *cis* fusion of the M and N rings as in all other halichondrins isolated to date. Key NOE enhancements from irradiation of H47 to H51 (1.4%) and to H49 (0.4%) also implied a *cis* relationship for these three protons. This implied an axial orientation for H47, H49 and H51 in the N ring and also assigned H49 as the axial proton and H49' as the equatorial proton, and therefore indicated a chair conformation existed for the N ring.

Table 2.5.1 ^{1}H NMR Data for Isohomohalichondrin B H45-H55

Proton	Multiplicity[a]	δ_H (ppm)[14]	J_{HH} (Hz)	NOE to (%)
H45		1.49		
H45'	dd	1.52	12.7, 12.7	
H46	m	2.18		
CH_3-46	d	0.90	6.9	H45/H45'(1.0%), H47(2.0%), H46(0.6%)
H47	d	3.23	2.3	CH_3-46(0.6%), H51(1.4%), H46(0.6%), H48(3.3%), H49(0.3%)
H48	br. s	3.75		H46(≈1.8%), H49'(≈1.8%), H49(0.4%), H47(3.3%)
H49	d	1.84	13.2	
H49'	d	2.13	13.2	
H50	s	3.52		
H51	dd	3.82	5.0, 8.0	
H52	dd	2.62	5.0, 15.7	
H52'	dd	2.93	8.0, 15.7	
H54/H54'	t	2.73	5.4, 5.4	
H55/H55'	t	3.86	5.4, 5.4	

[a] Abbreviations are as follows: dd = doublet of doublets, m = multiplet, d = doublet, br. = broad, s = singlet and t = triplet.

Another key point is that H50 appeared as a singlet resonance in the ^{1}H NMR spectrum of isohomohalichondrin B and H51 was coupled only into H52 and H52'. This implied that H50 and H51 were at a dihedral angle of around 90° and therefore that H50 was in an equatorial position. Similarly, as the H48 resonance was observed to be a broad singlet in the ^{1}H NMR spectrum of isohomohalichondrin B and H47 was a doublet with a small coupling constant, the dihedral angle between these two protons must be around 90°. These observations indicated an average chair conformation existed for the N ring as in a boat conformation these dihedral angles would be close to 0° and would therefore give rise to relatively large coupling constants for H47, H48 and H50, H51.

Dreiding models constructed of the chair/chair conformation fully supported the NMR observations discussed above.

2.5.3 Computer Modelling of Isohomohalichondrin B- M and N rings

Initially the chair/chair conformation of the M and N rings (the C44-C55 subunit) of isohomohalichondrin B was constructed using the CSC Chem3D Plus program. This structure was then minimised in MacroModel using a MM2* force field with PRCG as the conjugate gradient minimisation algorithm. Chloroform was selected as the solvent as this was the solvent used for the NMR experiments. The output structure generated was tested to ensure it was indeed a true minimum. This structure, having passed the minimum test, was then analysed to give vicinal coupling constants

($^3J_{HH}$) and interatomic distances between protons situated around the M and N rings (*ie* H45-H51).

Figure 2.5.2 depicts the minimised chair/chair conformation from the modelling output and gives the associated interatomic distances between protons with an experimentally observed NOE. Interatomic distances for NOE observations to and from CH_3-46 were not able to be calculated from the model because of the fixed orientation of the three equivalent CH_3-46 protons in the minimised conformation.

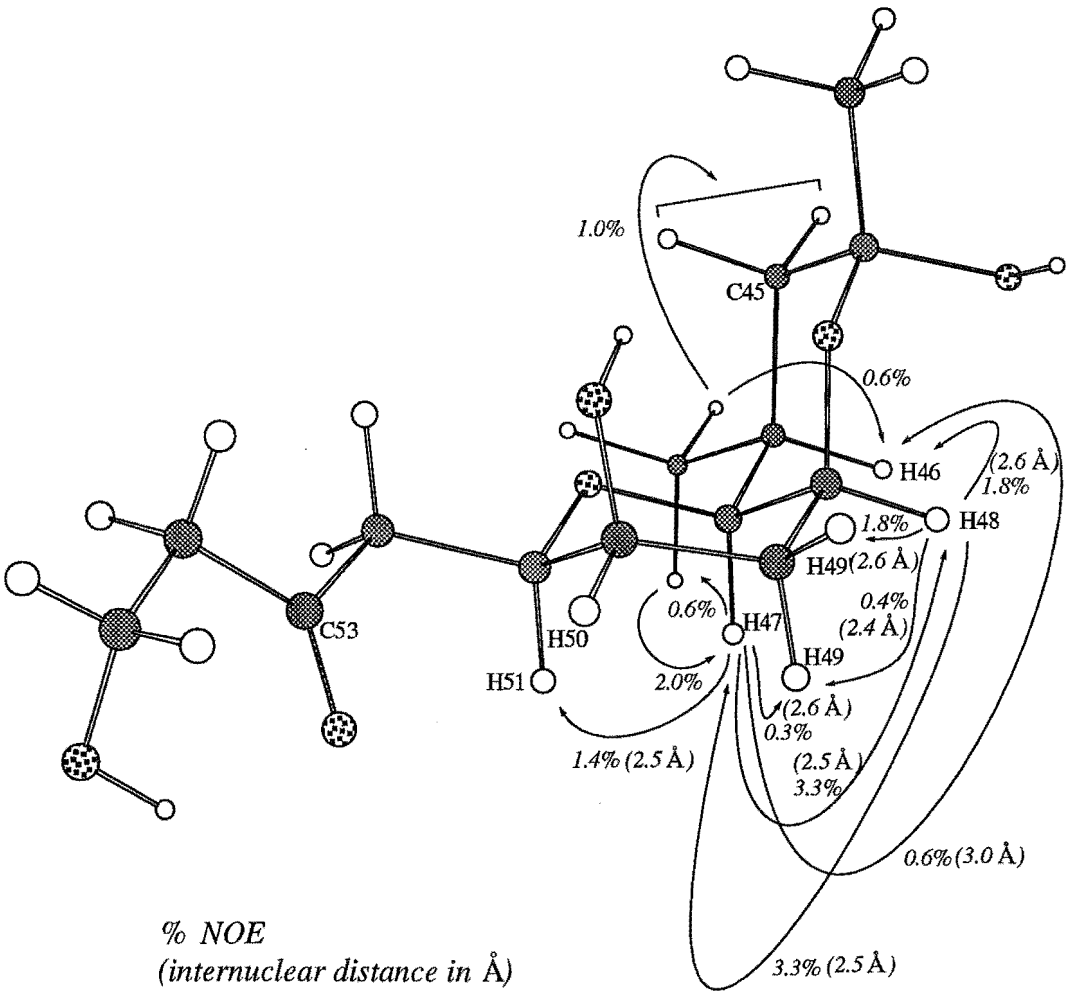

Figure 2.5.2 NOE Observations and Corresponding Modelling Distances

The interatomic distances between protons (taken from the minimised chair/chair model) which had an experimentally observed NOE, were within reason for a NOE observable distance. This therefore further supported the proposed chair/chair conformation of the terminal rings of isohomohalichondrin B.

The vicinal coupling constants collected from the minimised chair/chair conformation were compared to the experimentally obtained results and these data are given in **Table 2.5.2**.

Table 2.5.2 Comparison of Vicinal Coupling Constants- Experimental *vs* Modelling

Coupled protons	Experimental $^3J_{HH}$ (Hz)	Modelling $^3J_{HH}$ (Hz)
H46-H47	≤2.3	2.3
H47-H48	≤2.3	1.2
H48-H49	<5.8	3.0
H48-H49'	<5.8	3.0
H49-H50	<5.8	3.0
H49'-H50	<5.8	3.1
H50-H51	<2.9	1.0

The experimental coupling constants for H47-H46 and H47-H48 were assigned as being ≤2.3 Hz, as H47 appeared as a doublet in the ^{1}H NMR spectrum of isohomohalichondrin B, with a 2.3 Hz coupling to either H46 or H48. This meant that one proton had a coupling of 2.3 Hz and the other proton a coupling of less than

this, *ie* less than the linewidth of the peak which gave the appearance of no further splitting of the doublet. As the H49 and H49' resonances appeared to show no coupling apart from their geminal coupling, the vicinal coupling constant was given as the linewidth of these signals from a cross-section through H48 to give a F2 dimension trace from the 2D-TOCSY spectrum. F2 is the directly detected axis in a 2D NMR experiment and is therefore of higher resolution than F1, which is indirectly detected. Similarly, the H50-H51 coupling constant was approximated from the linewidth of H50 obtained from a cross-section through H48 in the F2 dimension of the 2D-TOCSY experiment. The experimental observation of small coupling constants for protons H47 to H51 appeared to justify the proposed chair/chair conformation of the terminal M and N rings of isohomohalichondrin B relative to the minimised model conformation of this region.

2.5.4 Optical Rotation of Isohomohalichondrin B

The absolute stereochemistry of isohomohalichondrin B (**1.2.9**) was initially based on the stereochemistry of the X-ray crystal structure of a norhalichondrin A derivative.[17] The ORD (Optical Rotatory Dispersion) spectrum of isohomohalichondrin B was recorded and the specific rotation ($[\alpha]_D$) calculated and compared to those of known halichondrins to give the assignment of the absolute stereochemistry further credibility. **Table 2.5.3** gives the specific rotations for isohomohalichondrin B and other known halichondrins. All specific rotations were measured in methanol.

The similarity of both the sign and the magnitude of the specific rotation for isohomohalichondrin B relative to the other halichondrins was indicative of the same absolute stereochemistry.

Table 2.5.3 Specific Rotation for Selected Halichondrins

Compound	$[\alpha]_D$ (°)	Concentration (mg/mL)
isohomohalichondrin B	-21.6	1.02
halichondrin B[18]	-58.9	0.94
norhalichondrin A[18]	-47.8	1.13
halichondrin C[18]	-41.6	0.49
homohalichondrin A[18]	-97.1	1.23
halistatin 1[19]	-58.4	0.57
halistatin 2[20]	-59.0	0.48

CHAPTER 3

Alterations to Terminal Groups of Halichondrins

3.1 Introduction

Initial investigations into the relationship between structure and the expression of biological activity in the halichondrin series were focused on manipulations of the oxidation level of functionalities at the terminal moiety region of selected halichondrins.

Acetylations of isohomohalichondrin B (**1.2.9**) and homohalichondrin B (**1.2.3**) were aimed at reducing the polarity of the terminal moiety. A monoacetylation of isohomohalichondrin B was undertaken to provide the C55 protected hydroxyl analogue to allow a selective oxidation of the C50 secondary alcohol to be attempted. It was anticipated that the C50 ketone derivative of isohomohalichondrin B would provide useful structure-activity information.

A reduction of the C53 ketone group in the "tail" of isohomohalichondrin B was undertaken with the objective of increasing the polarity in this region and, as such, to provide further biological activity data.

3.2 Acetylations

3.2.1 Acetylations of Isohomohalichondrin B

An acetylation was initially attempted on a small quantity of isohomohalichondrin B (**1.2.9**) prior to attempting the monoacetylation of the C55 primary hydroxyl group on larger scale.

Isohomohalichondrin B (**1.2.9**, 1.4 mg) was reacted overnight at room temperature with acetic anhydride dissolved in pyridine.[45] Silica TLC (*T*hin *L*ayer *C*hromatography) of the worked-up material indicated the presence of two spots of lower polarity relative to isohomohalichondrin B, the lower spot appearing as the major component.

A ^{1}H NMR spectrum acquired from the acetylation mixture, performed in $CDCl_3$/0.1% pyridine-d_5, indicated that the characteristic terminal H55/H55' triplet of isohomohalichondrin B at δ_H 3.86 ppm had moved by δ_H 0.46 ppm to a less shielded position at δ_H 4.32 ppm. Also apparent from the ^{1}H NMR spectrum of the acetylation mixture was the movement of the of the H54/H54' signal from δ_H 2.74 ppm in the ^{1}H NMR spectrum of isohomohalichondrin B to a less shielded position at δ_H 2.80 ppm. These chemical shifts described for the protons α (H55/H55') and β (H54/H54') to the C55 hydroxyl group were characteristic of an acetylation at the hydroxyl group.[46] The broad singlet resonance of the H50 proton was still visible at δ_H 3.52 ppm in the acetylation mixture, although it was likely that a less shielded H50 signal corresponding to diacetylation at both the H50 secondary hydroxyl and the C55 hydroxyl group was also present, but obscured by other resonances in the

spectrum. The acetate proton resonances were masked in the spectrum by a broad water peak at *ca* δ_H 2.00 ppm, so it was not possible to determine the relative amounts of monoacetylated and diacetylated isohomohalichondrin B present in the mixture. However, the relative intensity of the two silica TLC spots indicated that the major component was the more polar monoacetate derivative, with the diacetate present as a very minor component.

Low resolution FAB-MS (*F*ast *A*tom *B*ombardment *M*ass *S*pectrometry) performed on the product showed the presence of several parent ions corresponding to the monoacetate of isohomohalichondrin B (MH^+, MNa^+, MNa^+-AcO•) and one parent ion corresponding to the diacetate of isohomohalichondrin B (MH^+). The MS results therefore confirmed that the acetylation attempt had been successful with both the monoacetate (**3.2.1**) and the diacetate being formed in the reaction.

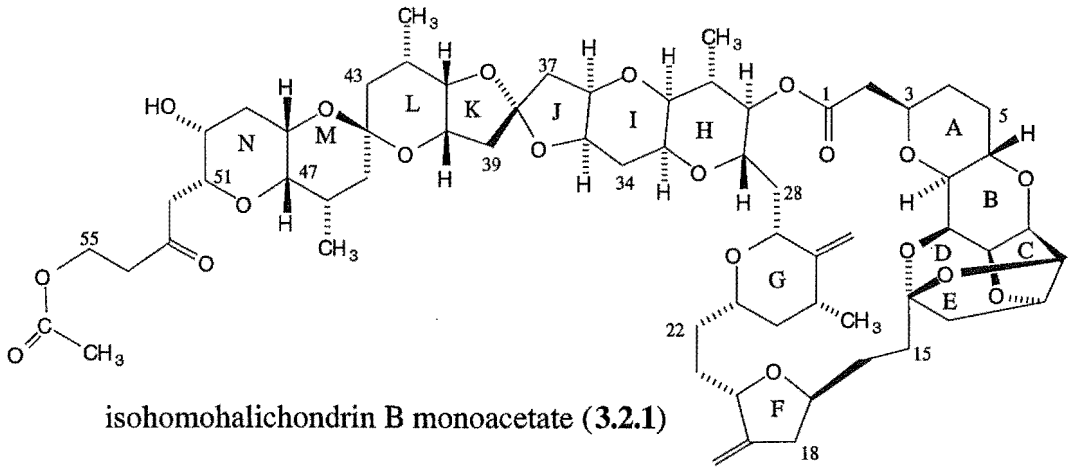

isohomohalichondrin B monoacetate (**3.2.1**)

A selective monoacetylation[47] of the C55 primary hydroxyl group was undertaken on a larger quantity (2.3 mg) of isohomohalichondrin B. Isohomohalichondrin B

(**1.2.9**) in pyridine was reacted with acetic anhydride at -5°C for three hours. Silica TLC of the product showed the appearance of a single spot at a higher R_f (*R*etention *f*actor) relative to that of isohomohalichondrin B. The R_f was identical with that of the monoacetate of the previously described acetylation. A ^1H NMR spectrum of the product (**Figure 3.2.1**), performed in $CDCl_3$/0.1% pyridine-d_5, was similar to that described previously. Now apparent in the spectrum was the distinctive CH_3 singlet proton resonance of the acetate protons at δ_H 2.02 ppm. A COSY experiment was also performed on this sample. An analysis of the COSY spectrum indicated that the chemical shifts around the A to M rings were identical with those of isohomohalichondrin B,[14] and that the changes were focused in the terminal region of the molecule. The COSY connectivities for the H45/H45' to H55/H55' region are depicted in **Figure 3.2.2**.

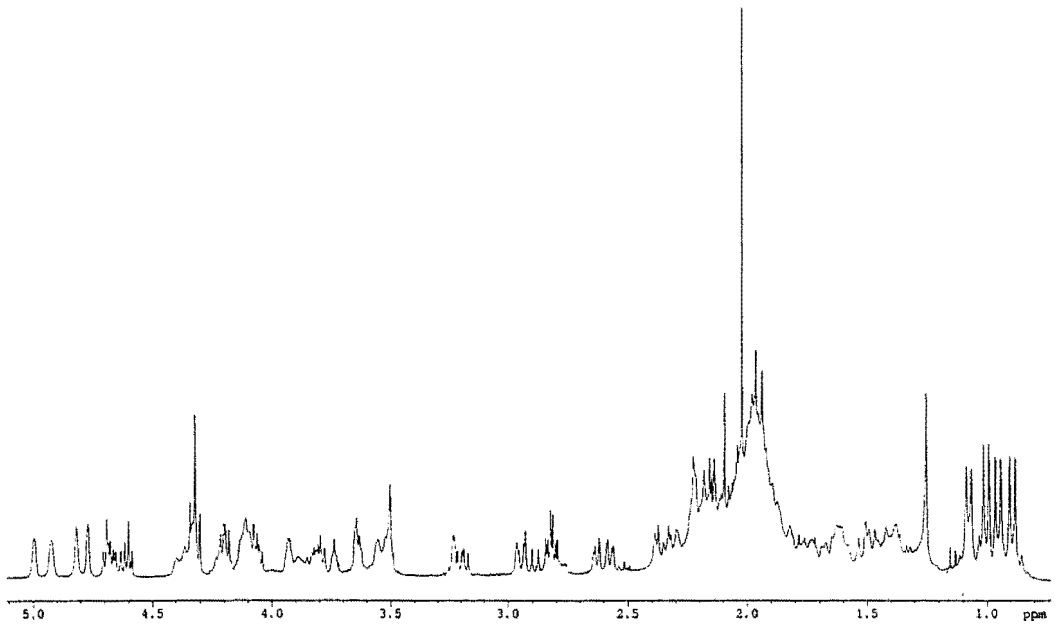

Figure 3.2.1 ^1H NMR Spectrum of Isohomohalichondrin B Monoacetylation Product

A strong COSY correlation was observed between two protons at δ_H 2.88 ppm and δ_H 2.80 ppm, which were assigned as corresponding to the H52' and H52 protons respectively. From these two protons, two correlations were observed into a methine proton at δ_H 3.81 ppm (H51). Two correlations from the relatively isolated H48 proton (at δ_H 3.74 ppm) to δ_H 1.82 ppm and δ_H 2.10 ppm assigned the chemical shifts of the H49 and H49' methylene protons respectively. A single correlation from H49 to a methine proton at δ_H 3.52 ppm located the H50 proton resonance. The chemical shift of the H50 proton was the same as that of isohomohalichondrin B, implying acetylation at this position had not occurred. The one COSY correlation remaining unassigned at δ_H 2.80 ppm/δ_H 4.32 ppm was assigned as corresponding to the H54/H54' and H55/H55' protons respectively. The ^{1}H NMR data for protons in the H45/H45' to H55/H55' region are cited in **Table 3.2.1** relative to the corresponding ^{1}H NMR chemical shifts of isohomohalichondrin B (**1.2.9**).[14] The observation of an unshifted H50 resonance and the α and β-shifts of the H55/H55' and H54/H54' methylene protons, relative to isohomohalichondrin B, implied that the C55 monoacetate of isohomohalichondrin B (**3.2.1**) had been formed, in support of the TLC evidence.

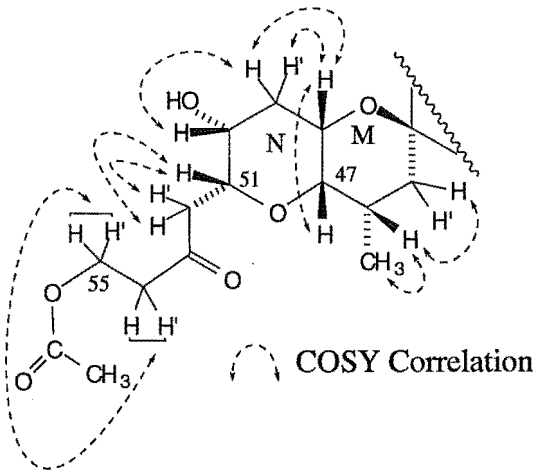

Figure 3.2.2 Isohomohalichondrin B Monoacetate- Terminal Region COSY Correlations

Table 3.2.1 ^{1}H NMR Data for Isohomohalichondrin B Monoacetate (**3.2.1**)- Terminal Region

Proton[a]	Isohomohalichondrin B[b] δ ppm[c]	Isohomohalichondrin B Monoacetate δ ppm[c]
H45	1.49	1.49
H45'	1.52	
H46	2.18	2.14
CH_3-46	0.90	0.89
H47	3.23	3.24
H48	3.75	3.74
H49	1.84	1.82
H49'	2.13	2.10
H50	3.52	3.52
H51	3.82	3.81
H52	2.62	2.62
H52'	2.93	2.88
H54	2.73	2.80
H54'	2.73	2.80
H55	3.86	4.32
H55'	3.86	4.32
C55-$OCOCH_3$		2.02

a The symbol ' represents the less shielded proton of a geminal pair.

b Appendix IV.

c Data recorded at 23 °C in $CDCl_3$ at 300 MHz with chemical shifts in ppm and referenced to $CHCl_3$, δ_H 7.25 ppm.

A small amount of isohomohalichondrin B monoacetate (**3.2.1**) was subsequently used as the starting material for an oxidation attempt of the C50 hydroxyl group; this reaction is described in Section 3.3.

3.2.1 Acetylation of Homohalichondrin B

There were two primary objectives in undertaking an acetylation of homohalichondrin B (**1.2.3**). The first objective was to protect the terminal C54, C55-diol group from periodate cleavage in the osmylation and periodate cleavage reactions of homohalichondrin B, which are described in detail in Chapter 4. The second objective was to generate additional biological activity data to further the understanding of structure-activity relationships.

The acetylation of homohalichondrin B (**1.2.3**) was initially attempted on a small scale, followed by a larger scale acetylation. The reaction of a small quantity of homohalichondrin B with acetic anhydride in pyridine was monitored by silica TLC at room temperature. After forty-five minutes reaction TLC indicated a small amount of homohalichondrin B, and two less polar spots indicating the formation of both the monoacetate and the diacetate product (**3.2.2**). After five hours reaction, TLC of the reaction mixture indicated the absence of starting material and the presence of only the least polar of the initially observed spots, indicating complete conversion of homohalichondrin B to the diacetate product. A ^{1}H NMR spectrum of the product, acquired in $CDCl_3$/0.1% pyridine-d_5, showed a new quintet at δ_H 5.13 ppm, and two acetate CH_3 singlet resonances at δ_H 2.04 ppm and δ_H 2.10 ppm, indicating formation of homohalichondrin B diacetate (**3.2.2**) was successful. The quintet at δ_H 5.13 ppm was assigned as the H54 methine resonance. Also apparent from the spectrum was the disappearance of the characteristic H55/H55' doublet at δ_H 3.69 ppm. An assignment of the ^{1}H and ^{13}C NMR resonances in the terminal region of the diacetate was achieved in the assignment of the homohalichondrin B diacetate diketone derivative (**4.3.3**); the NMR data and NMR correlations for **4.3.3** are given in **Tables 4.3.5** (^{1}H NMR data) and **4.3.6** (^{13}C NMR data) and in **Figure**

4.3.7 (NMR correlations). The ^1H NMR chemical shifts of **4.3.3** in the terminal region correlated well with the isolated signals of the terminal region in the ^1H NMR spectrum of **3.2.2**; namely H54, the two acetate CH_3 singlets and the methyl group CH_3-46.

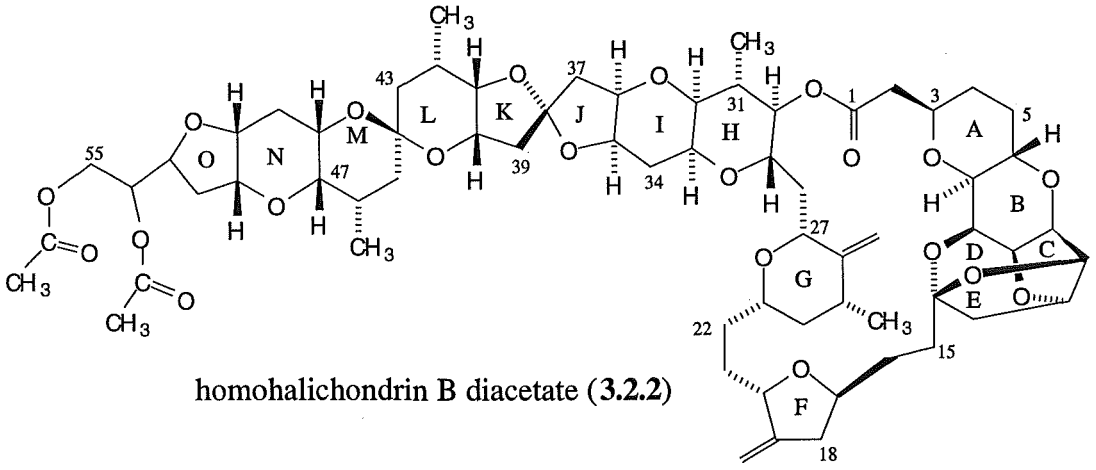

homohalichondrin B diacetate (**3.2.2**)

The diacetylation was repeated twice on a larger scale in overnight reactions, to provide sufficient material for the osmylation reactions described in Chapter 4, and for biological assay. Silica TLC and a ^1H NMR spectrum of each product (**Figure 3.2.3**), performed in $CDCl_3$/0.1% pyridine-d_5, were identical with that from the small scale reaction.

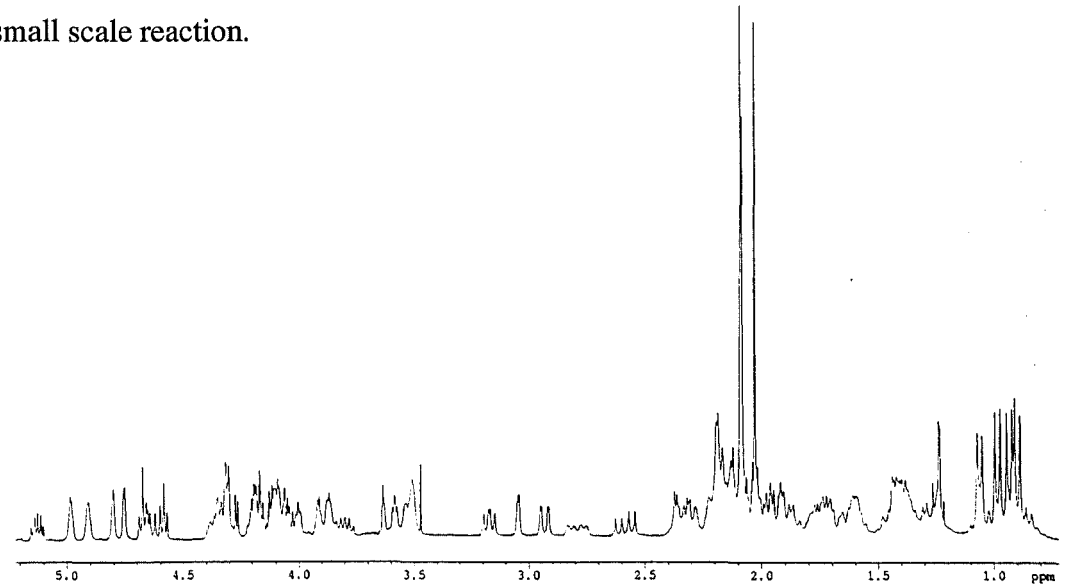

Figure 3.2.3 ^1H NMR Spectrum of Homohalichondrin B Diacetate

3.3 Oxidation

Oxidation of the C50 alcohol of isohomohalichondrin B monoacetate (**3.2.1**) was attempted using the readily prepared reagent pyridinium chlorochromate (PCC)[48] as the oxidising agent. A successful trial reaction was performed on a small quantity of cholesterol before committing **3.2.1** to the reaction conditions of the oxidation.

A small quantity of isohomohalichondrin B monoacetate (**3.2.1**) dissolved in dichloromethane was added to a suspension of PCC and sodium acetate (added to buffer the solution) in dichloromethane. The mixture was stirred vigorously at room temperature and the reaction progress was monitored by silica TLC. After sixty hours reaction, silica TLC indicated the formation of a new spot at a lower polarity relative to the starting material (**3.2.1**); some starting material was also visible in the mixture.

A ^{1}H NMR spectrum of the worked-up material in $CDCl_3$/0.1% pyridine-d_5 showed very weak proton resonances. However, it was possible to identify that the C55 acetate was intact, and that there were some minor differences in the spectrum relative to the ^{1}H NMR spectrum of isohomohalichondrin B monoacetate (**Figure 3.2.1**). Notably, the methyl region of the spectrum indicated the movement of the CH_3-42 and CH_3-46 doublets to more shielded positions, and some changes in the *ca* δ_H 3.20 ppm region where the H47 and H32 protons were situated in the ^{1}H NMR spectrum of isohomohalichondrin B monoacetate. It was not possible to observe changes in the region where the H50 resonance occurred at in the ^{1}H NMR spectrum of **3.2.1** (δ_H 3.52 ppm) as this position was obscured by other solvent related resonances.

It was difficult to assess if the C50 alcohol oxidation was successful given the small scale of the reaction and, as a result of this, the lack of supporting NMR and MS data. However, it did appear that some reaction had occurred, although an assessment of the product(s) formed and the reaction yield was not possible.

It was recognised that an assessment of the biological activity of the reaction material could give a further indication as to the success of the reaction. This aspect is discussed in Section 3.5.

To enable a full characterisation of the reaction product(s) from this reaction, it was decided to repeat the oxidation reaction of the monoacetate of isohomohalichondrin B on a larger scale. The oxidation was re-attempted on isohomohalichondrin B monoacetate (**3.2.1**) but the reaction that had been observed initially was not able to be reproduced; time and material constraints prohibited any subsequent investigations of this reaction. The identity of the initially observed product remains unknown.

3.4 Sodium Borohydride Reduction

The ketone located at position C53 in isohomohalichondrin B (**1.2.9**) was targeted in a sodium borohydride reduction reaction. It was recognised that there was the possibility of two diastereoisomeric alcohol derivatives being produced at the new C53 centre arising from hydride attack on either face of the ketone (**3.4.1** and **3.4.2**).

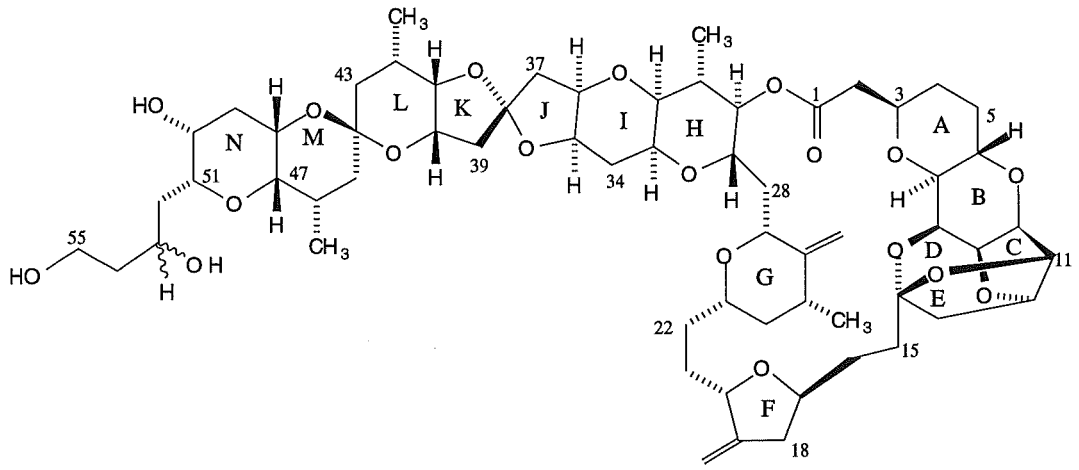

isohomohalichondrin B reduction isomers (**3.4.1** and **3.4.2**)

Initially a trial reaction on a small quantity of cholestan-3-one was undertaken to establish reaction conditions and work-up procedures. Having successfully achieved this, the reaction conditions were applied to a small amount of isohomohalichondrin B.

Sodium borohydride was added to isohomohalichondrin B (**1.2.9**) dissolved in isopropyl alcohol. The resulting suspension was stirred vigorously at room temperature, monitoring progress of the reaction by silica TLC. After fifteen minutes reaction, silica TLC of the reaction mixture indicated the presence of two new spots of increased polarity relative to an isohomohalichondrin B reference TLC spot; the less polar of the two spots being more intense, indicating that it was the major product. Also apparent from the TLC plate was the complete disappearance of isohomohalichondrin B from the reaction mixture, indicating that the reaction was complete. The reaction was quenched after thirty minutes and a ^{1}H NMR spectrum was obtained from the product (in $CDCl_3$/0.1% pyridine-d_5), and is displayed in **Figure 3.4.1**. Comparison of this spectrum with that of isohomohalichondrin B indicated several major changes. The methyl region indicated the movement of the CH_3-46 doublet resonance from δ_H 0.90 ppm to a less shielded position overlying the CH_3-42 doublet resonance at δ_H 0.94 ppm. The distinctive H55/H55' triplet at δ_H 3.86 ppm was no longer visible, and the resonances corresponding to the H52 (δ_H 2.62 ppm), H52' (δ_H 2.93 ppm) and H54/H54' (δ_H 2.73 ppm) protons had also moved to positions that were not immediately obvious. The final major change visible from this spectrum was the movement of the chemical shift of the characteristic H47 proton resonance to a less shielded position. This resonance appeared as a narrow doublet at δ_H 3.23 ppm in the ^{1}H NMR spectrum of isohomohalichondrin B, but was split into two separate and isolated narrow doublets at δ_H 3.32 ppm and δ_H 3.26 ppm in the spectrum of the reaction products. The sum of the integrals over both resonances was equivalent to the integral over a single unshifted olefinic proton resonance, indicating that these two resonances represented the two separate diastereoisomers produced in the reaction. The ratio of the integrals of the two H47 resonances was approximately 3:2 in favour of the less shielded resonance.

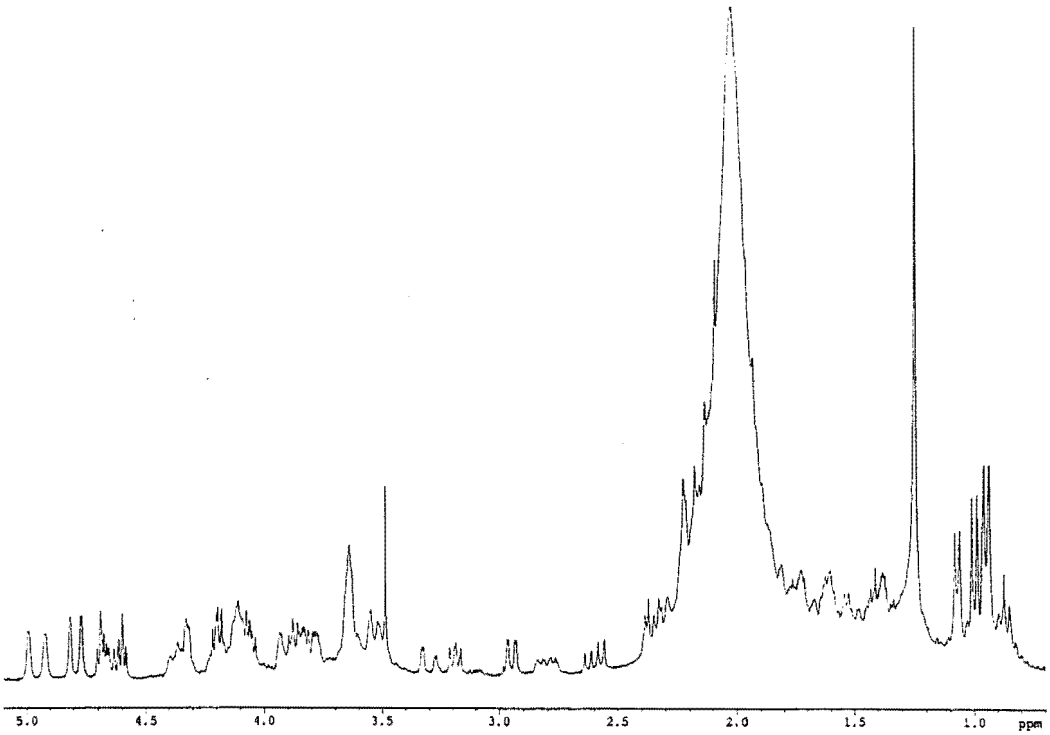

Figure 3.4.1 ^{1}H NMR Spectrum of Isohomohalichondrin B Reduction Products

The reaction was repeated on a slightly larger quantity of isohomohalichondrin B (**1.2.9**) to obtain sufficient material for separation of the two diastereoisomers. Silica TLC of the product was identical with that observed in the previous reaction. The products from the two separate reactions were combined prior to preparative HPLC (*H*igh *P*erformance *L*iquid *C*hromatography) separation. Separation of the two diastereoisomers was accomplished using a preparative C18 HPLC column, the chromatogram indicating that the less polar product was the major product. ^{1}H NMR spectra of the two products, performed in $CDCl_3$/0.1% pyridine-d_5, indicated that the separation was successful as evidenced by the clean separation of the two H47 proton resonances. The chemical shift of the H47 proton for the major, less polar product (**3.4.1**) was δ_H 3.32 ppm. The corresponding H47 resonance in the ^{1}H NMR spectrum of the minor, more polar product (**3.4.2**) was observed at δ_H 3.26 ppm. Other differences in the ^{1}H NMR spectra of the two products were apparent in the methyl region, with the less polar of the two products showing the CH_3-46 and

CH_3-42 doublet resonances as two very close, but separate doublet signals. For the more polar product they appeared at exactly the same chemical shift resulting in the appearance of a single doublet with twice the intensity of the adjacent CH_3-31 and CH_3-25 methyl resonances.

A relatively low recovery off the C18 column meant there was insufficient material to progress with the NMR spectral assignment of the two products. A further, large scale, sodium borohydride reduction was therefore repeated on isohomohalichondrin B (**1.2.9**), the products separated as previously and the products were combined with those from the first HPLC separation.

3.4.1 Reduction Isomer 3.4.1

The ^1H NMR spectrum of the major, less polar component, reduction isomer **3.4.1**, performed in $CDCl_3$/0.1% pyridine-d_5, is shown in **Figure 3.4.2**. The ^1H NMR spectrum indicated that there was more than 90% reduction isomer **3.4.1** present in the sample with respect to reduction isomer **3.4.2**, by integral. A ^{13}C NMR spectrum was acquired on this sample as there was sufficient material to obtain an adequate signal to noise ratio. Additionally, a range of selective 1D and 2D NMR experiments were performed on reduction isomer **3.4.1**, namely COSY, 2D-TOCSY (20 ms, 60 ms and 100 ms mixing times), NOE, HMQC and selective 1D-TOCSY experiments.

Analysis of the NMR experiments focused interest on changes in the terminal region of the molecule. The ^1H and ^{13}C NMR spectral assignments in the region of the A

to L rings were identical with those of isohomohalichondrin B (**1.2.9**).[14] The signals remaining in the various NMR spectra after assignment of the ^{1}H and ^{13}C signals in the A-L region were subsequently examined. The assignments in the terminal region of reduction isomer **3.4.1** are discussed. The assignments made for reduction isomer **3.4.1** are cited in **Table 3.4.1** for the ^{1}H NMR data and in **Table 3.4.2** for the ^{13}C NMR data. The important correlations from the various NMR experiments performed are depicted in **Figure 3.4.3**.

Table 3.4.1 ^{1}H NMR Data for Isohomohalichondrin B Reduction Isomer **3.4.1**

Proton[a]	δ ppm[b]	Proton[a]	δ ppm[b]	Proton[a]	δ ppm[b]
H2	2.34	**H21**	1.38	**H39**	2.22
H2'	2.58	**H21'**		**H39'**	2.22
H3	3.87	**H22**	1.62	**H40**	3.95
H4	1.37	**H22'**	1.62	**H41**	3.64
H4'	1.74	**H23**	3.53	**H42**	2.26
H5	1.38	**H24**	1.04	**CH_3-42**	0.94
H5'	2.08	**H24'**	1.70	**H43**	
H6	4.34	**H25**	2.20	**H43'**	
H7	2.94	**CH_3-25**	1.07	**H45**	1.48
H8	4.33	**26=CH**	4.75	**H45'**	1.53
H9	4.04	**26'=CH**	4.80	**H46**	2.22
H10	4.18	**H27**	3.53	**CH_3-46**	0.94
H11	4.60	**H28**	1.90	**H47**	3.32
H12	4.68	**H28'**	2.00	**H48**	3.78
H13	1.94	**H29**	4.18	**H49**	1.82
H13'	2.15	**H30**	4.64	**H49'**	2.14
H15		**H31**	2.02	**H50**	3.49
H15'		**CH_3-31**	0.99	**H51**	3.61
H16		**H32**	3.18	**H52**	1.56
H16'	2.14	**H33**	3.80	**H52'**	2.12
H17	4.10	**H34**	1.79	**H53**	4.16
H18	2.26	**H34'**		**H54**	1.72
H18'	2.79	**H35**	4.10	**H54'**	1.72
19=CH	4.91	**H36**	4.10	**H55**	3.83
19'=CH	4.98	**H37**	1.92	**H55'**	3.83
H20	4.38	**H37'**	2.36		

[a] The symbol ' represents the less shielded proton of a geminal pair.

[b] Data recorded at 23 °C in $CDCl_3$ at 300 MHz with chemical shifts in ppm and referenced to $CHCl_3$, δ_H 7.25 ppm.

Table 3.4.2 ^{13}C NMR Data for Isohomohalichondrin B Reduction Isomer **3.4.1**

Carbon	δ ppm[a]	Carbon	δ ppm[a]	Carbon	δ ppm[a]
C1	171.2	**C21**	29.5	**C39**	42.5
C2	40.4	**C22**	31.7	**C40**	71.1
C3	73.7	**C23**	74.9	**C41**	79.0
C4	30.7	**C24**	43.4	**C-CH_3-42**	25.7
C5	30.0	**C-CH_3-25**	35.9	**C-CH_3-42**	17.6
C6	68.2	**C-CH_3-25**	18.0	**C43**	
C7	77.6	**26C=CH_2**	151.6	**C44**	97.3
C8	74.3	**26C=CH_2**	104.2	**C45**	37.2
C9	73.8	**C27**	73.4	**C-CH_3-46**	28.4
C10	76.5	**C28**		**C-CH_3-46**	17.3
C11	82.1	**C29**	71.2	**C47**	76.2
C12	81.1	**C30**	77.2	**C48**	66.4
C13	48.3	**C-CH_3-31**	36.6	**C49**	34.4
C14	110.1	**C-CH_3-31**	15.0	**C50**	67.2
C15	34.4	**C32**	77.4	**C51**	81.1
C16	28.2	**C33**	66.4	**C52**	38.3
C17		**C34**	29.1	**C53**	71.8
C18	38.7	**C35**	75.1	**C54**	38.4
19C=CH_2	151.8	**C36**		**C55**	61.4
19C=CH_2	104.5	**C37**	43.2		
C20	75.4	**C38**			

[a] Data recorded at 23 °C in $CDCl_3$ at 75 MHz with chemical shifts in ppm and referenced to $CHCl_3$, δ_C 77.0 ppm. Some ^{13}C NMR chemical shifts assigned from HMQC spectrum at 300 MHz.

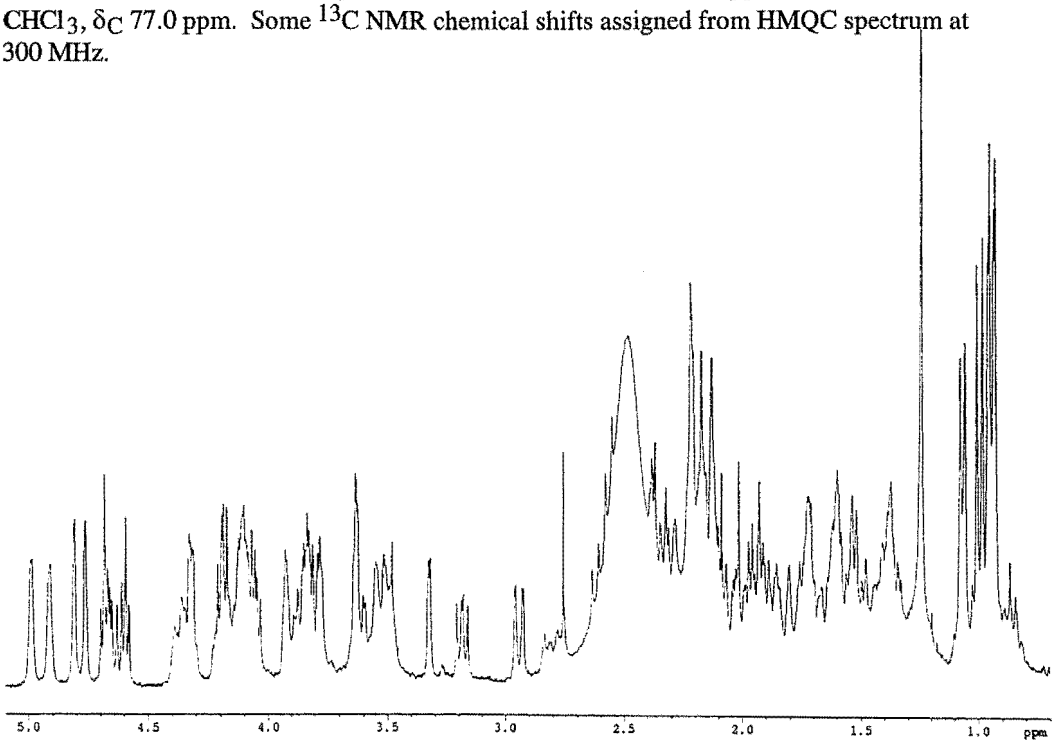

Figure 3.4.2 ^1H NMR Spectrum of Reduction Isomer **3.4.1**

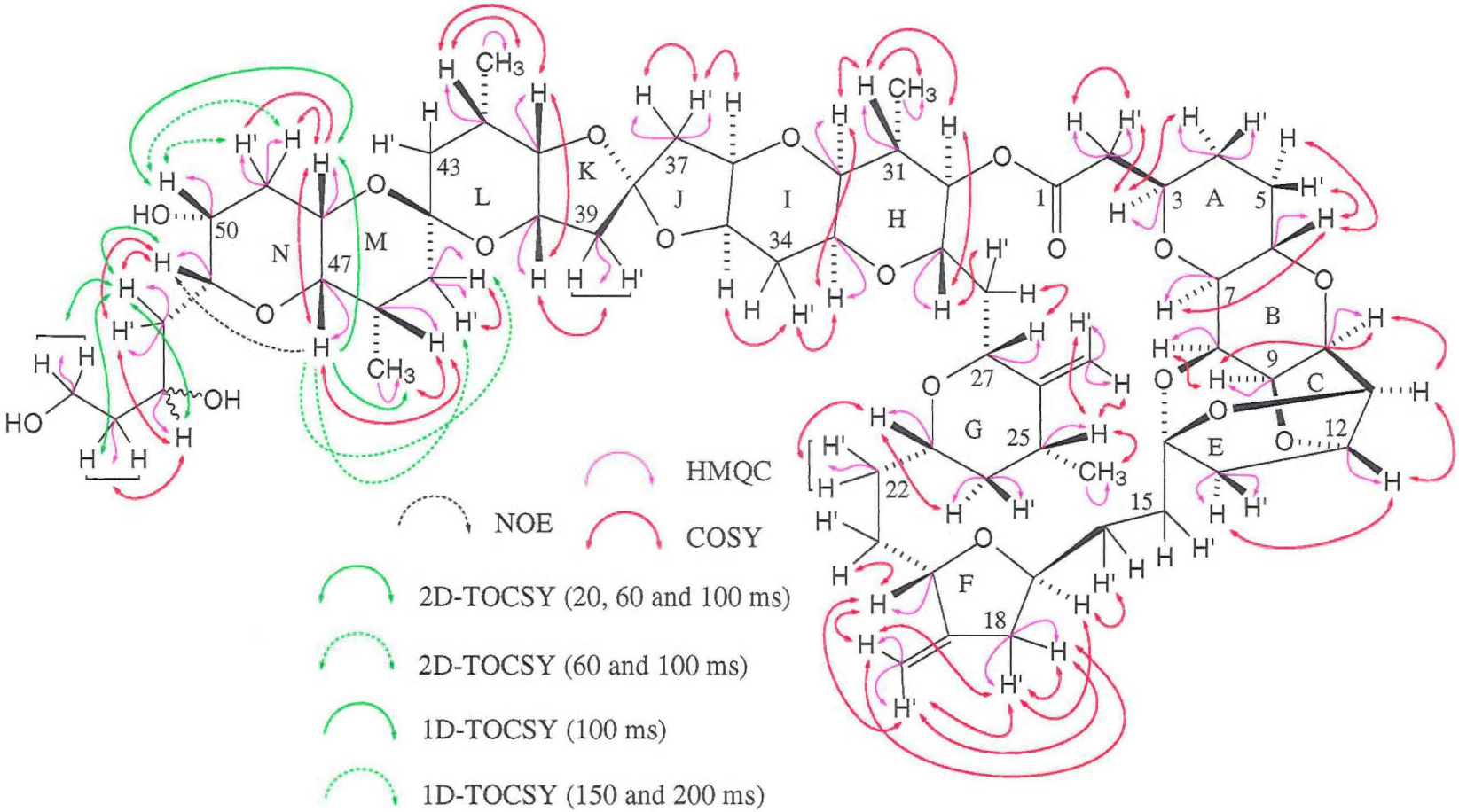

Figure 3.4.3 Isohomohalichondrin B Reduction Isomer **3.4.1**- Important NMR Correlations

The ^{13}C NMR spectrum of reduction isomer **3.4.1** indicated the presence of four new and isolated signals relative to isohomohalichondrin B: at δ_C 81.1 ppm, δ_C 71.8 ppm, δ_C 67.2 ppm, and δ_C 61.4 ppm. These signals were subsequently assigned as C51, C53, C50 and C55 respectively. The methyl group remaining unassigned in the ^1H NMR spectrum at δ_H 0.94 ppm was assigned as the CH_3-46 methyl resonance. These methyl protons showed a COSY correlation to a proton signal at δ_H 2.22 ppm which was assigned as the H46 resonance. A COSY correlation from H46 (δ_H 2.22 ppm) to δ_H 3.32 ppm confirmed the position of the H47 resonance. A COSY correlation from H47 was observed to a proton at δ_H 3.78 ppm (H48). Two COSY correlations from H48 to methylene protons at δ_H 1.82 ppm and δ_H 2.14 ppm located H49 and H49'. An isolated HMQC correlation was observed for a proton at δ_H 3.49 ppm attached to a carbon resonating at δ_C 67.2 ppm. TOCSY correlations from H49, H49' and H48 to the δ_H 3.49 ppm signal indicated that it was the H50 resonance. The H45 (δ_H 1.48 ppm) and H45' (δ_H 1.53 ppm) protons were located from two separate, selective 1D-TOCSY irradiations of the δ_H 3.32 ppm resonance (*ie* H47) with mixing times of 100 ms and 150 ms. A COSY correlation was observed between the H45 and H45' protons.

The COSY spectrum indicated the presence of a methine proton at δ_H 4.16 ppm correlated to two methylene protons, one at δ_H 2.12 ppm and the other at δ_H 1.72 ppm. From the HMQC spectrum it was apparent that the isolated correlation at δ_H 1.72 ppm/δ_C 38.4 ppm corresponded to two equivalent methylene protons attached to one carbon. This implied that the proton at δ_H 4.16 ppm was situated between two pairs of methylene protons. The only remaining assignment possible for the proton at δ_H 4.16 ppm was as the newly formed H53 proton. The methylene proton at δ_H 2.12 ppm also showed a COSY correlation to a methine proton at δ_H 3.61 ppm. This methine proton was correlated to a carbon at δ_C 81.1 ppm in the HMQC spectrum.

An NOE from irradiation at the H47 resonance to the methine proton at δ_H 3.61 ppm provided additional evidence that it was the H51 proton, and therefore the methylene proton at δ_H 2.12 ppm was assigned as the H52' proton, lying between H51 and H53. The equivalent methylene protons at δ_H 1.72 ppm were assigned as H54 and H54'. The methylene partner to H52 was assigned from a COSY correlation from H51 to a proton at δ_H 1.56 ppm. An isolated signal which remained unassigned in the ^{13}C NMR spectrum at δ_C 61.4 ppm, and appeared in the HMQC spectrum as an isolated correlation to a proton at δ_H 3.83 ppm was assigned as corresponding to the C55 carbon and H55/H55' protons respectively. Finally, the remaining unassigned carbons in the terminal region were able to be assigned from the ^{13}C NMR spectrum and the HMQC spectrum. All of the correlations described are shown in **Figure 3.4.3**.

As expected there were some significant changes in ^1H and ^{13}C NMR chemical shifts around the C53 centre. Two interesting observations are highlighted. Firstly, the H53 resonance at δ_H 4.16 ppm appeared at a relatively deshielded position for a methine proton in this environment. Secondly, the H47 proton recorded a chemical shift (δ_H 3.32 ppm) that was less shielded than H47 was in the ^1H NMR spectrum of isohomohalichondrin B (δ_H 3.23 ppm), although this position was significantly removed from the reaction centre at C53. These two observations could, in part, be explained by the occurrence of hydrogen bonding from the new C53 hydroxyl proton to the N-ring ether oxygen, resulting in deshielding of the H53 and H47 protons and a corresponding movement of chemical shifts for these proton resonances to less shielded positions in the ^1H NMR spectrum of the reduction isomer **3.4.1**.

High Resolution FAB-MS performed on reduction isomer **3.4.1** indicated the parent ion (MH^+), corresponding to a molecular formula of $C_{61}H_{88}O_{19}$; a gain of two

hydrogen atoms relative to isohomohalichondrin B. These data confirmed that isohomohalichondrin B had been successfully reduced to **3.4.1**.

3.4.2 Reduction Isomer 3.4.2

The NMR spectral assignment of the more polar and minor reduction product, reduction isomer **3.4.2**, was aided by the partial assignment of the ^{1}H and ^{13}C NMR spectra of reduction isomer **3.4.1**. The ^{1}H NMR spectrum of reduction isomer **3.4.2** is displayed in **Figure 3.4.4**. There was no reduction isomer **3.4.1** apparent in this ^{1}H NMR spectrum (by integral over the distinctive H47 signals), indicating an excellent HPLC separation had been achieved for this product.

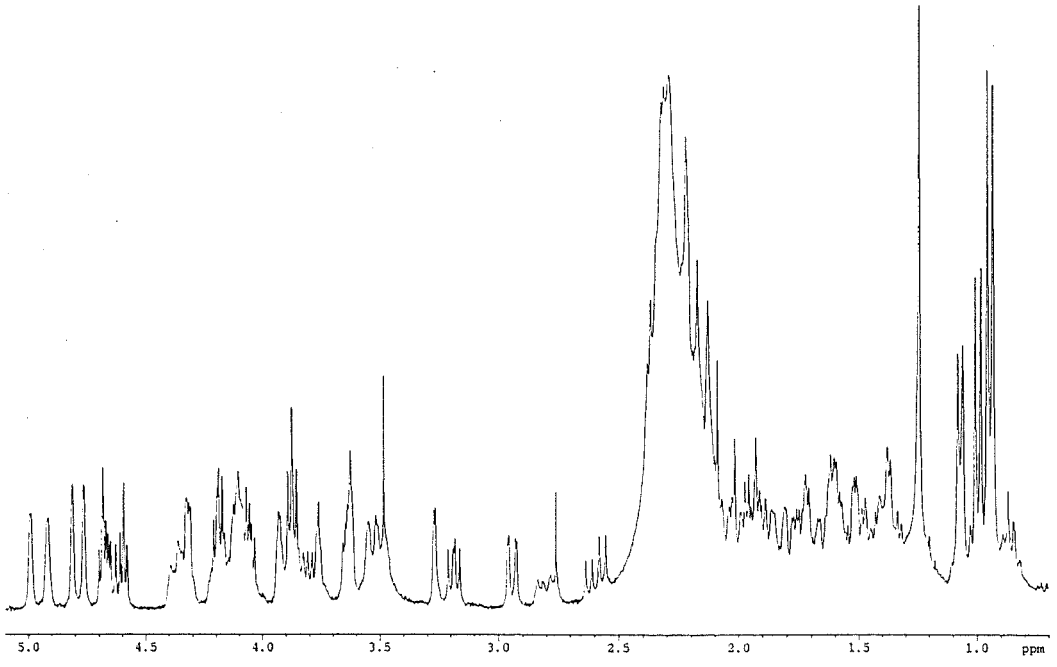

Figure 3.4.4 ^{1}H NMR Spectrum of Reduction Isomer **3.4.2**

A ^{13}C NMR spectrum was not acquired due to the reduced amount of reduction isomer **3.4.2** available compared to reduction isomer **3.4.1**. However, it was possible

to achieve a partial assignment of the ^{13}C NMR spectrum indirectly *via* an HMQC experiment. Two additional NMR experiments, which aided in the assignment of the ^{1}H NMR spectrum, were performed on reduction isomer **3.4.2**: a COSY experiment and a selective 1D-TOCSY experiment. The ^{1}H and ^{13}C NMR data for reduction isomer **3.4.2** are cited in **Tables 3.4.3** and **3.4.4** respectively.

Table 3.4.3 ^{1}H NMR Data for Isohomohalichondrin B Reduction Isomer **3.4.2**

Proton[a]	δ ppm[b]	Proton[a]	δ ppm[b]	Proton[a]	δ ppm[b]
H2	2.35	**H21**	1.38	**H39**	2.22
H2'	2.58	**H21'**		**H39'**	2.22
H3	3.87	**H22**	1.60	**H40**	3.93
H4	1.36	**H22'**	1.60	**H41**	3.63
H4'	1.74	**H23**	3.53	**H42**	2.26
H5		**H24**	1.04	**CH_3-42**	0.94
H5'	2.08	**H24'**	1.70	**H43**	
H6	4.34	**H25**	2.20	**H43'**	
H7	2.94	**CH_3-25**	1.07	**H45**	1.48
H8	4.32	**26=CH**	4.75	**H45'**	1.52
H9	4.04	**26'=CH**	4.80	**H46**	2.20
H10	4.18	**H27**	3.53	**CH_3-46**	0.94
H11	4.60	**H28**	1.92	**H47**	3.26
H12	4.68	**H28'**		**H48**	3.76
H13	1.93	**H29**	4.20	**H49**	1.83
H13'	2.15	**H30**	4.66	**H49'**	2.14
H15		**H31**	2.01	**H50**	3.48
H15'		**CH_3-31**	0.99	**H51**	3.63
H16		**H32**	3.18	**H52**	1.56
H16'	2.14	**H33**	3.81	**H52'**	2.10
H17	4.10	**H34**	1.78	**H53**	4.16
H18	2.26	**H34'**		**H54**	1.74
H18'	2.80	**H35**	4.10	**H54'**	1.74
19=CH	4.91	**H36**	4.10	**H55**	3.86
19'=CH	4.98	**H37**	1.92	**H55'**	3.86
H20	4.38	**H37'**	2.35		

[a] The symbol ' represents the less shielded proton of a geminal pair.

[b] Data recorded at 23 °C in $CDCl_3$ at 300 MHz with chemical shifts in ppm and referenced to $CHCl_3$, δ_H 7.25 ppm.

Table 3.4.4 ^{13}C NMR Data for Isohomohalichondrin B Reduction Isomer **3.4.2**

Carbon	δ ppm[a]	Carbon	δ ppm[a]	Carbon	δ ppm[a]
C1		**C21**		**C39**	42.3
C2	40.2	**C22**	31.7	**C40**	71.0
C3	73.6	**C23**	74.8	**C41**	79.0
C4		**C24**	43.4	**C-CH_3-42**	25.4
C5		**C-CH_3-25**		**C-CH_3-42**	17.5
C6	68.2	**C-CH_3-25**	18.0	**C43**	
C7	77.6	**26C=CH_2**		**C44**	
C8	74.3	**26C=CH_2**	104.2	**C45**	
C9	73.8	**C27**	73.4	**C-CH_3-46**	
C10	76.5	**C28**		**C-CH_3-46**	17.5
C11	82.1	**C29**	71.1	**C47**	76.0
C12	81.1	**C30**	77.0	**C48**	66.6
C13	48.3	**C-CH_3-31**		**C49**	34.3
C14		**C-CH_3-31**	15.0	**C50**	67.4
C15		**C32**	77.4	**C51**	77.0
C16		**C33**	66.6	**C52**	38.5
C17		**C34**		**C53**	69.8
C18	38.6	**C35**		**C54**	
19C=CH_2		**C36**		**C55**	62.0
19C=CH_2	104.5	**C37**	43.2		
C20	75.2	**C38**			

[a] Data recorded at 23° C in $CDCl_3$ with chemical shifts in ppm, assigned from an HMQC spectrum at 300 MHz.

The ^{13}C and ^{1}H NMR spectral data in the region of the A-L rings of reduction isomer **3.4.2** were consistent with those of reduction isomer **3.4.1** (Section 3.4.1) and isohomohalichondrin B (**1.2.9**).[14] Notable differences in the NMR data between the two reduction isomers were apparent, as expected, in the terminal (C44-C55) region. Apart from the H47 proton resonance, the ^{1}H NMR chemical shifts from H45/H45' to H55/H55' were only slightly different to those of reduction isomer **3.4.1**. The more obvious changes were apparent in terms of the ^{13}C NMR chemical shifts between the two diastereoisomers. The C51 ^{13}C NMR chemical shift of reduction isomer **3.4.2** at δ_C 77.0 ppm was observed at a more shielded position than the reduction isomer **3.4.1** C51 resonance (δ_C 81.1 ppm). Two other significant changes

were the shift of the C53 resonance to a more shielded position and the shift of the C55 carbon resonance to a less shielded position relative to reduction isomer **3.4.1**.

High Resolution FAB-MS performed on reduction isomer **3.4.2** gave the parent ion (MH^+), corresponding to a molecular formula of $C_{61}H_{88}O_{19}$; isobaric with reduction isomer **3.4.1**. These data confirmed that reduction isomer **3.4.1** and reduction isomer **3.4.2** were in fact related as diastereoisomers and that the two diastereoisomers, being the reduction products of isohomohalichondrin B (**1.2.9**), had been successfully produced.

3.4.3 Computer Modelling of Reduction Diastereoisomers

The relative stereochemistry at the new C53 centre was not able to be ascertained in terms of the NMR data collected for either reduction isomer **3.4.1** or reduction isomer **3.4.2**. It was anticipated that a knowledge of the solution conformation(s) of the two possible diastereoisomeric reduction products might provide evidence that could lead to their identification as either reduction isomer **3.4.1** or **3.4.2**. This knowledge could also provide useful information as to the conformational requirements for biological activity in the terminal C44-C55 region. The differing physical properties of the two isomers such as their polarities by silica TLC and C18 HPLC, and the observed differences in the NMR data provided evidence that their "average" solution conformations could be different. The "average" solution conformation describes a single, theoretical conformation, arising from a Boltzmann-weighted distribution of conformers with differing energies. This "average"

conformation is that observed on the NMR time-scale, arising from the presence, in solution, of the various populated conformers.

Computer modelling of the terminal region to determine the solution conformation(s) of each diastereoisomer was undertaken. Conformational searching of the terminal moiety of the two reduction diastereoisomers was carried out using the Monte Carlo search method in the program MacroModel V4.0 with the associated computational program BatchMin, using the parameters described previously in Section 2.3.2.

Initially the C43-C51 subunit was excised from the X-ray crystal structure of the norhalichondrin A *p*-bromophenacyl ester,[17] in the CSC Chem3D Plus program. The C43 methylene group was converted to a methyl group and the L-ring ether oxygen was converted to a free hydroxyl group. The C52-C55 "tail" was subsequently added as separate R and S chiralities at the C53 stereocentre to generate the two reduction product diastereoisomers. The conformational searching of each diastereoisomer is described.

3.4.3.1 Modelling of the C53-R Diastereoisomer

The R-diastereoisomer generated in Chem3D Plus was used as the starting conformation for a Monte Carlo conformational search in MacroModel using the chloroform GB/SA solvent model. Two additional searches were initiated from different starting geometries.

The global minimum and low energy conformers were identical for all three searches. Each conformer was subsequently tested to ensure that it was in fact a true local minima using the BatchMin minima test on the conformers in the output structure file. Having successfully passed this test, the Boltzmann-weighted

distribution of each conformer was calculated at 23°C resulting in three conformers contributing greater than 5% to the distribution. These three conformers are displayed in **Figure 3.4.5** along with their MM2* energies and percentage Boltzmann-weighted contributions to the distribution.

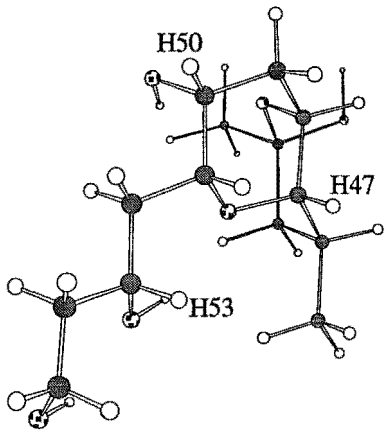

CONFORMATION ONE (64.6%)
MM2* Energy = - 150.9 kJ/ mol

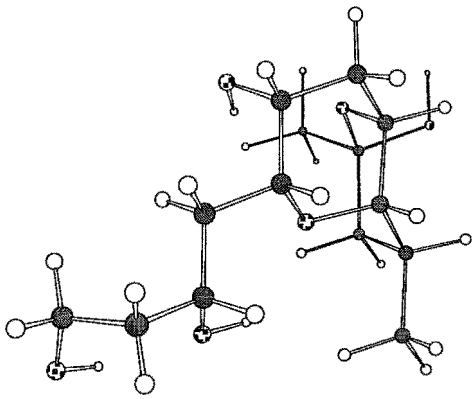

CONFORMATION TWO (15.1%)
MM2* Energy = - 147.3 kJ/ mol

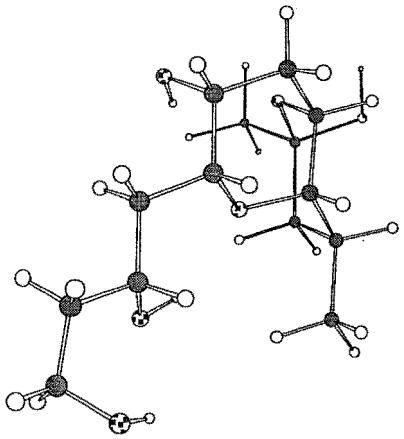

CONFORMATION THREE (6.5%)
MM2* Energy = - 145.2 kJ/ mol

Figure 3.4.5 R-Diastereoisomer Conformational Search Output

As can be seen in **Figure 3.4.5**, the M and N rings of the low energy conformers generated in the conformational search were all chair/chair in conformation, with the conformational variations occurring exclusively in the "tail" region of the structure.

3.4.3.2 Modelling of the C53-S Diastereoisomer

The S-diastereoisomer was modelled in the same manner as the R-diastereoisomer described above. Monte Carlo conformational searches initiated from two separate starting conformations yielded the same set of low energy conformers. Each conformer was tested using the BatchMin minima test to ensure that it was in fact a true local minima. Having successfully passed this test, the Boltzmann-weighted distribution of each conformer in the structure output file was calculated at 23°C, resulting in seven conformers contributing greater than 5% to the distribution. **Figure 3.4.6** depicts these seven conformers with their MM2* energies and Boltzmann-weighted contributions.

As with the R-diastereoisomer, the S-diastereoisomer conformational search output displayed identical chair/chair conformations for the terminal M and N rings. The "average" solution conformation of the "tail" region of the modelling output was calculated from Boltzmann-weighted vicinal coupling constants derived from dihedral angles (H-C-C-H) in MacroModel, for both the R and S-diastereoisomers. An attempt was made to collect experimental coupling constants in the "tail" region of reduction isomers **3.4.1** and **3.4.2** to relate to the modelling-derived Boltzmann-weighted "average" solution conformations. In principle, relating the experimentally-derived vicinal coupling constants for each diastereoisomer to the Boltzmann-weighted data from the modelling results for each diastereoisomer should have lead to the identification of the C53-stereochemistry of the reduction isomers. However, this was not possible due to the complex nature of the ^{1}H NMR resonances in the H51-H55/H55' regions of both diastereoisomers; all resonances appeared as complex or distorted signals.

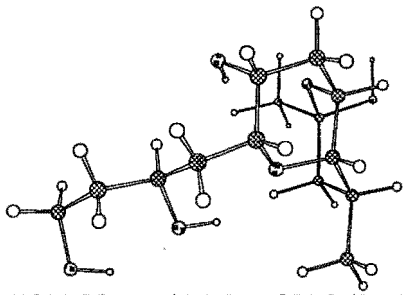

CONFORMATION ONE (22.9%)
MM2* Energy = - 147.1 kJ/ mol

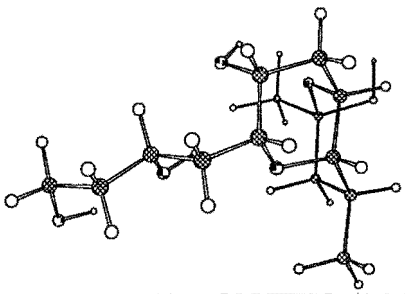

CONFORMATION TWO (15.8%)
MM2* Energy = - 146.2 kJ/ mol

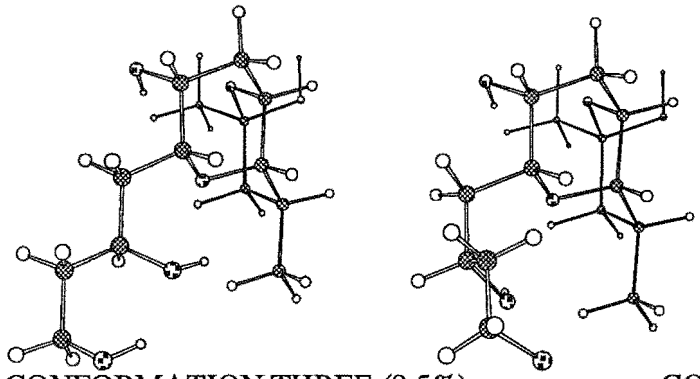

CONFORMATION THREE (9.5%)
MM2* Energy = - 144.9 kJ/ mol

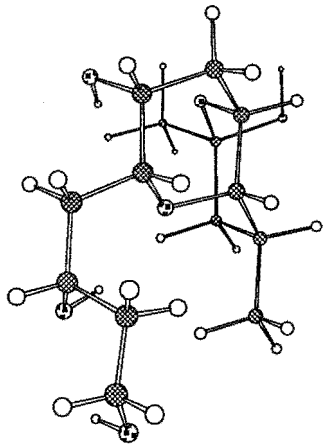

CONFORMATION FIVE (7.7%)
MM2* Energy = - 144.4 kJ/ mol

CONFORMATION FOUR (9.0%)
MM2* Energy = - 144.8 kJ/ mol

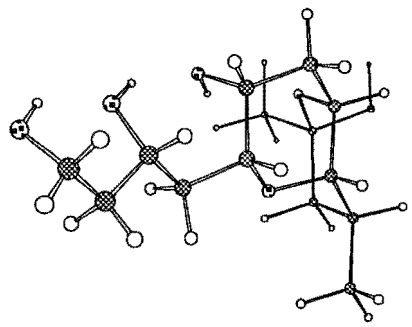

CONFORMATION SIX (5.6%)
MM2* Energy = - 143.6 kJ/ mol

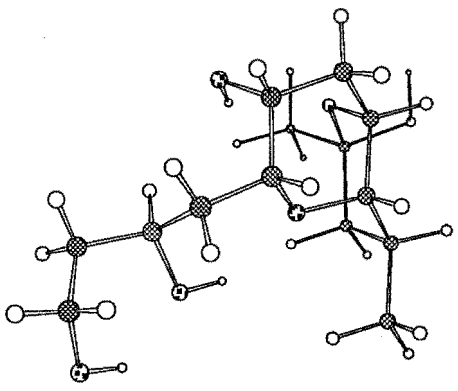

CONFORMATION SEVEN (5.2%)
MM2* Energy = - 143.4 kJ/ mol

Figure 3.4.6 S-Diastereoisomer Conformational Search Output

It is interesting to note the proximity of the C53 hydroxyl group to the N-ring ether oxygen in all of the R and S-diastereoisomers of **Figures 3.4.5** and **3.4.6**, except CONFORMATION SIX of the S-diastereoisomer conformational search output. This suggested that the presence of hydrogen bonding plays an important role in the "average" solution conformation of both diastereoisomers in chloroform. This was predicted in Section 3.4.1 from an analysis of the NMR data.

Although the solution conformations of the two diastereoisomers appeared to be quite different, it would be purely speculative to draw any conclusions relating the other physical differences between reduction isomers **3.4.1** and **3.4.2**, such as their relative polarities, to the conformations of the modelling output in order to assign a stereochemistry at the new C53 stereo centre.

3.5 Biological Activity Data

Table 3.5.1 lists the biological activities of the derivatives described in this Chapter. Included in this table are the P388 cytotoxicities of the five derivatives produced, the relevant parent halichondrins, and the GI_{50}s (over all sixty cell lines) of three derivatives described in this Chapter which underwent testing in the NCI's primary screening system. The COMPARE correlation coefficients are also listed for the NCI tested compounds.

Table 3.5.1 *In Vitro* Cytotoxicities of Selected Halichondrins

Compound	P388 IC_{50} (ng/mL)	NCI GI_{50} ($\times 10^{-10}$ M)	COMPARE Correlation[a]
homohalichondrin B (1.2.3)	0.22	3.16	0.95
isohomohalichondrin B (1.2.9)	0.18	1.15	0.74
isohomohalichondrin B monoacetate (3.2.1)	0.22	1.58	0.85
homohalichondrin B diacetate (3.2.2)	2.3		
isohomohalichondrin B monoacetate oxidation product	70.7		
reduction isomer 3.4.1	0.5	2.04	0.80
reduction isomer 3.4.2	0.6	1.78	0.87

a Correlation coefficients from the *Compare* pattern-recognition algorithm were calculated by computer using the GI_{50}-centred mean graph profiles of differential cellular sensitivities to each of the compounds. The GI_{50}-centred mean graph profile of halichondrin B (**1.2.1**) was used as the "seed" for all of the comparisons.

The biological activity of the isohomohalichondrin B monoacetate derivative (**3.2.1**) was very similar to the parent halichondrin *viz* isohomohalichondrin B (**1.2.9**), in both the P388 assay and the NCI primary screen results. While the similar activity results for **3.2.1** relative to **1.2.9** could be interpreted as implying hydrolysis of the terminal acetate of **3.2.1** was occurring in the assays, the COMPARE correlation coefficient suggested that the NCI mean graph profile was more like that of the halichondrin B "seed" mean graph profile than was isohomohalichondrin B (**1.2.9**). This tended to suggest that the acetate remained intact, modifying the mean graph profile of **3.2.1** relative to isohomohalichondrin B (**1.2.9**) while retaining a similar average cytotoxicity.

The homohalichondrin B diacetate derivative (**3.2.2**) displayed a greater than ten-fold reduction in P388 activity relative to homohalichondrin B (**1.2.3**). Therefore it appeared that the absence of free hydroxyl groups in the terminal moiety conferred a reduction in the observed P388 cytotoxicity.

As indicated in Section 3.3, it was anticipated that an assessment of the biological activity of the oxidation product would provide additional evidence as to the reaction or otherwise of isohomohalichondrin monoacetate (**3.2.1**) under PCC oxidation conditions. The cytotoxicity of the isohomohalichondrin B monoacetate oxidation product was more than three hundred times less active than the isohomohalichondrin B monoacetate derivative (**3.2.1**) in terms of their respective P388 activities. This implied that the monoacetate of isohomohalichondrin B (**3.2.1**) underwent reaction with PCC. However, nothing further could be said about the product formed in terms of structural identification *ie* whether the formation of the C50 ketone was successful.

Reduction isomer **3.4.1** displayed similar biological activity results to its C53 diastereoisomer, reduction isomer **3.4.2** in both the P388 assay and in the NCI primary screen. This implied that the conformational differences observed from the computer modelling conformational searches, conferred by the change in stereochemistry at C53, were not of great importance in determining the relative biological activities of the two diastereoisomers. The P388 and NCI primary screen cytotoxicities of reduction isomer **3.4.1** and reduction isomer **3.4.2** were slightly reduced relative to the parent halichondrin, isohomohalichondrin B (**1.2.9**). The COMPARE correlation coefficients however, suggested that the reduction isomers were more "halichondrin B-like" in terms of their mechanism of action as antimitotics than was isohomohalichondrin B.

In general terms, the biological activity data collected for the derivatives described in this Chapter suggested that the presence of at least one free hydroxyl group in the terminal moiety was essential for the expression of a high level of cytotoxicity. The addition of hydroxyl groups to the terminal moiety, as for the isohomohalichondrin B reduction isomers (**3.4.1** and **3.4.2**) did not appear to alter the observed biological activity to any significant degree.

Further discussion of these biological activities relative to a range of other halichondrin derivatives is made in Chapter 9.

CHAPTER 4

Modifications to Olefins

4.1 Introduction

The exocyclic double bonds at C19 and C26 in the halichondrin molecule were targeted in an investigation of their relative importance to the expression of biological activity. This involved the manipulation of the oxidation level at the C19 and C26 centres of selected halichondrins.

The preparation of a diketone derivative at positions C19 and C26 was the initial goal. As well as giving important structure-activity data, it was envisaged that this analogue would provide a useful starting point for further modifications.

Two approaches to generating the diketone were attempted: *via* ozonolysis and reductive cleavage of the ozonide formed, and *via* the di-osmate ester to the diol and cleavage to furnish the diketone derivative. It was envisaged that the intermediate C19 and C26 diol would also provide important biological activity information.

Other alterations to the exocyclic olefins included catalytic hydrogenation to produce the C19 and C26 methyl substituted derivatives which also provided useful bioactivity data. A reduction of the diketone compound at C19 and C26 was also attempted with the object of generating a dihydroxy compound at these positions.

4.2 Trial Ozonolysis

Ozonolysis was initially attempted on a model compound, β-pinene, which has an exocyclic olefinic functionality. This was undertaken to ensure reaction conditions and handling procedures were suitable to be applied to the halichondrins in terms of reaction yield and recovery of material on a small scale.

A method commonly used to cleave an ozonide to yield a ketone is the reductive zinc dust/acetic acid method.[49,50] Microscale ozonolysis to furnish the ozonide followed by a reductive zinc/aqueous acetic acid work-up to give the desired ketone was attempted on β-pinene.

An ozone generator capable of producing millimolar quantities of ozone was constructed, based on a novel design by Beroza and Bierl.[51] Ozonolysis was attempted on a small quantity of β-pinene dissolved in dichloromethane until ozone was detected in the outlet gases. This was followed by addition of a reductive zinc/aqueous acetic acid suspension to the solution. The resulting mixture was stirred vigorously overnight at room temperature and then extracted into ether. ^{1}H NMR spectroscopy of the resulting material indicated that considerable degradation had occurred.

Further investigations of β-pinene in a zinc/aqueous acetic acid suspension revealed that this step was resulting in the acid decomposition observed. It was decided therefore that the acidic work-up conditions would be too severe to be applied to the halichondrins and alternative methods of generating the diketone *via* osmylation were investigated.

4.3 Osmylation Reactions[52]

The generation of a ketone functional group from an olefin *via* osmylation can be accomplished by several distinct methodologies. The ketone may be directly accessed in a one-step reaction using a catalytic amount of osmium tetroxide and sodium perchlorate[53,54] or sodium periodate[55] to oxidatively cleave the osmate (VI) ester, regenerating osmium tetroxide. While this method has the advantage of using reduced amounts of expensive and toxic osmium tetroxide and minimising mass transfers, it was realised that a two-step method to yield the halichondrin diketone *via* the *vic*-diols at C19 and C26 would give an additional intermediate product for structure-activity evaluation.

Baran[56] describes a suitable pyridine-catalysed[57] osmylation to generate the corresponding osmate ester, followed by reductive cleavage in aqueous bisulfite solution to yield the desired *vic*-diol product. It was recognised that the halichondrin diketone could then be generated by periodate cleavage of the resulting two *vic*-diols.

Initially, a trial osmylation and reductive bisulfite reaction was carried out on β-pinene. The periodate cleavage step was carried out on benzoin which was cleaved to form benzoic acid and benzaldehyde. Finally, the stability of isohomohalichondrin B was tested under the periodate cleavage reaction conditions before committing it to the reaction.

4.3.1 Initial Studies

4.3.1.1 Trial Osmylation and Periodate Cleavage

A trial osmylation on a small quantity of β-pinene was successfully undertaken. The ^{1}H NMR spectrum of the reaction product acquired in $CDCl_3$/0.1% pyridine-d_5 indicated the complete loss of the olefinic proton signals and the appearance of a new doublet of doublets at δ_H 3.51 ppm. These protons were assigned as the diastereotopic diol methylene protons and it was concluded the reaction had been successful.

A trial periodate cleavage of benzoin to benzoic acid and benzaldehyde was also accomplished, a ^{1}H NMR spectrum of the reaction products showing a new resonance at δ_H 10.2 ppm, characteristic of an unsubstituted aromatic aldehyde proton.[58]

The reaction conditions applied to the two trial reactions were then utilised in the subsequent reactions of selected halichondrins.

4.3.1.2 Stability of Isohomohalichondrin B to Periodate

It was important to ensure that isohomohalichondrin B (**1.2.9**) was stable to the periodate reaction conditions to avoid the complication of possible side-reactions not associated with cleavage of the diol. A small sample of isohomohalichondrin B (**1.2.9**) was placed under the periodate reaction conditions to be applied to the diol of isohomohalichondrin B. TLC and ^{1}H NMR of the worked-up material indicated no reaction had occurred and therefore that isohomohalichondrin B was stable under these conditions.

4.3.2 Osmylation of Isohomohalichondrin B

An ether solution of osmium tetroxide was added to isohomohalichondrin B (**1.2.9**) dissolved in pyridine and the solution was stirred at room temperature for four hours. Sodium metabisulfite in water/pyridine was then added and the mixture was stirred at room temperature for a further twenty minutes.

Silica TLC of the product after work-up indicated the appearance of a single new spot of increased polarity relative to isohomohalichondrin B, and no evidence of starting material.

A ^{1}H NMR spectrum of the product clearly showed the complete loss of all four olefinic proton signals (**Figure 4.3.1**), indicating the reaction had gone to completion. A range of 2D NMR experiments (COSY, 2D-TOCSY (100 ms mixing time) and HMQC) were also performed on this sample, in $CDCl_3$/ 0.1% pyridine-d_5. A partial assignment of the ^{1}H and ^{13}C NMR spectra was accomplished and these data are given in **Tables 4.3.1** and **4.3.2** respectively, and the important correlations from the NMR experiments are depicted in **Figure 4.3.2**. It proved difficult to assign ^{1}H NMR chemical shift values to the terminal "hydroxy" methylene protons C19-$C\underline{H}_2$-O- and C26-$C\underline{H}_2$-O- and the methine protons adjacent to these two groups, namely H27 and H20.

The COSY spectrum showed a proton at δ_H 4.61 ppm strongly correlated to a proton resonance at δ_H 4.35 ppm. The HMQC spectrum showed these two protons to be correlated to the same carbon at δ_C 88.1 ppm, indicating that they were methylene protons. Similarly, a strong COSY correlation was observed between a proton at δ_H

4.56 ppm and another at δ_H 4.74 ppm which were also associated with a single carbon in the HMQC spectrum at δ_C 81.5 ppm. These ^1H NMR chemical shifts were too deshielded to be assigned as diastereotopic diol protons when related to the chemical shift of δ_H 3.51 ppm observed for the β-pinene diol methylene protons. Fortuitously, the osmate ester of β-pinene had been synthesised from β-pinene by David Stirling in the Marine Chemistry Group, the ^1H NMR spectrum of which showed the diastereotopic osmate ester methylene protons were situated at δ_H 4.20 ppm. This corresponded to a shift of δ_H 0.34 - 0.40 ppm, to a more shielded position, relative to the olefinic protons of β-pinene. This predicted ^1H NMR chemical shift to produce the osmate ester derivative is in the order of the chemical shifts observed for the new methylene protons of isohomohalichondrin B upon osmylation, relative to the olefinic protons. These observations indicated that the product formed from the osmylation of isohomohalichondrin B was the di-osmate ester (**4.3.1**). It proved difficult to assign ^1H and ^{13}C NMR chemical shifts around the two C19 and C26 centres, notably C20/H20 and C27/H27.

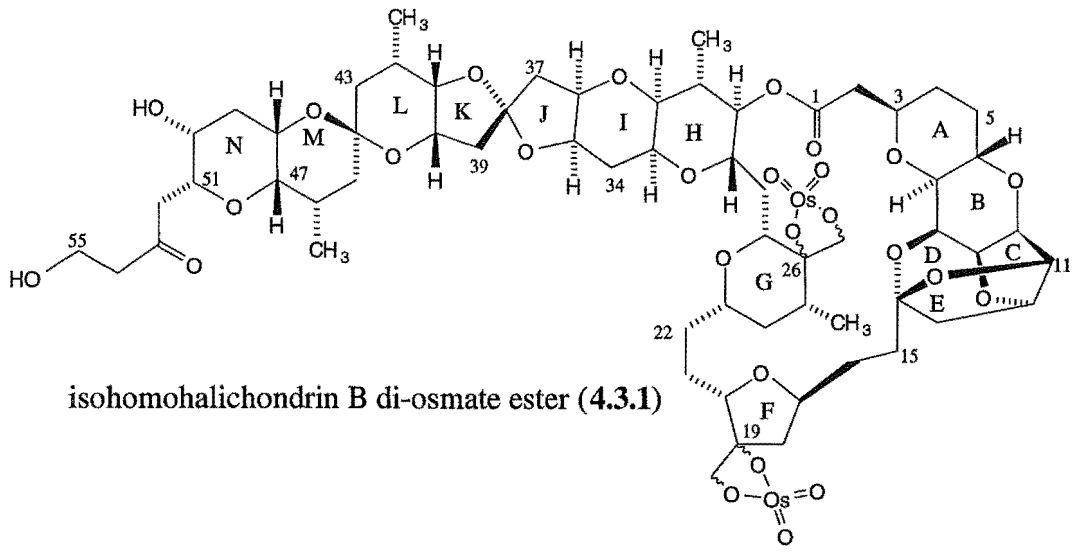

isohomohalichondrin B di-osmate ester (**4.3.1**)

Table 4.3.1 ^{1}H NMR Data for Isohomohalichondrin B Di-osmate Ester (**4.3.1**)

Proton[a]	δ ppm[b]	**Proton**[a]	δ ppm[b]	**Proton**[a]	δ ppm[b]
H2	2.42	**H21**		**H39**	2.22
H2'	2.52	**H21'**		**H39'**	2.22
H3	3.88	**H22**		**H40**	3.90
H4	1.40	**H22'**		**H41**	3.58
H4'	1.71	**H23**	3.50	**H42**	2.25
H5	1.50	**H24**	1.02	**CH_3-42**	0.92
H5'	2.23	**H24'**	1.67	**H43**	1.29
H6	4.36	**H25**	2.05	**H43'**	1.48
H7	2.88	**CH_3-25**	1.13	**H45**	1.45
H8	4.34	**26-CH-O**	4.56[c]	**H45'**	1.45
H9	4.00	**26'-CH-O**	4.74[c]	**H46**	2.12
H10	4.16	**H27**		**CH_3-46**	0.89
H11	4.57	**H28**		**H47**	3.23
H12	4.64	**H28'**		**H48**	3.72
H13	1.88	**H29**	4.08	**H49**	1.82
H13'	2.11	**H30**	4.71	**H49'**	2.08
H15		**H31**	2.00	**H50**	3.48
H15'		**CH_3-31**	0.95	**H51**	3.81
H16		**H32**	3.08	**H52**	2.60
H16'		**H33**	3.78	**H52'**	2.91
H17	4.05	**H34**	1.60	**H54**	2.73
H18	1.85	**H34'**	2.10	**H54'**	2.73
H18'	2.74	**H35**	4.04	**H55**	3.84
19 -CH-O	4.35[c]	**H36**	4.04	**H55'**	3.84
19' -CH-O	4.61[c]	**H37**	1.89		
H20		**H37'**	2.31		

[a] The symbol ' represents the less shielded proton of a geminal pair.

[b] Data recorded at 23 °C in $CDCl_3$ at 300 MHz with chemical shifts in ppm and referenced to $CHCl_3$, δ_H 7.25 ppm.

[c] Assignments of methylene pairs tentative - may be interchanged.

Table 4.3.2 ^{13}C NMR Data for Isohomohalichondrin B Di-osmate Ester (**4.3.1**)

Carbon	δ ppm[a]	Carbon	δ ppm[a]	Carbon	δ ppm[a]
C1		C21		C39	42.8
C2	41.0	C22		C40	71.4
C3		C23	75.4	C41	79.0
C4		C24	42.0	C-CH_3-42	
C5		C-CH_3-25		C-CH_3-42	17.5
C6	68.8	C-CH_3-25	15.4	C43	36.8
C7	78.0	26C-CH_2-O		C44	
C8	74.5	26C-CH_2-O	81.5[b]	C45	
C9	74.2	C27		C-CH_3-46	
C10	76.8	C28		C-CH_3-46	16.9
C11	82.5	C29		C47	76.1
C12	81.5	C30	77.2	C48	66.7
C13	48.5	C-CH_3-31		C49	45.4
C14		C-CH_3-31	15.0	C50	66.6
C15		C32	78.8	C51	76.5
C16		C33		C52	45.4
C17		C34		C53	
C18	35.0	C35		C54	46.2
19C-CH_2-O		C36		C55	58.3
19C-CH_2-O	88.1[b]	C37	36.8		
C20		C38			

a ^{13}C NMR spectral data assigned from HMQC experiment, recorded at 23° C in $CDCl_3$ at 300 MHz with chemical shifts in ppm.

b Assignments tentative - may be interchanged.

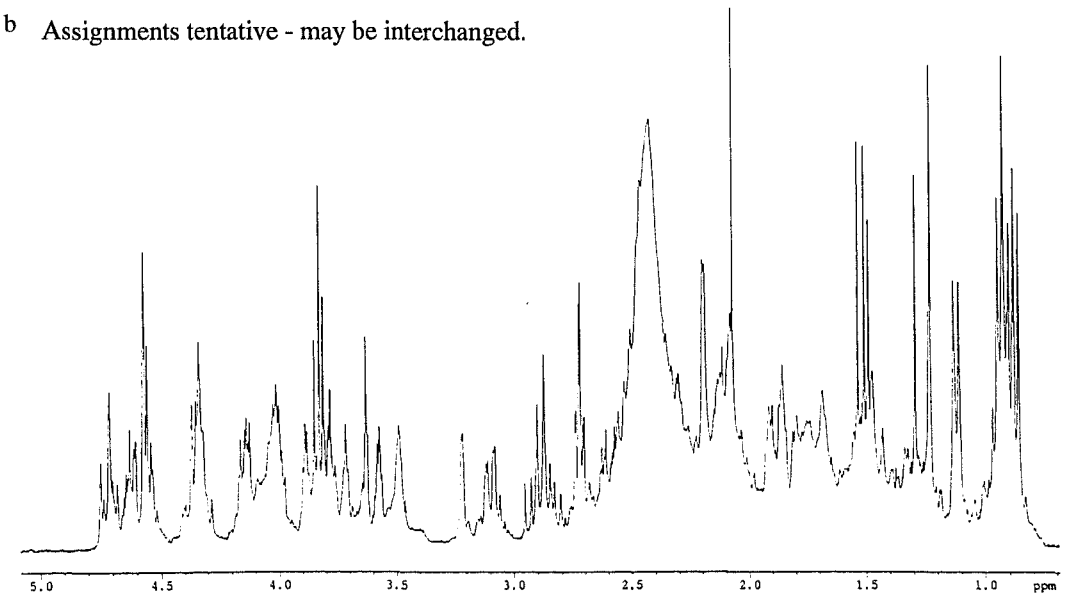

Figure 4.3.1 ^{1}H NMR Spectrum of Isohomohalichondrin B Di-osmate Ester (**4.3.1**)

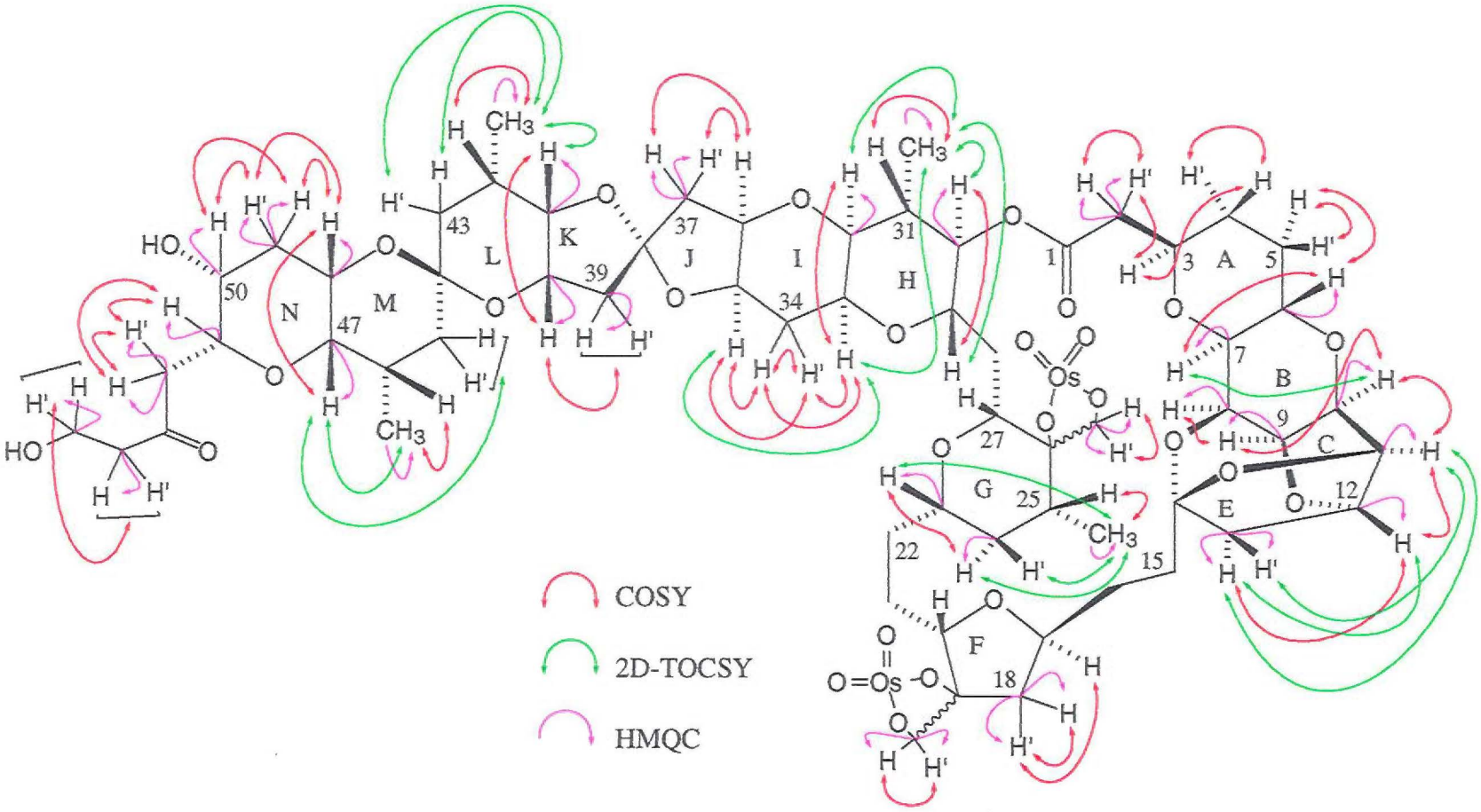

Figure 4.3.2 Isohomohalichondrin B Di-osmate Ester- Important NMR Correlations

One-sixth of this material was retained for bioassay and mass spectrometry analysis. The remaining five-sixths was used to produce the diketone. At this stage it was anticipated that FAB-MS would confirm the diol as the molecular ion as an analysis of the NMR data had not been undertaken. No parent ion corresponding to the diol product was detected. It was noted that the product was black in solution, and a subsequent analysis of the NMR data aroused the strong suspicion that the osmate ester (which is usually black[59]) had not been cleaved to form the diol at the bisulfite step. Repeated FAB-MS some time later was unable to detect the parent ion corresponding to the di-osmate ester product, perhaps indicating that decomposition of the product had occurred.

Prior to submitting the isohomohalichondrin B di-osmate ester (**4.3.1**) for biological evaluation, it was passed through a small C18 column to remove any remaining osmium tetroxide (which is cytotoxic), to remove the possibility of misinterpretation of the biological activity.

4.3.3 Periodate Cleavage of Isohomohalichondrin B Osmylation Product

The isohomohalichondrin B osmylation product (**4.3.1**) was cleaved to the diketone product of isohomohalichondrin B (**4.3.2**) by reaction with sodium periodate in a methanol/water[60] mix. The reaction was stirred at room temperature in the dark and monitored by silica TLC. The reaction was carried out in the dark, to avoid possible periodate decomposition.[61] Completion of the reaction, after four days, was

indicated by the formation of a single silica TLC spot of lower polarity relative to the osmylation product and of a similar polarity to that of isohomohalichondrin B.

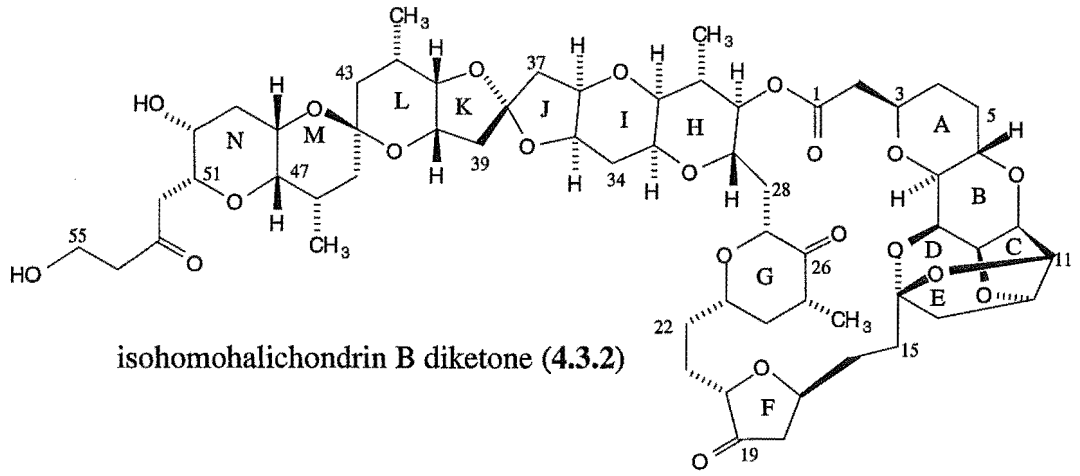

isohomohalichondrin B diketone (**4.3.2**)

A ^{1}H NMR spectrum of the product (**Figure 4.3.3**) showed several significant changes relative to the spectra of the osmylation product and isohomohalichondrin B (**1.2.9**). The CH_3-25 doublet was apparent at δ_H 1.09 ppm, in a more shielded position compared to the osmylation product CH_3-25 (δ_H 1.13 ppm) and slightly less shielded relative to isohomohalichondrin B (δ_H 1.05 ppm). The doublet at δ_H 1.13 ppm was still visible in the ^{1}H NMR spectrum of the product, contributing <8% to the total material (by integral), indicating the reaction yield was >92%. The region from δ_H 4.60 ppm to δ_H 4.70 ppm appeared to contain a reduced number of proton resonances when compared to the ^{1}H NMR spectrum of the osmylation product and this region appeared very similar to the ^{1}H NMR spectrum of isohomohalichondrin B.

A range of selective 1D and 2D NMR experiments (COSY, 2D-TOCSY (100 ms mixing time), NOE, HMQC and HMBC) were acquired from the product (**4.3.2**). An analysis of these data gave a partial assignment of the ^{1}H and ^{13}C NMR spectra of the product formed and indicated that ketone functionalities had been formed at C19 and C26. The important NMR correlations from these experiments are depicted in **Figure 4.3.4**. The ^{1}H and ^{13}C NMR data are cited in **Tables 4.3.3** and **4.3.4** respectively.

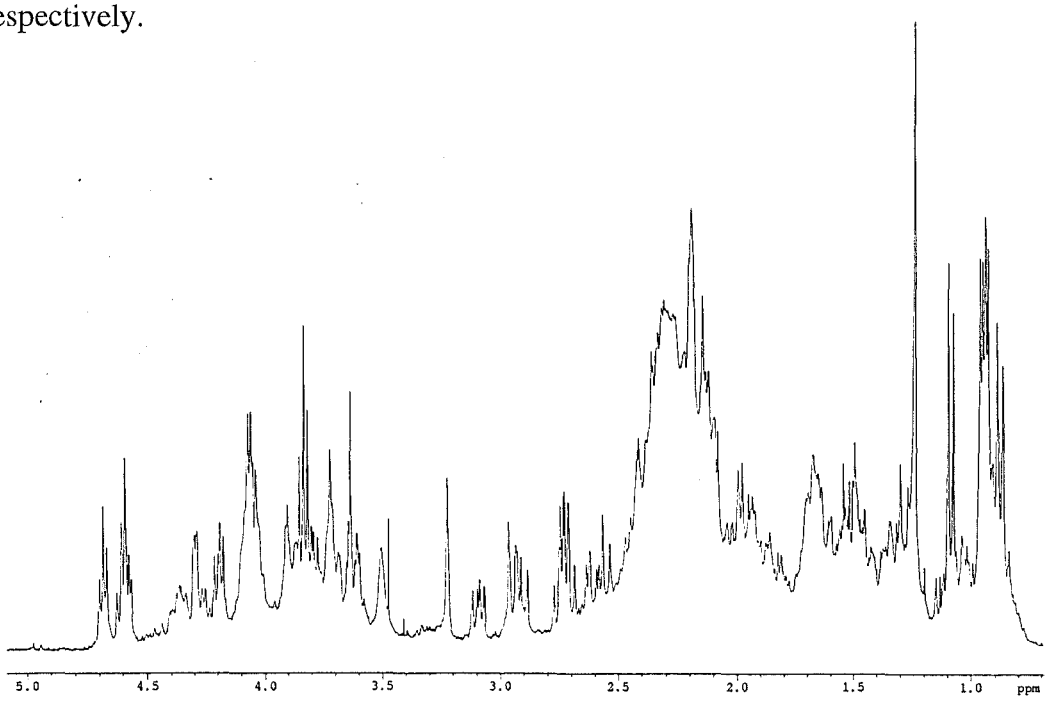

Figure 4.3.3 ^{1}H NMR Spectrum of Isohomohalichondrin B Diketone (**4.3.2**)

The HMBC spectrum of the product showed the presence of two new ^{13}C NMR signals situated at δ_C 208.9 ppm and δ_C 216.9 ppm, characteristic positions for carbonyl carbon resonances, which were assigned as C26 and C19 respectively. The C19 carbonyl carbon showed HMBC correlations to H20, H18 and H18', and the C26 carbonyl showed correlations to the H25, CH_3-25 and H24' protons. Unfortunately, no HMBC correlation was observed from C26 to the H27 proton. Apart from this region, the other ^{1}H and ^{13}C NMR chemical shifts were very similar to those of isohomohalichondrin B.

Table 4.3.3 ^{1}H NMR Data for Isohomohalichondrin B Diketone (**4.3.2**)

Proton[a]	δ ppm[b]	**Proton**[a]	δ ppm[b]	**Proton**[a]	δ ppm[b]
H2	2.38	**H21**		**H39**	2.22
H2'	2.59	**H21'**		**H39'**	2.22
H3	3.87	**H22**	1.69	**H40**	3.93
H4	1.33	**H22'**		**H41**	3.62
H4'	1.70	**H23**	3.76	**H42**	2.30
H5	1.38	**H24**	1.62	**CH_3-42**	0.94
H5'	2.12	**H24'**	2.00	**H43**	1.35
H6	4.26	**H25**	2.45	**H43'**	1.52
H7	2.95	**CH_3-25**	1.09	**H45**	1.49
H8	4.32	**H27**		**H45'**	1.49
H9	4.05	**H28**		**H46**	2.18
H10	4.20	**H28'**		**CH_3-46**	0.88
H11	4.60	**H29**	4.05	**H47**	3.25
H12	4.70	**H30**	4.62	**H48**	3.74
H13	1.96	**H31**	2.04	**H49**	1.85
H13'	2.18	**CH_3-31**	0.96	**H49'**	2.14
H15		**H32**	3.12	**H50**	3.53
H15'		**H33**	3.71	**H51**	3.81
H16		**H34**		**H52**	2.58
H16'	2.18	**H34'**		**H52'**	2.94
H17	4.39	**H35**	4.07	**H54**	2.75
H18	2.15	**H36**	4.12	**H54'**	2.75
H18'	2.74	**H37**	1.92	**H55**	3.85
H20	3.83	**H37'**	2.35	**H55'**	3.85

[a] The symbol ' represents the less shielded proton of a geminal pair.

[b] Data recorded at 23 °C in $CDCl_3$ at 300 MHz with chemical shifts in ppm and referenced to $CHCl_3$, δ_H 7.25 ppm.

Table 4.3.4 ^{13}C NMR Data for Isohomohalichondrin B Diketone (**4.3.2**)

Carbon	δ ppm[a]	Carbon	δ ppm[a]	Carbon	δ ppm[a]
C1	171.2	**C21**		**C39**	42.7
C2	39.5	**C22**		**C40**	71.5
C3	74.9	**C23**	74.0	**C41**	79.2
C4		**C24**	42.5	**C-CH$_3$-42**	
C5		**C-CH$_3$-25**	43.0	**C-CH$_3$-42**	17.8
C6	68.3	**C-CH$_3$-25**	14.8	**C43**	36.9
C7	78.4	**C26**	208.9	**C44**	
C8	75.2	**C27**		**C45**	37.2
C9		**C28**		**C-CH$_3$-46**	
C10	76.5	**C29**		**C-CH$_3$-46**	17.3
C11	82.5	**C30**	76.8	**C47**	76.1
C12	81.2	**C-CH$_3$-31**		**C48**	66.3
C13	48.2	**C-CH$_3$-31**	14.7	**C49**	
C14	110.0	**C32**	78.2	**C50**	66.4
C15		**C33**	77.2	**C51**	76.5
C16		**C34**		**C52**	
C17	73.8	**C35**		**C53**	211.1
C18		**C36**		**C54**	46.2
C19	216.9	**C37**		**C55**	58.3
C20		**C38**	112.5		

a ^{13}C NMR spectral data assigned from HMQC and HMBC experiments, recorded at 23°C in $CDCl_3$ at 300 MHz with chemical shifts in ppm.

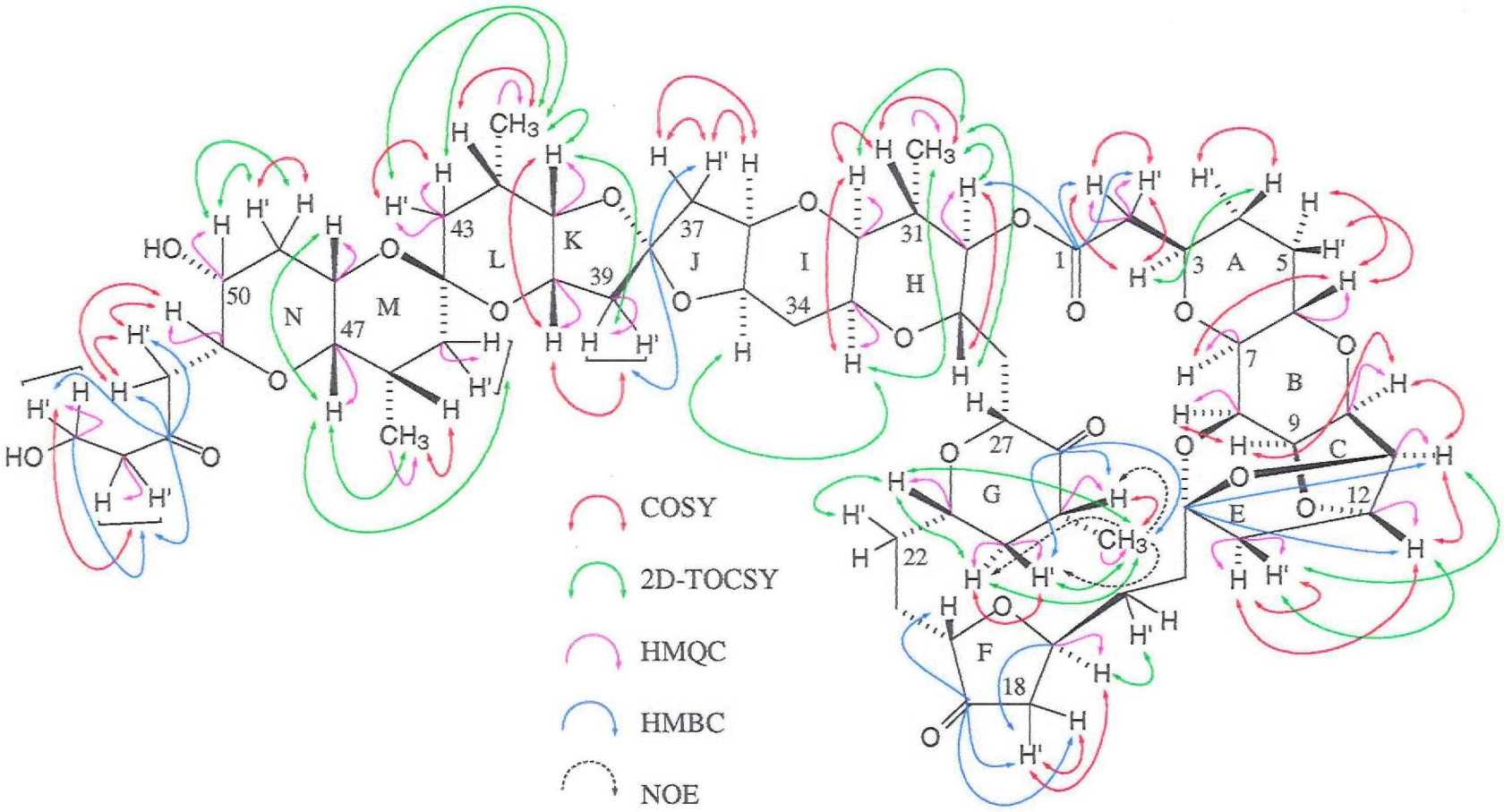

Figure 4.3.4 Isohomohalichondrin B Diketone- Important NMR Correlations

The periodate cleavage product (**4.3.2**) was subjected to HPLC and C18 column chromatography to remove any osmium tetroxide (or osmylation product) in the reaction mixture before submitting **4.3.2** for biological assay and MS.

The high resolution FAB-MS spectrum of **4.3.2** gave the parent ion (MK^+) corresponding to a molecular formula of $C_{59}H_{82}O_{21}$, a loss of two carbon and four hydrogen atoms and the addition of two oxygen atoms, relative to isohomohalichondrin B ($C_{61}H_{86}O_{19}$). This data confirmed the diketone of isohomohalichondrin B (**4.3.2**) was formed in the reaction.

4.3.4 Osmylation and Periodate Cleavage of Homohalichondrin B Diacetate

The hemi-synthesis of the diketone derivative of homohalichondrin B (**4.3.3**) provided the starting point for the production of two further derivatives. It was envisaged that the reaction of the diketone with an isotopically labelled ylide in a Wittig reaction would provide a labelled homohalichondrin B molecule that could be useful in pharmacokinetic studies. This reaction is discussed in Section 8.4.

The diketone of homohalichondrin B also provided the starting point for the sodium borohydride reduction of the C19 and C26 diketone, the idea being to increase the polarity in this region and thus provide useful structure-activity information. This reaction is discussed in Section 4.4.

The C19 and C26 diketone of isohomohalichondrin B (**4.3.2**) was not able to be used for the two further reactions described above, as the C53 ketone would be expected

to react under the conditions of both the Wittig and the sodium borohydride reactions. Alternatively, the use of homohalichondrin B to produce the diketone derivative necessitated protection of the terminal diol, which would be expected to cleave under the periodate oxidation conditions.

Reactivity tables[62] report that the diacetate derivative of a diol is stable to osmium tetroxide, bisulfite, sodium periodate, sodium borohydride and Wittig reaction conditions. Thus it was decided that protection of homohalichondrin B as a diacetate derivative would provide suitable protection for the planned reaction sequence. The diacetylation of homohalichondrin B was described in Section 3.2.1. The immediate objective was therefore to produce the homohalichondrin B diacetate diketone derivative (**4.3.3**).

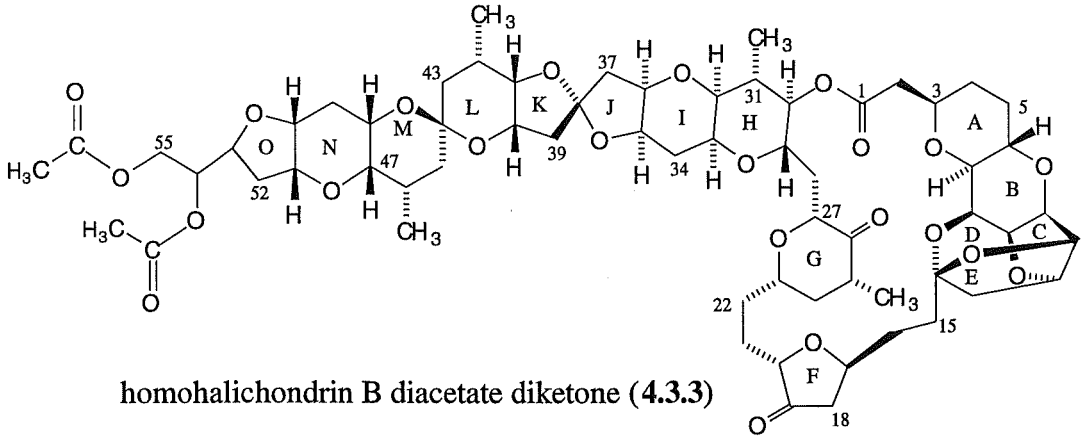

homohalichondrin B diacetate diketone (**4.3.3**)

The sodium periodate stability of the diacetate of homohalichondrin B (**3.2.2**, Section 3.2.1) was tested, under the conditions to be performed on the osmylation product, prior to committing the material to the initial osmylation. Silica TLC and a

^{1}H NMR spectrum (in $CDCl_3$/ 0.1% pyridine-d_5) of the material after work-up indicated that homohalichondrin B diacetate was unreactive under the periodate reaction conditions.

Having passed the stability test, an ether solution of osmium tetroxide was added to homohalichondrin B diacetate (**3.2.2**) dissolved in pyridine and stirred at room temperature for four and a half hours, followed by addition of sodium metabisulfite ($Na_2S_2O_5$) in water/pyridine. This mixture was stirred for twenty minutes at room temperature. Silica TLC of the product showed that no starting material remained.

A ^{1}H NMR spectrum obtained from the product (in $CDCl_3$/ 0.1% pyridine-d_5) indicated the presence of the two acetate CH_3 singlet signals at δ_H 2.04 ppm and δ_H 2.10 ppm and a quintet at δ_H 5.13 ppm corresponding to the H54 methine proton, indicating that the diacetate remained intact (**Figure 4.3.5**).

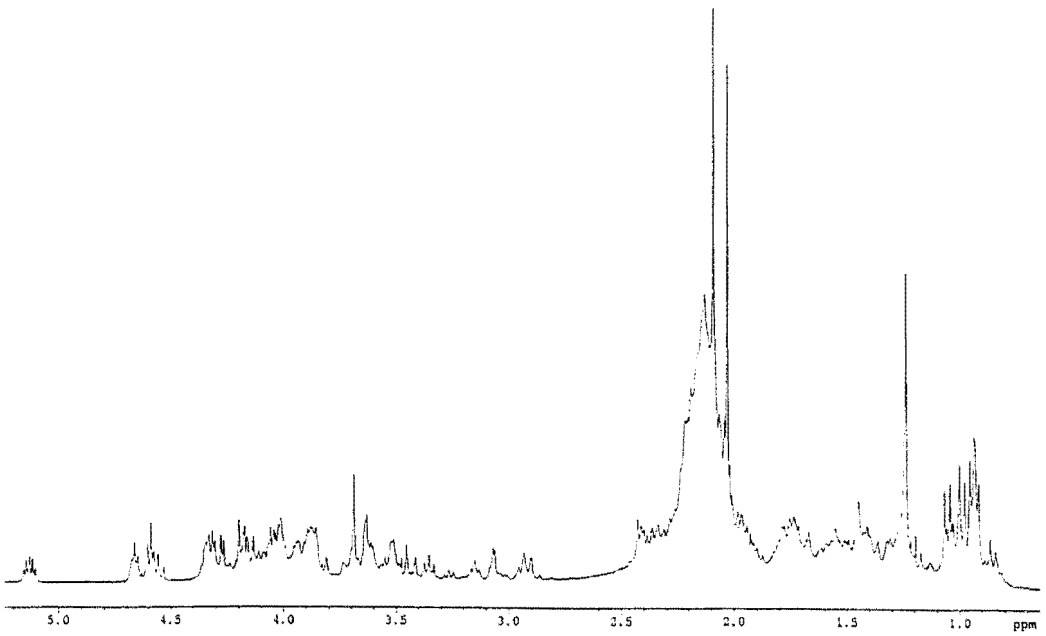

Figure 4.3.5 ^{1}H NMR Spectrum of Homohalichondrin B Diacetate Osmylation Product

Also apparent was the absence of the olefinic resonances from the spectrum. However, the Me-25 doublet appeared at δ_H 1.04 ppm compared to δ_H 1.13 ppm for the Me-25 resonance of the isohomohalichondrin B di-osmate ester (**4.3.1**). The ^1H NMR spectrum also showed an apparent reduction in the number of resonances in the δ_H 4.50 ppm to δ_H 4.80 ppm region relative to the ^1H NMR spectrum of the isohomohalichondrin B di-osmate ester (**Figure 4.3.1**). The resonances in this region of the spectrum were assigned as corresponding to the osmate ester methylene protons, H30, H11 and H12. These were resonances that would not have been expected to significantly alter in the ^1H NMR spectrum of the corresponding homohalichondrin B diacetate osmylation product derivative as they were well removed from the differing terminal moiety. Along with the difference in the chemical shift of the Me-25 protons, it suggested that the product in this case was more likely to be the diol at positions C19 and C26, with the new diastereotopic methylene protons obscured by other resonances in the *ca* δ_H 3.60 ppm to δ_H 4.00 ppm region of the spectrum. This material was subsequently committed for the periodate cleavage step.

The osmylation/bisulfite reaction material was dissolved in a methanol/water periodate solution, stirred in the dark at room temperature, and the reaction progress was monitored by silica TLC. The reaction was worked-up when silica TLC indicated the formation of a single, less polar spot relative to homohalichondrin B and the starting material, and the complete disappearance of homohalichondrin B diacetate osmylation product, after two days reaction. A ^1H NMR spectrum acquired from this material (in $CDCl_3$/ 0.1% pyridine-d_5 , **Figure 4.3.6**) indicated that the diacetate had remained intact during the reaction sequence as predicted. The characteristic Me-25 doublet that appeared at a chemical shift of δ_H 1.09 ppm in the ^1H NMR spectrum of the diketone of isohomohalichondrin B (**Figure 4.3.1**) was also observed for this product. A range of 2D NMR experiments were performed on

this product (*viz* COSY, 2D-TOCSY (100 ms mixing time), HMQC and HMBC experiments) which enabled a partial assignment of the ^{1}H and ^{13}C NMR spectra to be achieved (**Tables 4.3.5** and **4.3.6** respectively), and confirmed that the C19 and C26 diketone of homohalichondrin B diacetate (**4.3.3**) had been formed. The important correlations from these NMR experiments are summarised in **Figure 4.3.7**. The NMR data were consistent with those of the diketone of isohomohalichondrin B (**4.3.2**) in the region of the A-L rings.

Table 4.3.5 ^{1}H NMR Data for Homohalichondrin B Diacetate Diketone (**4.3.3**)

Proton[a]	δ ppm[b]	Proton[a]	δ ppm[b]	Proton[a]	δ ppm[b]
H2	2.38	**H21'**	1.92	**H40**	3.92
H2'	2.56	**H22**	1.65	**H41**	3.58
H3	3.87	**H22'**		**H42**	2.32
H4	1.29	**H23**	3.74	**CH_3-42**	0.93
H4'	1.70	**H24**	1.58	**H43**	1.30
H5	1.36	**H24'**	1.96	**H43'**	1.48
H5'	2.12	**H25**	2.44	**H45**	1.40
H6	4.26	**CH_3-25**	1.09	**H45'**	1.40
H7	2.95	**H27**		**H46**	2.12
H8	4.30	**H28**		**CH_3-46**	0.90
H9	4.05	**H28'**		**H47**	3.05
H10	4.19	**H29**	4.04	**H48**	3.51
H11	4.60	**H30**	4.60	**H49**	1.74
H12	4.68	**H31**	2.01	**H49'**	2.12
H13	1.94	**CH_3-31**	0.96	**H50**	3.88
H13'	2.17	**H32**	3.09	**H51**	4.02
H15	1.78	**H33**	3.70	**H52**	1.73
H15'	2.22	**H34**	1.80	**H52'**	1.98
H16		**H34'**	2.10	**H53**	4.34
H16'		**H35**		**C54-$OCOCH_3$**	2.10
H17	4.38	**H36**	4.09	**H54**	5.13
H18	2.15	**H37**	1.88	**C55-$OCOCH_3$**	2.04
H18'	2.73	**H37'**	2.34	**H55**	4.18
H20		**H39**	2.18	**H55'**	4.30
H21	1.45	**H39'**	2.18		

[a] The symbol ' represents the less shielded proton of a geminal pair.

[b] Data recorded at 23°C in $CDCl_3$ at 300 MHz with chemical shifts in ppm and referenced to $CHCl_3$, δ_H 7.25 ppm.

Table 4.3.6 ^{13}C NMR Data for Homohalichondrin B Diacetate Diketone (**4.3.3**)

Carbon	δ ppm[a]	Carbon	δ ppm[a]	Carbon	δ ppm[a]
C1	171.2	**C23**	73.4	**C-$\underline{C}H_3$-42**	17.4
C2	39.2	**C24**	41.7	**C43**	36.7
C3	74.2	**$\underline{C}$-CH_3-25**		**C44**	
C4		**C-$\underline{C}H_3$-25**	14.4	**C45**	36.5
C5		**C26**	208.6	**$\underline{C}$-CH_3-46**	
C6	68.1	**C27**		**C-$\underline{C}H_3$-46**	17.0
C7	77.8	**C28**		**C47**	72.7
C8	74.5	**C29**		**C48**	63.4
C9		**C30**	76.3	**C49**	
C10	76.2	**$\underline{C}$-CH_3-31**		**C50**	74.2
C11	82.1	**C-$\underline{C}H_3$-31**	14.0	**C51**	76.2
C12	80.8	**C32**	78.2	**C52**	
C13	48.0	**C33**	66.1	**C53**	75.9
C14	110.1	**C34**		**C54**	72.2
C15	33.2	**C35**		**C54-O$\underline{C}$OCH_3**	170.7
C16		**C36**		**C54-OCO$\underline{C}H_3$**	20.6
C17	73.2	**C37**	42.8	**C55**	63.6
C18	42.7	**C38**		**C55-O$\underline{C}$OCH_3**	170.7
C19	217.0	**C39**	42.1	**C55-OCO$\underline{C}H_3$**	20.4
C20		**C40**	70.5		
C21		**C41**	79.2		
C22		**$\underline{C}$-CH_3-42**			

a ^{13}C NMR spectral data assigned from HMQC and HMBC experiments, recorded at 23 °C in $CDCl_3$ at 300 MHz with chemical shifts in ppm.

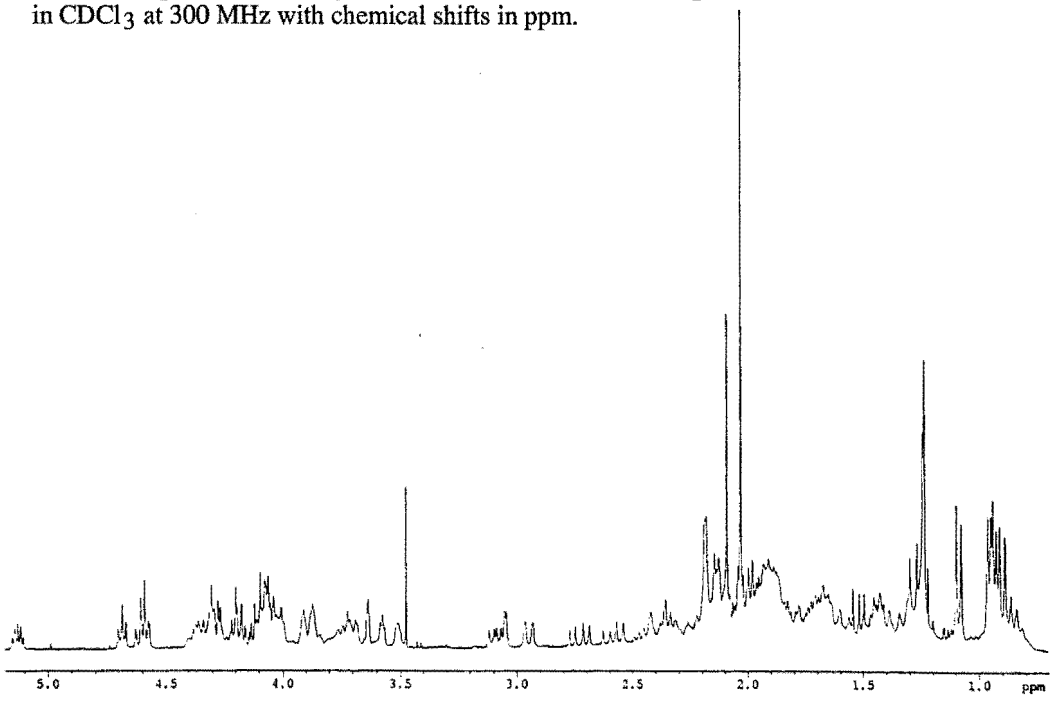

Figure 4.3.6 ^{1}H NMR Spectrum of Homohalichondrin B Diacetate Diketone (**4.3.3**)

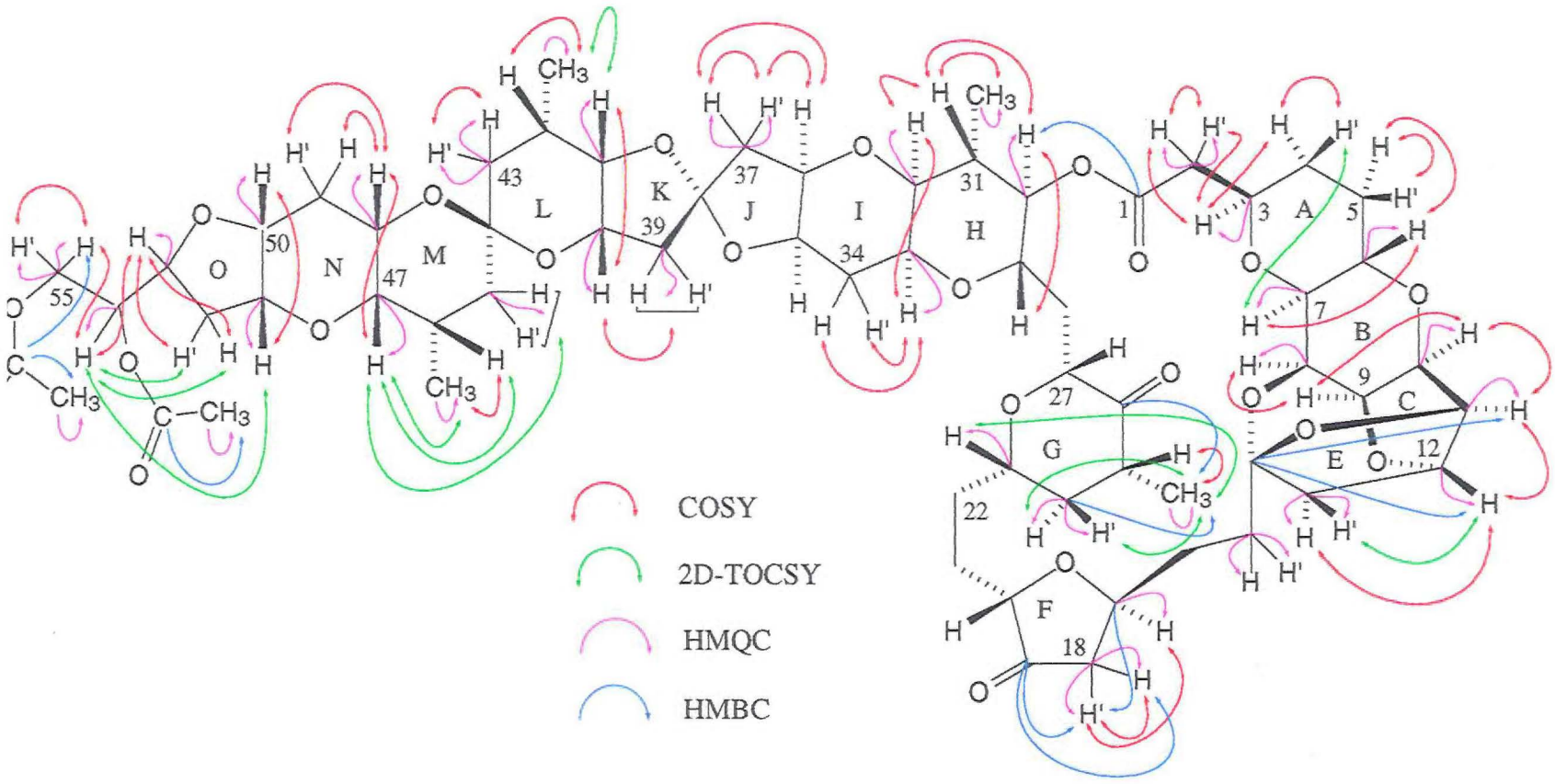

Figure 4.3.7 Homohalichondrin B Diacetate Diketone- Important NMR Correlations

These reactions provided the material for the Wittig reaction described in Section 8.4. It was necessary to repeat the reactions described above, on a similar scale, to yield sufficient material for the sodium borohydride reduction reaction (Section 4.4). A malfunction of a micropipette during the addition of osmium tetroxide, resulting in the delivery of less than a two-fold molar quantity of osmium tetroxide solution to homohalichondrin B diacetate, provided interesting evidence of the differential reactivity of the C19 and C26 olefinic groups. A ^{1}H NMR spectrum of the osmium tetroxide/bisulfite work-up material indicated that the CH_2=26 olefinic protons (δ_H 4.75 ppm and δ_H 4.80 ppm) had completely disappeared and that the CH_2=19 olefinic protons at δ_H 4.91 ppm and δ_H 4.98 ppm were *ca* 20-25 % of their original size in terms of integral. This indicated that the CH_2=26 group had reacted more readily under these conditions than the corresponding CH_2=19 group. The Uemura *et al* X-ray crystal structure conformation of norhalichondrin A[17] and the solution conformations of halichondrin B and homohalichondrin B indicated by NMR spectroscopy (described in Sections 2.3 and 2.4 respectively), which suggested that the CH_2=19 group was directed into the lactone ring and was less exposed than the CH_2=26 group which pointed towards the outside of the lactone, were consistent with this observation. This material was then re-reacted with osmium tetroxide/bisulfite prior to periodate cleavage, as described previously, to produce the diketone derivative of homohalichondrin B diacetate (**4.3.3**).

4.4 Homohalichondrin B Diacetate Diketone Reduction

Homohalichondrin B diacetate diketone (**4.3.3**) was dissolved in 20% dichloromethane/isopropyl alcohol. A suspension of sodium borohydride in isopropyl alcohol was added to **4.3.3** in solution; the resulting suspension was stirred at room temperature and the reaction monitored by silica TLC. After eighteen hours reaction, silica TLC indicated the formation of two more polar spots relative to both homohalichondrin B (**1.2.9**) and the starting material (**4.3.3**), and the absence of starting material in the reaction mixture.

A ^{1}H NMR spectrum of the product acquired in $CDCl_3$/0.1% pyridine-d_5 indicated the material was a mixture of at least two different components. It appeared from this spectrum that the C19 ketone had fully reacted, as the distinctive H18' methylene proton signal at δ_H 2.73 ppm had moved. Also obvious in this spectrum was the unexpected loss of one of the terminal acetate groups, as the H54 quintet was not present, and only one of the CH_3 proton singlet resonances remained. The methyl region of the spectrum also indicated several overlapping resonances, with the δ_H 1.09 ppm CH_3-25 doublet of the starting material no longer present. Separation of the two components that were visible by TLC was achieved on a small diol column, providing sufficient material to perform a ^{1}H NMR spectrum of each.

The ^{1}H NMR spectrum of the least polar fraction indicated that it was probably still a mixture of several components as the methyl region of the spectrum was still complex. However, the CH_3-25 doublet that appeared at δ_H 1.09 ppm in the spectrum of **4.3.3** had moved to a more shielded position. There was insufficient material to make further progress with these products.

The ^{1}H NMR spectrum of the more polar fraction also indicated a mixture of components were present, and that only one acetate group remained intact. A methyl doublet appeared at a relatively deshielded position in the spectrum at a chemical shift of δ_H 1.14 ppm. Again, there was insufficient material to make further progress with these products.

It appeared that the unexpected cleavage of an acetate group had occurred during the reaction, and although it was likely that the products represented the C19 and C26 alcohol derivatives with four diastereoisomeric product combinations possible, it would have been impossible to determine the identity of the products without committing more material to the reaction to obtain mass spectrometry data and generate good NMR data that would aid in the analysis.

4.5 Hydrogenation

Two methods of hydrogenation were attempted to gain access to the C19 and C26 methyl derivatives of homohalichondrin B (**4.5.1**); using palladium on carbon[63] as a catalyst and by using Adams' catalyst.[64]

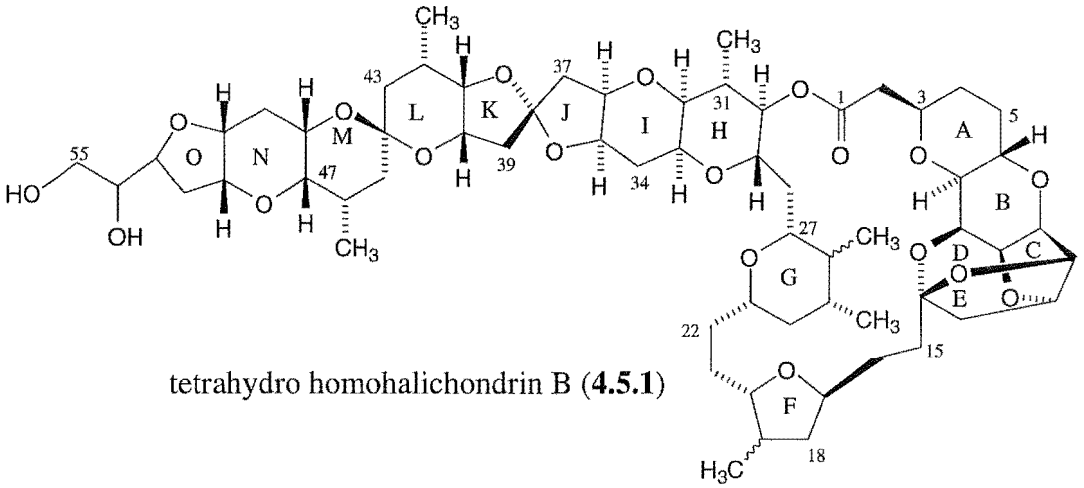

tetrahydro homohalichondrin B (**4.5.1**)

It was anticipated that **4.5.1** would provide useful biological activity data as to the relative importance of the sp^2 hybridisation of the C19 and C26 centres. Although it is possible to produce four diastereoisomers from this reaction, it was recognised that the relative inaccessibility of the hydrogen bound catalyst to one face of the C19 olefin could result in only two possible diastereoisomers being produced.

4.5.1 Catalyst : Palladium on Carbon

Homohalichondrin B (**1.2.3**) dissolved in ethanol was stirred over 0.5% palladium on carbon catalyst under hydrogen at a slightly positive atmospheric pressure. After stirring the reaction overnight at room temperature there was no apparent reaction by ^{1}H NMR spectroscopy, as the spectrum was identical with that of homohalichondrin B. The reaction was then attempted using an alternative hydrogenation catalyst- Adams' catalyst.

4.5.2 Catalyst : Adams' Catalyst

A suspension of Adams' catalyst (PtO_2) in ethyl acetate was pre-reduced under hydrogen for thirty minutes prior to the introduction of homohalichondrin B (**1.2.3**). A ^{1}H NMR spectrum of the product, after four hours reaction at ambient temperature, was acquired in $CDCl_3$/ 0.1% pyridine-d_5, and is displayed in **Figure 4.5.1**. The spectrum indicated the complete disappearance of the olefinic CH_2=19 and CH_2=26 proton resonances of homohalichondrin B, and the movement of the distinctive homohalichondrin B H18' multiplet at δ_H 2.79 ppm. The reaction was therefore assumed to have gone to completion, with no homohalichondrin B (**1.2.3**) detectable by ^{1}H NMR spectroscopy. A range of selective 1D and 2D NMR experiments were performed on this material, *ie* COSY, 1D and 2D-TOCSY (100 ms mixing time), HMQC and NOE experiments. The important connectivities established from these experiments are depicted in **Figure 4.5.2**. The corresponding ^{1}H and ^{13}C NMR data are summarised in **Tables 4.5.1** and **4.5.2** respectively.

Table 4.5.1 ^{1}H NMR Data for Tetrahydro Homohalichondrin B (**4.5.1**)

Proton[a]	δ ppm[b]	Proton[a]	δ ppm[b]	Proton[a]	δ ppm[b]
H2	2.39	**H21**		**H39**	2.18
H2'	2.52	**H21'**		**H39'**	2.18
H3	3.92	**H22**	1.55	**H40**	3.92
H4	1.36	**H22'**	1.55	**H41**	3.55
H4'	1.78	**H23**	3.28	**H42**	2.32
H5	1.35	**H24**	0.98	**CH_3-42**	0.91
H5'	2.08	**H24'**	1.18	**H43**	1.23
H6	4.38	**H25**		**H43'**	1.44
H7	2.94	**CH_3-25**		**H45**	1.40
H8	4.30	**H26**		**H45'**	1.40
H9	4.04	**CH_3-26**		**H46**	2.15
H10	4.19	**H27**		**CH_3-46**	0.90
H11	4.60	**H28**		**H47**	3.06
H12	4.67	**H28'**		**H48**	3.53
H13	1.89	**H29**	3.97	**H49**	1.75
H13'	2.13	**H30**	4.67	**H49'**	2.13
H15		**H31**	1.98	**H50**	3.90
H15'		**CH_3-31**	0.96	**H51**	4.04
H16		**H32**	3.12	**H52**	1.98
H16'		**H33**	3.68	**H52'**	1.98
H17		**H34**	1.80	**H53**	4.25
H18		**H34'**	2.12	**H54**	3.55
H18'		**H35**	4.10	**H55**	3.66
H19		**H36**	4.10	**H55'**	3.66
CH_3-19		**H37**	1.86		
H20		**H37'**	2.33		

[a] The symbol ' represents the less shielded proton of a geminal pair.

[b] Data recorded at 23 °C in $CDCl_3$ at 300 MHz with chemical shifts in ppm and referenced to $CHCl_3$, δ_H 7.25 ppm.

Table 4.5.2 ^{13}C NMR Data for Tetrahydro Homohalichondrin B (**4.5.1**)

Carbon	δ ppm[a]	Carbon	δ ppm[a]	Carbon	δ ppm[a]
C1		**C21**		**C38**	
C2	40.4	**C22**	32.5	**C39**	42.3
C3	74.6	**C23**	74.5	**C40**	70.6
C4		**C24**	34.8	**C41**	79.2
C5		**C-CH_3-25**		**C-CH_3-42**	
C6	68.0	**C-CH_3-25**		**C-CH_3-42**	17.4
C7	77.5	**C-CH_3-26**		**C43**	
C8	73.9	**C-CH_3-26**		**C44**	
C9		**C27**		**C45**	
C10	76.3	**C28**		**C-CH_3-46**	
C11	81.9	**C29**		**C-CH_3-46**	17.3
C12	80.8	**C30**	77.0	**C47**	72.5
C13	48.0	**C-CH_3-31**		**C48**	63.7
C14		**C-CH_3-31**	14.6	**C49**	31.2
C15		**C32**	75.7	**C50**	73.0
C16		**C33**	66.0	**C51**	76.0
C17		**C34**		**C52**	36.8
C18		**C35**		**C53**	79.5
C19		**C36**		**C54**	71.9
C20		**C37**	43.0	**C55**	65.7

a ^{13}C NMR spectral data assigned from HMQC experiment, recorded at 23 °C in $CDCl_3$ at 300 MHz with chemical shifts in ppm.

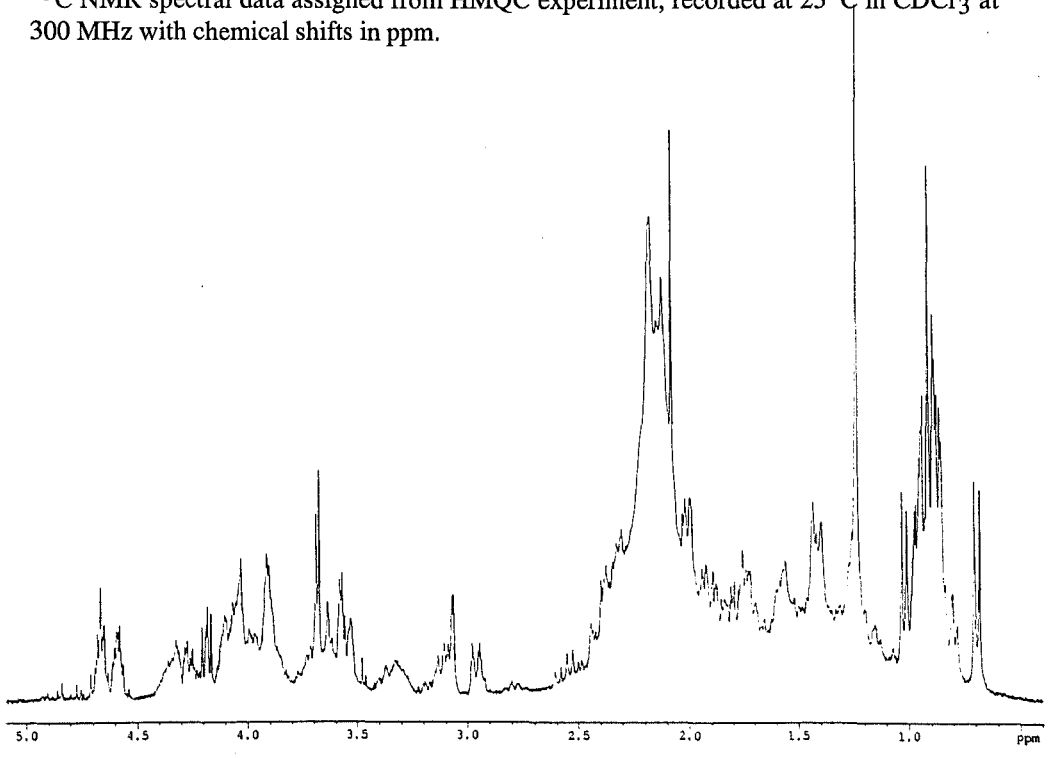

Figure 4.5.1 ^{1}H NMR Spectrum of Tetrahydro Homohalichondrin B (**4.5.1**)

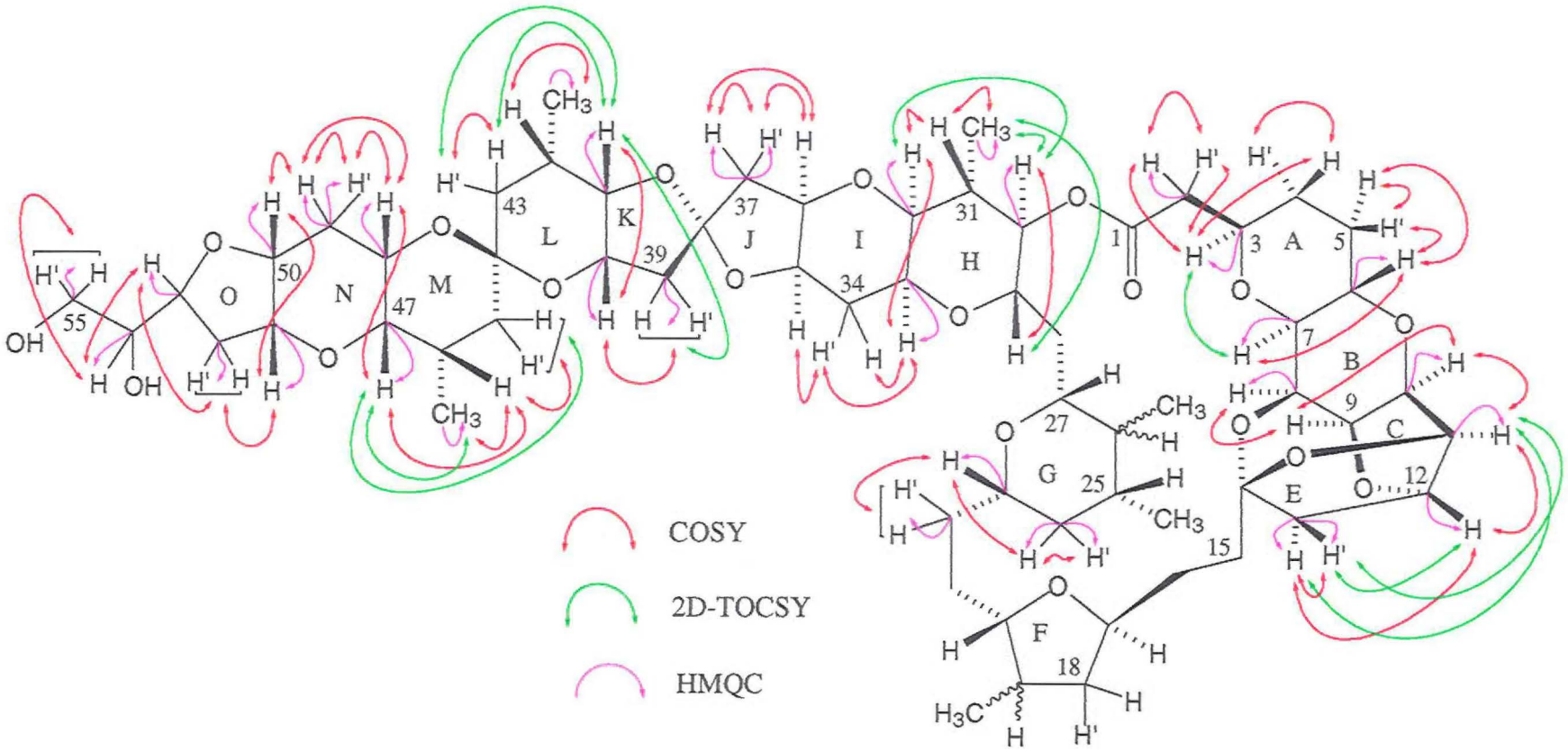

Figure 4.5.2 Tetrahydro Homohalichondrin B- Important NMR Correlations

Analysis of the NMR experiments performed on the hydrogenation product(s) indicated that the A-E and H-O rings were intact, and that the ^{1}H and ^{13}C NMR data were consistent with those of homohalichondrin B (**1.2.3**) in these regions. It proved difficult to assign chemical shifts around the F and G rings. The HMQC spectrum showed at least five new C-H correlations in the methyl region, and three correlations corresponding to CH_3-46, CH_3-42 and CH_3-31 which appeared at similar chemical shifts to those of homohalichondrin B. The observation of at least five new correlations in the HMQC spectrum implied that there were diastereoisomers present. However, the assignment of the individual diastereoisomers was not possible due to the complex nature of the spectra in the methyl region. An HMQC correlation at δ_H 0.69 ppm/δ_C 5.2 ppm appeared as an isolated doublet in the ^{1}H NMR spectrum of the homohalichondrin B hydrogenation products (**Figure 4.5.1**). A doublet appearing in this region is characteristic of methyl protons coupled to a methine proton on a directly attached carbon, and this signal also showed a 2D-TOCSY correlation to another methyl doublet signal at δ_H 0.88 ppm. These two methyl groups probably represented an individual diastereoisomer of the C25-C26 dimethyl system. It was also possible to assign chemical shifts for the H24 and H24' methylene protons, the C24 carbon, the H23 proton, the C23 carbon and the H22/H22' protons and C22 carbon based on COSY, 2D-TOCSY and HMQC connectivities.

High resolution FAB-MS showed the presence of the MNa^+ parent ion corresponding to a molecular formula of $C_{61}H_{90}O_{19}$, representing a gain of four hydrogen atoms relative to homohalichondrin B. This confirmed that the hydrogenation of homohalichondrin B had been successful and the tetrahydro homohalichondrin B derivatives (**4.5.1**) had been formed.

4.6 Biological Activity Data

The biological activity results for selected derivatives described in this Chapter are listed in **Table 4.6.1**. Included in this table are the P388 cytotoxicities of the diketone derivative (**4.3.2**), the di-osmate ester derivative (**4.3.1**), the tetrahydro reduction product (**4.5.1**) and the relevant parent halichondrins. Also included in this table are the cytotoxicities of these derivatives and the parent halichondrins which underwent testing in the NCI's primary screening system (GI_{50}s over all sixty cell lines) against selected tumour cell lines. Also included are the COMPARE correlation coefficients for the NCI tested compounds.

Table 4.6.1 *In Vitro* Cytotoxicities of Selected Halichondrins

Compound	P388 IC_{50} (ng/mL)	NCI GI_{50} ($\times 10^{-10}$ M)	COMPARE Correlation[a]
homohalichondrin B (1.2.3)	0.22	3.16	0.95
isohomohalichondrin B (1.2.9)	0.18	1.15	0.74
isohomohalichondrin B di-osmate ester (4.3.1)	>1250	>1000	<0.71
isohomohalichondrin B diketone (4.3.2)	21.9	95.5	0.82
tetrahydro homohalichondrin B (4.5.1)	12.6	362	0.87

a Correlation coefficient from the *Compare* pattern-recognition algorithm were calculated by computer using the GI_{50}-centred mean graph profiles of differential cellular sensitivities to each of the compounds. The GI_{50}-centred mean graph profile of halichondrin B was used as the "seed" for all of the comparisons.

From the data in **Table 4.6.1** it can be seen that there was a significant reduction in the cytotoxicity which was observed for all three derivatives in the P388 assay relative to their parent halichondrins. The isohomohalichondrin B di-osmate ester derivative (**4.3.1**) was inactive in terms of the IC_{50} and the GI_{50} result, relative to isohomohalichondrin B. The COMPARE correlation coefficient for the di-osmate ester of <0.71 suggested that this derivative had lost the ability to act as a polymerisation inhibitor of tubulin. The loss of activity observed for the isohomohalichondrin B di-osmate ester (**4.3.1**) probably reflected the conformational changes arising from a change to sp^3 hybridisation, and an increase in polarity and bulk of the osmate esters at C19 and C26.

It was interesting to see the return of activity upon cleavage of the osmylation product to produce the diketone derivative of isohomohalichondrin B (**4.3.2**). A <8% contribution of uncleaved osmylation product to the diketone of isohomohalichondrin B (as discussed in Section 4.3.3) would be expected result in a <8% decrease in the observed biological activity. This is not considered particularly significant in terms of the biological nature of the assays. An eighty-fold reduction in biological activity was observed in the NCI primary screen for isohomohalichondrin B diketone (**4.3.2**) relative to isohomohalichondrin B (**1.2.9**) in terms of the GI_{50} result. This implied that the maintenance of sp^2 character was not the only requirement for the C19 and C26 centres, but the nature of the substituent was also an important contributor to the expression of biological activity. It appeared that the relatively polar nature of the ketones, the absence of attached hydrogens and/or the conformational consequences of this, lead to the observed reduction in activity.

In considering of the biological activity of the tetrahydro homohalichondrin B diastereoisomers (**4.5.1**), it was assumed that the P388 assay result and the NCI GI_{50}

result represented an average result for all the diastereoisomers produced. A sixty-fold reduction in the P388 activity for **4.5.1** relative to homohalichondrin B (**1.2.3**) indicated the relative importance of maintaining the sp^2 nature and geometry of the C19 and C26 centres to retain the biological activity of the halichondrins. The GI_{50} result was over a hundred fold less active than homohalichondrin B (**1.2.3**). It appeared that the P388 cell line was slightly less sensitive than the averaged NCI cell line to this modification. The relatively high COMPARE correlation (0.87) suggested that the tetrahydro homohalichondrin B (**4.5.1**) derivative was still able to display a similar antimitotic mean-graph profile to that of halichondrin B (**1.2.1**) and homohalichondrin B (**1.2.3**).

In general terms, these results indicated the relative importance of the C19 and C26 olefinic groups in the expression of biological activity. It appeared that it was not just the sp^2 nature of the C19 and C26 centres that governed the expression of biological activity; it appeared that there was a specific requirement for the attached groups to be olefinic.

The biological activities of these derivatives in relation to other halichondrin derivatives are discussed further in Chapter 9.

CHAPTER 5

Lactone Alterations

5.1 Introduction

The twenty-two membered lactone ring (C1-C30), a characteristic functionality of the halichondrins, was targeted in an investigation of its relative importance to the expression of biological activity in the halichondrin series.

Efforts were initially focused on opening the C1-O-C30 linkage *via* methanolysis. Methanolysis was initially attempted on a small quantity of isohomohalichondrin B (**1.2.9**), before scaling up the reaction. The methanolysis of homohalichondrin B (**1.2.3**) was subsequently undertaken. A reductive cleavage of the lactone was also attempted on homohalichondrin B.

5.2 Methanolysis

5.2.1 Methanolysis of Isohomohalichondrin B

A solution of sodium methoxide in methanol was added to a small quantity of isohomohalichondrin B (**1.2.9**). The reaction was stirred at room temperature, monitoring the reaction by silica TLC. After two hours, no reaction was apparent by TLC so the sodium methoxide concentration was increased, and the reaction was stirred overnight. After this time, silica TLC indicated the appearance of a single spot of reduced polarity relative to isohomohalichondrin B, and the disappearance of starting material from the reaction mixture. The reaction was worked-up and silica TLC of the product showed a single, *more polar* spot relative to isohomohalichondrin B. An account of these observations, in light of the identified product, is discussed later. A ^{1}H NMR spectrum of the product, performed in $CDCl_3$/ 0.1% pyridine-d_5, indicated no starting material was present and that there were several major changes relative to the ^{1}H NMR spectrum of isohomohalichondrin B. Notable changes were apparent in the methyl region of the spectrum, with the movement of the methyl doublet at δ_H 1.00 ppm (CH_3-31) to a new position at δ_H 1.13 ppm. At δ_H 3.33 ppm in the ^{1}H NMR spectrum, a new singlet signal was apparent (integral corresponding to three protons); a characteristic position and appearance of a methoxyl resonance. Also apparent was the movement of the H32 resonance (from δ_H 3.20 ppm) and the H18' resonance (from δ_H 2.80 ppm), and the movement of other signals into this region of the spectrum.

The reaction was repeated on a larger scale, giving a product with a ^{1}H NMR spectrum (**Figure 5.2.1**, in $CDCl_3$/ 0.1% pyridine-d_5) identical to that from the

previous reaction. This material was combined with that of the previous reaction and a series of NMR experiments were performed (*viz* DQ COSY, 2D-TOCSY (100 ms mixing time), NOE, NOESY, HMQC and HMBC experiments). A partial assignment of the ^{1}H and ^{13}C NMR spectra was achieved from an analysis of the NMR experiments. These assignments are given in **Tables 5.2.1** (^{1}H NMR data) and **5.2.2** (^{13}C NMR data), and the important correlations from the NMR experiments are depicted in **Figure 5.2.2**.

Table 5.2.1 ^{1}H NMR Data for Lactone-Opened Isohomohalichondrin B (**5.2.1**)

Proton[a]	δ ppm[b]	**Proton**[a]	δ ppm[b]	**Proton**[a]	δ ppm[b]
H2		**H21**	1.67	**H39**	2.22
H2'		**H21'**		**H39'**	2.22
H3	3.84	**H22**	1.62	**H40**	3.92
H4	1.42	**H22'**	1.62	**H41**	3.63
H4'	1.78	**H23**	3.60	**H42**	2.27
H5	1.40	**H24**	1.07	**CH_3-42**	0.95
H5'	2.06	**H24'**	1.77	**H43**	1.32
H6	4.27	**H25**	2.26	**H43'**	1.52
H7	2.96	**CH_3-25**	1.06	**H45**	1.45
H8	4.52	**26=CH**	4.81	**H45'**	1.45
H9	4.06	**26'=CH**	4.90	**H46**	2.12
H10	4.18	**H27**	3.95	**CH_3-46**	0.90
H11	4.60	**H28**	1.96	**H47**	3.23
H12	4.66	**H28'**	2.05	**H48**	3.73
H13	1.96	**H29**	3.66	**H49**	1.83
H13'	2.16	**H30**	3.18	**H49'**	2.12
H15		**H31**	1.84	**H50**	3.49
H15'		**CH_3-31**	1.13	**H51**	3.80
H16		**H32**	3.36	**H52**	2.63
H16'		**H33**	3.84	**H52'**	2.90
H17	4.05	**H34**	1.94	**H54**	2.74
H18	2.22	**H34'**	2.05	**H54'**	2.74
H18'	2.64	**H35**	4.14	**H55**	3.63
19=CH	4.86	**H36**	4.06	**H55'**	3.63
19'=CH	4.95	**H37**	1.96	**C55-OCH_3**	3.33
H20	4.48	**H37'**	2.40		

[a] The symbol ' represents the less shielded proton of a geminal pair.

[b] Data recorded at 23 °C in $CDCl_3$ at 300 MHz with chemical shifts in ppm and referenced to $CHCl_3$, δ_H 7.25 ppm.

Table 5.2.2 ^{13}C NMR Data for Lactone-Opened Isohomohalichondrin B (**5.2.1**)

Carbon	δ ppm[a]	Carbon	δ ppm[a]	Carbon	δ ppm[a]
C1		C21		C39	43.6
C2		C22		C40	71.3
C3	76.2	C23	77.8	C41	79.0
C4		C24	42.5	C-CH_3-42	25.5
C5		C-CH_3-25	35.9	C-CH_3-42	17.0
C6	68.3	C-CH_3-25	17.5	C43	36.8
C7	77.3	26C=CH_2		C44	97.2
C8	74.3	26C=CH_2		C45	
C9	73.9	C27	75.3	C-CH_3-46	
C10	75.4	C28		C-CH_3-46	16.5
C11	82.2	C29	73.4	C47	76.0
C12	81.0	C30	72.1	C48	66.3
C13	46.9	C-CH_3-31	39.2	C49	
C14	110.4	C-CH_3-31	15.0	C50	66.2
C15		C32	76.9	C51	76.2
C16		C33	66.5	C52	45.0
C17	76.8	C34		C53	207.9
C18	38.6	C35	75.4	C54	43.7
19C=CH_2		C36	75.0	C55	67.1
19C=CH_2		C37	45.0	C55-OCH_3	58.6
C20	79.7	C38	112.0		

[a] Data recorded at 23°C in $CDCl_3$ with chemical shifts in ppm, assigned from HMQC and HMBC spectra at 300 MHz.

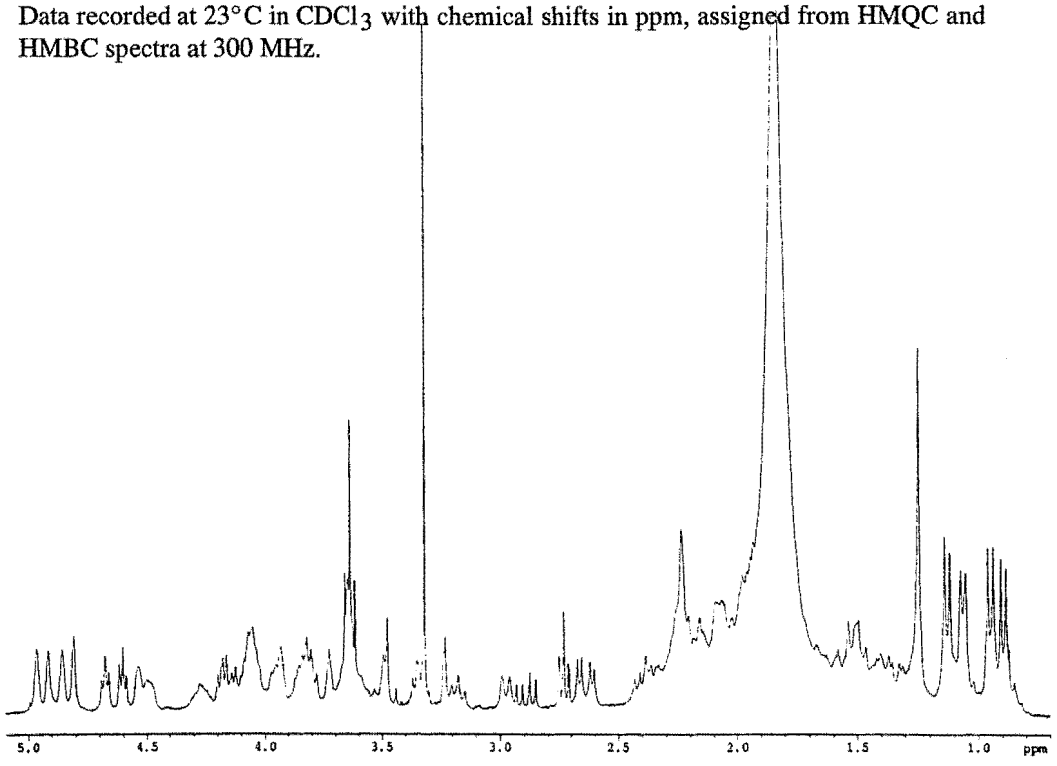

Figure 5.2.1 ^{1}H NMR Spectrum of Lactone-Opened Isohomohalichondrin B (**5.2.1**)

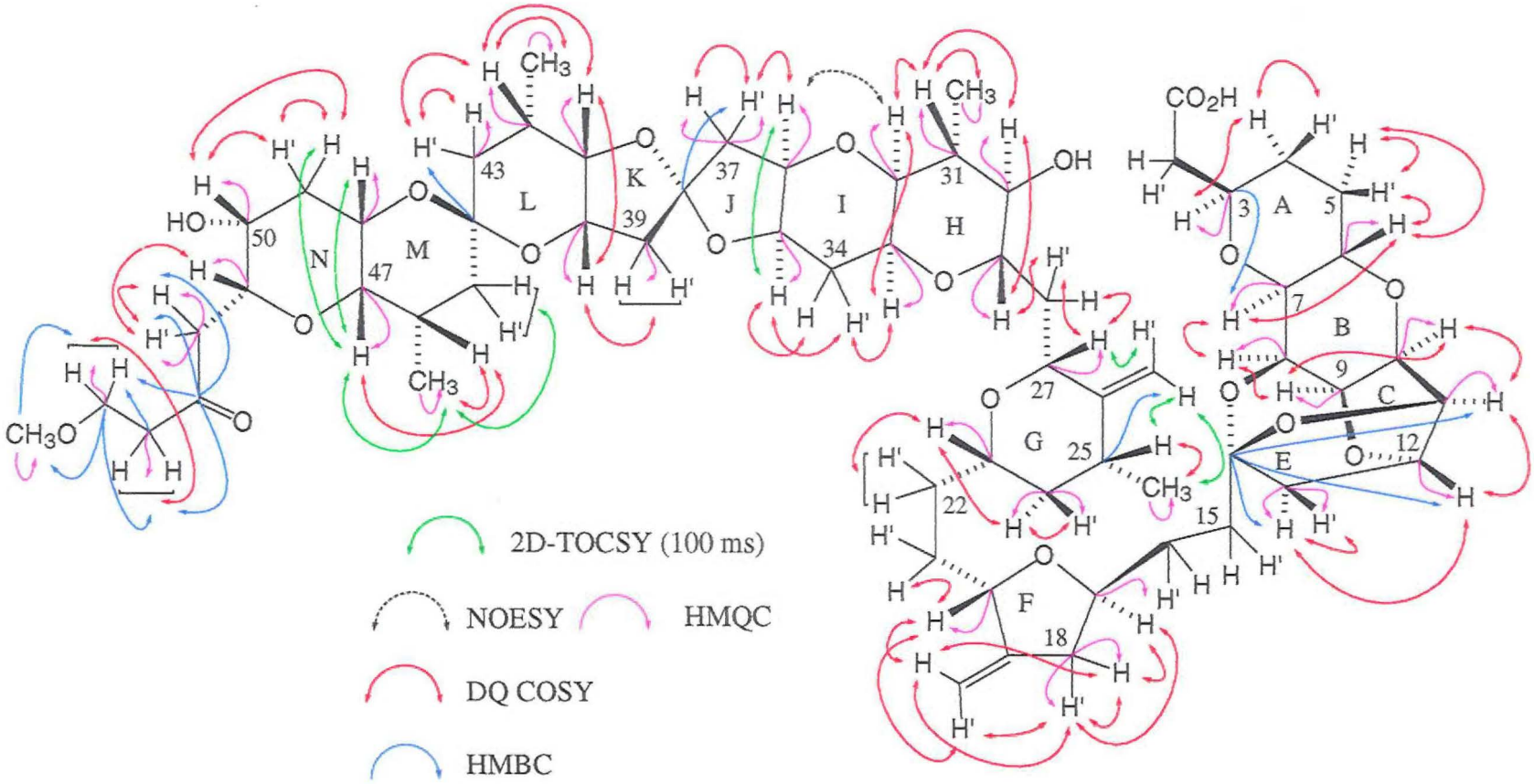

Figure 5.2.2 Lactone-Opened Isohomohalichondrin B- Important NMR Correlations

Analysis of the NMR data indicated that the methoxyl group was not attached at the C1 position, but at the terminal C55 position. An isolated HMQC correlation was observed for the methoxyl group carbon at δ_C 58.6 ppm to the methoxyl protons (δ_H 3.33 ppm). An HMBC correlation was observed from this carbon to the H55/H55' protons at δ_H 3.63 ppm. The C55 carbon at δ_C 67.1 ppm showed an HMBC correlation to the H54/H54' protons (δ_H 2.74 ppm) and to the methoxyl protons at δ_H 3.33 ppm. The observed ^{1}H NMR chemical shifts in this region were consistent with those observed for Me-isohomohalichondrin B-b (**1.2.12**),[65] the naturally occurring C55 methoxyl derivative of isohomohalichondrin B. Reaction at the terminal hydroxyl group was not anticipated under the reaction conditions used. A mechanism to account for this most unusual, and unexpected, finding is given in **Figure 5.2.3**. This mechanism involves initial formation of an enolate and elimination of the terminal hydroxyl group to give an α,β-unsaturated compound followed by Michael addition of a methoxyl group to regenerate the enolate and reformation of the C53 ketone.

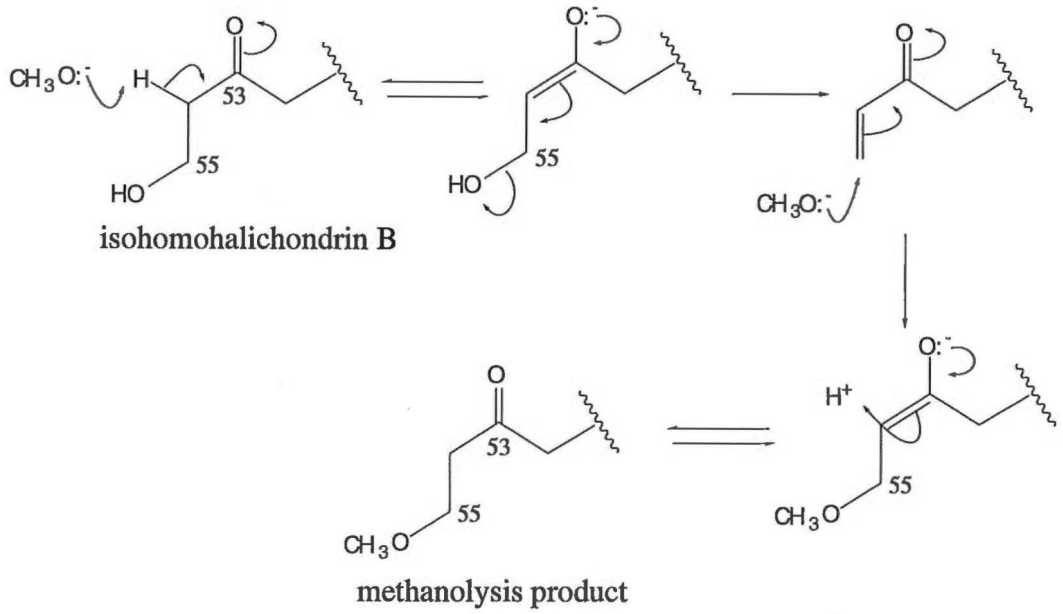

Figure 5.2.3 Proposed Mechanism for Terminal Methoxy Formation

COSY correlations and a key NOESY correlation were used primarily to assign the ^{1}H NMR chemical shifts around the H and I rings. A NOESY correlation from the unidentified resonance at δ_H 3.36 ppm to a proton at δ_H 4.06 ppm (H36) aided in the assignment of the chemical shift of the H32 proton. COSY correlations from δ_H 3.36 ppm (H32) to δ_H 3.84 ppm and δ_H 1.84 ppm located the H33 and H31 proton resonances respectively. A COSY correlation was observed from H31 (δ_H 1.84 ppm) to the previously assigned CH_3-31 doublet resonance at δ_H 1.13 ppm. The COSY spectrum also revealed the location of the H30 resonance; a correlation from H31 (δ_H 1.84 ppm) was observed to a resonance at δ_H 3.18 ppm. The signal at δ_H 3.18 ppm (H30) was correlated to another proton resonating at δ_H 3.66 ppm, which was assigned as the H29 resonance.

The large change in the ^{1}H NMR chemical shift observed for H30, from δ_H 4.66 ppm in isohomohalichondrin B to δ_H 3.18 ppm in the methanolysis product, implied that the C1-O-C30 bond had been cleaved to give the alcohol derivative at C30. It was not possible to locate the H2 and H2' protons, or the C1 or C2 carbon in the NMR spectra of the product, although there were some minor changes observed in the ^{1}H and ^{13}C NMR chemical shifts observed around the A and B rings, that were consistent with lactone cleavage.

The NOESY and difference NOE NMR spectra showed the NOE correlations as negative signals, as opposed to the positive correlations observed in the NOESY and NOE spectra of homohalichondrin B and halichondrin B, and the other derivatives isolated. It is likely that the opening of the lactone ring resulted in the molecule behaving more like a macromolecule in solution, arising from the splaying out of the released lactone ring, giving a relatively long correlation time (τ_c) and resulting in the observation of negative NOEs.

An infrared (IR) spectrum was performed on the product (**5.2.1**). The IR spectrum lacked the distinctive υ 1732 cm^{-1} lactone stretch present in the IR spectrum of isohomohalichondrin B, and the other halichondrins isolated to date. A new band at υ 1574 cm^{-1} was also observed, characteristic of a carboxylate stretch band.[66]

High resolution FAB-MS performed on the product (**5.2.1**) showed the parent ion corresponding to a molecular formula of $C_{62}H_{90}O_{20}$, a gain of one carbon atom, four hydrogen atoms and one oxygen atom relative to isohomohalichondrin B (**1.2.9**). This indicated that a CH_3 group and a hydroxyl group had been added to isohomohalichondrin B in the reaction.

The observation of carboxylate functionality in the IR spectrum, combined with the MS result confirmed that the lactone had been cleaved to produce the C1 carboxylate, *via* hydrolysis of the initially formed C1 methyl ester. This was also indicated by the TLC evidence before (a less polar product) and after work-up (the formation of a more polar product). The structure of the isohomohalichondrin B methanolysis product was therefore given as **5.2.1**. The observance of either a carboxylate or a carboxylic acid (as for **5.2.1**) being a function of pH.

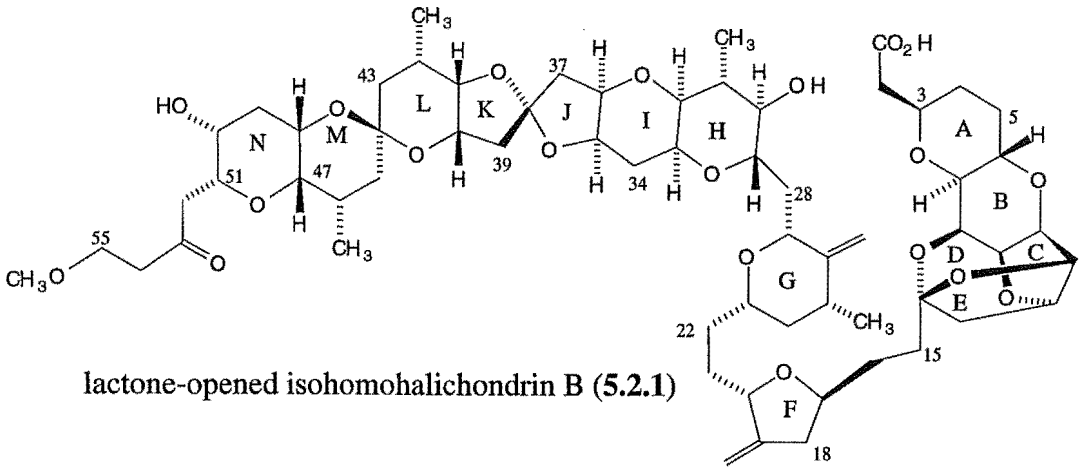

lactone-opened isohomohalichondrin B (**5.2.1**)

5.2.2 Methanolysis of Homohalichondrin B

To demonstrate that the opening of the lactone ring to give the carboxylate at C1 *via* methanolysis was a general reaction of the halichondrin series, and to avoid the complication of terminal moiety involvement in the reaction, methanolysis was attempted on homohalichondrin B (**1.2.3**).

Homohalichondrin B (**1.2.3**) was reacted with sodium methoxide in methanol, stirring the reaction overnight at room temperature. Silica TLC of the reaction mixture indicated the appearance of a less polar component. After reaction work-up, TLC performed on the product indicated the presence of a more polar spot relative to homohalichondrin B. These TLC observations were consistent with those observed in the methanolysis of isohomohalichondrin B (Section 5.2.1). A ^{1}H NMR spectrum performed on the product indicated that the reaction was incomplete, with approximately 50% homohalichondrin B and 50% reaction product in the reaction mixture. The mixture was committed for re-reaction with sodium methoxide, stirring the reaction overnight at room temperature, and monitoring the reaction by TLC. A ^{1}H NMR spectrum (**Figure 5.2.4**) performed after this time (in $CDCl_3$/ 0.1% pyridine-d_5) indicated that 90% of the halichondrin had been transformed into product with about 10% homohalichondrin B remaining. The CH_3-31 doublet resonance, present at δ_H 0.99 ppm in the ^{1}H NMR spectrum of homohalichondrin B, was absent in the spectrum of the reaction product. Other notable changes in the ^{1}H NMR spectrum of the product, relative to that of homohalichondrin B, was the movement of the H30 signal from δ_H 4.65 ppm and the movement of the H18' (from δ_H 2.79 ppm) and H32 (from δ_H 3.17 ppm) resonances, and the appearance of a new doublet of doublets at δ_H 3.34 ppm. The methoxyl resonance present in the ^{1}H NMR

spectrum of lactone opened isohomohalichondrin B (**Figure 5.2.1**), was absent from the spectrum of the homohalichondrin B methanolysis product (**Figure 5.2.4**).

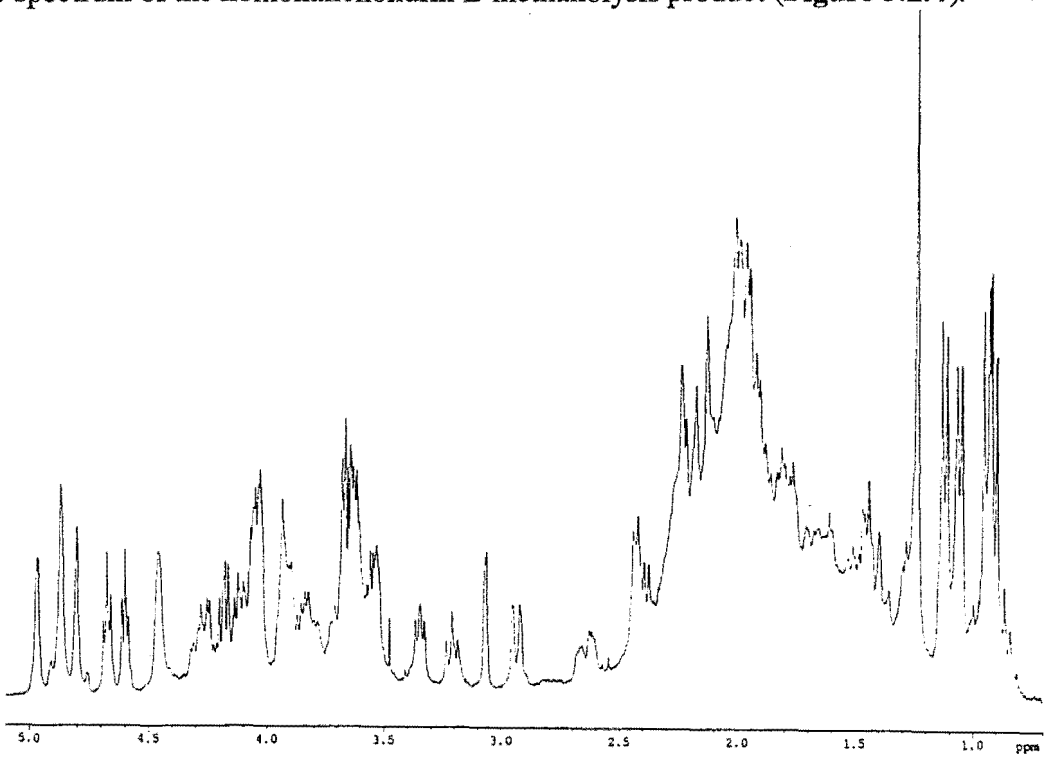

Figure 5.2.4 ^{1}H NMR Spectrum of Lactone-Opened Homohalichondrin B (**5.2.2**)

A series of NMR experiments were performed on the product (**5.2.2**), namely COSY, 2D-TOCSY (100 ms mixing time), NOE, HMQC and HMBC experiments. An analysis of the data generated from these experiments enabled a partial assignment of the ^{1}H and ^{13}C NMR spectra to be achieved. These ^{1}H and ^{13}C NMR data are cited in **Tables 5.2.3** and **5.2.4** respectively, and the important NMR correlations from these experiments are shown in **Figure 5.2.5**.

Relative to the ^{1}H and ^{13}C NMR data for homohalichondrin B (**Tables 2.4.1** and **2.4.2**), the NMR data for the methanolysis product of homohalichondrin B (**5.2.2**) were significantly different in the region of the A-J rings, focusing interest more specifically in changes around the A and H rings. Irradiation of the isolated doublet

of doublets at δ_H 3.34 ppm gave negative NOEs for resonances at δ_H 4.06 ppm (H36), δ_H 1.13 ppm (CH_3-31) and δ_H 3.86 ppm (H33), indicating that the irradiated signal was the H32 resonance. Irradiation of the isolated doublet of doublets at δ_H 3.23 ppm gave NOEs to proton resonances at δ_H 3.34 ppm (H32), δ_H 3.86 ppm (H33), indicating that the signal at δ_H 3.23 ppm was the H30 resonance.

Table 5.2.3 ^{1}H NMR Data for Lactone-Opened Homohalichondrin B (**5.2.2**)

Proton[a]	δ ppm[b]	**Proton**[a]	δ ppm[b]	**Proton**[a]	δ ppm[b]
H2	2.35	**H21**	1.64	**H39**	2.22
H2'		**H21'**		**H39'**	2.22
H3	3.82	**H22**		**H40**	3.95
H4	1.45	**H22'**		**H41**	3.61
H4'	1.80	**H23**	3.60	**H42**	2.30
H5	1.40	**H24**	1.05	**CH_3-42**	0.94
H5'	2.06	**H24'**	1.80	**H43**	1.30
H6	4.26	**H25**	2.27	**H43'**	1.49
H7	2.94	**CH_3-25**	1.06	**H45**	1.45
H8	4.48	**26=CH**	4.80	**H45'**	1.45
H9	4.06	**26'=CH**	4.86	**H46**	2.15
H10	4.18	**H27**	3.95	**CH_3-46**	0.92
H11	4.60	**H28**		**H47**	3.06
H12	4.67	**H28'**	2.02	**H48**	3.53
H13	1.93	**H29**	3.70	**H49**	1.78
H13'	2.17	**H30**	3.23	**H49'**	2.15
H15		**H31**	1.85	**H50**	3.90
H15'		**CH_3-31**	1.13	**H51**	4.03
H16	1.74	**H32**	3.34	**H52**	2.00
H16'	2.00	**H33**	3.86	**H52'**	2.00
H17	4.10	**H34**	1.92	**H53**	4.26
H18	2.25	**H34'**	2.10	**H54**	3.55
H18'	2.62	**H35**	4.14	**H55**	3.67
19=CH	4.86	**H36**	4.06	**H55'**	3.67
19'=CH	4.97	**H37**	1.95		
H20	4.48	**H37'**	2.40		

[a] The symbol ' represents the less shielded proton of a geminal pair.

[b] Data recorded at 23°C in $CDCl_3$ at 300 MHz with chemical shifts in ppm and referenced to $CHCl_3$, δ_H 7.25 ppm.

Table 5.2.4 ^{13}C NMR Data for Lactone-Opened Homohalichondrin B (**5.2.2**)

Carbon	δ ppm[a]	Carbon	δ ppm[a]	Carbon	δ ppm[a]
C1		C21		C39	43.5
C2	43.6	C22		C40	70.8
C3	76.0	C23	77.7	C41	79.2
C4		C24	42.5	C-CH_3-42	25.5
C5		C-CH_3-25	35.5	C-CH_3-42	17.0
C6	68.4	C-CH_3-25	18.1	C43	
C7	77.5	26C=CH_2	150.8	C44	
C8	74.2	26C=CH_2		C45	
C9		C27		C-CH_3-46	28.0
C10	76.5	C28	36.8	C-CH_3-46	18.0
C11	82.1	C29	73.6	C47	72.6
C12	81.0	C30	72.2	C48	63.5
C13	47.0	C-CH_3-31	39.0	C49	
C14		C-CH_3-31	15.4	C50	74.6
C15		C32	76.6	C51	76.4
C16		C33	66.3	C52	
C17		C34		C53	79.6
C18	38.5	C35		C54	72.0
19C=CH_2		C36	75.4	C55	65.3
19C=CH_2		C37	45.0		
C20	79.4	C38			

[a] Data recorded at 23 °C in $CDCl_3$ with chemical shifts in ppm, assigned from HMQC and HMBC spectra at 300 MHz.

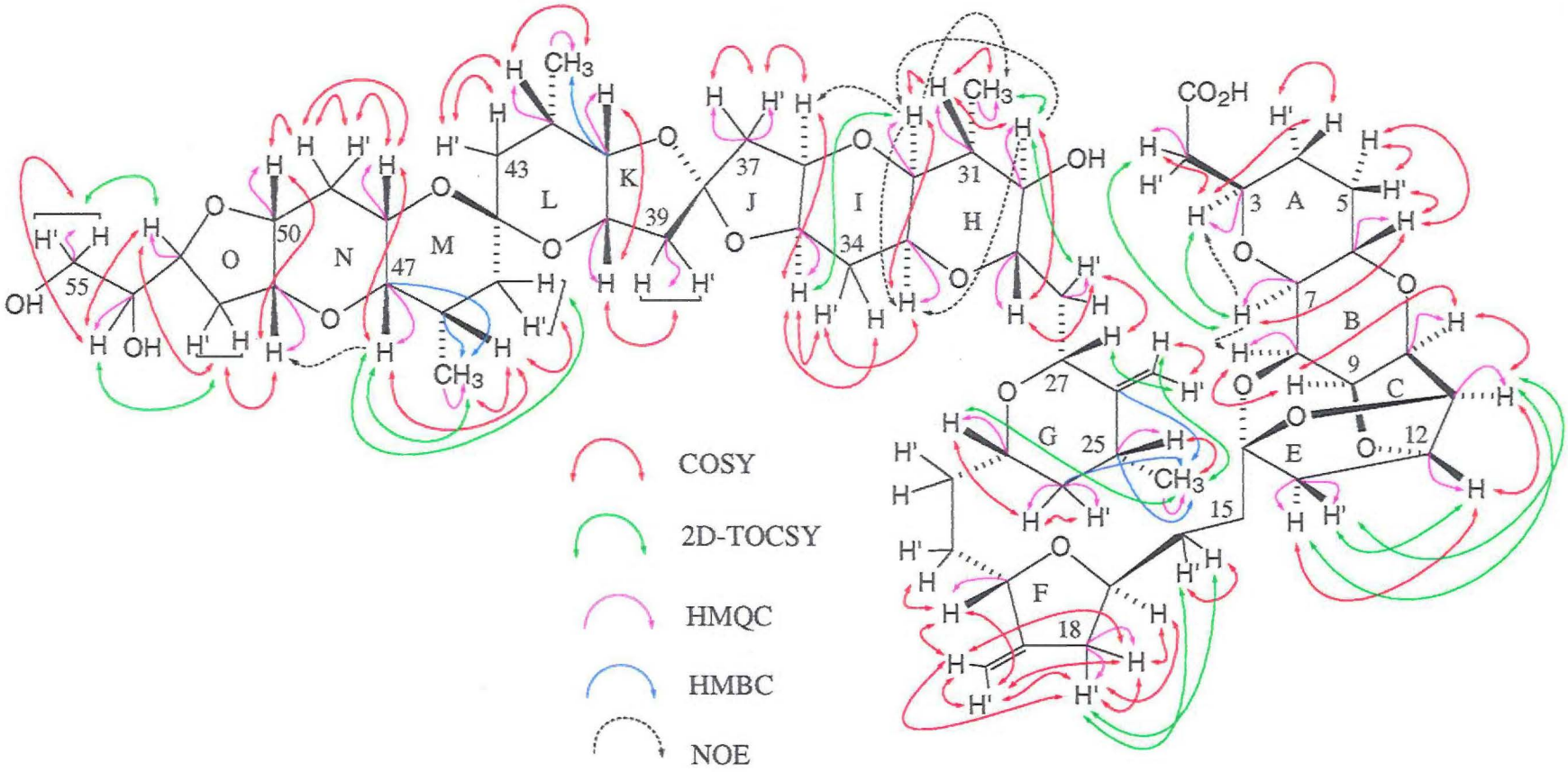

Figure 5.2.5 Lactone-Opened Homohalichondrin B- Important NMR Correlations

The ^{1}H and ^{13}C NMR data in the terminal spin system (C45-C55) were very similar to those of homohalichondrin B (**1.2.3**), indicating that the terminal moiety was unmodified.

High resolution FAB-MS performed on the methanolysis product (**5.2.2**) gave the parent ion corresponding to a molecular formula of $C_{61}H_{88}O_{20}$, a gain of one oxygen and two hydrogen atoms relative to homohalichondrin B (**1.2.3**). These data confirmed that **5.2.2** had been formed in the reaction.

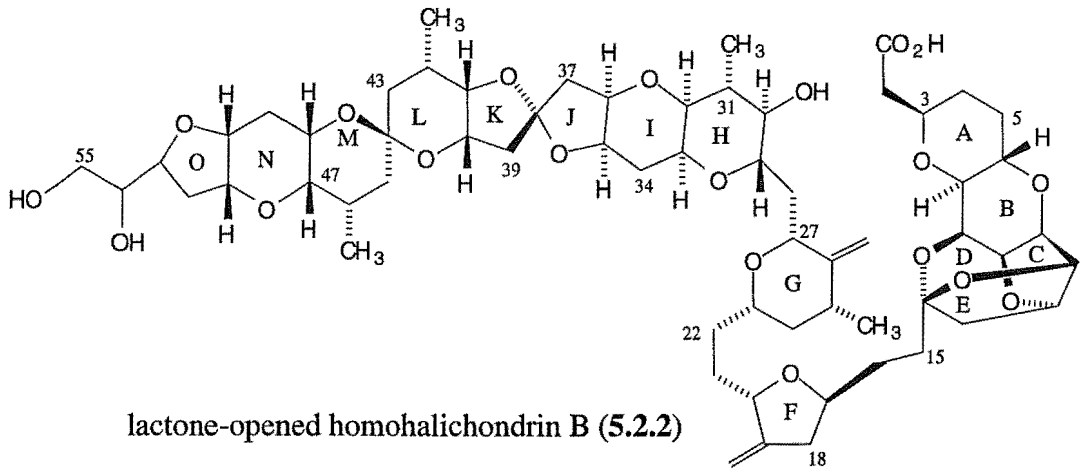

lactone-opened homohalichondrin B (**5.2.2**)

5.3 Lithium Aluminium Hydride Reduction

A lithium aluminium hydride reduction of the C1-C30 lactone of homohalichondrin B (**1.2.3**) was undertaken with the objective being to produce the lactone-cleaved C1 and C30 alcohol derivative (**5.3.1**).

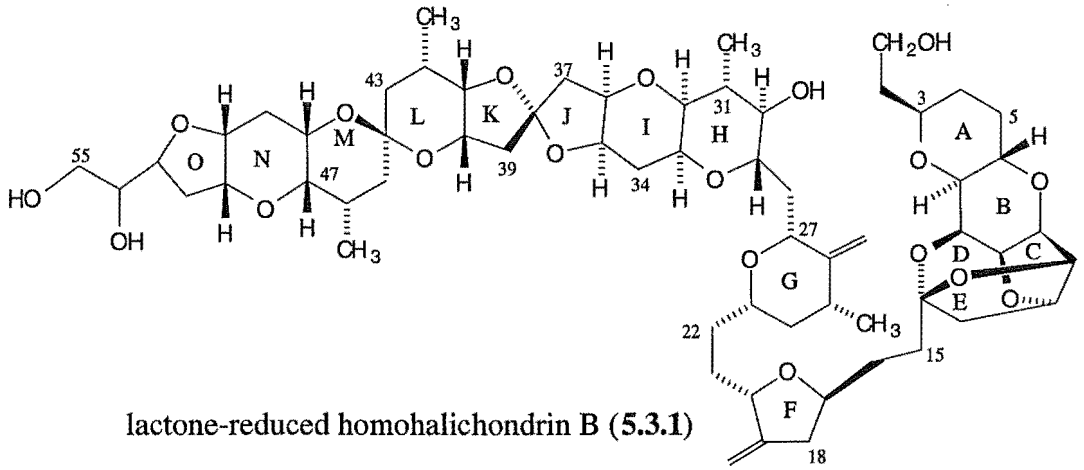

lactone-reduced homohalichondrin B (**5.3.1**)

Homohalichondrin B (**1.2.3**) was dissolved in dry tetrahydrofuran before the addition of fresh lithium aluminium hydride. The resulting suspension was stirred vigorously for four hours, at room temperature. Reaction work-up involved quenching the reaction with acidified water and extracting the halichondrin material on a small C18 column, washing the column with water to remove lithium salts and eluting with methanol to obtain the halichondrin material. The C18 column work-up procedure was tested on a small quantity of homohalichondrin B, without lithium aluminium hydride added, to ensure the halichondrin material was stable to the work-up conditions and that a high recovery was attainable.

TLC performed on the reaction mixture showed a single, more polar spot relative to a homohalichondrin B reference spot. A ^{1}H NMR spectrum of the product, acquired in $CDCl_3$/ 0.1% pyridine-d_5, is displayed in **Figure 5.3.1**. Several major changes were apparent in this spectrum relative to the ^{1}H NMR spectrum of homohalichondrin B (**Figure 2.4.1**). In the methyl region of the spectrum, it was apparent that the doublet resonance corresponding to the CH_3-31 protons had moved from δ_H 0.99 ppm to a new position at δ_H 1.13 ppm. Also apparent from the spectrum was the loss of one proton resonance (by integral) in the δ_H 4.65 ppm region where the H30 and H12 resonances were situated in the ^{1}H NMR spectrum of homohalichondrin B. A new doublet of doublets was observed at δ_H 3.37 ppm and the distinctive H2' resonance (δ_H 2.58 ppm) was no longer visible. The distinctive H18' multiplet at δ_H 2.79 ppm in homohalichondrin B was visible at δ_H 2.62 ppm in the spectrum of the product and no homohalichondrin B H18' signal was apparent at δ_H 2.79 ppm, indicating that there was no starting material remaining from the reaction.

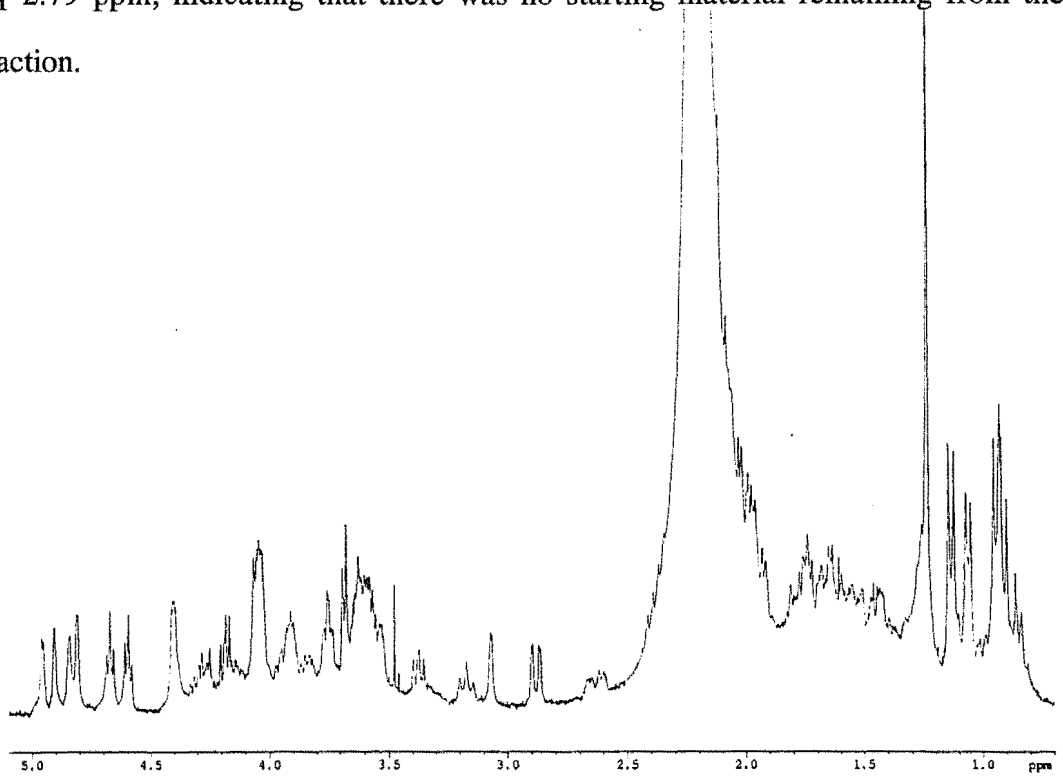

Figure 5.3.1 ^{1}H NMR Spectrum of Homohalichondrin B Lactone Reduction Product (**5.3.1**)

A series of NMR experiments were performed on the product : COSY, 2D-TOCSY (100 ms mixing time), 1D-TOCSY, NOE and HMQC experiments. A partial assignment of the ^{1}H and ^{13}C NMR spectra was achieved from an analysis of the various NMR spectra. The important correlations from these experiments are depicted in **Figure 5.3.2**. The ^{1}H and ^{13}C NMR data are cited in **Tables 5.3.1** and **5.3.2** respectively.

Table 5.3.1 ^{1}H NMR Data for Lactone-Reduced Homohalichondrin B (**5.3.1**)

Proton[a]	δ ppm[b]	**Proton**[a]	δ ppm[b]	**Proton**[a]	δ ppm[b]
H1	3.75	**19'=CH**	4.95	**H37**	1.96
H1'	3.75	**H20**	4.38	**H37'**	2.38
H2	1.72	**H21**	1.62	**H39**	2.22
H2'	1.72	**H21'**		**H39'**	2.22
H3	3.61	**H22**		**H40**	3.92
H4	1.55	**H22'**		**H41**	3.62
H4'	1.70	**H23**	3.54	**H42**	2.27
H5	1.36	**H24**	1.06	**CH_3-42**	0.94
H5'	2.08	**H24'**	1.75	**H43**	1.38
H6	4.30	**H25**	2.20	**H43'**	1.50
H7	2.88	**CH_3-25**	1.06	**H45**	1.42
H8	4.40	**26=CH**	4.81	**H45'**	1.42
H9	4.04	**26'=CH**	4.91	**H46**	2.10
H10	4.19	**H27**	3.92	**CH_3-46**	0.92
H11	4.59	**H28**	2.03	**H47**	3.07
H12	4.67	**H28'**	2.03	**H48**	3.55
H13	1.94	**H29**	3.62	**H49**	1.78
H13'	2.15	**H30**	3.17	**H49'**	2.15
H15		**H31**	1.79	**H50**	3.90
H15'		**CH_3-31**	1.13	**H51**	4.03
H16		**H32**	3.37	**H52**	2.00
H16'		**H33**	3.85	**H52'**	2.00
H17	4.05	**H34**	1.93	**H53**	4.25
H18	2.22	**H34'**	2.03	**H54**	3.55
H18'	2.62	**H35**	4.14	**H55**	3.70
19=CH	4.84	**H36**	4.04	**H55'**	3.70

[a] The symbol ' represents the less shielded proton of a geminal pair.

[b] Data recorded at 23° C in $CDCl_3$ at 300 MHz with chemical shifts in ppm and referenced to $CHCl_3$, δ_H 7.25 ppm.

Table 5.3.2 ^{13}C NMR Data for Lactone-Reduced Homohalichondrin B (**5.3.1**)

Carbon	δ ppm[a]	Carbon	δ ppm[a]	Carbon	δ ppm[a]
C1	60.6	**C21**		**C39**	44.0
C2		**C22**		**C40**	71.2
C3	73.5	**C23**	78.1	**C41**	79.5
C4		**C24**	42.5	**C**-CH_3-42	
C5		**C**-CH_3-25		**C**-**C**H_3-42	17.8
C6	68.6	**C**-**C**H_3-25	18.5	**C43**	
C7	78.0	26**C**=CH_2		**C44**	
C8	79.3	26**C**=**C**H_2		**C45**	
C9		**C27**		**C**-CH_3-46	
C10		**C28**		**C**-**C**H_3-46	18.0
C11	82.3	**C29**		**C47**	73.0
C12	81.1	**C30**	72.3	**C48**	63.7
C13	47.4	**C**-CH_3-31		**C49**	
C14		**C**-**C**H_3-31	15.7	**C50**	
C15		**C32**	77.0	**C51**	
C16		**C33**		**C52**	
C17		**C34**		**C53**	
C18		**C35**		**C54**	72.5
19**C**=CH_2		**C36**		**C55**	65.8
19**C**=**C**H_2		**C37**	45.5		
C20	74.6	**C38**			

[a] Data recorded at 23°C in $CDCl_3$ with chemical shifts in ppm, assigned from an HMQC spectrum at 300 MHz.

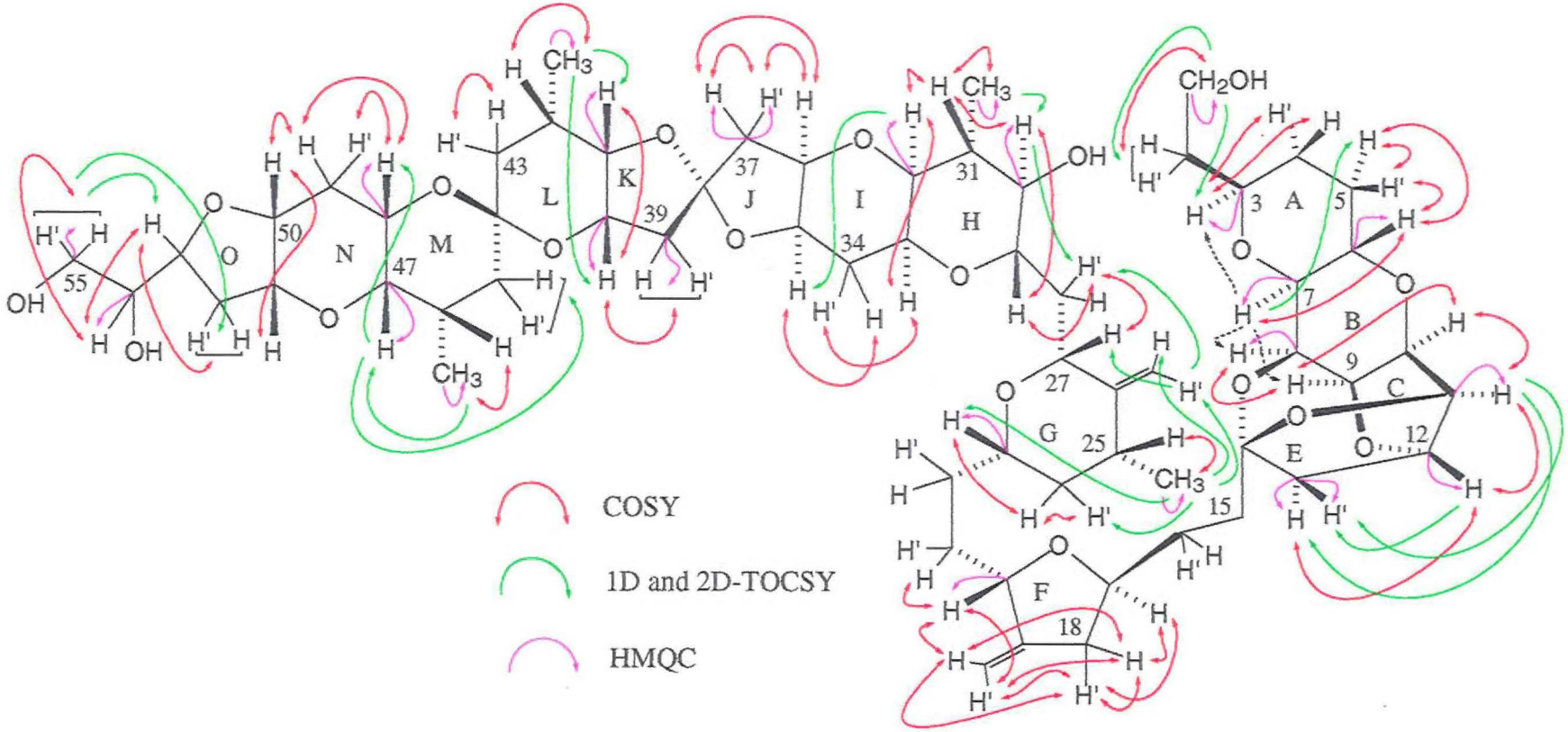

Figure 5.3.2 Lactone-Reduced Homohalichondrin B- Important NMR Correlations

The ^{1}H and ^{13}C NMR assignments for the terminal region of the molecule (C38-C55) were consistent with those observed for homohalichondrin B. As expected, the changes in chemical shifts were centred around the A to J rings, with the most notable differences being observed around the regions of the A, H and I rings.

The assignments of ^{1}H NMR chemical shifts around the H to J rings were similar to those observed for the lactone opened homohalichondrin B (**5.2.2**). The H30 proton resonance was observed at δ_H 3.17 ppm in the lactone reduction product (**5.3.1**), a shift of δ_H 1.48 ppm to a more shielded position relative to homohalichondrin B. This was consistent with the H30 ^{1}H NMR resonance observed for the lactone-opened homohalichondrin B product (**5.2.2**), situated at δ_H 3.23 ppm, and implied that the lactone had been cleaved using lithium aluminium hydride to give the secondary C30 alcohol. The ^{1}H NMR chemical shifts of other protons in this region were also consistent with those observed for the lactone-opened homohalichondrin B (**5.2.2**).

As with the lactone-opened homohalichondrin B (**5.2.2**), some changes in the ^{1}H and ^{13}C NMR chemical shifts were observed around the regions of the C to G rings. COSY correlations around the A to E rings assigned the chemical shifts of the protons in this region. The H3 resonance was observed at δ_H 3.61 ppm, shielded by δ_H 0.30 ppm compared to the shift observed for the H3 resonance of homohalichondrin B (**1.2.3**). An isolated HMQC correlation was observed for a carbon at δ_C 60.6 ppm, correlated to protons at δ_H 3.75 ppm, typical ^{13}C and ^{1}H NMR chemical shifts for an aliphatic -CH_2-OH. As the terminal C55 primary alcohol had already been assigned, the δ_H 3.75 ppm resonance was assigned as corresponding to the new, equivalent, H1 and H1' protons and the δ_C 60.6 ppm resonance as the C1 carbon. A COSY correlation was observed from the H1 and H1'

protons to protons resonating at δ_H 1.72 ppm, which were assigned as the resonances of the H2 and H2' methylene protons. Additionally, from the δ_H 3.75 ppm resonance (H1/H1'), 1D and 2D-TOCSY correlations were observed to the previously assigned H3 proton at δ_H 3.61 ppm, and to the δ_H 1.72 ppm protons (H2/H2').

Interestingly, the NOEs observed for this product were positive, as opposed to the negative NOEs observed for both the homohalichondrin B and isohomohalichondrin B methanolysis products (**5.2.2** and **5.2.1** respectively). This implied a solution behaviour more like that observed for the other halichondrins, with a relatively short correlation time (τ_c), resulting in the observation of positive NOEs. It was possible that in $CDCl_3$ solution, the C1 hydroxyl group of **5.3.1** was involved in an intramolecular hydrogen bond to the C30 alcohol group, resulting in a conformation of the C1-C30 region that was similar to homohalichondrin B (**1.2.3**) and halichondrin B (**1.2.1**), and thus gave rise to a "halichondrin-like" solution behaviour. Conversely, the presence of the ionic C1 carboxylate (or carboxylic acid) group in the products **5.2.1** and **5.2.2** was possibly forcing the carboxylate end of the lactone ring away from interaction with C30, resulting in splaying out of the molecule.

High resolution FAB-MS performed on the reduction product (**5.3.1**) established that the parent ion corresponding to a molecular formula of $C_{61}H_{90}O_{19}$ was present, a gain of four hydrogen atoms relative to the molecular formula of homohalichondrin B. This confirmed that **5.3.1** was the product formed in the lithium aluminium hydride reduction of homohalichondrin B.

5.4 Biological Activity Data

The biological activities of the three derivatives discussed in this Chapter are listed in **Table 5.4.1**. Listed are the cytotoxicities against the P388 cell line of all three compounds, with the NCI-derived GI_{50}s (averaged over all sixty cell lines) and COMPARE correlations for these three derivatives. The relevant parent halichondrins: homohalichondrin B (**1.2.3**), isohomohalichondrin B (**1.2.9**) and Me-isohomohalichondrin B-b (**1.2.12**) have their cytotoxicities given in terms of their IC_{50} and GI_{50} results for comparison.

All of the derivatives produced showed a significant increase in IC_{50} and GI_{50} concentrations relative to their respective parent compounds. In terms of the P388 IC_{50} results the lactone-opened isohomohalichondrin B (**5.2.1**) product displayed a 3500-fold decrease in activity relative to isohomohalichondrin B (**1.2.9**). The naturally occurring C55 methoxyl derivative of isohomohalichondrin B (**1.2.12**) resulted in a greater than fifty-fold decrease in P388 activity relative to isohomohalichondrin B. Providing that the reduction in biological activity conferred by the presence of a terminal methyl group at C55 was independent of the reduction in biological activity conferred by the opening of the lactone ring to give **5.2.1**, then the biological activity (*ie* the IC_{50}) due to the lactone opening of isohomohalichondrin B only could be seen as being *ca* 11 ng/ mL or a greater than sixty-fold reduction in cytotoxicity relative to isohomohalichondrin B (**1.2.9**). The homohalichondrin B lactone-opened product (**5.2.2**), given the 10% contribution by homohalichondrin B, presented at least a twenty-four fold reduction in P388 activity relative to homohalichondrin B (**1.2.3**), although synergistic or antagonistic effects due to the presence of homohalichondrin B could not be discounted. A similar analysis of the NCI GI_{50} results indicated *ca* 280-fold decrease in biological activity

for the lactone-opened isohomohalichondrin B product (**5.2.1**) relative to isohomohalichondrin B, or a reduction in activity of about 160-fold for opening of the lactone ring only, by taking into account the reduction in activity conferred by terminal methylation. In comparison, the homohalichondrin B lactone-opened product (**5.2.2**) recorded at least a 260-fold reduction in activity relative to homohalichondrin B (**1.2.3**). Generally, the P388 cytotoxicity results suggested that the P388 cell line was less sensitive to the effect of opening the lactone ring than in the NCI primary screen which is averaged over sixty different cell lines.

Table 5.4.1 *In Vitro* Cytotoxicities of Selected Halichondrins

Compound	P388 IC_{50} (ng/mL)	NCI GI_{50} ($\times 10^{-10}$ M)	COMPARE Correlation[a]
homohalichondrin B (1.2.3)	0.22	3.16	0.95
isohomohalichondrin B (1.2.9)	0.18	1.15	0.74
Me-isohomohalichondrin B-b (1.2.12)	10	2.00	0.72
lactone-opened isohomohalichondrin B (5.2.1)	630	324	<0.71
lactone-opened homohalichondrin B (5.2.2)	5.4	851	0.81
lactone-reduced homohalichondrin B (5.3.1)	56	490	0.73

a Correlation coefficient from the *Compare* pattern-recognition algorithm were calculated by computer using the GI_{50}-centred mean graph profiles of differential cellular sensitivities to each of the compounds. The GI_{50}-centred mean graph profile of halichondrin B was used as the "seed" for all of the comparisons.

In terms of the COMPARE correlation coefficient for the isohomohalichondrin B lactone-opened derivative (**5.2.1**), the reduction in the similarity of its GI_{50}-centred profile to either halichondrin B (COMPARE defined as being 1.00) or isohomohalichondrin B (**1.2.9**) probably reflected a reduction in the ability to act as antimitotic compound. The lactone-opened homohalichondrin B derivative (**5.2.2**) appeared to display only a slight reduction in the COMPARE coefficient relative to homohalichondrin B, even though the cytotoxicity of this compound was significantly reduced.

The lactone-reduced homohalichondrin B product (**5.3.1**) also showed a significant reduction in the P388 cytotoxicity assay of greater than 250-fold relative to the parent halichondrin, homohalichondrin B (**1.2.3**). Similarly, the GI_{50} result indicated a greater than 150-fold reduction in activity relative to homohalichondrin B (**1.2.3**). The COMPARE correlation coefficient indicated a significant reduction in the ability of **5.3.1** to display the characteristic antimitotic mean-graph profile observed for homohalichondrin B (**1.2.3**).

In general terms, the lactone ring was observed to play a significant role in the expression of cytotoxicity in the halichondrins.

A further discussion of the biological activities of these analogues in relation to other halichondrin analogues is found in Chapter 9.

CHAPTER 6

Acid Stability Studies

6.1 Introduction

In order to gain an insight into the general chemistry of the halichondrins, an investigation of the acid stability of selected members of the halichondrin series was undertaken. It was anticipated that a knowledge of this stability would give useful information as to the ability to react other reagents with halichondrins under specific acidic reaction conditions without acid decomposition.

Hirata and Uemura[18] reported in 1986 that halichondrins underwent decomposition in acidic solution, although the authors did not report conditions or a specific mode(s) of decomposition.

In 1993, Cooper *et al* reported a specific mode of acid decomposition in a synthetic C1-C21 "B family" halichondrin fragment as part of their synthetic efforts towards the total synthesis of halichondrin B (**1.2.1**).[31] The authors reported the 50% conversion of a C14-ketal synthetic fragment to a furan derivative (refer to Appendix III) "presumably owing to traces of HCl in the solvent" ($CDCl_3$). They further suggested that "this reactivity has biological significance".[31]

A series of trial reactions were performed, placing selected halichondrins under acidic conditions using a range of acids of varying acid strengths and concentrations, with the objective of isolating and identifying specific acid catalysed reaction products.

Once a suitable reaction conditions were developed which enabled the generation of a series of acid catalysed reaction products, a method of separating these products

was developed and subsequently performed. Structural characterisation of the isolated derivatives was then undertaken.

A study of the interaction and possible equilibration between the various acid catalysed reaction products under similar reaction conditions was undertaken, in closely monitored time-scale reactions, performed on the individual products.

In the total synthesis of halichondrin B (**1.2.1**) and norhalichondrin B (**1.2.2**) reported by Kishi's group,[67] the final step in the synthesis was the formation of the C38 spiro centre with camphor sulfonic acid in dichloromethane (refer to Appendix III). No data on the stereoselectivity of this transformation was given, except to say that it was "very high". It was therefore important to consider the effect of the acidic reaction conditions on the stereoselectivity of the closure of the spiro centre and the effect of acid on the rest of the halichondrin molecule. A time-scale reaction study of the acid catalysed reaction of homohalichondrin B (**1.2.3**) in camphor sulfonic acid solution (in dichloromethane) was therefore undertaken.

6.2 Acid Stability Studies

Kishi and co-workers reported[67] the formation of the C14 spiro centre in a C1-C38 synthetic fragment using a mild acid, pyridinium *p*-toluene sulfonate (PPTS), in dichloromethane to effect ketalisation in the total synthesis of halichondrin B and norhalichondrin B. A more detailed description of this reaction in the context of the overall total synthesis can be found in Appendix III. An initial point for studying the acid stability of homohalichondrin B (**1.2.3**) was therefore undertaken using PPTS in dichloromethane solution. Subsequently, a stronger acid, *p*-toluene sulfonic acid (PTSA), and finally trifluoroacetic acid (TFA) were investigated in acid stability studies of homohalichondrin B (**1.2.3**).

6.2.1 PPTS Stability Studies of Homohalichondrin B

The reaction of a small quantity (0.3 mg) of homohalichondrin B (**1.2.3**) with PPTS in deuterochloroform was monitored by ^{1}H NMR spectroscopy. A reference ^{1}H NMR spectrum of homohalichondrin B in deuterochloroform was obtained, then PPTS was added to give a 1:3 ratio of PPTS to homohalichondrin B. The reaction was left standing at room temperature and monitored at regular time intervals. After forty-five minutes no reaction was observed by ^{1}H NMR spectroscopy, so additional PPTS was added to give a 1:1 ratio of PPTS to homohalichondrin B in the NMR tube.

After seventy-seven hours at a 1:1 ratio and at room temperature, a ^{1}H NMR spectrum obtained from the solution indicated the appearance of new signals and the reduction in the intensity of other, homohalichondrin B resonances. A new doublet of doublets was apparent at δ_H 3.12 ppm (lying between the H32 and H47 resonances), and the intensity of the CH_3-46 doublet at δ_H 0.90 ppm was reduced relative to the ^{1}H NMR spectrum of homohalichondrin B (**Figure 2.4.1**). Also apparent from the ^{1}H NMR spectrum was the increase in the intensity of the doublet resonance situated at δ_H 0.99 ppm (CH_3-31).

After six days, a ^{1}H NMR spectrum obtained from the mixture indicated some additional changes relative to the spectrum acquired after seventy-seven hours. The regions around δ_H 4.25 ppm, δ_H 3.52 ppm and δ_H 3.80 ppm showed an increase in complexity and the resonances at δ_H 3.12 ppm and δ_H 0.99 ppm continued to increase in intensity while the δ_H 0.90 ppm resonance continued to decrease in intensity.

After ten days, a ^{1}H NMR spectrum of the reaction mixture showed a number of additional resonances appearing in the region of the olefinic 19=CH_2 and 26=CH_2 resonances and three resonances centred about δ_H 6.34 ppm.

After fifteen days reaction, the ^{1}H NMR spectrum showed an increase in the number of signals in the methyl region of the spectrum, although the intensity of the δ_H 0.90 ppm resonance was still decreasing and the resonance at δ_H 0.99 ppm was still increasing in intensity.

Finally, after twenty-two days reaction, the ^{1}H NMR spectrum showed three new resonances centred about δ_H 6.25 ppm, and a continuation of the trends previously

described. At this point the reaction was quenched and worked-up as the (almost) complete disappearance of the CH_3-46 doublet at δ_H 0.90 ppm indicated that there was very little homohalichondrin B (**1.2.3**) remaining in the NMR tube. Furthermore, and that there was a mixture of several components present. A ^1H NMR spectrum of the reaction product was identical with that observed before work-up.

Silica TLC performed on the reaction mixture indicated the appearance of a single spot, with the same R_f as the starting material, homohalichondrin B (**1.2.3**). Reverse phase analytical HPLC indicated the presence of several apparently major, more polar components, relative to homohalichondrin B; some homohalichondrin B; and some less polar components. In light of the unusual HPLC behaviour of the acid products (discussed in Section 6.2.3), it was likely that some of the products from the reaction had not been observed as they were found to be very late eluting with the chosen solvent system. A preparative HPLC collection of the peaks observed to be eluting off the column was attempted. However, there was insufficient material to progress further with.

In general, this reaction indicated that the halichondrins were stable under the PPTS conditions described, as long as reaction times were less than seventy-seven hours. This should prove useful information for reactions of halichondrins which need to be undertaken in acidic reaction conditions.

At this stage it was decided to attempt a more rapid generation of the acid products using the related, but stronger acid, PTSA.

6.2.2 PTSA Stability Studies of Homohalichondrin B

Two methods of rapidly generating the acid catalysed reaction of homohalichondrin B (**1.2.3**) were attempted. Initially, a two-phase reaction was attempted and later a one-phase system was undertaken.

6.2.2.1 Two-phase PTSA Reaction

As a gentle way of introducing a stronger acid (relative to PPTS) to homohalichondrin B (**1.2.3**), a two-phase reaction was initially attempted. PTSA in aqueous solution was added to small quantity (0.3 mg) of homohalichondrin B (**1.2.3**) dissolved in dichloromethane to give a PTSA : homohalichondrin B ratio of 1:360. The reaction was stirred vigorously at room temperature and monitored by reverse phase HPLC with time. No reaction was apparent by HPLC after forty-seven hours so the reaction was worked-up. A ^{1}H NMR spectrum of this material confirmed that no reaction had occurred with only homohalichondrin B (**1.2.3**) being identified in the spectrum.

This material was committed for re-reaction with PTSA in a two-phase reaction, increasing the amount of PTSA present, to give a 1:1 ratio of PTSA to homohalichondrin B (**1.2.3**). Again, the reaction was monitored by reverse phase HPLC. No reaction was apparent by HPLC after forty-eight hours vigorously stirring at room temperature, so the reaction was worked-up. ^{1}H NMR spectroscopy confirmed that no reaction had occurred. At this stage it was decided to try a single phase solvent system to generate the acid reaction of homohalichondrin B.

6.2.2.2 One-phase PTSA Reaction

A solution of PTSA in dichloromethane was added to the unreacted homohalichondrin B (from the two-phase reactions) in dichloromethane to give a *ca* 220:1 ratio of PTSA to homohalichondrin B (**1.2.3**). The resulting solution was stirred at room temperature for forty-eight hours . A ^{1}H NMR spectrum obtained from the product after this time showed the presence of only homohalichondrin B, indicating that no reaction had occurred. More severe reaction conditions were then attempted with TFA as the acid.

These reactions indicated that the halichondrins were stable under the PTSA conditions described, as long as reaction times were less than forty-eight hours. As with the PPTS reaction, this information should prove useful for reactions of halichondrins which need to be performed in acidic reaction conditions.

6.2.3 TFA Reaction Studies of Homohalichondrin B

A series of reactions aimed at producing acid catalysed reaction products of homohalichondrin B for characterisation and biological activity evaluation were undertaken. Initially, a time-scale reaction of homohalichondrin B with TFA in CD_3OD was monitored by ^{1}H NMR spectroscopy. Subsequently, a series of TFA reactions in dichloromethane were developed to allow the generation of a series of acid products and the development of an HPLC method capable of separating them for structural determination and biological activity assessment.

6.2.3.1 TFA Reaction in Methanol

A ^{1}H NMR spectrum of a small quantity (0.3 mg) of homohalichondrin B (**1.2.3**) in CD_3OD was acquired before a TFA solution (in CD_3OD) was added, to give a *ca* 1:20 ratio of homohalichondrin B to TFA in the NMR tube. The reaction was monitored with time by ^{1}H NMR spectroscopy. Immediately after addition of TFA to homohalichondrin B, a ^{1}H NMR spectrum obtained from the mixture indicated a reduction in intensity of one of the multiplet resonances at *ca* δ_H 4.62 ppm, where the H30 and H11 proton resonances were situated in the ^{1}H NMR spectrum of homohalichondrin B. After three hours reaction, a ^{1}H NMR spectrum acquired from the reaction mixture showed several new resonances in the methyl and olefinic regions of the spectrum. The reaction was quenched after this time by the addition of triethylamine (TEA) and the reaction was worked-up; the product was transferred back to an NMR tube with $CDCl_3$/ 0.1% pyridine-d_5. A ^{1}H NMR spectrum obtained from this material indicated several minor changes relative to the ^{1}H NMR spectrum of homohalichondrin B (**Figure 2.4.1**). The CH_3-46 methyl doublet at δ_H 0.90 ppm had decreased in intensity while the doublet at δ_H 0.99 ppm, where the CH_3-31 resonance was situated in the ^{1}H NMR spectrum of homohalichondrin B, had increased in intensity. Also visible was a new, relatively broad resonance at δ_H 3.82 ppm. From this spectrum it was apparent that there was a minor amount (<10%) of homohalichondrin B present and one other, unidentified major component as well as some TFA and TEA in the reaction product.

COSY, 2D-TOCSY (100 ms mixing time) and HMQC spectra were acquired from the mixture, enabling a partial assignment of the ^{1}H and ^{13}C NMR spectra to be achieved. This acid reaction product was later recognised as being the C38 epimer of homohalichondrin B (**6.3.3**), and the NMR spectroscopic assignment of this compound is described in Section 6.3.3.

Silica TLC of the reaction mixture relative to homohalichondrin B (**1.2.3**) indicated a very slight decrease in polarity of the major component. C18 bench column chromatography was performed on the reaction mixture to separate the TFA and TEA from the halichondrin material. The product was dissolved in a small quantity of the mobile phase (55% acetonitrile/ water) and placed on the equilibrated column; eight fractions were then collected off the column. The column was stripped with 100% acetonitrile and this was collected in two fractions. Fractions were combined on the basis of silica TLC results to give two halichondrin-containing fractions: fractions four to nine (major fraction) and fraction ten (minor fraction, <10% of total material). The final acetonitrile-stripped fraction (fraction ten) appeared to contain halichondrin material of a *higher* polarity than the earlier halichondrin-eluting fractions by silica TLC. A ^{1}H NMR spectrum was obtained from each of the combined fractions in $CDCl_3$/ 0.1% pyridine-d_5. The ^{1}H NMR spectrum of the major fraction identified the material as pure homohalichondrin B (**1.2.3**). The ^{1}H NMR spectrum of the minor fraction had a very poor signal to noise ratio, but did not appear to resemble either homohalichondrin B or the major reaction product (**6.3.3**). From these observations, it appeared that the reaction was reversible under certain conditions. This aspect is described in the time-scale acid reaction studies described later in Section 6.4.

6.2.3.2 TFA Reactions in Dichloromethane

TFA in dichloromethane (a standardised solution) was added to a small quantity (0.3 mg) of homohalichondrin B (**1.2.3**) dissolved in dichloromethane to give an eleven-fold excess of TFA relative to homohalichondrin B. The resulting solution was stirred at room temperature for four hours. After this time the reaction was quenched by the addition of water and dilute sodium hydroxide to pH 7.5-8.0. The water layer

was removed and the dichloromethane layer was washed with water before extracting the halichondrin material in dichloromethane.

A ^{1}H NMR spectrum obtained from the product (in $CDCl_3$/ 0.1% pyridine-d_5) indicated that there was a mixture of several components present. There were several new resonances in the δ_H 5.80 - 6.30 ppm region of the spectrum, and an apparent loss or movement of the isolated H12 doublet of doublets signal at δ_H 4.68 ppm. There was no evidence of the previously observed acid product (**6.3.3**) from the TFA in CD_3OD reaction (Section 6.2.3.1). It was apparent that the reaction had been taken too far, resulting in severe acid decomposition of homohalichondrin B. It was decided to reduce both the ratio of acid to homohalichondrin B and the duration of the reaction.

The reaction was repeated on a larger quantity (2.2 mg) of homohalichondrin B (**1.2.3**) with a 1.5:1 ratio of TFA to homohalichondrin B in dichloromethane. The solution was stirred at room temperature for thirty minutes before working-up the reaction. A ^{1}H NMR spectrum obtained from the product (in $CDCl_3$/ 0.1% pyridine-d_5) indicated that a mixture of components was present. There were only two resonances in the δ_H 5.80 - 6.30 ppm region of the spectrum (**Figure 6.2.1**)- one at δ_H 5.95 ppm (doublet) and one at δ_H 6.18 ppm (with the appearance of a triplet). Also apparent was a new, isolated, broad singlet resonance at δ_H 5.08 ppm. There was some evidence of the product from the CD_3OD reaction: a doublet of doublets (slightly obscured) at δ_H 3.12 ppm, and the broad singlet signal at δ_H 3.82 ppm. The methyl region of the spectrum indicated a mixture of components was present, as several overlapping doublets of differing relative intensities were visible.

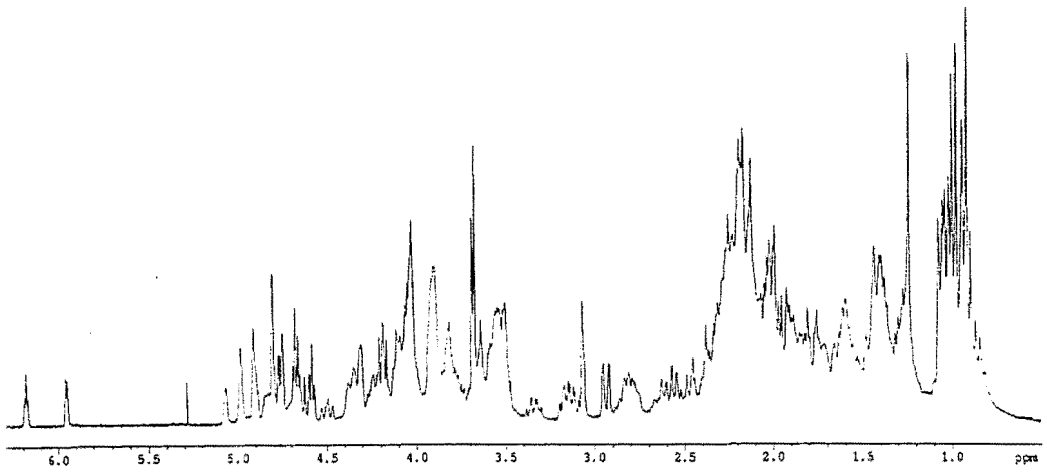

Figure 6.2.1 ^{1}H NMR Spectrum of Products From TFA Reaction of Homohalichondrin B

At this stage, analytical reverse phase HPLC (utilising an analytical C18 HPLC column) was investigated as a method of separating the products of the reaction. A series of acetonitrile/water solvent mixtures were investigated as possible mobile phases, with injections of the reaction mixture, using pure homohalichondrin B (**1.2.3**) as a reference. At a solvent mix of 50% acetonitrile/ water, the standard method of observing the individual naturally-occurring halichondrins by analytical C18 HPLC, evidence of carry-over peaks from previous injections of the reaction mixture was observed, indicating a less polar solvent mixture was required. At 60% acetonitrile/ water, a peak in the chromatogram at *ca* 230 s corresponding to homohalichondrin B was observed in the reaction mixture. Also observed in the chromatogram of the reaction mixture was a minor peak at *ca* 550 s. The uv spectrum of this component showed absorbance maxima at λ 193 nm and λ 230 nm. Homohalichondrin B, like the other halichondrins isolated to date, exhibited end-absorption only, at *ca* λ 193 nm. The observance of a product with an absorbance maximum of λ 230 nm suggested an increase in conjugation had occurred in the reaction. The reaction was repeated to obtain more material for HPLC separation.

The reaction was carried out on a similar scale (2.1 mg) and under identical conditions to the previous reaction. A ^{1}H NMR spectrum obtained in $CDCl_3$/ 0.1% pyridine-d_5 was very similar to that of the previous reaction. Preparative reverse phase HPLC using an analytical C18 column, with 60% acetonitrile/ water as the mobile phase, was used to separate the peaks at *ca* 230 s and 550 s. A ^{1}H NMR spectrum obtained from the fraction eluting at *ca* 230 s was identified as homohalichondrin B (**1.2.3**). The ^{1}H NMR spectrum of the peak eluting at 550 s appeared to be one product. The peaks at δ_H 5.95 ppm and at δ_H 6.18 ppm were visible in the spectrum and the methyl region appeared much cleaner. The structural assignment of this component (**6.3.1**) was able to be made once sufficient material had been obtained, and this is described in Section 6.3.1. There was insufficient material to analyse further so the reaction was repeated on yet a larger scale (4.4 mg) under identical reaction conditions.

HPLC separation of the product was performed using multiple injections on an analytical C18 column to separate the homohalichondrin B peak eluting at *ca* 230 s from the acid product (**6.3.1**) eluting at 550 s. A fraction was collected of the peak at 230 s and another fraction containing the eluent from 550 s and the material eluting after this peak was collected. The solvent was removed from the two fractions, and they were re-injected to ascertain the quality of the separation. The chromatograms of the two injections showed both homohalichondrin B (230 s) and the acid product **6.3.1** (550 s). At this stage it was realised that 0.05% TFA had been added to the HPLC water (as a polar modifier). TFA would have concentrated when the solvent was removed from the two fractions resulting in re-reaction which was detected on re-injection of the separated fractions. The homohalichondrin B and acid product fractions were recombined and subsequently re-separated using 60% acetonitrile/ water (with no TFA added) as the mobile phase. The solvent was removed from the

two fractions (eluting at 230 s and 550 s) and they were re-analysed by HPLC, which indicated a good separation of the two components had been achieved.

The reaction was repeated again on a large scale (4.0 mg) under identical reaction conditions. Preparative reverse phase HPLC using 60% acetonitrile/ water as the mobile phase was performed on the products. The peaks at 230 s (homohalichondrin B) and 550 s (**6.3.1**) were collected separately, along with the material from between injections. A ^{1}H NMR spectrum was acquired on the material from between injections- this indicated a large amount of halichondrin material was present (half the total reaction material in terms of mass). This material appeared to be a mixture of two components; a product with resonances at δ_H 5.95 ppm and δ_H 6.18 ppm and another product lacking these signals. It was realised at this stage that the HPLC conditions were such that two additional acid reaction products were not being observed as they were less polar than any other halichondrins that had previously been analysed on a C18 column. The solvent mix was changed to 70% acetonitrile/ water and analytical-scale injections were performed on the homohalichondrin B and the acid product **6.3.1**. The chromatogram of the homohalichondrin B (**1.2.3**) separated previously showed one peak at *ca* 200 s whereas the chromatogram of the acid product **6.3.1** showed one uv-active component (absorbance maxima at λ 193 nm and λ 230 nm) eluting at *ca* 300 s (**6.3.1**). An analytical injection of the two additional acid products showed two components in the chromatogram, one at *ca* 800 s and the other at *ca* 1000 s, similar in magnitude. The uv spectrum of the peak eluting at 800 s was similar in appearance to the component eluting at 300 s; with absorbance maxima at λ 193 nm and λ 230 nm. The structural characterisation of this component is described in Section 6.3.2 (**6.3.2**), performed once sufficient quantities had been obtained. The peak eluting at 1000 s had a uv spectrum identical with that of homohalichondrin B; with only end-absorption at λ 193 nm. The structural characterisation of this component was made once sufficient material was

obtained, and is described in Section 6.3.3 (**6.3.3**). The two-component mixture (**6.3.2** and **6.3.3**) was separated preparatively by HPLC, *via* multiple injections on the analytical C18 column. Diol and silica TLC performed on the three acid products (**6.3.1**, **6.3.2** and **6.3.3**) did not show any significant difference in polarity relative to homohalichondrin B (**1.2.3**).

The interaction of the three acid products on silica and diol appeared to be quite different to their behaviour on C18. This may be attributed to the interaction of polar groups such as hydroxyl groups with silica and diol to produce the differences in polarity observed, whereas interactions with C18 are partly a function of the relative hydrophobicity of the components. The halichondrins possess both polar functionalities and hydrophobic regions which may have contributed to the effective "polarity" differences observed for normal and reverse stationary phases. Conformational differences between the products may also contribute to the differing interactions of the products with C18 relative to silica or diol as the stationery phase.

There was still insufficient material to analyse the products so two final, large scale reactions (4.0 mg and 4.8 mg) of homohalichondrin B (**1.2.3**) under identical reaction conditions were performed. This enabled HPLC separation of enough material to allow structural identification and biological activity assessments to be performed, with the unreacted homohalichondrin B (**1.2.3**) from each reaction being fed into the next reaction. Once separated, the three acid products (*viz* **6.3.1**, **6.3.2** and **6.3.3**) were individually re-injected on an analytical scale to ensure the separation and purity of the products was adequate. These reactions gave a total of 2.0 mg of **6.3.1**, 1.8 mg of **6.3.2** and 2.0 mg of **6.3.3** for further study.

6.3 Characterisation of TFA Reaction Products

Each of the three acid products from the HPLC separation were individually characterised, primarily by NMR spectroscopy and MS.

6.3.1 Assignment of Acid Product 6.3.1

The uv spectrum of the component eluting at *ca* 300 s off the analytical C18 HPLC column at 70% acetonitrile/ water (**6.3.1**) showed absorbance maxima at λ 193 nm and λ 230 nm. High resolution FAB-MS performed on the acid product **6.3.1** gave the parent ion corresponding to a molecular formula of $C_{61}H_{86}O_{19}$, isobaric with that of homohalichondrin B (**1.2.3**).

The ^1H NMR spectrum ($CDCl_3$/ 0.1% pyridine-d_5) of acid product **6.3.1** is displayed in **Figure 6.3.1**. The spectrum indicated several major changes relative to the ^1H NMR spectrum of homohalichondrin B (**Figure 2.4.1**). Notable, was the appearance of the two isolated doublets at δ_H 5.95 ppm and δ_H 6.18 ppm. Other new, isolated resonances were apparent: a broad singlet at δ_H 5.10 ppm; a doublet at δ_H 4.90 ppm; a doublet of doublets at δ_H 4.52 ppm; a broad singlet at δ_H 4.70 ppm and a doublet of doublets at δ_H 3.35 ppm. Movement of the methyl doublets was apparent with two overlying doublets at δ_H 1.03 ppm and two doublets overlapping at δ_H 0.92 ppm and δ_H 0.90 ppm. Several distinctive resonances characteristic of the ^1H NMR spectrum of homohalichondrin B were no longer apparent in the ^1H NMR spectrum of **6.3.1**: the H32 doublet of doublets resonance at δ_H 3.17 ppm, the H7 resonance at

δ_H 2.94 ppm, the H2' resonance at δ_H 2.58 ppm, and the H11 and H12 resonances at δ_H 4.58 ppm and δ_H 4.68 ppm respectively. However, there were some isolated resonances in the spectrum of the acid product **6.3.1** that remained unshifted relative to the ^{1}H NMR spectrum of homohalichondrin B (**Figure 2.4.1**); the isolated H47 resonance at δ_H 3.06 ppm and the H55/H55' resonance at δ_H 3.69 ppm. This indicated that the terminal region of the molecule remained intact.

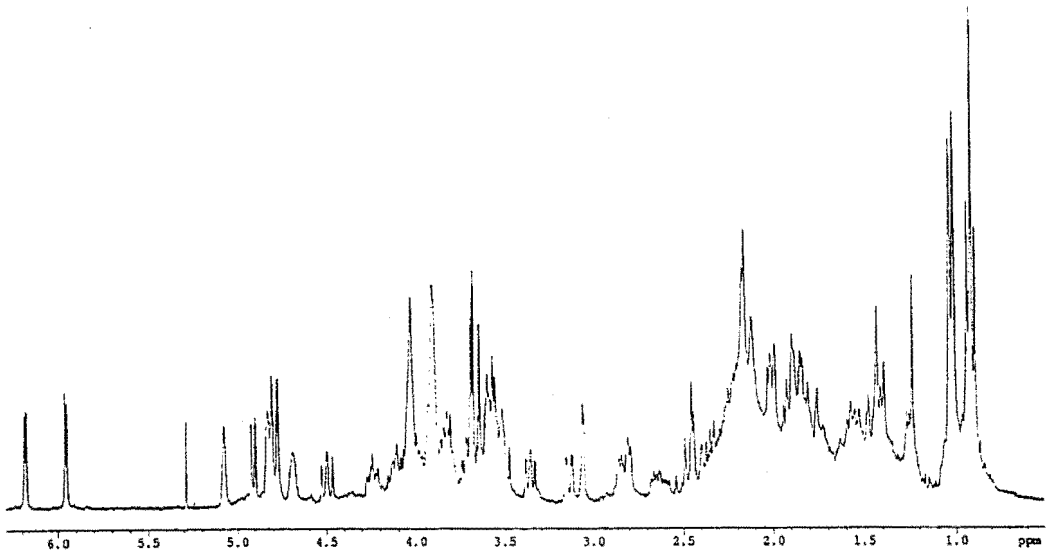

Figure 6.3.1 ^{1}H NMR Spectrum of Acid Product **6.3.1**

A series of NMR experiments were performed on the acid product **6.3.1** *viz* COSY, 2D-TOCSY (mixing times of 20 ms, 50 ms and 100 ms), 1D-TOCSY, HMQC, HMBC, NOESY and NOE experiments. From an analysis of the data generated from these experiments, a partial assignment of the ^{1}H and ^{13}C NMR spectra of acid product **6.3.1** was achieved. These data are cited in **Tables 6.3.1** (^{1}H NMR data) and

6.3.2 (^{13}C NMR data), with the important correlations from the NMR experiments depicted in **Figure 6.3.2**.

Table 6.3.1 ^{1}H NMR Data for Furan Acid Product (**6.3.1**)

Proton[a]	δ ppm[b]	Proton[a]	δ ppm[b]	Proton[a]	δ ppm[b]
H2	2.43	**H21**	1.60	**H37'**	2.35
H2'	2.53	**H21'**		**H39**	2.18
H3	3.95	**H22**	1.40	**H39'**	2.18
H4	1.40	**H22'**	1.58	**H40**	3.90
H4'	1.70	**H23**	3.60	**H41**	3.60
H5	1.48	**H24**	0.94	**H42**	2.32
H5'	2.08	**H24'**	1.85	**CH_3-42**	0.92
H6	3.98	**H25**	2.20	**H43**	1.29
H7	3.12	**CH_3-25**	1.03	**H43'**	1.45
H8	4.04	**26=CH**	4.78	**H45**	1.42
C8-OH	3.57	**26'=CH**	4.81	**H45'**	1.42
H9	3.90	**H27**	3.70	**H46**	2.15
H10	4.90	**H28**	1.55	**CH_3-46**	0.90
H12	6.18	**H28'**	2.25	**H47**	3.06
H13	5.95	**H29**	3.80	**H48**	3.53
H15	2.60	**H30**	4.52	**H49**	1.79
H15'	2.82	**H31**	1.88	**H49'**	2.15
H16	1.75	**CH_3-31**	1.03	**H50**	3.90
H16'		**H32**	3.35	**H51**	4.04
H17	3.87	**H33**	3.82	**H52**	2.02
H18	2.20	**H34**	1.90	**H52'**	2.02
H18'	2.82	**H34'**		**H53**	4.25
19=CH	4.82	**H35**	4.12	**H54**	3.55
19'=CH	5.10	**H36**	4.04	**H55**	3.69
H20	4.70	**H37**	1.89	**H55'**	3.69

[a] The symbol ' represents the less shielded proton of a geminal pair.

[b] Data recorded at 23 °C in $CDCl_3$ at 300 MHz with chemical shifts in ppm and referenced to $CHCl_3$, δ_H 7.25 ppm.

Table 6.3.2 ^{13}C NMR Data for Furan Acid Product (**6.3.1**)

Carbon	δ ppm[a]	Carbon	δ ppm[a]	Carbon	δ ppm[a]
C1	172.0	**C21**		**C39**	42.8
C2	40.5	**C22**	30.2	**C40**	70.7
C3	75.4	**C23**	77.1	**C41**	79.1
C4		**C24**	43.2	**C-CH_3-42**	25.8
C5		**C-CH_3-25**	36.0	**C-CH_3-42**	17.5
C6	68.9	**C-CH_3-25**		**C43**	37.0
C7	78.8	**26C=CH_2**	151.0	**C44**	96.5
C8	64.6	**26C=CH_2**	105.0	**C45**	36.8
C9	69.0	**C27**	74.6	**C-CH_3-46**	29.0
C10	71.0	**C28**	33.8	**C-CH_3-46**	17.2
C11	151.0	**C29**	70.8	**C47**	72.6
C12	108.6	**C30**	75.8	**C48**	63.4
C13	106.0	**C-CH_3-31**	38.0	**C49**	31.2
C14	155.0	**C-CH_3-31**		**C50**	74.5
C15	24.2	**C32**	76.4	**C51**	76.0
C16		**C33**	67.2	**C52**	36.8
C17	77.0	**C34**		**C53**	79.5
C18	39.7	**C35**	75.2	**C54**	71.8
19C=CH_2		**C36**		**C55**	65.3
19C=CH_2	105.4	**C37**	44.2		
C20	78.3	**C38**	112.4		

a ^{13}C NMR spectral data assigned from HMQC and HMBC experiments, recorded at 23°C in $CDCl_3$ at 300 MHz with chemical shifts in ppm.

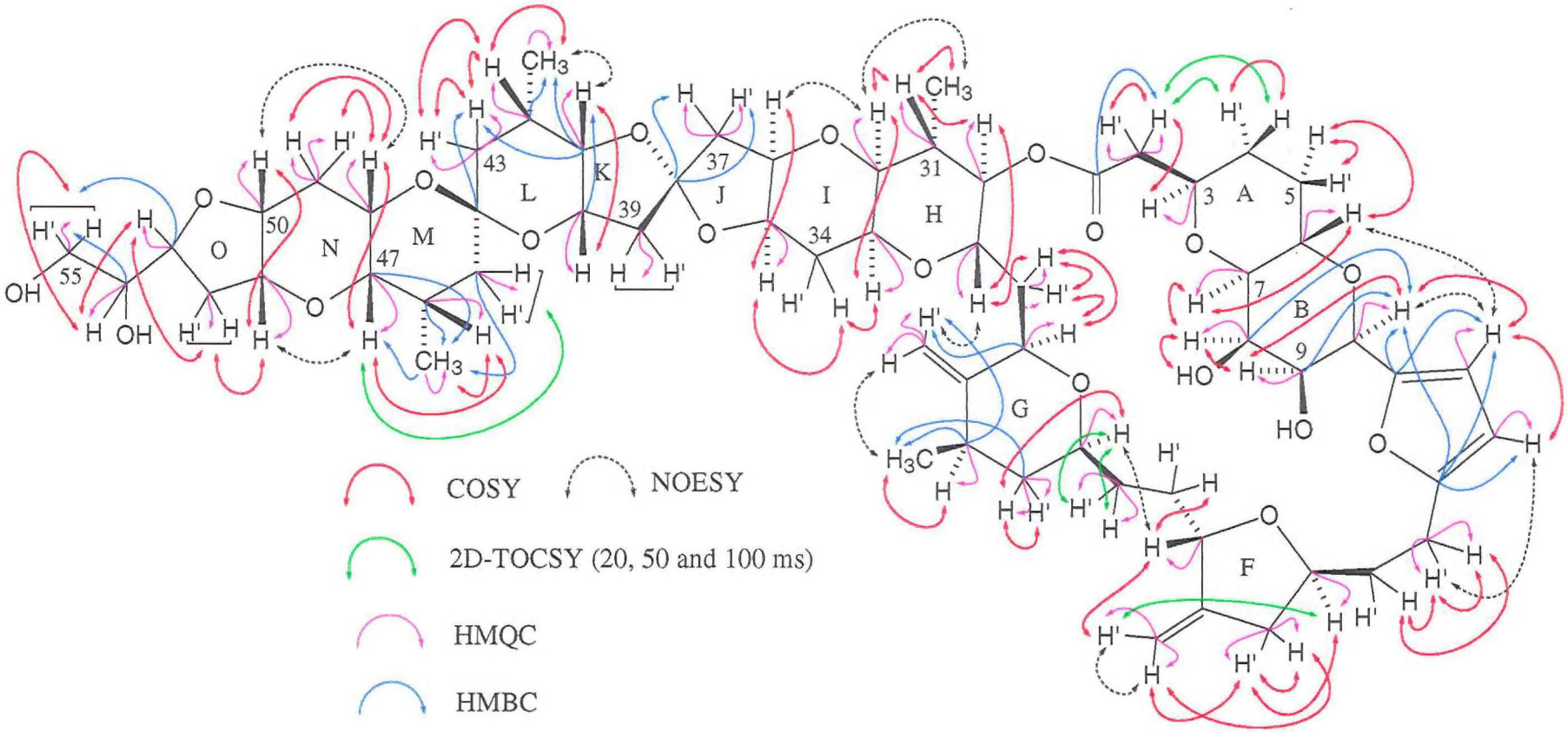

Figure 6.3.2 Furan Acid Product- Important NMR Correlations

Initial interest centred on the two ^1H NMR narrow doublet resonances at δ_H 5.95 ppm and δ_H 6.18 ppm (**Figure 6.3.1**). An integral over each doublet signal, relative to the unshifted H47 resonance at δ_H 3.06 ppm, indicated one proton was contributing to each resonance. A +5.0% NOE enhancement of the δ_H 5.95 ppm resonance was observed from irradiation of the δ_H 6.18 resonance. Correspondingly, irradiation of the δ_H 5.95 ppm resonance gave a +3.0% NOE enhancement of the δ_H 6.18 ppm resonance, indicating that the two protons were situated close in space. The COSY and 2D-TOCSY spectra revealed strong correlations between the two resonances. The chemical shifts and multiplicity of these resonances were characteristic of the protons at the three and four positions of either a furan or dihydrofuran type system.[68,69] For a dihydrofuran, the $^3J_{HH}$ coupling constant between the protons at positions three and four would typically be *ca* 6.0 Hz,[69] whereas the vicinal coupling between the protons at the three and four positions of a furan would be 3.4 Hz.[68] The actual coupling constant for both doublets was measured at 3.0 Hz, indicating they were coupled together as furan-type protons. The uv spectrum of **6.3.1** was consistent with that of a furan-type compound, with absorption maxima at λ 193 nm and λ 230 nm.[70]

An analysis of the NMR experiments confirmed that the terminal region (C38-C55) of the molecule was intact, with the ^1H and ^{13}C NMR data consistent with those of homohalichondrin B (**1.2.3**) in this region. Chemical shift changes were apparent around the C1-C37 region of the molecule, with the most significant changes occurring around the C3-C14 region, indicating that the furan was a part of this system.

It was anticipated that the furan had formed from the "E-ring" of homohalichondrin B, as had occurred in Salomon's synthetic fragment.[31] An analysis of the COSY

spectrum revealed some apparent anomalies for this anticipated product. The H7 proton had moved from δ_H 2.94 ppm in the ^1H NMR spectrum of homohalichondrin B to a new position at δ_H 3.12 ppm. COSY correlations from this resonance were observed to δ_H 3.98 ppm (H6) and δ_H 4.04 ppm (H8). However, the H8 resonance showed *two* additional correlations to resonances at δ_H 3.57 ppm and to δ_H 3.90 ppm (a weak correlation). The δ_H 3.90 ppm resonance was correlated to the isolated doublet resonance at δ_H 4.90 ppm in the COSY spectrum. The COSY spectrum revealed the doublet at δ_H 4.90 ppm was correlated to the furan resonance at δ_H 6.18 ppm, the result of allylic coupling. The resonance at δ_H 4.90 ppm was therefore assigned as the H10 methine proton resonance, and the δ_H 6.18 ppm resonance as the H12 proton resonance, leaving the other furan signal at δ_H 5.95 ppm assignable as the H13 proton resonance. The resonance at δ_H 3.90 ppm was assigned as the H9 proton resonance. However, this left the assignment of the remaining resonance at δ_H 3.57 ppm unaccounted for. The HMQC spectrum revealed that no correlation was apparent for a proton at δ_H 3.57 ppm to a directly attached carbon, indicating that this proton was not in fact a methine (or methylene) proton but rather a slowly exchanging hydroxyl proton, *viz* the newly created C8 substituted hydroxyl proton. It is likely that the hydroxyl proton was hydrogen-bonded to the newly created C9 substituted hydroxyl oxygen resulting in its slow exchange with the surrounding solvent and thus its appearance in the spectrum.

A series of selective 1D-TOCSY experiments, irradiating the δ_H 4.90 ppm resonance (H10), with varied mixing times, showed the contribution of the δ_H 3.90 ppm signal (H9) with a mixing time of 10 ms, while the δ_H 4.04 ppm (H8) and δ_H 3.57 ppm resonances were observed only with a longer mixing time of 40 ms. Another series of selective 1D-TOCSY experiments, irradiating the isolated H7 resonance at δ_H 2.94 ppm, revealed the δ_H 4.04 ppm (H8) and δ_H 3.57 ppm resonances with a mixing time of 10 ms, whereas the δ_H 3.90 ppm resonance (H9) was only visible with a

relatively long mixing time of 50 ms. These experiments also supported the theory that the unidentified δ_H 3.57 ppm resonance was the C8 hydroxyl proton as its order in the spin system suggested it was attached at the C8 position.

To test whether the proton at δ_H 3.57 ppm was exchangeable, a D_2O shake test of the product (**6.3.1**) was undertaken. This involved acquiring a reference ^1H NMR spectrum and a selective 1D-TOCSY spectrum (irradiating at δ_H 4.90 ppm (H10), mixing time 80 ms) from the acid product in $CDCl_3$/ 0.1% pyridine-d_5. One drop of D_2O was then added to the NMR tube and the resulting mixture was vigorously shaken. After five minutes standing at room temperature, ^1H NMR and 1D-TOCSY spectra were acquired under identical NMR experimental conditions. The spectra were re-acquired after another one and a half hours standing at room temperature. A comparison of these spectra with the spectra acquired before D_2O addition revealed key differences. The ^1H NMR spectra showed a reduction in the size of the resonances at δ_H 3.57 ppm after D_2O addition, and a slight increase in the intensity of the δ_H 4.04 ppm (H8) resonance. Similarly, the 1D-TOCSY spectra obtained after D_2O addition showed a decrease in the intensity of the δ_H 3.57 ppm resonance relative the reference spectrum, with time. Also notable was the increase in intensity and decrease in complexity of the δ_H 4.04 ppm resonance (H8) after D_2O addition, reflecting the loss of coupling to the δ_H 3.57 ppm resonance. This experiment confirmed that the δ_H 3.57 ppm resonance was the C8 hydroxyl proton resonance.

The HMQC spectrum revealed the directly attached carbons of the δ_H 5.95 ppm and δ_H 6.18 ppm resonances, at δ_C 106.0 ppm and δ_C 108.6 ppm respectively, (appearing as foldbacks to δ_C 16.0 ppm and δ_C 18.6 ppm in the spectrum), similar to the carbon shifts of unsubstituted C3 and C4 furan carbons (δ_C 109.9 ppm).[71]

The HMBC spectrum showed two important correlations from carbons at δ_C 151.0 ppm and δ_C 155.0 ppm (appearing as foldback carbons at δ_C 61.0 ppm and δ_C 65.0 ppm respectively) to the furan proton at δ_H 6.18 ppm (H12). A strong HMBC correlation from the carbon at δ_C 151.0 ppm to the methine proton at δ_H 4.90 ppm (H10), and a much weaker correlation from δ_C 155.0 ppm to the H10 proton resonance (a four-bond correlation), supported the assignment of δ_C 155.0 ppm as the C14 carbon, and δ_C 151.0 ppm as the C11 carbon.

The NMR data was therefore consistent with **6.3.1** as the structure of the acid product. This compound was also isobaric with homohalichondrin B (**1.2.3**), as required by the MS result.

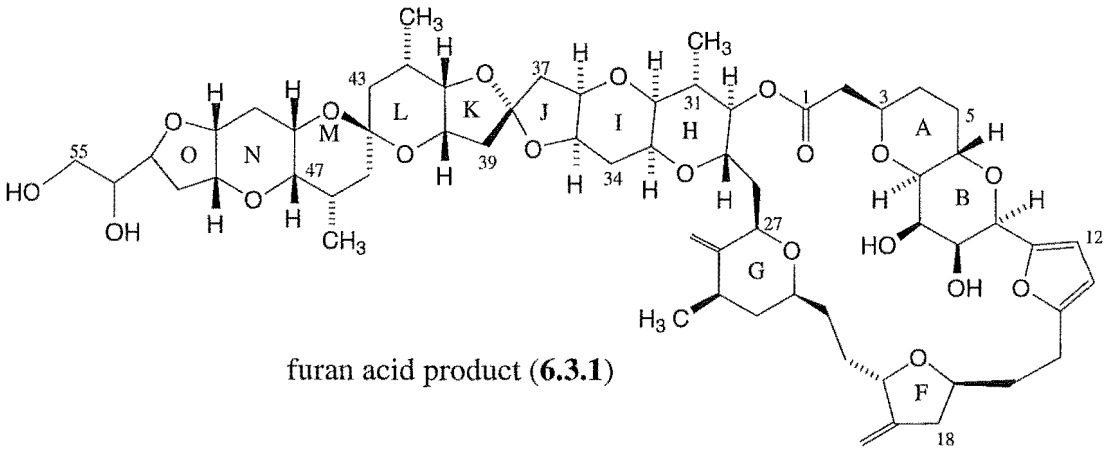

furan acid product (**6.3.1**)

A likely mechanism for the formation of **6.3.1** is depicted in **Figure 6.3.3**. The mechanism involves protonation of the C and D-ring ether protons in acid solution, facilitating the elimination of one of the H13 protons and the H12 proton to form the

E-ring furan, and opening the C and D-rings to give the C8 and C9 hydroxyl derivative. This reaction probably occurs *via* stepwise protonations and eliminations rather than as the simultaneous process depicted in **Figure 6.3.3**.

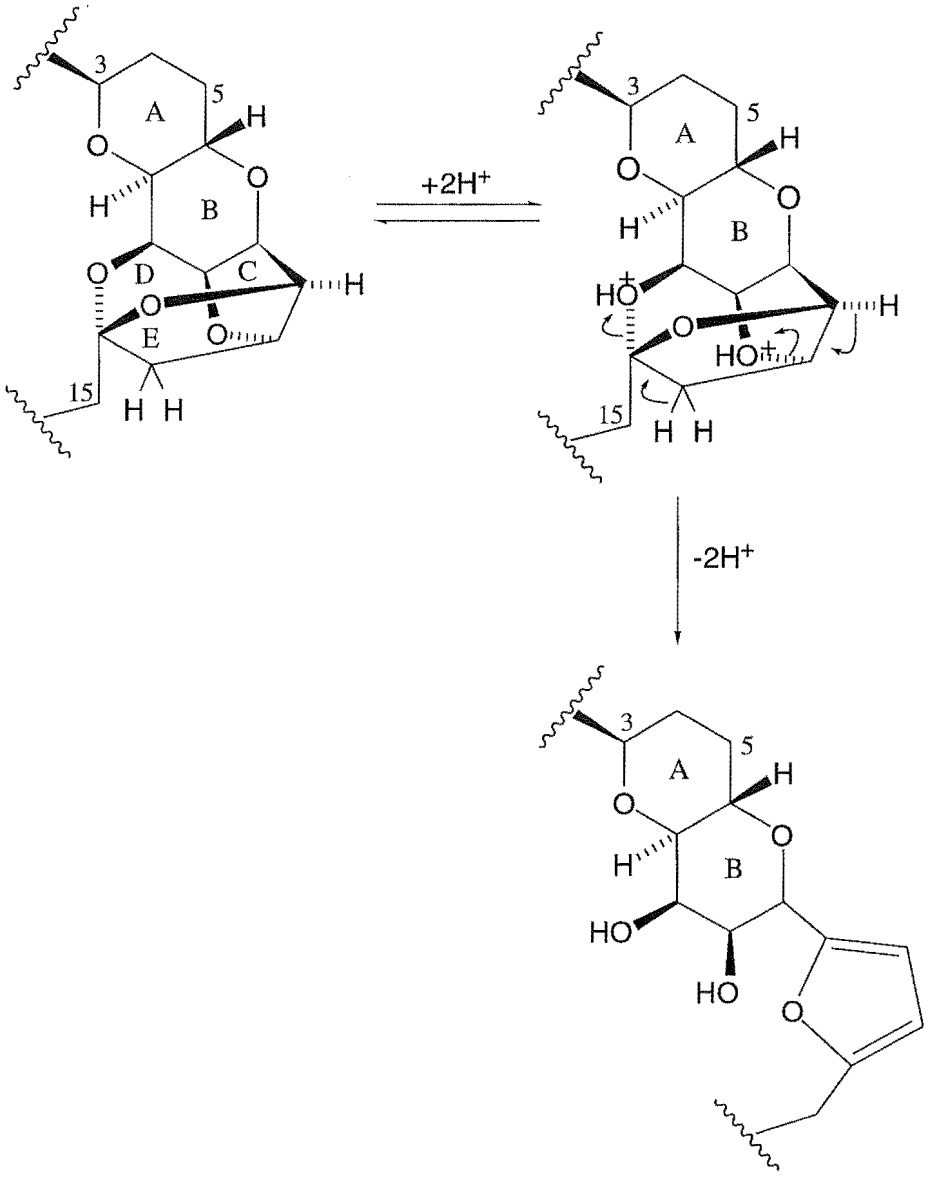

Figure 6.3.3 Proposed Mechanism of Furan Formation

The NOESY spectrum of **6.3.1** showed several interesting correlations from the furan ring protons. A NOESY correlation was observed from the furan proton at δ_H

5.95 ppm (H13) to a methylene proton at δ_H 2.82 ppm (H15'). The other furan proton resonance at δ_H 6.18 ppm (H12) showed NOESY correlations to δ_H 4.90 ppm (H10) and δ_H 3.98 ppm (H6). A cursory glance at the structure of **6.3.1** suggested that the stereochemistry of the H6 proton would preclude it from an NOE interaction with H12. Models of the C1-C15 system were able to confirm that the NOEs observed were feasible, as was a subsequent computer modelling analysis.

The C2-C15 subunit from the computer modelling studies of halichondrin B (Section 2.3.2.1) was modified using the computer program Chem3D Plus to generate the C2-C15 furan derivative **6.3.1**. The C10-C11 bond was rotated to give a conformation allowing both H6 and H10 to be in close proximity to H12. The energy (MM2) of the resulting conformation was minimised. The resulting structure is displayed in **Figure 6.3.4**, along with the interatomic distances for the H12-H6 and H12-H10 NOESY interactions for this conformation.

The interatomic distances for the minimised structure were within the typical limits for the observation of an NOE interaction. Construction of a model of the C1-C30 structure of the furan derivative indicated that the H13 to H15' NOE interaction and the H12-H6 and H12-H10 NOE interactions were possible within the constraints of the lactone ring, although the position of the furan ring H12 proton relative to H6 and H10 could not be rotated significantly without exceeding the distance constraints of an NOE observation.

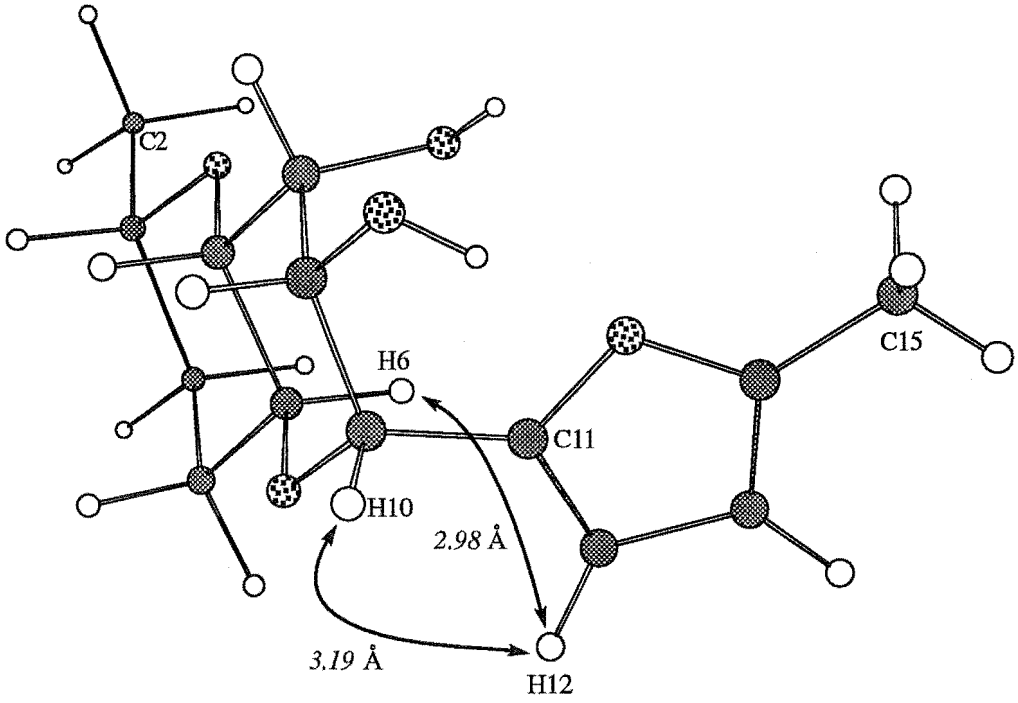

Figure 6.3.4 C2-C15 Furan Modelling Output

The NOESY spectrum lacked the correlations across the lactone ring from the H2' proton to H20 and 19=CH, which were observed in the NOESY spectrum of homohalichondrin B (and halichondrin B). The changes in chemical shift observed for protons around the H ring, such as the H32 proton (from δ_H 3.17 ppm to δ_H 3.35 ppm in **6.3.1**) may have resulted from a change in the conformation of the lactone ring imposed by the presence of the furan ring.

6.3.2 Assignment of Acid Product 6.3.2

The uv spectrum of the component eluting at *ca* 800 s off the analytical HPLC C18 column with 70% acetonitrile/ water (**6.3.2**) showed absorbance maxima at λ 193 nm and λ 230 nm. High resolution FAB-MS, performed on acid product **6.3.2**, gave a molecular formula of $C_{61}H_{86}O_{19}$, isobaric with that of homohalichondrin B (**1.2.3**). This indicated that no gain or loss of protons had occurred in the formation of acid product **6.3.2** from homohalichondrin B.

The ^1H NMR spectrum of acid product **6.3.2** is displayed in **Figure 6.3.5**. This spectrum was obtained in $CDCl_3$/ 0.1% pyridine-d_5 and shows some major changes relative to the ^1H NMR spectrum of homohalichondrin B (**Figure 2.4.1**) but relatively minor changes relative to the spectrum of the furan acid product **6.3.1** (**Figure 6.3.1**).

The resonances at δ_H 5.95 ppm and δ_H 6.19 ppm were recognisable as the previously assigned H12 and H13 furan signals. However, the CH_3-46 and CH_3-42 doublets at δ_H 0.90 ppm and δ_H 0.92 ppm respectively, which had the appearance of a triplet in the ^1H NMR spectrum of **6.3.1**, appeared as separate doublets at δ_H 0.92 ppm and δ_H 0.96 ppm respectively in the ^1H NMR spectrum of acid product **6.3.2**. Other resonances appeared to have moved slightly, and a new broad resonance at δ_H 3.85 ppm and the loss of the broad singlet resonance at δ_H 3.60 ppm were also visible. The distinctive H55/H55' doublet at δ_H 3.69 ppm and the isolated H47 resonance at δ_H 3.07 ppm were still apparent, indicating that the terminal moiety was intact. These differences (and similarities) relative to the ^1H NMR spectrum of the furan acid product **6.3.1** indicated that the acid product **6.3.2** was a furan derivative with a

subtle change occurring in another part of the molecule, which was not in the terminal region.

A range of NMR experiments were performed on acid product **6.3.2**. COSY, 1D-TOCSY, 2D-TOCSY (mixing times of 20 ms, 40 ms and 100 ms), HSMQC, HMBC, NOESY and NOE experiments enabled a partial assignment of the ^{1}H and ^{13}C NMR spectra of **6.3.2** to be achieved. These data, obtained from an analysis of the NMR experiments are listed in **Tables 6.3.3** (^{1}H NMR data) and **6.3.4** (^{13}C NMR data) and the important correlations from the NMR experiments are shown in **Figure 6.3.6**.

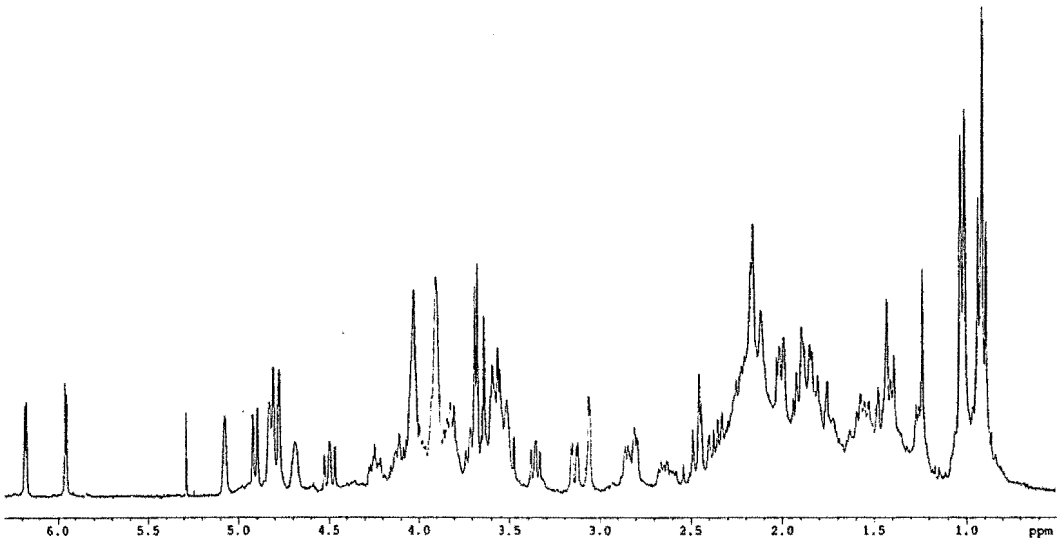

Figure 6.3.5 ^{1}H NMR Spectrum of Acid Product **6.3.2**

Table 6.3.3 ^{1}H NMR Data for *Epi*-Furan Acid Product (**6.3.2**)

Proton[a]	δ ppm[b]	Proton[a]	δ ppm[b]	Proton[a]	δ ppm[b]
H2	2.45	**H21**	1.55	**H37'**	2.19
H2'	2.55	**H21'**	1.65	**H39**	2.02
H3	3.95	**H22**	1.40	**H39'**	2.26
H4	1.42	**H22'**	1.55	**H40**	3.94
H4'	1.72	**H23**	3.62	**H41**	3.85
H5	1.48	**H24**	0.94	**H42**	2.26
H5'	2.09	**H24'**	1.87	**CH_3-42**	0.96
H6	4.02	**H25**	2.15	**H43**	1.30
H7	3.17	**CH_3-25**	1.03	**H43'**	
H8	4.00	**26=CH**	4.78	**H45**	1.28
C8-OH	3.56	**26'=CH**	4.82	**H45'**	1.45
H9	3.90	**H27**	3.68	**H46**	2.08
H10	4.90	**H28**	1.60	**CH_3-46**	0.92
H12	6.19	**H28'**	2.20	**H47**	3.07
H13	5.95	**H29**	3.80	**H48**	3.52
H15	2.66	**H30**	4.50	**H49**	1.79
H15'	2.82	**H31**	1.95	**H49'**	2.15
H16	1.80	**CH_3-31**	1.03	**H50**	3.92
H16'	1.80	**H32**	3.32	**H51**	4.04
H17	3.90	**H33**	3.78	**H52**	2.02
H18	2.20	**H34**	1.92	**H52'**	2.02
H18'	2.80	**H34'**	2.08	**H53**	4.25
19=CH	4.86	**H35**	4.12	**H54**	3.55
19'=CH	5.08	**H36**	4.02	**H55**	3.69
H20	4.70	**H37**	2.19	**H55'**	3.69

[a] The symbol ' represents the less shielded proton of a geminal pair.

[b] Data recorded at 23 °C in $CDCl_3$ at 300 MHz with chemical shifts in ppm and referenced to $CHCl_3$, δ_H 7.25 ppm.

Table 6.3.4 ^{13}C NMR Data for *Epi*-Furan Acid Product (**6.3.2**)

Carbon	δ ppm[a]	Carbon	δ ppm[a]	Carbon	δ ppm[a]
C1	171.0	**C21**		**C39**	44.3
C2	40.2	**C22**		**C40**	71.4
C3	75.2	**C23**	77.2	**C41**	78.8
C4		**C24**	43.2	**$\underline{C}$-CH_3-42**	25.8
C5		**$\underline{C}$-CH_3-25**	36.0	**C-$\underline{C}H_3$-42**	17.5
C6	68.9	**C-$\underline{C}H_3$-25**	17.6	**C43**	36.8
C7	79.0	**26$\underline{C}$=CH_2**	151.1	**C44**	96.0
C8	64.8	**26C=$\underline{C}H_2$**	104.5	**C45**	36.8
C9	69.0	**C27**	74.9	**$\underline{C}$-CH_3-46**	28.9
C10	71.2	**C28**	33.8	**C-$\underline{C}H_3$-46**	17.0
C11	151.0	**C29**	71.4	**C47**	72.7
C12	109.1	**C30**	76.2	**C48**	63.4
C13	105.9	**$\underline{C}$-CH_3-31**	36.5	**C49**	31.0
C14	155.0	**C-$\underline{C}H_3$-31**	14.6	**C50**	74.6
C15	24.0	**C32**	76.2	**C51**	76.3
C16	34.0	**C33**	68.0	**C52**	36.7
C17	77.2	**C34**		**C53**	79.7
C18	39.6	**C35**	78.0	**C54**	72.1
19$\underline{C}$=CH_2		**C36**		**C55**	65.5
19C=$\underline{C}H_2$	105.2	**C37**	44.2		
C20	78.6	**C38**	114.0		

a ^{13}C NMR spectral data assigned from HSMQC and HMBC experiments, recorded at 23°C in $CDCl_3$ at 300 MHz with chemical shifts in ppm.

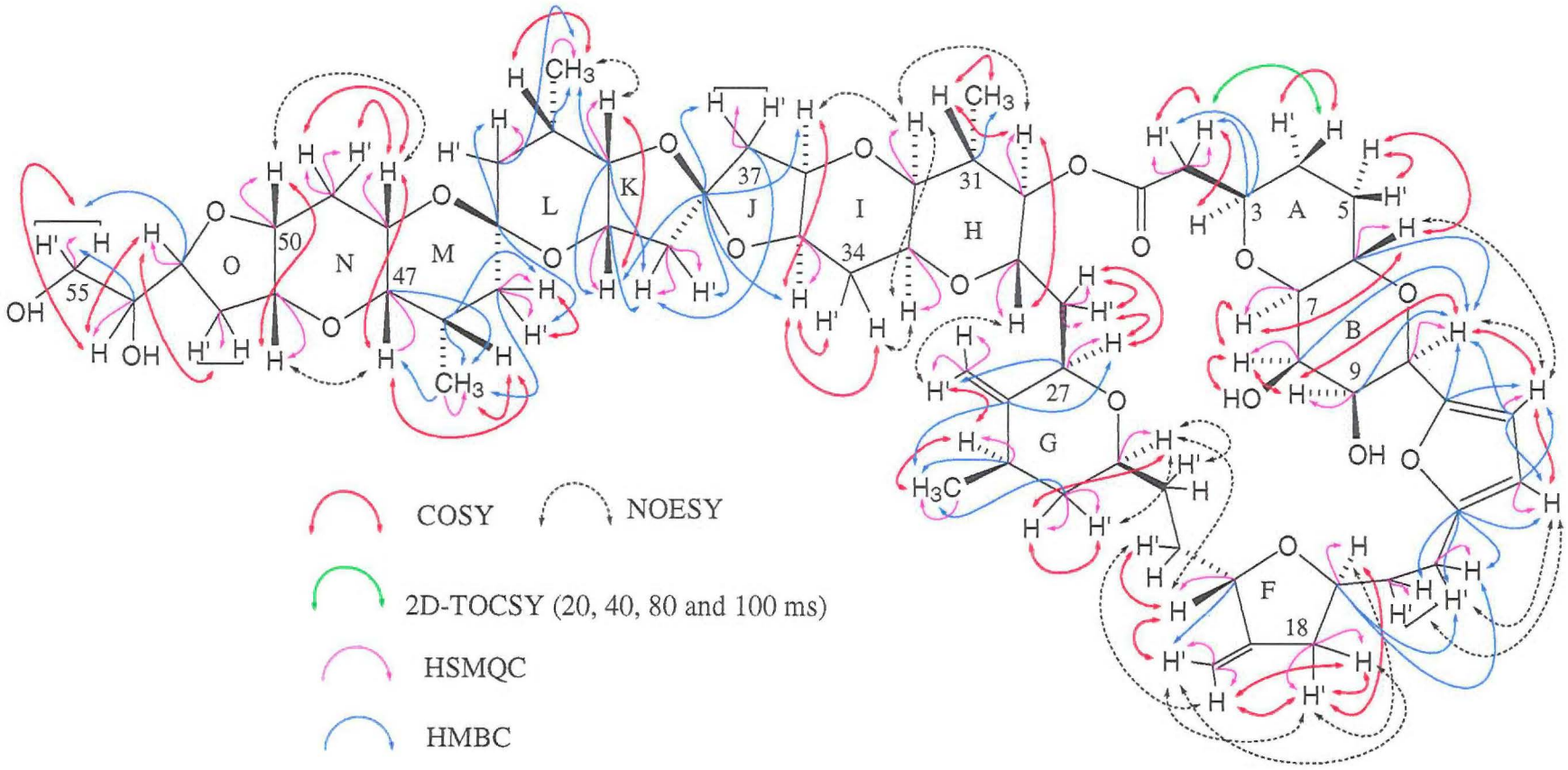

Figure 6.3.6 *Epi*-Furan Acid Product- Important NMR Correlations

An analysis of the NMR experiments showed that the connectivities in the terminal region were similar to homohalichondrin B (**1.2.3**) and acid product **6.3.1**, with only small differences in chemical shift data. The NMR correlations and the ^{1}H and ^{13}C NMR data in the C1-C14 region were consistent with formation of the "E-ring" furan derivative as observed for the furan acid product, **6.3.1**. The region from the I ring to the L ring became the focus of attention in terms of differences relative to the furan acid product **6.3.1**.

The methyl group remaining unassigned after analysis of the terminal region (C44-C55) and the A-H rings, *viz* the CH_3-42 doublet, was situated at δ_H 0.96 ppm. A COSY correlation from this methyl resonance to a proton resonating at δ_H 2.26 ppm assigned the chemical shift of the H42 methine proton. From the CH_3-42 resonance, a correlation to a proton resonating at δ_H 3.85 ppm was observed in the 2D-TOCSY spectra (for 20 ms, 40 ms, 80 ms and 100 ms mixing times). This resonance was assigned to the H41 proton. In the COSY spectrum, a correlation was observed between the proton at δ_H 3.85 ppm (H41) and a proton resonating at δ_H 3.94 ppm, assigning the chemical shift of the H40 proton. The HSMQC spectrum showed an unassigned correlation for a carbon at δ_C 78.8 ppm to the H41 proton at δ_H 3.85 ppm, locating the chemical shift of the C41 carbon resonance. An HMBC correlation from a carbon at δ_C 36.8 ppm to the CH_3-42 methyl protons assigned the chemical shift of the C43 carbon. The previously assigned C44 spiro carbon (at δ_C 96.0 ppm) showed a correlation to H45' (assigned a chemical shift of δ_H 1.45 ppm) as well as to a proton at δ_H 1.30 ppm. The proton at δ_H 1.30 ppm was correlated in the HSMQC spectrum to the C43 carbon, so this resonance was attributed to the H43 proton. HMBC correlations were observed from the C41 carbon to the CH_3-42 protons and to a resonance at δ_H 2.02 ppm. This resonance was assigned as one of the H39 proton resonances. An HMBC correlation from C40 to δ_H 2.02 ppm supported this assignment.

The HSMQC spectrum revealed three unassigned and distinct correlations: one from at carbon at δ_C 44.2 ppm to two equivalent methylene protons at δ_H 2.19 ppm; the other correlation from a carbon at δ_C 44.3 ppm to two equivalent methylene protons at δ_H 2.02 ppm (H39) and δ_H 2.26 ppm. This implied that the methylene partner to the H39 proton (at δ_H 2.02 ppm) was situated at δ_H 2.26 ppm, and that the C39 carbon chemical shift was δ_C 44.3 ppm. The δ_H 2.19 ppm proton resonance was assigned to the equivalent H37 and H37' protons, and the δ_C 44.2 ppm signal as the C37 resonance. The C38 spiro centre carbon at δ_C 114.0 ppm gave HMBC correlations to the H37/H37' protons (at δ_H 2.19 ppm) and to the H39' proton at δ_H 2.26 ppm. The C38 carbon also gave HMBC correlations to the H40, H35 and H36 protons.

Once assigned, the NMR data for acid product **6.3.2** were compared to the ^1H and ^{13}C NMR data around the I to K rings relative to those of the furan acid product (**6.3.1**) and homohalichondrin B (**1.2.3**). In general, the changes in chemical shifts were most significant around the C38 centre.

In terms of specific ^{13}C NMR chemical shifts, the C38 spiro centre recorded a large change, from δ_C 112.4 ppm in homohalichondrin B and in furan acid product **6.3.1,** to δ_C 114.0 ppm in acid product **6.3.2**. The C39 carbon located at δ_C 42.5 ppm in homohalichondrin B and δ_C 42.8 ppm in the furan acid product **6.3.1**, moved to δ_C 44.3 ppm in the ^{13}C NMR spectrum of acid product **6.3.2**.

In terms of specific changes in ^1H NMR chemical shifts, the H41 proton (at δ_H 3.85 ppm in **6.3.2**) recorded a large change, by δ_H 0.15 ppm, to a more deshielded position relative to the chemical shift of H41 in the spectra of both homohalichondrin B (**1.2.3**) and the furan acid product (**6.3.1**). Larger changes in chemical shift were observed for the H37 and H39 protons. The H37 and H37' ^1H NMR resonances

appeared as two separate signals at δ_H 1.90 ppm and δ_H 2.35 ppm respectively in the spectrum of homohalichondrin B (**Figure 2.4.1**). In the furan acid product **6.3.1**, these resonances were located at δ_H 1.89 ppm (H37) and δ_H 2.35 ppm (H37'). In acid product **6.3.2**, H37 and H37' were equivalent, at δ_H 2.19 ppm. Conversely, the H39 and H39' proton signals were equivalent in homohalichondrin B (δ_H 2.21 ppm) and acid product **6.3.1** (δ_H 2.18 ppm), but appeared as separate resonances (δ_H 2.02 ppm and δ_H 2.26 ppm) in the ^{1}H NMR spectrum of the acid product (**6.3.2**).

This information pointed to a change around the C38 spiro centre *ie* epimerisation to give the *epi*-furan acid product **6.3.2**.

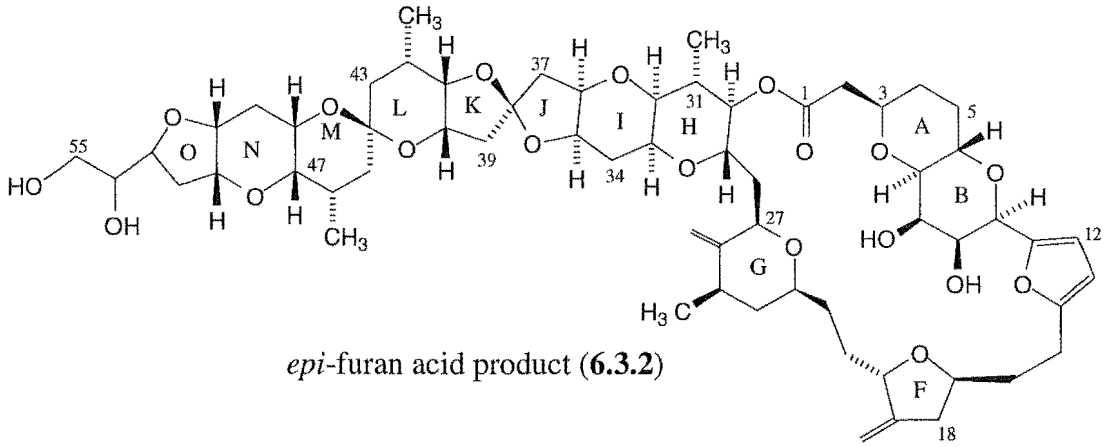

epi-furan acid product (**6.3.2**)

It proved difficult to determine the stereochemistry about the C38 centre. Construction of a model of the H to L rings suggested that NOEs might be observed between the H37/H37' and H39/H39' methylene protons for both the naturally occurring C38 stereochemistry and the *epi*-stereochemistry as these protons were situated close in space. Unfortunately, no NOEs were observed across the C38 spiro

centre in the NOESY spectra of either homohalichondrin B (**1.2.3**) or acid product **6.3.2**.

It was hypothesised that an inversion in stereochemistry at the C38 centre could induce conformational changes in the surrounding rings. This aspect is discussed in Section 6.3.4.

Like the furan acid product (**6.3.1**), the NOESY spectrum of **6.3.2** lacked the H2' to H20 and 19=CH correlations that were apparent in the NOESY spectra of homohalichondrin B and halichondrin B. Observed were the H13 to H15' and H12 to H6 and H12 to H10 correlations seen in the NOESY spectrum of the furan acid product (**6.3.1**). The ^{1}H NMR resonances around the H-ring were also similar to those of **6.3.1**, suggesting that the conformation of the lactone ring was similar in the two acid products (**6.3.1** and **6.3.2**) to give a similar electronic environment for protons around the H-ring, and the NOESY correlations observed for the furan protons.

A possible mechanism for formation of the C38 epimer in the absence of water is depicted in **Figure 6.3.7**. This mechanism involves protonation of either the J or K ring ether oxygens, opening of the protonated cyclic ether and formation of the central oxonium ion species. From this species, attack of the hydroxyl group on either face of the oxonium ion to give either a retention or inversion of stereochemistry at the spiro centre, would result in homohalichondrin B or its C38 epimer respectively.

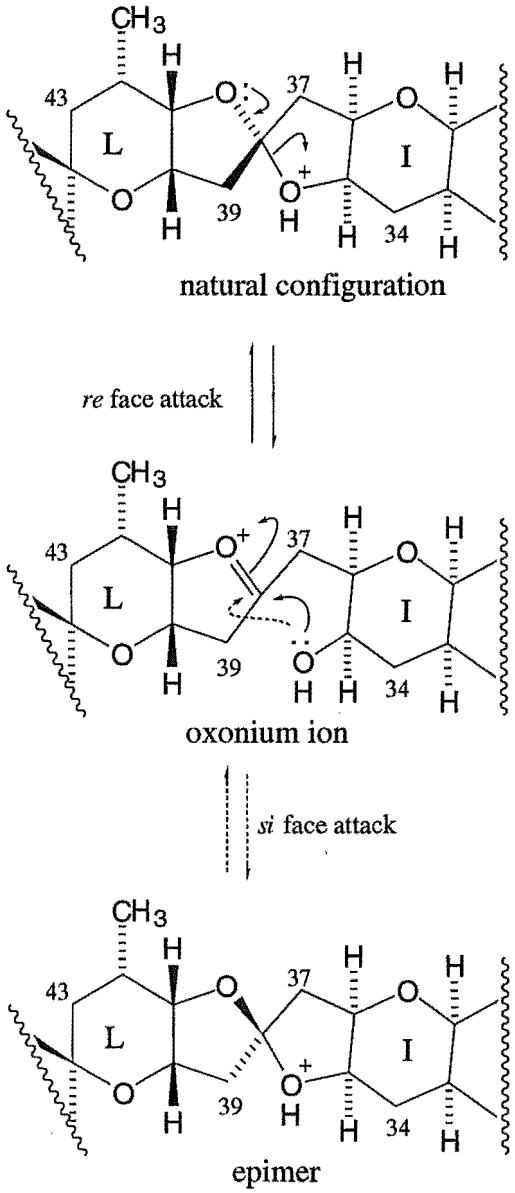

Figure 6.3.7 Proposed Mechanism of C38 Epimer Formation, Following Protonation of J-ring Ether Oxygen

6.3.3 Assignment of Acid Product 6.3.3

The uv spectrum of the least polar of the three acid products (eluting off the analytical C18 HPLC column at *ca* 1000 s in 70% acetonitrile/ water), **6.3.3**, indicated that this compound contained no uv chromophore, with end-absorption at *ca* 193 nm; a uv spectrum identical to that of homohalichondrin B (**1.2.3**). High resolution FAB-MS performed on the acid product **6.3.3** gave a parent ion corresponding to a molecular formula of $C_{61}H_{86}O_{19}$. This molecular formula was isobaric with homohalichondrin B (**1.2.3**).

The ^1H NMR spectrum of acid product **6.3.3** is displayed in **Figure 6.3.8**. This spectrum (obtained in $CDCl_3$/ 0.1% pyridine-d_5) lacked the distinctive furan resonances observed in the spectra of both the furan acid product (**6.3.1**) and the *epi*-furan acid product (**6.3.2**). There were several minor changes apparent relative to the ^1H NMR spectrum of homohalichondrin B (**Figure 2.4.1**). In the methyl region of the spectrum, two methyl doublet resonances at δ_H 0.99 ppm appeared as one overlapping doublet, with another doublet corresponding to one methyl group, in a more deshielded position at δ_H 1.04 ppm and another more shielded, single methyl group, at δ_H 0.94 ppm. The following distinctive resonances were still apparent in the ^1H NMR spectrum of acid product **6.3.3**, with little or no change in chemical shift relative to the spectrum of homohalichondrin B: H47, H7, H18', H2', H55/H55', H50, H11, 19=CH_2 and 26=CH_2 (at δ_H 3.06 ppm, δ_H 2.94, δ_H 2.79, δ_H 2.58, δ_H 3.69, δ_H 3.90, δ_H 4.58, δ_H 4.91, δ_H 4.98, δ_H 4.75 and δ_H 4.80 ppm respectively, in the ^1H NMR spectrum of homohalichondrin B). The H32 proton resonance appeared to have moved to a slightly more shielded position, from δ_H 3.17 ppm in the ^1H NMR spectrum of homohalichondrin B to δ_H 3.12 ppm in **6.3.3**. A new,

broad singlet resonance was apparent at δ_H 3.82 ppm, while the region around δ_H 3.60 ppm showed minor changes in the multiplicity of some of the overlapping resonances. The information obtained from comparison of the ^1H NMR spectrum of **6.3.3** (**Figure 6.3.8**) with that of homohalichondrin B (**Figure 2.4.1**) indicated that the terminal (C44-C55) and the C1-C30 regions were intact and unaltered.

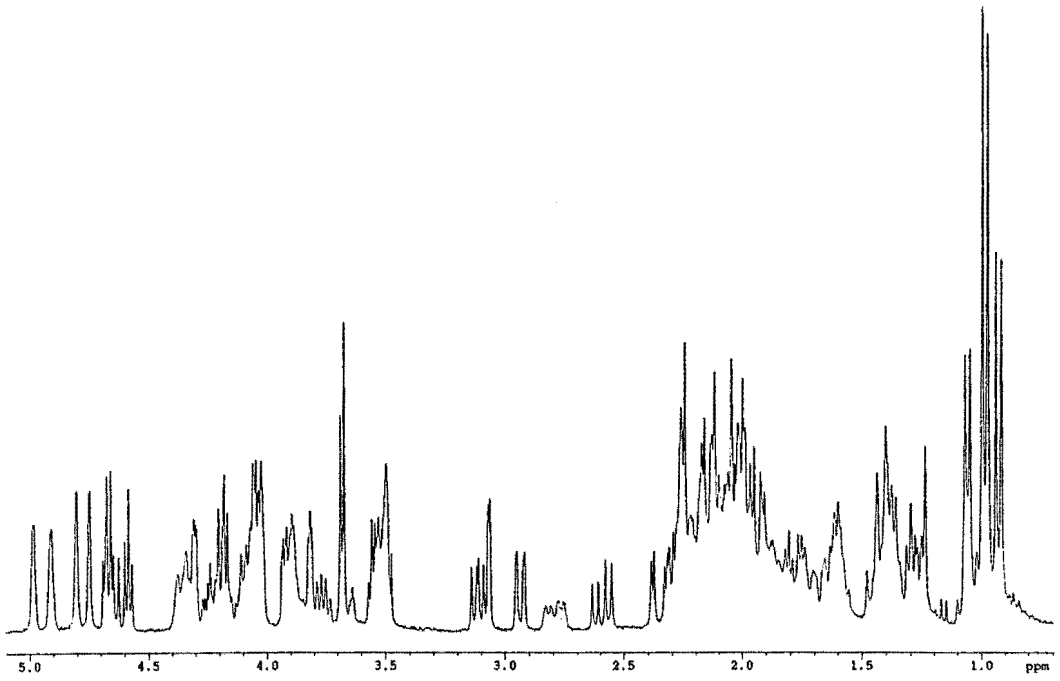

Figure 6.3.8 ^1H NMR Spectrum of Acid Product **6.3.3**

Various NMR experiments were performed on acid product **6.3.3**, *viz* COSY, 1D-TOCSY, 2D-TOCSY (with mixing times of 20 ms, 50 ms and 100 ms), HMQC, HMBC, NOE and NOESY experiments. These experiments were analysed to give a partial assignment of the ^1H and ^{13}C NMR spectra of **6.3.3**. The ^1H and ^{13}C NMR data are cited in **Tables 6.3.5** and **6.3.6** respectively, and the important correlations from these experiments are shown in **Figure 6.3.9**.

Table 6.3.5 ^{1}H NMR Data for *Epi* Acid Product (**6.3.3**)

Proton[a]	δ ppm[b]	Proton[a]	δ ppm[b]	Proton[a]	δ ppm[b]
H2	2.35	**H21**		**H39**	2.02
H2'	2.62	**H21'**	1.85	**H39'**	2.28
H3	3.86	**H22**	1.60	**H40**	3.92
H4	1.35	**H22'**	1.60	**H41**	3.82
H4'	1.75	**H23**	3.50	**H42**	2.26
H5	1.38	**H24**	1.05	**CH_3-42**	0.99
H5'	2.08	**H24'**	1.68	**H43**	1.25
H6	4.33	**H25**	2.20	**H43'**	1.40
H7	2.94	**CH_3-25**	1.04	**H45**	1.29
H8	4.31	**26=CH**	4.75	**H45'**	1.42
H9	4.04	**26'=CH**	4.81	**H46**	2.08
H10	4.18	**H27**	3.50	**CH_3-46**	0.94
H11	4.59	**H28**	1.96	**H47**	3.06
H12	4.67	**H28'**	1.96	**H48**	3.50
H13	1.93	**H29**	4.18	**H49**	1.76
H13'	2.14	**H30**	4.66	**H49'**	2.15
H15	1.62	**H31**	2.05	**H50**	3.90
H15'	2.14	**CH_3-31**	0.99	**H51**	4.01
H16		**H32**	3.12	**H52**	2.00
H16'		**H33**	3.76	**H52'**	2.00
H17	4.06	**H34**		**H53**	4.25
H18	2.25	**H34'**	2.14	**H54**	3.55
H18'	2.80	**H35**	4.08	**H55**	3.69
19=CH	4.91	**H36**	4.04	**H55'**	3.69
19'=CH	4.98	**H37**	2.22		
H20	4.36	**H37'**	2.22		

[a] The symbol ' represents the less shielded proton of a geminal pair.

[b] Data recorded at 23 °C in $CDCl_3$ at 300 MHz with chemical shifts in ppm and referenced to $CHCl_3$, δ_H 7.25 ppm.

Table 6.3.6 ^{13}C NMR Data for *Epi* Acid Product (**6.3.3**)

Carbon	δ ppm[a]	Carbon	δ ppm[a]	Carbon	δ ppm[a]
C1	171.0	**C21**		**C39**	44.5
C2	40.3	**C22**	32.0	**C40**	71.3
C3	73.6	**C23**	74.5	**C41**	78.6
C4		**C24**	43.2	**C-CH$_3$-42**	25.3
C5		**C-CH$_3$-25**	35.9	**C-CH$_3$-42**	17.9
C6	68.0	**C-CH$_3$-25**	18.0	**C43**	37.0
C7	77.4	**26C=CH$_2$**	151.8	**C44**	96.8
C8	74.1	**26C=CH$_2$**	104.0	**C45**	37.0
C9	73.7	**C27**	73.2	**C-CH$_3$-46**	29.0
C10	76.3	**C28**		**C-CH$_3$-46**	17.3
C11	81.8	**C29**	71.0	**C47**	72.5
C12	80.8	**C30**	76.8	**C48**	63.4
C13	48.2	**C-CH$_3$-31**	36.2	**C49**	31.2
C14	110.0	**C-CH$_3$-31**	14.7	**C50**	
C15	34.2	**C32**	77.1	**C51**	
C16		**C33**	67.0	**C52**	
C17		**C34**		**C53**	79.4
C18	38.6	**C35**		**C54**	71.8
19C=CH$_2$		**C36**		**C55**	65.3
19C=CH$_2$	104.8	**C37**	43.9		
C20	75.0	**C38**	114.0		

a ^{13}C NMR spectral data assigned from HMQC and HMBC experiments, recorded at 23°C in $CDCl_3$ at 300 MHz with chemical shifts in ppm.

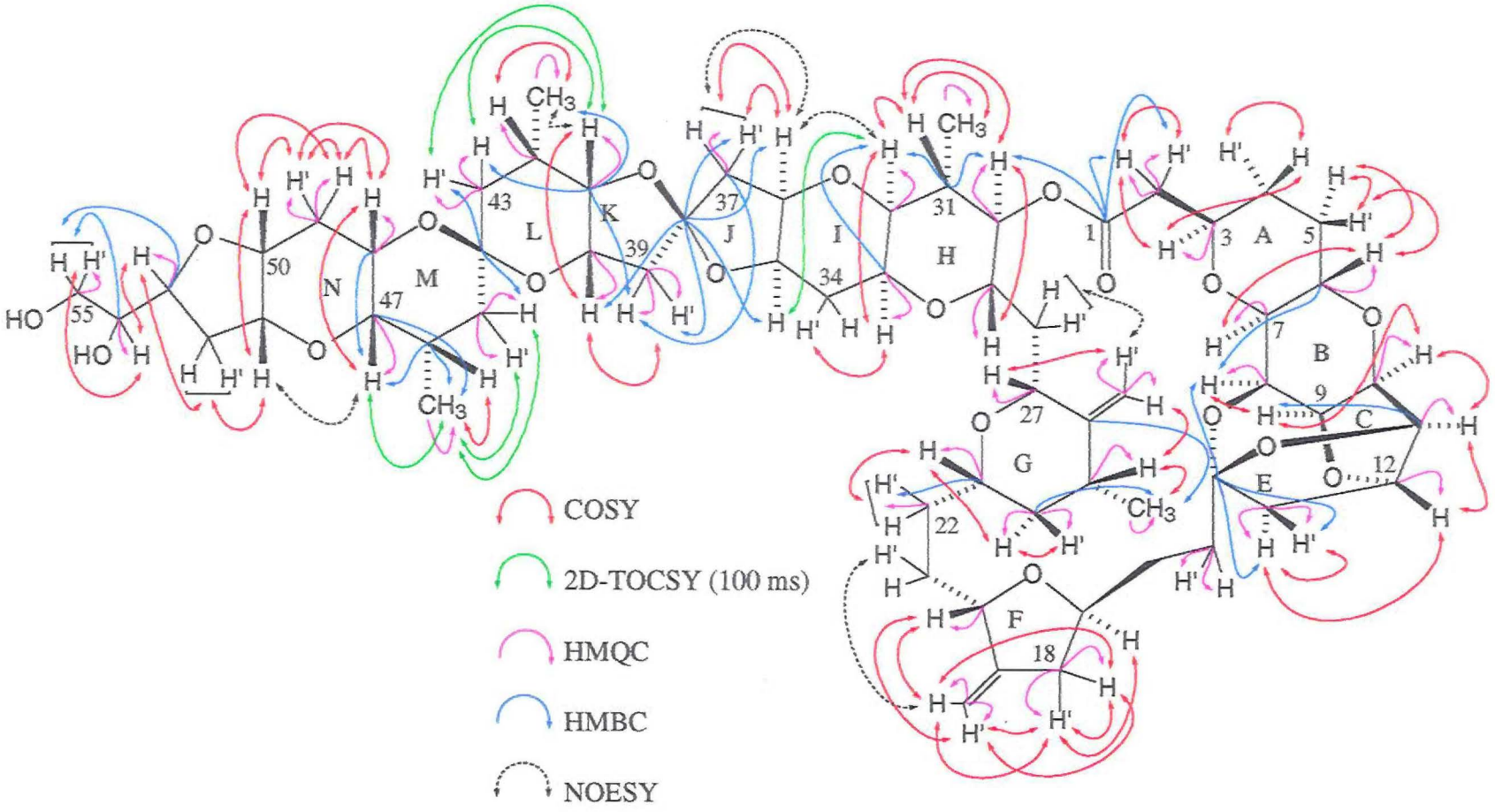

Figure 6.3.9 *Epi* Acid Product- Important NMR Correlations

These data confirmed that the connectivities and NMR chemical shifts around the C1-C30 and C44-C55 regions were identical with those of homohalichondrin B. It was apparent that the changes were again most significant around the C38 centre. The rings around this centre appeared to be intact, and the ^{1}H and ^{13}C NMR data compared well with those data observed for the *epi*-furan acid product (**6.3.2**). The H41 resonance was observed at δ_H 3.82 ppm, the H39 and H39' protons at δ_H 2.02 ppm and δ_H 2.28 ppm and the H37 and H37' protons at δ_H 2.22 ppm. These resonances were at very similar chemical shifts compared to **6.3.2**, but at quite different positions compared to homohalichondrin B. The C38 carbon resonance was observed at δ_C 114.0 ppm, identical to the C38 *epi*-furan acid product **6.3.2**. The C41 (δ_C 78.6 ppm), C39 (δ_C 44.5 ppm) and C37 (δ_C 43.9 ppm) resonances were also consistent with the *epi*-furan acid product (**6.3.2**).

These NMR data indicated that the acid product was the C38 epimer of homohalichondrin B, with the structure **6.3.3**.

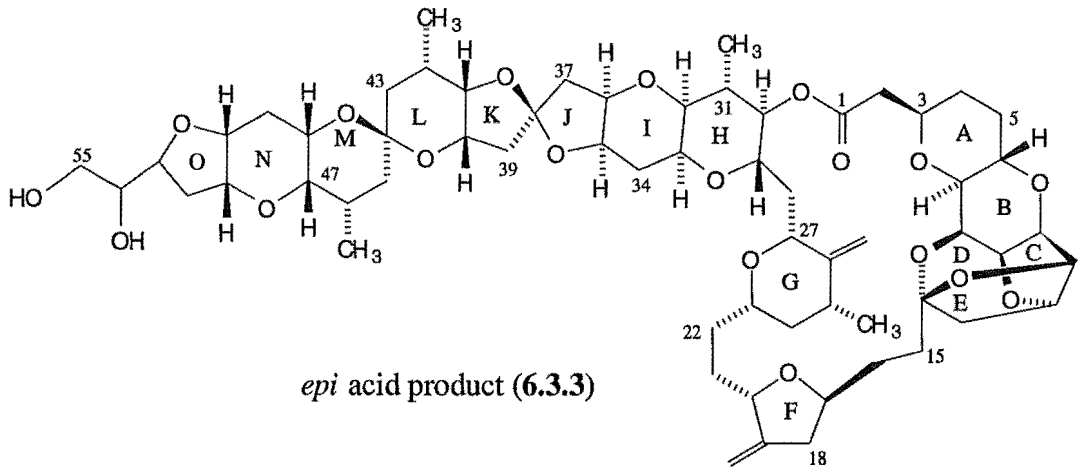

epi acid product (**6.3.3**)

The ^{1}H NMR chemical shifts around the A-H rings, notably CH_3-31 (δ_H 0.99 ppm), H29 (δ_H 4.18 ppm), H30 (δ_H 4.66 ppm), H31 (δ_H 2.05 ppm) and H32 (δ_H 3.12 ppm), were close to those observed in homohalichondrin B as opposed to those observed in the furan acid product **6.3.1** and the *epi*-furan acid product **6.3.2**. This was probably a reflection of the chemical shift changes invoked by the presence of the furan ring, and the conformational effects of its presence on the lactone ring and thus the electronic environment around the H ring. The NOESY spectrum showed a correlation between H2' (at δ_H 2.79 ppm) and 19=CH (at δ_H 4.91 ppm), implying a similar folding of the lactone ring to that observed in homohalichondrin B (and halichondrin B). This correlation was not observed in the NOESY spectra of the furan acid product (**6.3.1**) and the *epi*-furan acid product (**6.3.2**).

6.3.4 Computer Modelling of C38 Epimer Acid Product

In an effort to support the assignment of the *epi* stereochemistry at the C38 centre for the acid products **6.3.2** and **6.3.3**, computer modelling of the C28-C44 fragment with the "natural" C38 stereochemistry and the corresponding C38 epimer was undertaken. The resulting conformers were analysed to give vicinal coupling constants from the dihedral angles. These were compared to the vicinal coupling constants derived from homohalichondrin B, the *epi*-furan acid product **6.3.2** and the *epi* acid product **6.3.3**.

From the X-ray crystal structure of the norhalichondrin B derivative,[17] the C28-C44 portion of the molecule was excised to give the C29-methyl, C30-hydroxyl, C44-

hydroxyl and C44-methyl substituted derivative using the program Chem3D Plus. This structure was manipulated to give the epimer at C38. The energies of the X-ray crystallographic-derived structure and its epimer were subsequently minimised in Chem3D Plus. The resulting output is displayed in **Figure 6.3.10** for the natural (X-ray) and *epi* C38 stereochemistry.

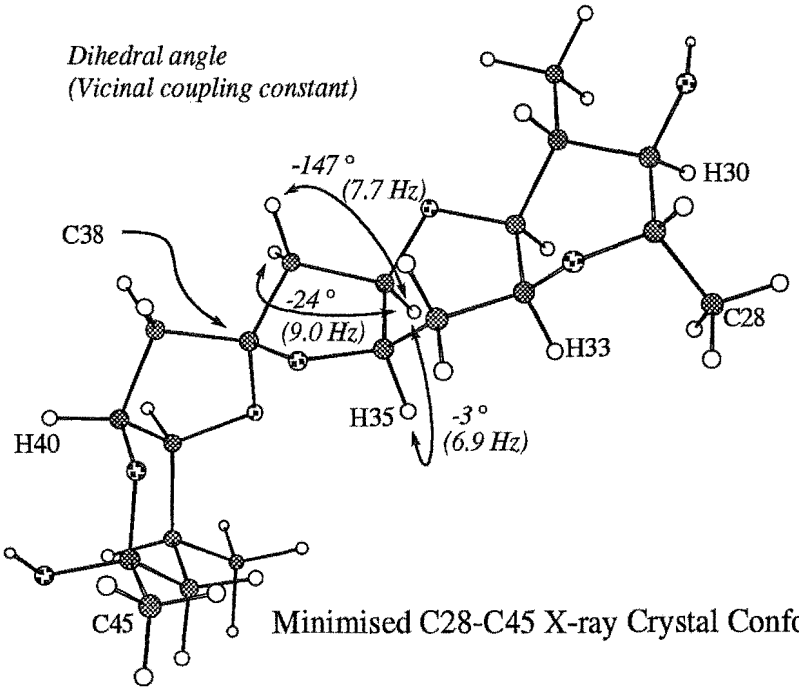

Minimised C28-C45 X-ray Crystal Conformer

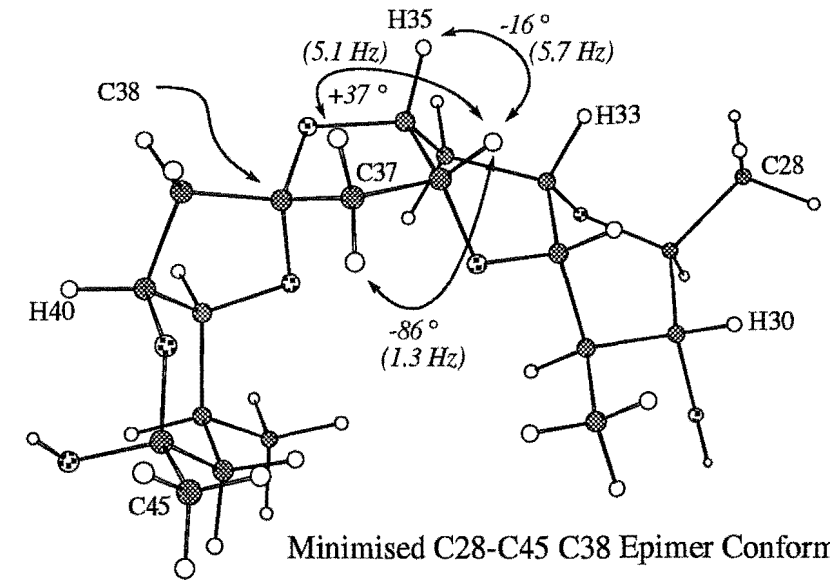

Minimised C28-C45 C38 Epimer Conformer

Figure 6.3.10 Chem3D Plus Minimised Structures of X-ray and *Epi* C38 Stereochemistry

The conformation of the structure with the X-ray crystal structure stereochemistry was little altered from that of the original X-ray crystal structure. Conversely, the conformation of the C38 epimer was markedly different to that of the X-ray crystal structure conformation. The main conformational change was apparent in the J-ring, which showed a greater degree of puckering relative to the X-ray crystal structure conformation and X-ray crystal structure-derived minimised conformations. An analysis of dihedral angles and vicinal coupling constants (obtained from MacroModel) indicated that the conformation of the H, K and L rings was relatively unchanged compared to the minimised X-ray crystal structure C28-C44 values. The key changes were associated with the H35-H36, H36-H37 and H36-H37' dihedral angles and coupling constants. These values are depicted in **Figure 6.3.10**. The H35-C-C-H36 dihedral angle was observed to increase from -3° to -16° on minimisation. One of the H36-C-C-H37 dihedral angles moved from -147° to -87°, while the other moved from -24° to +37°. The calculated coupling constants corresponding to these dihedral angles are given in **Figure 6.3.10**.

Construction of a model of this region indicated that if the C37 protons were pushed away from an interaction with the ether oxygen of the K-ring, the H35-H36 dihedral angle would be expected to increase and the J-ring would pucker, resulting in a "bent" molecule. It was discovered that the H and I rings could accommodate this puckering with little conformational change.

It was anticipated that the collection of experimental coupling constants, especially for the H35, H36, H37 and H37' protons for homohalichondrin B (**1.2.3**), the *epi*-furan and *epi* acid products (**6.3.2** and **6.3.3**) would provide evidence of this difference in the average solution conformation. Coupling constants were collected from the NMR experiments for these compounds for the H30-H37' region and are

listed in **Table 6.3.7** along with the predicted values for the minimised conformations from the computer modelling.

The H36 proton was only accessible through an NOE interaction from the isolated H32 proton of the *epi*-furan acid product (**6.3.2**) and homohalichondrin B (**1.2.3**). Unfortunately, the complex appearance of the H36 multiplet was difficult to interpret in terms of coupling constants. However, the coupling constants for the H30 and H32 protons for the *epi*-furan and *epi* acid products (**6.3.2** and **6.3.3**) were consistent with those of homohalichondrin B (**1.2.3**) and the minimised computer generated conformers, indicating an average boat conformation existed for the *epi* and *epi*-furan acid products.

Table 6.3.7 Vicinal Coupling Constants: Calculated and Experimental

Coupled	Calculated $^3J_{HH}$ (Hz)		Experimental $^3J_{HH}$ (Hz)		
protons	**X-ray**	**C38 *epi***	**1.2.3**	**6.3.2**	**6.3.3**
H30-H31	10.4	10.3	10.0	10.3	10.0
H31-H32	10.9	11.1	7.8	9.4	8.8
H32-H33	7.5	7.7	6.2	7.0	6.6
H33-H34	4.7	4.5	5.7		
H33-H34'	11.2	11.2	11.2		
H34-H35	10.8	9.6			
H34'-H35	5.6	7.0			
H35-H36	6.9	5.7			
H36-H37	9.0[a]	5.1[a]			
H36-H37'	7.7[a]	1.3[a]			

[a] Assignments may be interchanged.

No conclusions could be drawn on the average solution conformation of the *epi* or the *epi*-furan acid products from a comparison of the modelling results with the NMR data that would support epimerisation at the C38 centre in the acid products **6.3.2** and **6.3.3**, because the experimental coupling constants for the H35-H37 protons could not be obtained from any of the NMR experiments performed.

Despite the difficulties in obtaining the necessary coupling constants to assist in the assignment of the C38 stereochemistry of **6.3.2** and **6.3.3**, there was no evidence from the analysis of the NMR data to suggest that the changes observed in **6.3.3** (and **6.3.2**) could have been elsewhere in the molecule.

6.4 Time-Scale Acid Reactions

An investigation was undertaken to determine the inter-relationship of the three acid products (**6.3.1**, **6.3.2** and **6.3.3**) and homohalichondrin B (**1.2.3**), under the acid reaction conditions.

The time-scale reaction of CSA in dichloromethane with homohalichondrin B was also performed, with regard to the final step in the Kishi total synthesis of halichondrin B (refer to Appendix II) which involved ketalisation with CSA to form the final C38 spiro centre. Also of interest were the identities of the products formed in relation to the TFA reactions.

These reactions were monitored closely by HPLC with time. A ^{1}H NMR spectrum was acquired on a standard mixture, comprising the three acid products (**6.3.1**, **6.3.2**, **6.3.3**) and homohalichondrin B (**1.2.3**), and this standard was also injected into the HPLC. A calculation of the molar absorptivity (ε) of the furan products (**6.3.1** and **6.3.2**) relative to the non-furan products (**1.2.3** and **6.3.3**) was undertaken so that an accurate quantification of the HPLC component peaks could be calculated at each stage in the reaction. In the ^{1}H NMR spectrum, an integral over the H12 and H13 furan resonances at δ_H 5.95 ppm and δ_H 6.18 ppm relative to the H7 resonance (δ_H 2.94 ppm), common to homohalichondrin B (**1.2.3**) and the *epi* acid product (**6.3.3**), gave the true ratio of furan products relative to non-furan products. Integration of the four peaks in the HPLC chromatogram of the standard mixture at λ 199 nm, gave the sum of the furan *vs* non-furan components. Comparison with the ratios from the ^{1}H NMR spectrum gave the ratio of the molar absorptivities of the furan products *vs* the non-furans. This ratio was calculated at 5.9 : 1 for $\varepsilon_{furans} : \varepsilon_{non\text{-}furans}$. Implicit in this calculation was the assumption that the molar absorptivities of the two furans

(**6.3.1** and **6.3.2**) were the same, and that the molar absorptivities of the non-furan compounds (**1.2.3** and **6.3.3**) were also the same.

6.4.1 Time-Scale TFA Reaction of Furan Acid Product

A small quantity of the furan acid product (**6.3.1**) was dissolved in dichloromethane and an aliquot removed for HPLC analysis, as a reference chromatogram. Standardised TFA in dichloromethane solution was added to the furan acid product to give a 2 to 1 molar ratio of **6.3.1** to TFA. The reaction was stirred at room temperature and analysed by HPLC (analytical C18 column, mobile phase 70% acetonitrile/ water). Samples were extracted from the reaction mixture at regular intervals (after 10 min, 30 min, 1 hr, 2.5 hr, 3.5 hr, 4.5 hr, 7 hr, 11 hr, 18 hr, 35.5 hr, 49 hr and 73.5 hr of reaction) for immediate HPLC analysis. The peaks in the HPLC chromatograms were integrated at λ 199 nm, and each identified component was expressed as a relative percentage of the total amount of identified components present at that time.

Figure 6.4.1 displays a graph of the relative percentage of each component with increasing reaction time. The proportion of furan acid product (**6.3.1**) was observed to decrease as its C38 epimer, the *epi*-furan acid product **6.3.2**, formed. The decay was observed to level off after approximately 18 hours reaction, and after 49 hours reaction a slight excess of the *epi*-furan acid product (**6.3.2**) over the furan acid product (**6.3.1**) was observed. After this time, contributions from other, more polar unidentified components made an analysis of subsequent HPLC chromatograms

unreliable. No evidence of either homohalichondrin B (**1.2.3**) or the *epi* acid product (**6.3.3**) was observed at any time.

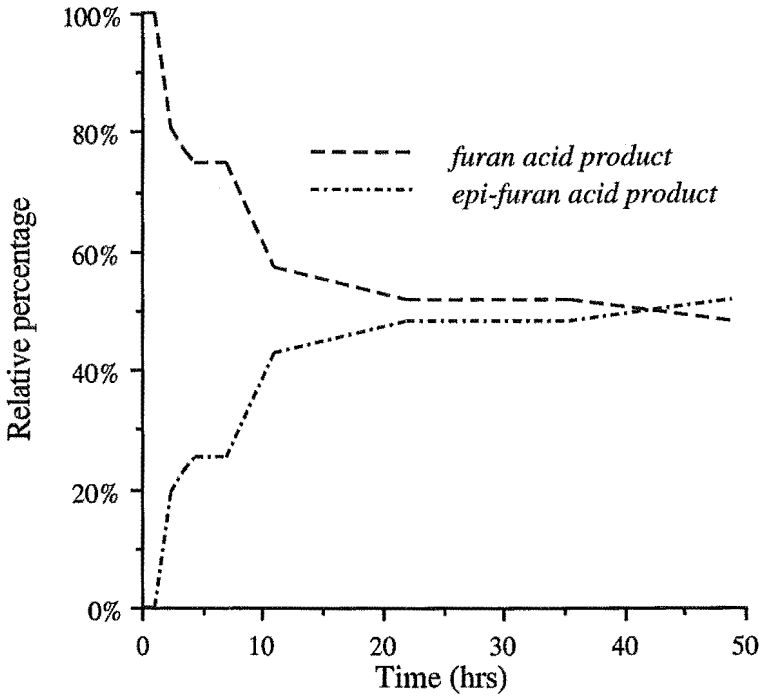

Figure 6.4.1 Graph of TFA Acid Reaction of Furan Acid Product (**6.3.1**)

These results suggested that the furan product was an end-product of the acid reaction of homohalichondrin B (*ie* it was not reversible to regenerate homohalichondrin B). Also apparent from these results was the relationship between the furan acid product (**6.3.1**) and the *epi*-furan acid product (**6.3.2**), suggesting an equilibrium existed between the two products under these reaction conditions. However, the equilibrium appeared to be relatively slow to establish, and contributions from subsequent acid decomposition mechanisms meant that the

analysis of the furan and *epi*-furan acid products became unreliable after 49 hours, perhaps before the equilibrium had time to fully establish.

6.4.2 Time-Scale TFA Reaction of *Epi*-Furan Acid Product

A small quantity of the *epi*-furan acid product (**6.3.2**) was dissolved in dichloromethane, and a small aliquot of this solution was taken for HPLC analysis (using an analytical C18 column with 70% acetonitrile/ water as the mobile phase), for reference purposes.

To this solution, a standard solution of TFA in dichloromethane was added, to give a molar ratio of 2 moles *epi*-furan acid product (**6.3.2**) to 1 mole of TFA. This solution was stirred at room temperature and the reaction progress was monitored at regular intervals (*viz* after 15 min, 1 hr, 2 hr, 3 hr, 4 hr, 7 hr, 22 hr, and 48 hr reaction) by HPLC. Each identified component peak in the chromatogram was integrated at λ 199 nm, and its contribution to the total of the identified component integrals in the chromatogram was expressed as a relative percentage. A plot of the percentage of each component at each point in time during the course of the reaction, is shown in **Figure 6.4.2**.

From this graph, it was apparent that the *epi*-furan acid product (**6.3.1**) underwent decay to an equilibrium value, as the furan acid product (**6.3.2**) formed with time, to reach an equilibrium value after twenty-two hours reaction. This equilibrium appeared to be in favour of the *epi*-furan acid product (**6.3.2**). After forty-eight hours reaction, the reaction appeared to be leading off into subsequent acid decomposition

products. No adjustment was made to the graph for the appearance of these unidentified products. No evidence was observed, at any time, of the formation of homohalichondrin B or the *epi* acid product (**6.3.3**).

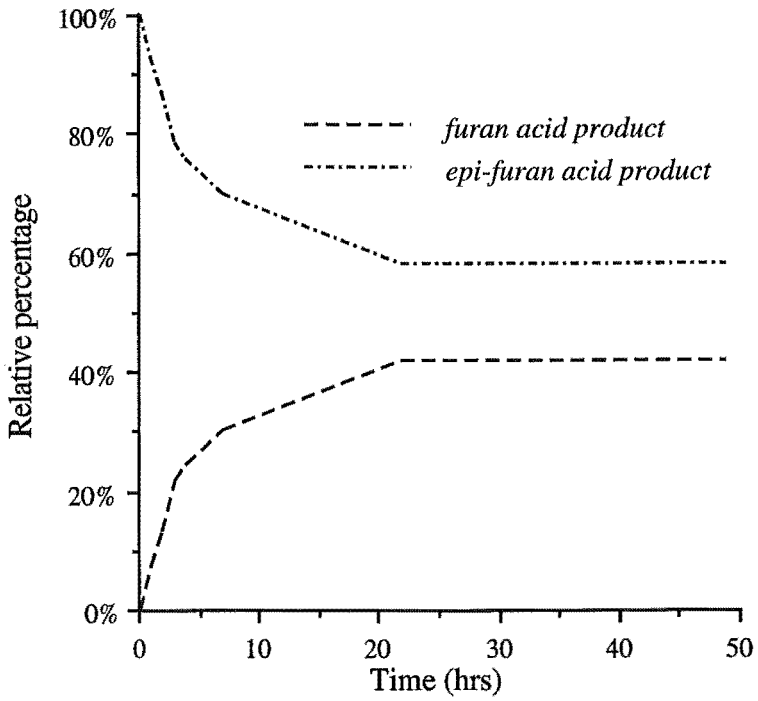

Figure 6.4.2 Graph of TFA Acid Reaction of *Epi*-Furan Acid Product (**6.3.2**)

These observations were consistent with the observations for the reaction of the furan acid product (**6.3.1**), and supported the belief that the reaction to produce the furan was not reversible. It also supported the theory that an equilibrium existed between the two furan acid products (**6.3.1** and **6.3.2**).

6.4.3 Time-Scale TFA Reaction of *Epi* Acid Product

A small quantity of the *epi* acid product (**6.3.3**) was dissolved in dichloromethane, and an aliquot of this solution was analysed by HPLC, using the conditions previously described, for reference. Standard TFA solution in dichloromethane was added to the *epi* acid product (**6.3.3**) to give a 2 : 1 molar ratio of **6.3.3** to TFA. The reaction was stirred at room temperature and monitored by HPLC with time. The identified component peaks in the chromatograms were integrated (at λ 199 nm), corrected for the appropriate ε values, and the relative percentage of each component was calculated. The reaction mixture was analysed by HPLC after 15 min, 45 min, 1.17 hr, 1.75 hr, 2.5 hr, 3 hr, 3.5 hr, 4.5 hr, 7 hr, 20.5 hr and 47 hr. **Figure 6.3.4** displays the graph of the variation in the relative percentage of each component with time.

A decay from 100% to 0% *epi* acid product (**6.3.3**) was observed over a reaction period of forty-seven hours. Initially, the build-up of homohalichondrin B (**1.2.3**) was observed, along with a build-up in both furan acid products (**6.3.1** and **6.3.2**). The build-up of the furan acid product (**6.3.1**) appeared to lag behind that of the *epi*-furan acid product (**6.3.2**). As the homohalichondrin B (**1.2.3**) and *epi* acid product (**6.3.3**) decayed, the proportion of furan acid products (**6.3.1** and **6.3.2**) continued to increase. After about twenty hours reaction, the relative amounts of the furan acid product (**6.3.1**) to the *epi*-furan product (**6.3.2**) reached an equilibrium in favour of the latter acid product.

From the time-scale reactions of the furan acid product (**6.3.1**) and the *epi*-furan acid product (**6.3.2**), described in Sections 6.4.1 and 6.4.2 respectively, it was apparent

that the formation of the furan products was not reversible under the reaction conditions. This implied that formation of homohalichondrin B in the time-scale reaction of the *epi* acid product (**6.3.3**) originated from epimerisation of **6.3.3**. It was likely that furan formation from the *epi* acid product (**6.3.3**) and homohalichondrin B (**1.2.3**) gave the relevant furan derivative.

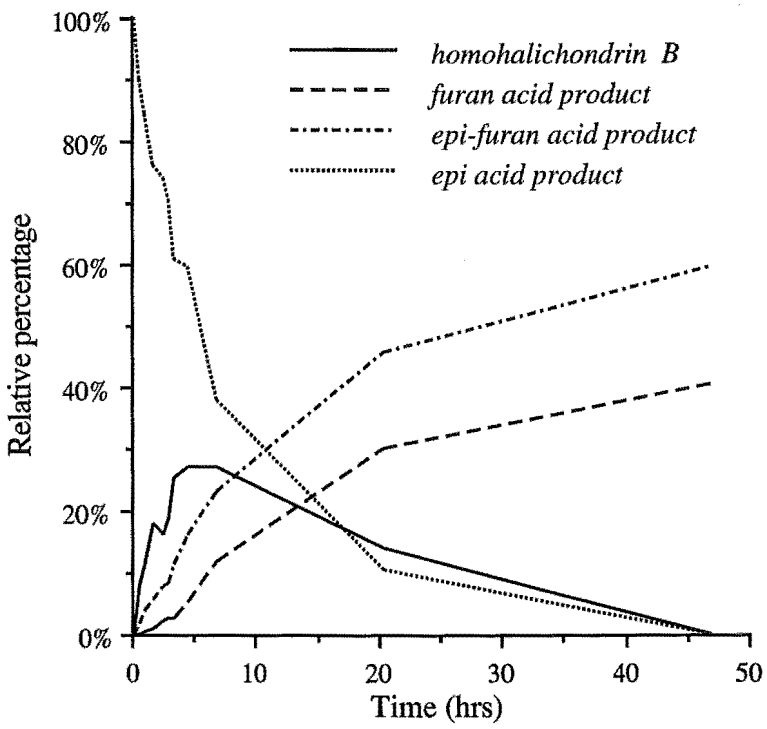

Figure 6.4.3 Graph of TFA Acid Reaction of *Epi* Acid Product (**6.3.3**)

6.4.4 Time-Scale TFA Reaction of Homohalichondrin B

To complete the series of time-scale reactions of the components involved in the TFA acid reactions, a time-scale study of homohalichondrin B (**1.2.3**) under the same reaction conditions was undertaken.

Initially, a small quantity of homohalichondrin B (**1.2.3**) was dissolved in dichloromethane and an aliquot of this solution was removed for HPLC analysis using the procedure described for the previous reactions. A standardised solution of TFA in dichloromethane was added to the homohalichondrin B solution to give a 2 : 1 molar ratio of homohalichondrin B to TFA. The reaction was stirred at room temperature and the reaction progress was monitored by HPLC. Aliquots of the reaction mixture were removed at regular intervals (after 15 min, 1 hr, 1.5 hr, 2.5 hr, 3 hr, 4 hr, 5 hr, 7 hr, 8 hr, 10 hr, 18 hr, 32 hr and 44 hr) and the solvent was immediately removed before HPLC injection in the mobile phase. For each injection, the resulting chromatogram was integrated at λ 199 nm, over each of the four identified components. Correction was made for the difference in molar absorptivities to give a quantification of the components in the reaction mixture at that point in time. A graph of the results of this experiment is given in **Figure 6.4.4**.

From **Figure 6.4.4**, it is apparent that the furan acid product (**6.3.1**) was the first product to form, after two and a half hours reaction. Subsequently, the *epi* acid product (**6.3.3**) and the *epi*-furan acid product (**6.3.2**) were observed, after four hours reaction. A slow build-up of furan acid products was observed as the proportion of homohalichondrin B slowly decreased with time. After forty-four hours reaction, no *epi* acid product (**6.3.3**) was observed in the reaction mixture, but some

homohalichondrin B (**1.2.3**) was still present. At this time the proportion of the *epi*-furan acid product (**6.3.2**) became dominant over the furan acid product (**6.3.1**). Unfortunately, after this time, the presence of additional and unidentified peaks in the chromatograms arose, making the analysis in terms of the four known components unreliable.

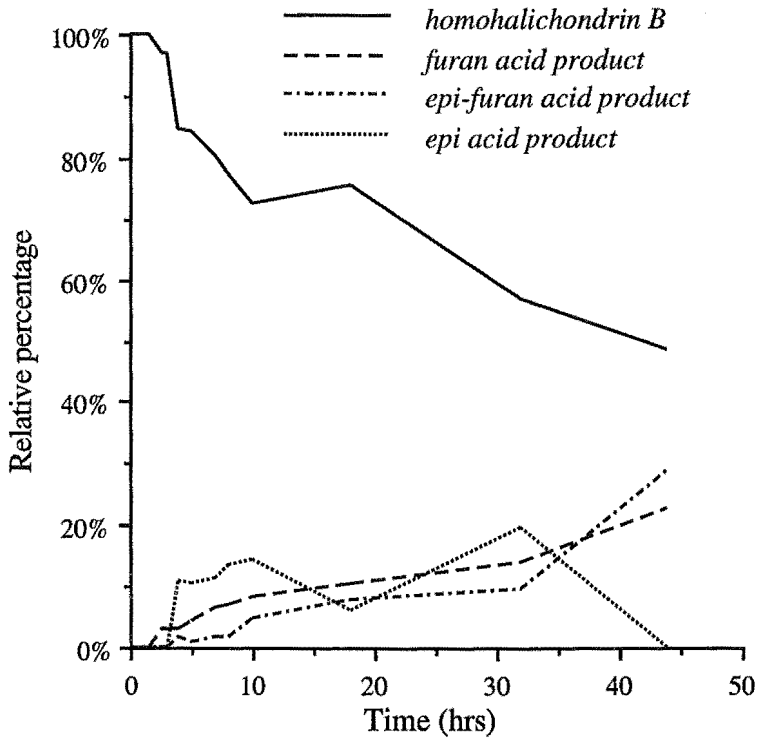

Figure 6.4.4 Graph of TFA Acid Reaction of Homohalichondrin B (**1.2.3**)

In comparison to the *epi* acid product (**6.3.3**) time-scale reaction, it was apparent that homohalichondrin B (**1.2.3**) had a longer lifetime under the TFA reaction conditions. The graph of the time-scale reaction of the *epi* acid product (**Figure 6.4.3**) shows a relatively rapid reaction of **6.3.3** occurring with time, whereas **Figure 6.4.4** shows

the persistence of homohalichondrin B in the reaction mixture, with a "shallower" curve. The reasons behind these observations were not clear. However, it was possible that conformational differences between the *epi* and "natural" C38 stereochemistry may have resulted in the observed differences in the rates of reaction.

In a qualitative sense, it was apparent that the furans (**6.3.1** and **6.3.2**) represented end-products of the reaction, while an equilibrium appeared to exist between the C38 epimeric products.

6.4.5 Time-Scale CSA Reaction of Homohalichondrin B

As discussed in Section 6.1, it was important to consider the effect of the acid CSA on homohalichondrin B (**1.2.3**). Kishi and co-workers reported the final C38 ketalisation step in the total synthesis of norhalichondrin B (**1.2.2**) and halichondrin B (**1.2.1**) with CSA in dichloromethane.[67] Their description of this reaction was lacking in detail as no indication as to the acid concentration or the duration of the reaction was given.

Initially, a small quantity of homohalichondrin B (**1.2.3**) was dissolved in dichloromethane. An aliquot of this solution was analysed by HPLC (analytical C18 column with 70% acetonitrile/ water as the mobile phase), for reference purposes. CSA in dichloromethane was then added to the homohalichondrin B (**1.2.3**) solution, to give a molar ratio of 10 : 1 for **1.2.3** to CSA. The reaction was stirred at room temperature and was monitored by HPLC after half an hour, one hour and two hours

and ten minutes of reaction. After this time, no reaction was apparent by HPLC so the CSA concentration was increased to give a 3 : 1 molar ratio of **1.2.3** to CSA. This reaction was stirred at room temperature and monitored with time (after 0.5 hr, 1 hr, 1 hr 40 min, 3 hr and 22 hr at a 3 :1 molar ratio), by HPLC. Identified peaks in the chromatogram (at λ 199 nm) were integrated and differences in the molar absorptivities were corrected, to allow quantification of the components. The data from this reaction is displayed in **Figure 6.4.5**, showing the proportion of each component at each point in time. After twenty-two hours reaction, contributions were observed from other, unidentified components, making the analysis in terms of the known products unreliable.

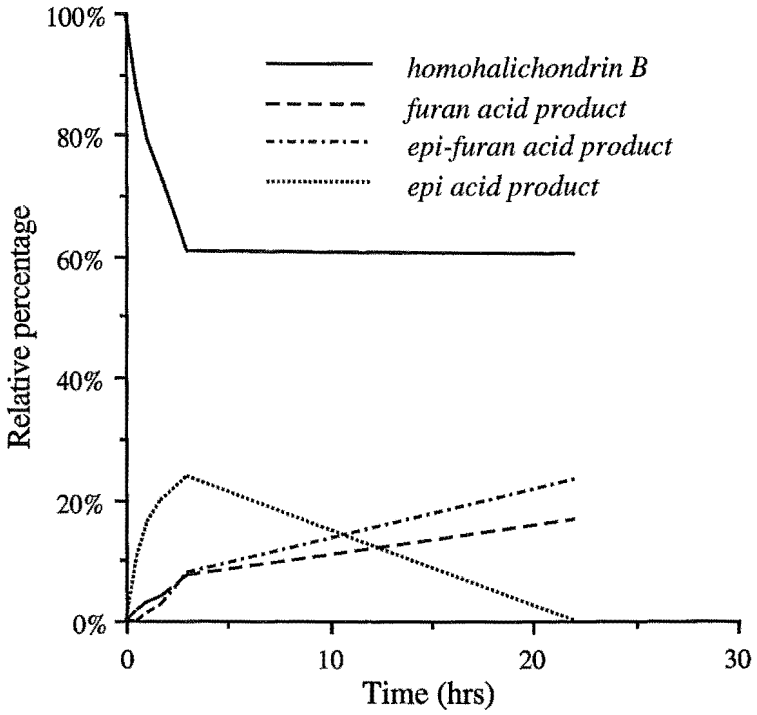

Figure 6.4.5 Graph of CSA Acid Reaction of Homohalichondrin B (**1.2.3**)

This reaction appeared to follow the same trends as the TFA reaction of homohalichondrin B (**1.2.3**), described in Section 6.4.4. Homohalichondrin B (**1.2.3**) appeared to react slowly as the two furan products (**6.3.1** and **6.3.2**) formed. Also observed was the *epi* acid product (**6.3.3**), although, as observed previously, this too reacted, presumably to the *epi*-furan acid product (**6.3.2**) as the reaction proceeded. The *epi*-furan product (**6.3.2**) appeared to be dominant over the furan product (**6.3.1**), after twenty-two hours reaction.

The significance of these results in relation to the total synthesis of halichondrin B (**1.2.1**) and norhalichondrin B (**1.2.2**) is discussed in Section 6.5.

6.5 Biological Activity Data

The biological activities of the three acid products (**6.3.1**, **6.3.2** and **6.3.3**), described in Section 6.3, were evaluated in the *in vitro* P388 assay and in the NCI primary *in vitro* antitumour screen. These data are cited in **Table 6.5.1**, along with those for the relevant parent halichondrin, homohalichondrin B (**1.2.3**).

Table 6.5.1 *In Vitro* Cytotoxicities of Selected Halichondrins

Compound	P388 IC_{50} (ng/mL)	NCI GI_{50} ($\times 10^{-10}$ M)	COMPARE Correlation[a]
homohalichondrin B (1.2.3)	0.22	3.16	0.95
furan acid product (6.3.1)	4.1	117	0.91
***epi*-furan acid product (6.3.2)**	8.4	478	0.69
***epi* acid product (6.3.3)**	15.0	475	0.86

a Correlation coefficient from the *Compare* pattern-recognition algorithm were calculated by computer using the GI_{50}-centred mean graph profiles of differential cellular sensitivities to each of the compounds. The GI_{50}-centred mean graph profile of halichondrin B was used as the "seed" for all of the comparisons.

Analysis of the cytotoxicity data (**Table 6.5.1**) indicated that for all the acid products, a decrease in cytotoxicity was observed in both the P388 assay and the NCI *in vitro* primary screen. The results of the P388 assay indicated that the furan acid product (**6.3.1**) was the most active of the three acid products, with a *ca* forty-fold reduction in activity relative to homohalichondrin B (**1.2.3**). The *epi*-furan and *epi*

acid products (**6.3.2** and **6.3.3**) recorded a larger decrease in P388 cytotoxicity relative to the furan acid product (**6.3.3**).

Similar trends were observed for the biological activities of the acid products in the NCI primary screen. The furan acid product (**6.3.1**) was the most active of the acid products in terms of the GI_{50} result (averaged over all sixty cell lines), with a *ca* thirty-five-fold reduction in biological activity relative to homohalichondrin B (**1.2.3**). The biological activities of the *epi*-furan and *epi* acid products (**6.3.2** and **6.3.3**) were very similar, with a *ca* one hundred and fifty-fold decrease in activity relative to homohalichondrin B (**1.2.3**).

The P388 cell line appeared to be less sensitive to changes in stereochemistry at the C38 centre than the averaged result over the sixty cell lines comprising the NCI screen, as the *epi*-furan acid product (**6.3.2**) recorded only a *ca* forty-fold decrease in P388 activity, and the *epi* acid product (**6.3.3**) only a *ca* seventy-fold decrease in P388 activity, relative to homohalichondrin B (**1.2.3**).

The COMPARE correlation coefficients for the furan acid product (**6.3.1**) and the *epi* acid product (**6.3.3**) were slightly reduced relative to the parent compound, homohalichondrin B (**1.2.3**), indicating that the mechanism of action for these acid products was still "halichondrin-like". The acid product with the C38 *epi* centre and furan ring (**6.3.2**) recorded a significant decrease in the COMPARE correlation coefficient (0.69).

In general terms, the formation of the E-ring furan derivative did not produce as large a decrease in activity as would have be expected for such a major structural change. However, it seems that the stereochemistry at the C38 centre is of greater significance in determining the biological activity in the halichondrin series.

A further discussion of these results in relation to those of other halichondrin analogues is found in Chapter 9.

These results indicate that the activity of the halichondrins (particularly the B series halichondrins) may be compromised if they were to be administered orally. In the acidic environment of the stomach (pH <1) the halichondrins would undergo rapid acid reaction to the acid products (**6.3.1**, **6.3.2** and **6.3.3**) and probably into subsequent decomposition products. Therefore, the administered halichondrin *eg* halichondrin B (**1.2.1**) would not reach the bloodstream, but rather a less potent derivative.

It is worthwhile at this stage to speculate on the significance of these reactions in relation to the total synthesis of halichondrin B and norhalichondrin B reported by Kishi and co-workers.[67] They indicated that the identity of the final halichondrin B product was confirmed "on the basis of spectroscopic (^{1}H NMR, MS, IR, $[\alpha]_D$) and chromatographic data". These authors make no comment on how the product was purified. From the observations of the acid reactions of homohalichondrin B in CSA solutions (and in TFA and PTSA), described in this Chapter, it would seem possible that the final reaction step in the total synthesis of halichondrin B could have given a mixture of products; halichondrin B and the acid reaction products.

Kishi's synthetic halichondrin B which was initially submitted to the NCI for biological testing, was less active than the naturally-derived material (a GI_{50} of 8.40 $\times 10^{-10}$ M). Given the biological activity data results of the acid products, it would appear possible that the decrease in biological activity observed for the synthetic material may have arisen from contamination with one or more of the acid products.

The ^1H NMR spectra (obtained in C_6D_6) of the synthetic halichondrin B was obtained. Unfortunately, there was no way of knowing if this was the same sample that was submitted for biological assessment. It is likely that if either of the furan acid products had been produced, that this would be obvious in a ^1H NMR spectrum of the product mixture. However, the presence of the *epi* acid product (**6.3.3**) would be more difficult to detect.

The ^1H NMR spectrum of homohalichondrin B (**1.2.3**) and the *epi* acid product (**6.3.3**) was obtained in C_6D_6. A comparison of these two spectra indicated that there would be significant differences in the appearance of some resonances in this solvent. Inspection of the ^1H NMR spectrum of the synthetic halichondrin B material (obtained in C_6D_6) did not reveal any obvious, distinctive resonances for the *epi* acid product (**6.3.3**).

CHAPTER 7

Base Stability and Chelation Studies

7.1 Introduction

Two aspects of the general chemistry of the halichondrins are described in this Chapter.

The stability of the halichondrins under basic conditions was investigated with the objective of opening the twenty-two membered lactone ring.

An investigation of the possibility of cation binding by the halichondrins was also initiated. As well as giving an insight into the general chemistry of the halichondrins, it was conceivable that the expression of biological activity in the halichondrins was related to an ability to chelate a metal ion under physiological conditions. The antibiotics valinomycin and nonactin for example, "which contain ether, ester, and amide bonds in 32-36-membered rings",[72] are known to bind Na^+ and K^+ cations to exert their biological effects. Halichondrins exert their mechanism of antimitotic action *via* binding in the vinca domain of tubulin, inhibition of GTP hydrolysis, nucleotide exchange on tubulin[24] (refer Section 1.2.3); it is possible that this mode of action may be facilitated by metal ion binding.

7.2 Base Stability Studies

A dilute solution of sodium hydroxide (0.1 M) in 10% methanol/ water was added to a small quantity of isohomohalichondrin B (**1.2.9**). Methanol was added to solubilise the halichondrin. The solution was stirred at room temperature overnight. A ^1H NMR spectrum obtained from the worked-up material (in $CDCl_3$/ 0.1% pyridine-d_5) indicated that no reaction had occurred, with only isohomohalichondrin B (**1.2.9**) being identified in the spectrum.

The stability of homohalichondrin B (**1.2.3**) to lithium hydroxide was tested as part of the Wittig reaction investigations and this is described in Section 8.4. Homohalichondrin B (**1.2.3**) was found to be stable to dilute aqueous lithium hydroxide.

The base hydrolysis of isohomohalichondrin B (**1.2.9**), and subsequently of homohalichondrin B (**1.2.3**), was investigated using sodium methoxide. Both halichondrins were found to be labile in the presence of sodium methoxide in methanol solution. A full description of these reactions is given in Section 5.2.

It appeared that the halichondrins were relatively stable in dilute alkaline solutions, but less stable in the presence of more nucleophilic, Lewis bases, such as sodium methoxide.

7.3 Chelation Studies

Pedersen estimated that a "hole" 4 Å in diameter was "enough to accommodate any unsolvated or uncoordinated inorganic cation" in a macrocyclic polyether molecule.[73] This author also commented that complexes in such molecules were "formed by ion-dipole interaction between the cation and the negative dipoles of the oxygens of the polyether ring".[73]

The X-ray crystal structure of the norhalichondrin A derivative[17] was investigated for possible metal chelation sites. It was apparent from an inspection of the overall conformation of the molecule that chelation, if it were to occur, would probably occur in the region of the folded lactone ring as there were several oxygens of the cyclic ethers in this region that could complex a single metal ion species. There appeared to be a large enough site to accommodate a metal ion species. However, the positions of the ether oxygens were not in any kind of "symmetrical" relationship to this site. This indicated that if metal chelation were to occur, the conformation of the lactone ring would be required to change significantly to achieve a symmetrical arrangement of the oxygens.

Prestegard and Chan reported the investigation of cation-binding properties of the macrocyclic antibiotic nonactin by ^{1}H NMR spectroscopy.[74] These authors reported the observation of conformational changes in the nonactin ring upon ion complexation. James *et al* reported significant (up to δ_H 0.27 ppm) changes in ^{1}H NMR chemical shifts of Ag^+ binding to the oxazole portion of dihydrohalichondramide.[75] It was decided to initiate ion chelation studies in the halichondrins by investigating the relatively small (0.98 Å ionic radius), and

physiologically prevalent, Na^+ ion using ^1H NMR spectroscopy to detect the conformational changes and the electronic effects of metal ion binding.

A ^1H NMR spectrum of a small quantity of isohomohalichondrin B (**1.2.9**) in CD_3OD with two drops of D_2O was obtained as a reference spectrum. Sodium perchlorate in D_2O was added to the NMR tube to give a 1:1 ratio of Na^+: isohomohalichondrin B (**1.2.9**). A ^1H NMR spectrum was acquired on this solution; no changes were indicated relative to the reference ^1H NMR spectrum. Sodium perchlorate (in D_2O) was added to the NMR tube to give stepwise increments in the ratio of Na^+: isohomohalichondrin B (*ie* 2:1, 3:1, 4: 1, 5:1 and 10:1 molar ratios). ^1H NMR spectra were acquired on the solution after each addition. No changes were apparent in the ^1H NMR spectra up to a ratio of 10:1 Na^+: isohomohalichondrin B that indicated that Na^+ chelation was occurring.

Obviously, a wide range of alternative chelating ions such as K^+, Fe^{2+}, Ca^{2+}, Mg^{2+} and Fe^{2+} would need to be investigated before the possibility of metal binding in the halichondrins could be eliminated. Time constraints meant a fuller investigation was not possible.

CHAPTER 8

Labelling Studies

8.1 Introduction

Critical to the development of the halichondrins as anticancer drugs, will be the ability to study the kinetics of drug absorption, distribution, metabolism, and excretion (*ie* the pharmacokinetics) of the molecule *in vivo*. To facilitate the detection and quantification of very small quantities (sub ng) of halichondrins in a biological matrix such as blood serum, it is necessary to "label" the molecule. This labelling may involve hapten binding for enzyme-linked immunoassay (ELISA); isotopic labelling for radio immunoassay (RIA), NMR spectroscopic or MS detection; or fluorescent tagging for detection by HPLC.

Several methods of generating selected, "labelled" halichondrins were investigated. Initially, a deuterium exchange reaction was attempted on isohomohalichondrin B (**1.2.9**) with the objective of producing a deuterium-labelled derivative; thus establishing a means for obtaining a tritium-labelled derivative. Subsequently, the sodium borodeuteride reduction of isohomohalichondrin B (**1.2.9**) was also undertaken using methodology previously established. This would establish a methodology for the inclusion of a stable tritium label. Efforts were also focused on the production of an isotopically-labelled halichondrin derivative produced *via* a Wittig reaction on a previously synthesised analogue.

Additionally, derivatisations of selected halichondrins to give fluorescent-labelled halichondrins were undertaken.

8.2 Deuterium Exchange

The deuterium exchange of isohomohalichondrin B (**1.2.9**) was attempted as a simple method of generating a deuterium-labelled derivative. It was anticipated that the protons adjacent to the C53 ketone (*viz* H52/H52' and H54/H54') of isohomohalichondrin B (**1.2.9**) would be exchangeable in basic solution.

The deuterium exchange of isohomohalichondrin B (**1.2.9**) was monitored by ^{1}H NMR spectroscopy. A solution of sodium deuteroxide (NaOD) in deuterium oxide (D_2O) was added to a small quantity of isohomohalichondrin B (**1.2.9**) in CD_3OD, and the solution was mixed thoroughly. A ^{1}H NMR spectrum acquired on this solution immediately after mixing indicated that reaction had occurred. The reaction mixture was worked-up and a ^{1}H NMR spectrum was re-acquired in $CDCl_3$/ 0.1% pyridine-d_5 solution to facilitate comparison with the ^{1}H NMR spectrum of isohomohalichondrin B (**1.2.9**) in this solvent.

Although the signal to noise ratio of this spectrum was very poor, it was apparent that there was a decrease in the intensity of the H54 and H54' (δ_H 2.73 ppm), H52 (δ_H 2.62 ppm) and H52' (δ_H 2.93 ppm) proton resonances, relative to the ^{1}H NMR spectrum of isohomohalichondrin B (**1.2.9**). The H2' resonance, which was observed as a doublet of doublets in the ^{1}H NMR spectrum of isohomohalichondrin B (**1.2.9**) at δ_H 2.61 ppm, was now predominantly visible as a doublet resonance. This indicated the exchange of the H2 proton (obscured in the spectrum at δ_H 2.36 ppm) was resulting in a loss of geminal coupling to the H2' resonance and the collapse of the doublet of doublets to give a doublet resonance. This stereospecific loss of the H2 proton was consistent with the conformational studies of halichondrin B and (*vide* Section 2.3) which suggested that the H2' proton was directed into the lactone

ring and the H2 proton was in a relatively exposed environment. The stereospecific deuteration at the C2 position appeared to be exclusively on the *re* face of the enolate.

FAB-MS performed on the worked-up material showed the presence of an envelope of parent ions, corresponding to the incorporation of one, two, three, four and five deuterium atoms, replacing the equivalent number of hydrogen atoms of isohomohalichondrin B (**1.2.9**). The envelope was symmetrical about the most intense peak corresponding to the exchange of three hydrogen atoms with three deuterium atoms. High resolution FAB-MS performed on the central parent ion gave a molecular formula corresponding to $C_{61}H_{83}D_3O_{19}$ or the incorporation of three deuterium atoms relative to the molecular formula of isohomohalichondrin B (**1.2.9**).

It was likely that there was not 100% exchange occurring at each centre- the poor signal to noise ratio in the ^1H NMR spectrum made a quantitative assessment of this impossible. This was reflected in the appearance of the FAB-MS cluster of d_1-d_5 peaks centred on d_3.

8.3 Sodium Borodeuteride Reduction

The sodium borodeuteride reduction of isohomohalichondrin B (**1.2.9**) was undertaken with the objective of producing the C53-deuterated derivative of the isohomohalichondrin B reduction isomers (**3.4.1** and **3.4.2**), as described in Section 3.4.

A small quantity of isohomohalichondrin B (**1.2.9**) was dissolved in dry isopropyl alcohol and sodium borodeuteride was added. The resulting suspension was stirred vigorously at room temperature for one hour, monitoring the reaction progress by silica TLC. After one hour, TLC performed on the reaction mixture indicated the appearance of two new spots of increased polarity relative to isohomohalichondrin B (**1.2.9**) and no evidence of starting material. The reaction was subsequently quenched and worked-up. A ^{1}H NMR spectrum and a COSY spectrum were acquired from the product (in $CDCl_3$/ 0.1% pyridine-d_5).

The ^{1}H NMR spectrum of the product appeared to be identical with that performed on the isohomohalichondrin B sodium borohydride reduction isomers (**Figure 3.4.1**). The H53 resonance was located at an obscured position, at δ_H 4.16 ppm in the spectrum of the sodium borohydride reduction isomers (**3.4.1** and **3.4.2**), and this resonance would be expected to be relatively broad due to coupling to the methylene protons on adjacent carbons. Therefore its absence from the spectrum of the sodium borodeuteride reduction products would not be detectable from an inspection of the ^{1}H NMR spectrum. A reduction in complexity of the H54/H54' and H52 and H52' resonances would be expected in the spectrum of the sodium borodeuteride reduction products due to a loss in coupling to the H53 proton. These methylene protons, H54/H54' (δ_H 1.74 ppm), H52 (δ_H 1.56 ppm) and H52' (δ_H 2.10 ppm) were also

obscured in the ^1H NMR spectrum of the isohomohalichondrin B reduction isomers (**Figure 3.4.1**).

The COSY spectrum performed on the sodium borodeuteride reduction products was compared to the spectrum performed on the sodium borohydride reduction isomers (**3.4.1** and **3.4.2**). Apart from two notable differences, the spectra were identical (**Figure 8.3.1**). The key differences were two COSY correlations which were observed in the COSY spectrum of the sodium borohydride isomers (upper spectrum, **Figure 8.3.1**), but were absent in the spectrum of the sodium borodeuteride reduction products (lower spectrum, **Figure 8.3.1**). These correlations were the H53 and H52' correlation, at δ_H 4.16 ppm/δ_H 2.10 ppm (slightly obscured); and the H53/H54/H54' correlation at δ_H 4.16 ppm/δ_H 1.74 ppm in the COSY spectrum of the sodium borohydride reduction isomers. This indicated that the H53 proton was not present in the sodium borodeuteride reduction product, and that the corresponding C53 deuteride isomers **8.3.1** and **8.3.2** had been produced in the reaction.

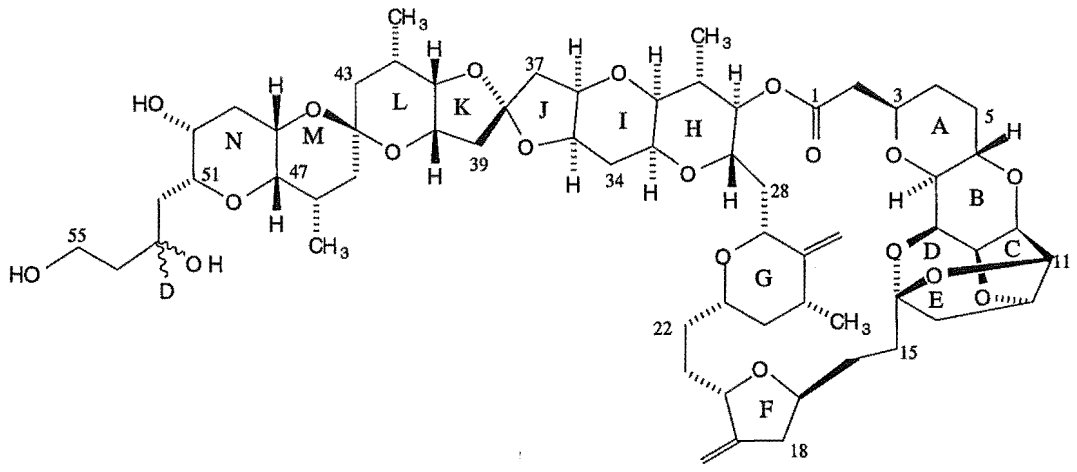

isohomohalichondrin B sodium borodeuteride reduction isomers (**8.3.1** and **8.3.2**)

High resolution FAB-MS performed on the sodium borodeuteride reduction isomers (**8.3.1** and **8.3.2**) gave the parent ion corresponding to a molecular formula of $C_{61}H_{87}DO_{19}$ (100% incorporation), the addition of one hydrogen and one deuterium atom relative to the molecular formula of isohomohalichondrin B (**1.2.9**). This confirmed that the C53-deuteride derivatives of **3.4.1** and **3.4.2** (**8.3.1** and **8.3.2**) had been produced in the reaction of isohomohalichondrin B (**1.2.9**) with sodium borodeuteride.

COSY Spectrum of Borohydride Reduction Products

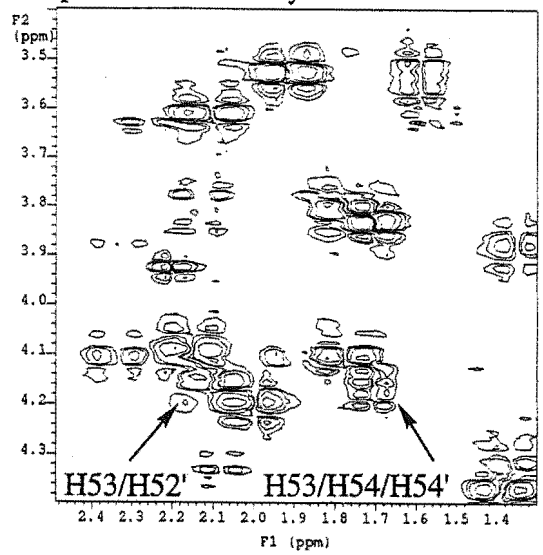

COSY Spectrum of Borodeuteride Reduction Products

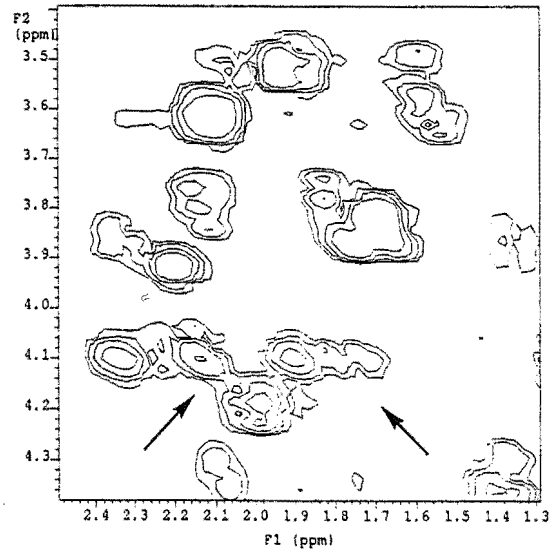

Figure 8.3.1 COSY Spectra of Reduction Products

8.4 Wittig Reaction

It was envisaged that isotopic carbon atoms (^{13}C or ^{14}C) could be inserted into a halichondrin molecule at the 19=CH_2 and 26=CH_2 positions *via* a Wittig reaction with a C19 and C26 diketone halichondrin derivative using the appropriately labelled ylide.[76]

Homohalichondrin B diacetate diketone (**4.3.3**) was selected as the diketone derivative to undertake the Wittig reaction on. The synthesis of this derivative was described in Section 4.3.4. It was anticipated that reaction at the C19 and C26 ketone centres of **4.3.3** with a labelled ylide would regenerate labelled homohalichondrin B (as the diacetate derivative). The isohomohalichondrin B diketone derivative (**4.3.2**), described in Section 4.3.3, was not suitable for the conditions of the Wittig reaction because of the potential for reaction of the ylide with the C53 ketone functionality.

Initially, a series of trial Wittig reactions on cholestan-3-one were developed to give suitable reaction and handling conditions for applying to the diacetate diketone derivative of homohalichondrin B (**4.3.3**).

The reactions were initially attempted using methyl triphenylphosphonium iodide ($MePh_3P^+I^-$) as an "unlabelled" Wittig reagent with the objective of developing suitable reaction conditions for the regeneration of the olefinic functionalities. It was anticipated that once the reaction conditions were developed they could be applied using an isotopically labelled Wittig reagent to give the corresponding isotopically labelled halichondrin.

8.4.1 Trial Wittig Reaction

A trial reaction of cholestan-3-one with the Wittig reagent $MePh_3^+I^-$ was undertaken, based on a literature method.[77] The Wittig reagent, $MePh_3P^+I^-$, was suspended in dry ether and *n*-butyllithium in hexane was added to the suspension to generate the ylide (CH_2=PPh_3). Cholestan-3-one, dissolved in dry ether, was added to the ylide. The resulting solution was stirred overnight at room temperature.

A ^1H NMR spectrum acquired on the product (in $CDCl_3$) showed the presence of a broad singlet resonance at δ_H 4.54 ppm which was assigned as the olefinic 3=CH_2 resonance of 3-methylene cholestane. Also apparent from the ^1H NMR spectrum was the movement of the CH_3-18 singlet resonance from δ_H 0.66 ppm to δ_H 0.63 ppm, and the CH_3-19 singlet resonance from δ_H 0.99 ppm to δ_H 0.83 ppm. No starting material was identifiable in the spectrum.

8.4.2 Wittig Reaction of Homohalichondrin B Diacetate Diketone

The stability of homohalichondrin B (**1.2.3**) to lithium hydroxide (generated from reaction of *n*-butyllithium) was tested before committing the diacetate diketone of homohalichondrin B (**4.3.3**) to the Wittig reaction conditions. A small quantity of homohalichondrin B (**1.2.3**) was dissolved in water and an aqueous solution of lithium hydroxide was added. The reaction was stirred overnight at room

temperature. Silica TLC performed on the product indicated homohalichondrin B (**1.2.3**) was stable under these conditions.

The Wittig reagent ($MePh_3P^+I^-$) was suspended in dry ether and *n*-butyllithium in hexane was added to the suspension to generate the ylide ($CH_2=PPh_3$). Homohalichondrin B diacetate diketone (**4.3.3**) in dry ether, was added to the ylide. The resulting solution was stirred overnight at room temperature. After this time, the ether was removed and the reaction mixture was extracted with hexanes and filtered.

A ^1H NMR spectrum of the product showed very weak halichondrin resonances. However, it was possible to determine that this material was unreacted homohalichondrin B diacetate diketone (**4.3.3**) as several resonances, characteristic of the ^1H NMR spectrum of **4.3.3** were still apparent in the spectrum. The distinctive CH_3-25 doublet at δ_H 1.09 ppm was unshifted, indicating that the C26 ketone was intact. The isolated quintet of the H54 resonance (at δ_H 5.13 ppm) was also visible, indicating that the diacetate remained intact. No evidence was seen in the olefinic region that would support formation of the $26=CH_2$ and $19=CH_2$ homohalichondrin B diacetate derivative (**3.2.2**).

The filtered solid from the work-up was subsequently extracted with 20% dichloromethane/ hexane to remove any more polar halichondrin material present. A ^1H NMR spectrum (in $CDCl_3$) of this material showed very weak halichondrin resonances. The H54 quintet resonance at δ_H 5.13 ppm was a fraction of its former intensity in the spectrum indicating that the major component had either one or two acetate groups cleaved. Reactivity tables indicated that acetate functionalities would be unstable to alkyl lithium and stable to ylides.[62] An equimolar amount of *n*-butyllithium had been added to the Wittig reagent to generate the ylide to avoid this potential problem. However, it was possible that *n*-butyllithium had not fully reacted

with the Wittig reagent ($MePh_3P^+I^-$) to form the ylide before addition of the halichondrin material.

Silica TLC was performed on the two extracts. The material from the hexane extract showed a single spot with the same polarity as homohalichondrin B diacetate diketone (**4.3.3**). The 20% dichloromethane/ hexane extract showed two spots by silica TLC; one minor spot with the same polarity as **4.3.3**, and the other, major spot of increased polarity relative to **4.3.3**. This supported the NMR observations that the hexane extract was unreacted **4.3.3**, whereas the dichloromethane/ hexane extract contained predominantly a diacetate-cleaved derivative (from the R_f of the spot). The two extracts were combined and the reaction was reattempted under identical conditions.

The reaction was worked-up as previously, with the hexane and dichloromethane/ hexane extracts combined. A ^1H NMR spectrum acquired on the combined material (in $CDCl_3$) appeared to be similar to the previous reaction, indicating a mixture of acetylated and non-acetylated homohalichondrin B diketone material was present. No evidence of 26=CH_2 or 19=CH_2 olefinic resonances were observed in this spectrum. There was insufficient material to progress further with.

Two explanations for the non-reaction observed were postulated. It was possible that the conformation of the diketone may have precluded a close approach by the ylide to the C19 and C26 ketone centres. Also possible was the low solubility observed for the starting material, homohalichondrin B diacetate diketone (**4.3.2**) in ether, resulting in non-reaction with the ylide.

8.5 Fluorescent Labelling

The majority of fluorescent labels have been developed for the labelling of primary and secondary amino acids.[78] A few reagents, such as anthracene-isocyanate (AIC)[79], 4-dimethylamino-1-naphthoylnitrile (DMA-NN)[80] and naphthyl-isocyanate (NIC),[81] have been developed for the labelling of hydroxyl functional groups. Other, traditional and readily available fluorescent labels such as the acid chloride 5-dimethylaminonaphthalene-1-sulfonylchloride (dansyl chloride, **8.5.1**) are reported to react slowly[82] with hydroxyl groups.

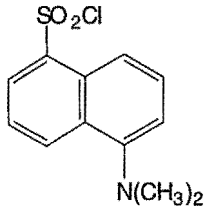

dansyl chloride (**8.5.1**)

Detection of halichondrins in blood serum using a fluorescent label would, in theory, involve derivatisation in blood serum and possible purification, or alternatively, extraction of the halichondrin material prior to derivatisation, followed by HPLC quantification, using a fluorescence detector to give increased analytical sensitivity.

For a fluorescent label to be of analytical use, the derivatisation reaction should ideally give a 100% yield. However, a derivatisation that gives a reproducible yield of less than 100% may still be of analytical use, although in this situation the detection limit of the analytical method would be compromised.

Dansyl chloride (**8.5.1**) was selected as a fluorescent label for the terminal hydroxyl group of selected halichondrins. Initially, a series of trial reactions were performed on *n*-hexanol before applying the reaction conditions to selected halichondrins.

8.5.1 Trial Reactions of Dansyl Chloride

To a solution of *n*-hexanol dissolved in pyridine, dansyl chloride in pyridine was added at 0°C while stirring to give a 1:1 molar ratio of dansyl chloride to *n*-hexanol. The solution was then stirred at room temperature for four and a half hours. The reaction was worked-up after this time and a ^{1}H NMR spectrum acquired on the product in $CDCl_3$/ 0.1% pyridine-d_5. The ^{1}H NMR spectrum showed the shift of the terminal hydroxyl methylene protons from δ_H 3.64 ppm in *n*-hexanol to δ_H 3.98 ppm, indicating dansylation had occurred at the hydroxyl group. Changes in the chemical shift of the aromatic dansyl proton resonances and in the other *n*-hexanol resonances were also apparent. No evidence of either unreacted starting material or reagent was apparent in the spectrum.

The NMR solution fluoresced green under a visible wavelength (λ 380-400 nm) lamp. The fluorescence excitation wavelength for dansyl derivatives is typically λ 375 nm to give fluorescence at λ 540 nm (green).[83]

Reactions were also attempted using carbonate as the base with either ethyl acetate or acetone as the solvents.

To a solution of *n*-hexanol in ethyl acetate, dansyl chloride and sodium carbonate were added to give a molar ratio of 1:2:6 *n*-hexanol: dansyl chloride : sodium carbonate. The reaction was stirred overnight at 35°C. A ^{1}H NMR spectrum acquired from the product (in $CDCl_3$/ 0.1% pyridine-d_5) indicated a 70% conversion to dansylated *n*-hexanol, by integration over the terminal hydroxyl methylene triplets.

The reaction of *n*-hexanol in ethyl acetate was subsequently repeated on the incompletely dansylated material from the previous reaction, under identical reaction conditions. A ^{1}H NMR spectrum of the product obtained in $CDCl_3$/ 0.1% pyridine-d_5 showed a 100% conversion of *n*-hexanol to its dansylated derivative.

A trial reaction using an alternative aqueous solvent (acetone) was subsequently undertaken. To a solution of *n*-hexanol in acetone, dansyl chloride and sodium carbonate were added to give a molar ratio of 1:1:3 *n*-hexanol: dansyl chloride: sodium carbonate. The resulting mixture was stirred overnight at room temperature. The reaction was worked-up and a ^{1}H NMR spectrum acquired from this material (in $CDCl_3$/ 0.1% pyridine-d_5) indicated a 78% conversion to dansylated *n*-hexanol, by integration.

8.5.2 Dansyl Chloride Reactions With Homohalichondrin B

A series of reactions of homohalichondrin B (**1.2.3**) with dansyl chloride were performed with the objective of producing dansyl homohalichondrin B (**8.5.2**) in quantitative yield.

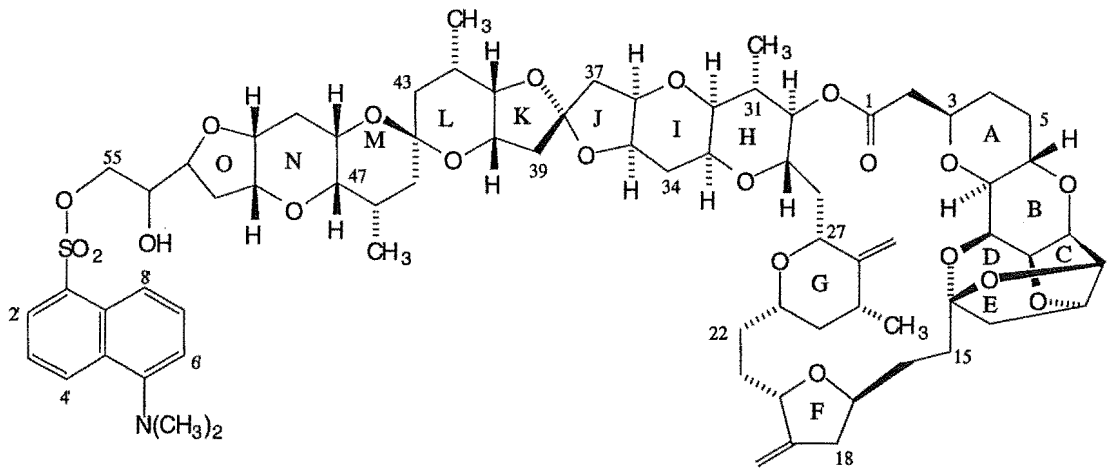

dansyl homohalichondrin B (**8.5.2**)

Homohalichondrin B (**1.2.3**) was dissolved in pyridine and dansyl chloride (1 mole equivalent) in pyridine was added, at 0°C. The solution was stirred at room temperature for four hours. Silica TLC and a ^{1}H NMR spectrum obtained from the product (in $CDCl_3$/ 0.1% pyridine-d_5) indicated only unreacted homohalichondrin B (**1.2.3**) was present. This material was committed for the next reaction.

Homohalichondrin B (**1.2.3**) was dissolved in pyridine, and dansyl chloride in pyridine was added at 0°C to give a 5:1 molar ratio of dansyl chloride: **1.2.3**. The solution was stirred at room temperature for four hours. A ^{1}H NMR spectrum acquired on the reaction product (in $CDCl_3$/ 0.1% pyridine-d_5) indicated that no reaction had occurred, as only homohalichondrin B (**1.2.3**) was present. This material was again used in the next reaction.

The reaction was performed as described previously except fifteen mole equivalents of dansyl chloride were added to homohalichondrin B (**1.2.3**). No reaction was apparent by silica TLC or ^{1}H NMR spectroscopy on the product. The material from this reaction was subsequently submitted for the next reaction.

At this stage it was decided to increase the reaction temperature. Homohalichondrin B (**1.2.3**) was dissolved in pyridine and ten mole equivalents of dansyl chloride (in pyridine) were added at room temperature. The resulting solution was stirred at 35°C. After four hours reaction at 35°C, silica TLC performed on the reaction mixture indicated the presence of two components. One component had an R_f identical to that of homohalichondrin B (**1.2.3**); the other component, possessing a greater R_f, was observed as a fluorescent yellow spot under a visible wavelength (λ 380-400 nm) lamp. Both components were stained blue by phosphomolybdic acid spray and heat (the standard TLC detection method used for the halichondrins). After nine hours reaction, silica TLC performed on the reaction mixture indicated no change in the relative intensities of the two components, so the reaction was worked-up.

A ^1H NMR spectrum obtained from the product (in $CDCl_3$/ 0.1% pyridine-d_5) indicated the presence of two components. The spectrum showed the presence of two H47 resonances, one unshifted homohalichondrin B (**1.2.3**) H47 resonance at δ_H 3.06 ppm, the other at δ_H 3.02 ppm. Also apparent in the spectrum was the decrease in the intensity of the δ_H 3.69 ppm (H55/H55') doublet resonance. The CH_3-42 and CH_3-46 doublet resonances appeared to be split into new resonances overlapping in the region where the homohalichondrin B CH_3-46 (δ_H 0.90 ppm) and CH_3-42 (δ_H 0.93 ppm) doublets resonated. This spectrum also showed several resonances in the aromatic region, and a singlet at δ_H 2.88 ppm, which were attributed to the dansyl $N(CH_3)_2$ methyl groups. Comparison of these "dansyl" resonances with a ^1H NMR spectrum of dansyl chloride (in $CDCl_3$/ 0.1% pyridine-d_5) indicated several differences. The doublet at δ_H 8.68 ppm (in the ^1H NMR spectrum of dansyl chloride) was apparent at δ_H 8.60 ppm in the ^1H NMR spectrum of the product. A doublet (integral corresponding to two protons) present at δ_H 8.26 ppm in the ^1H NMR spectrum of the product appeared to have arisen from overlap of the δ_H 8.42

ppm (doublet) and δ_H 8.35 ppm (doublet of doublets) resonances observed in the ^1H NMR spectrum of dansyl chloride. Two doublet of doublets (appearing as two triplets) at δ_H 7.69 ppm and δ_H 7.56 ppm in the ^1H NMR spectrum of dansyl chloride, were visible as a "quintet" (*ie* two overlapping "triplets") resonance at δ_H 7.58 ppm and δ_H 7.52 ppm in the ^1H NMR spectrum of the product. This information indicated that dansyl homohalichondrin B (**8.5.2**) was formed in the reaction. An integral over the two H47 resonances indicated that there was 51% homohalichondrin B (**1.2.3**) and 49% dansyl homohalichondrin B (**8.5.2**) present in the reaction product.

This material was re-reacted with the objective of increasing the amount of product formed.

Thirteen mole equivalents of dansyl chloride (in pyridine) were added to the material from the previous reaction dissolved in pyridine. The resulting solution was stirred at 35°C for seventeen hours. Silica TLC performed on the reaction mixture did not indicate any change in the relative amounts of homohalichondrin B (**1.2.3**) or dansyl homohalichondrin B (**8.5.2**). A ^1H NMR spectrum obtained from the reaction product indicated that a mixture of 56% dansyl homohalichondrin B (**8.5.2**) and 44% homohalichondrin B (**1.2.3**) was present. This was little improvement in terms of reaction yield, relative to the initial reaction.

An analysis of several TLC stationary phases and solvent systems indicated that either C18 or diol stationary phases would provide a good basis for chromatographic separation of the two components in the product.

Analytical reverse phase HPLC (using a C18 column), performed on the product, indicated homohalichondrin B (**1.2.3**) was eluting slightly before a uv-active component. The uv spectrum of this component showed absorbance maxima at λ 195 nm, 215 nm, 245 nm and 330 nm. A standard injection of dansyl chloride gave a uv spectrum with absorbance maxima at λ 208 nm, 264 nm and 369 nm for the only peak in the chromatogram. However, a base-line separation of the two components was not able to be achieved on the analytical C18 HPLC column which would provide a good basis for a preparative separation.

A diol cartridge column was investigated as a potential separation method. The product was placed onto a cartridge diol column, eluting with acetonitrile and increasing isopropyl alcohol/ acetonitrile mixtures. Silica TLC of the resulting fractions indicated that the presence of halichondrin material was predominantly in the first three fractions. The first fraction appeared to be pure dansyl homohalichondrin B (**8.5.2**), the second fraction appeared to be a mixture of dansyl homohalichondrin B and homohalichondrin B (**1.2.3**) while the third fraction appeared to be pure homohalichondrin B. It was decided that the column should be started with a less polar solvent to retain the halichondrins on the column longer to provide a better separation. The three fractions were recombined and placed on a cartridge diol column equilibrated to dichloromethane. Fractions eluting with dichloromethane and increasing acetonitrile/ dichloromethane mixtures were collected before stripping the column with acetonitrile. The progress of the fluorescent material through the column was able to be followed by shining the visible lamp on the column and observing the movement of the yellow fluorescence. Silica TLC indicated that the halichondrins were spread over the first eight fractions. The first fraction appeared to contain only dansyl homohalichondrin B (**8.5.2**), while fractions three through to eight contained homohalichondrin B (**1.2.3**). Fractions were combined on the basis of the TLC results.

A ^{1}H NMR spectrum (in $CDCl_3$/ 0.1% pyridine-d_5) acquired on the combined fractions three through to eight from the diol column, showed very weak signals. However, it was possible to detect the distinct H55/H55' doublet (at δ_H 3.69 ppm) and the isolated H47 resonance (at δ_H 3.06 ppm), characteristic of homohalichondrin B (**1.2.3**). No evidence of the aromatic or $N(CH_3)_2$ resonances of dansyl homohalichondrin B (**8.5.2**) were observed in the spectrum.

A ^{1}H NMR spectrum of the least polar component from the diol column (in $CDCl_3$/ 0.1% pyridine-d_5) showed the presence of very weak signals. The H47 resonance was apparent at δ_H 3.02 ppm, and the $N(CH_3)_2$ methyl singlet was also apparent at δ_H 2.88 ppm. No H47 resonance was apparent at δ_H 3.06 ppm, as would be the case if homohalichondrin B (**1.2.3**) was present. The NMR tube was observed to fluoresce strongly yellow under the visible lamp. These observations supported the TLC evidence that the sample was pure dansyl homohalichondrin B (**8.5.2**). There were insufficient quantities of this sample to progress further with.

A modified method for generating dansyl homohalichondrin B (**8.5.2**) was attempted with the objectives of increasing the yield of the reaction and providing sufficient material to allow a NMR spectroscopic assignment of the product.

Homohalichondrin B (**1.2.3**) was dissolved in dichloromethane and dansyl chloride and pyridine (a slight excess relative to dansyl chloride) were added to the solution to give five mole equivalents of dansyl chloride. The solution was stirred at room temperature. After three hours reaction, silica TLC indicated some evidence of the dansyl derivative forming. The reaction was continued with stirring overnight at room temperature. TLC performed on the reaction mixture after this time indicated no change, relative to the TLC performed after three hours reaction. The molar ratio

of dansyl chloride ratio was increased to 10:1 and additional pyridine was added. The reaction was stirred at 35°C for a further three hours. TLC performed after this time indicated an increase in the relative amount of dansyl homohalichondrin B (**8.5.2**), although homohalichondrin B (**1.2.3**) appeared to be the major component of the reaction mixture. After six hours at 35°C, TLC indicated the major component of the reaction was dansyl homohalichondrin B (**8.5.2**). After ten hours at 35°C, no change in the appearance of the TLC of the reaction mixture was evident. The molar ratio of dansyl chloride was increased again to give fifteen mole equivalents and more pyridine was added. The resulting solution was stirred overnight at 35°C. No change in the appearance of the TLC of the reaction mixture was apparent, so the reaction was worked-up.

This material was combined with the dansyl homohalichondrin B (**8.5.2**) separated previously from the diol column and a diol cartridge separation of the combined mixture was undertaken. Fractions of 10% hexane/ dichloromethane elutions were collected and analysed by silica TLC. When TLC indicated the two components had been successfully separated, the remaining homohalichondrin B (**1.2.3**) was stripped off the column with methanol. Fractions were combined on the basis of the TLC results.

A ^{1}H NMR spectrum acquired from the more polar, non-fluorescent component (in $CDCl_3$/ 0.1% pyridine-d_5), was identified as being homohalichondrin B (**1.2.3**) with very minor dansyl-related impurities (as evidenced by the presence of the $N(CH_3)_2$ singlet at δ_H 2.88 ppm).

A ^{1}H NMR spectrum acquired from the less polar, fluorescent yellow component was identical with the previously described spectrum of dansyl homohalichondrin B

(**8.5.2**). This spectrum was obtained in $CDCl_3$/ 0.1% pyridine-d_5 and is displayed in **Figure 8.5.1**.

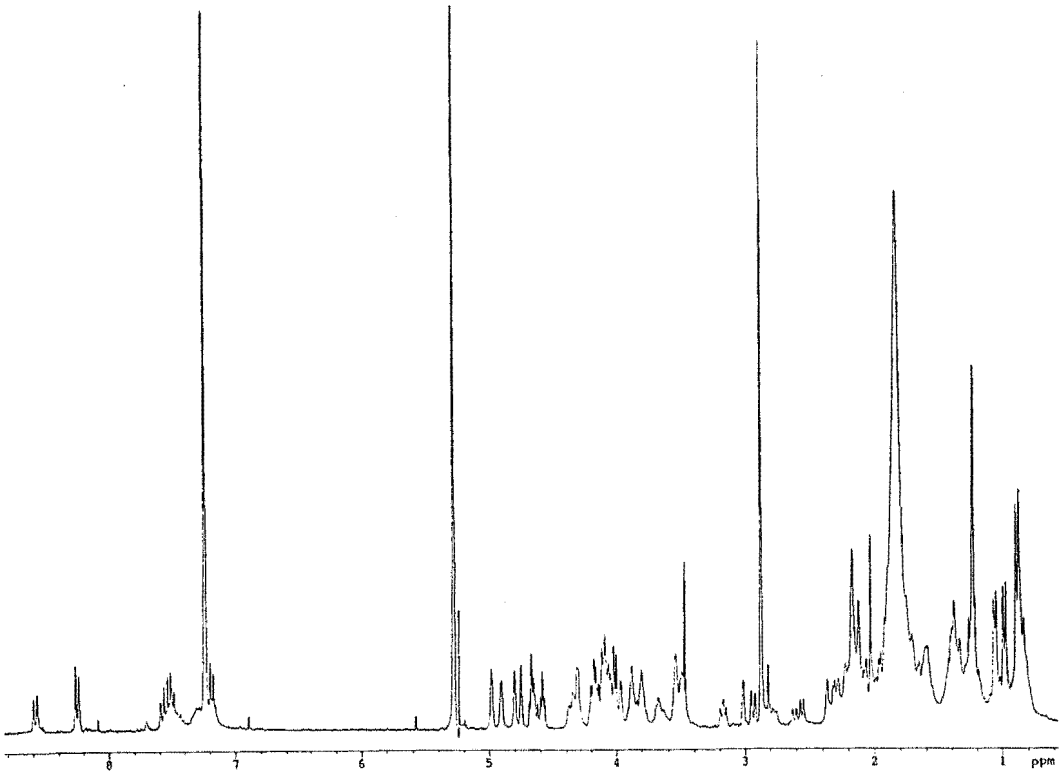

Figure 8.5.1 ^1H NMR Spectrum of Dansyl Homohalichondrin B (**8.5.2**)

COSY, 2D-TOCSY (100 ms mixing time) and HMQC experiments, acquired from the product, enabled the partial assignment of the ^1H and ^{13}C NMR spectra to be achieved. The HMQC spectrum acquired gave a low signal to noise ratio, a reflection of the small sample size (0.4 mg). This meant only a few correlations were observed and consequently only a few ^{13}C resonances were able to be assigned. The important correlations from these experiments are depicted in **Figure 8.5.2** and the ^1H and ^{13}C NMR data are listed in **Tables 8.5.1** and **8.5.2** respectively.

Table 8.5.1 ^{1}H NMR Data for Dansyl Homohalichondrin B (**8.5.2**)

Proton[a]	δ ppm[b]	Proton[a]	δ ppm[b]	Proton[a]	δ ppm[b]
H2	2.34	**H23**	3.52	**CH_3-42**	0.89
H2'	2.58	**H24**	1.05	**H43**	1.26
H3	3.89	**H24'**	1.70	**H43'**	1.42
H4	1.35	**H25**	2.20	**H45**	
H4'		**CH_3-25**	1.06	**H45'**	1.36
H5	1.37	**26=CH**	4.75	**H46**	2.10
H5'	2.07	**26'=CH**	4.80	**CH_3-46**	0.89
H6	4.33	**H27**	3.50	**H47**	3.02
H7	2.94	**H28**		**H48**	3.47
H8	4.32	**H28'**		**H49**	1.70
H9	4.04	**H29**	4.19	**H49'**	2.07
H10	4.18	**H30**	4.65	**H50**	3.79
H11	4.58	**H31**	2.04	**H51**	3.96
H12	4.68	**CH_3-31**	0.99	**H52**	1.88
H13	1.94	**H32**	3.17	**H52'**	1.88
H13'	2.16	**H33**	3.78	**H53**	4.12
H15		**H34**		**H54**	3.67
H15'		**H34'**	2.14	**H55**	4.02
H16		**H35**	4.10	**H55'**	4.02
H16'		**H36**		**H2'**	8.60
H17	4.09	**H37**	1.90	**H3'**	7.52
H18	2.25	**H37'**	2.33	**H4'**	8.26
H18'	2.79	**H39**	2.17	**$N(CH_3)_2$**	2.88
19=CH	4.90	**H39'**	2.17	**H6'**	7.25
19'=CH	4.98	**H40**	3.87	**H7'**	7.58
H20	4.37	**H41**	3.54	**H8'**	8.26
H22'		**H42**	2.28		

[a] The symbol ' represents the less shielded proton of a geminal pair.

[b] Data recorded at 23 °C in $CDCl_3$ at 300 MHz with chemical shifts in ppm and referenced to $CHCl_3$, δ_H 7.25 ppm.

Table 8.5.2 ^{13}C NMR Data for Dansyl Homohalichondrin B (**8.5.2**)

Carbon	δ ppm[a]	Carbon	δ ppm[a]	Carbon	δ ppm[a]
C1		C24		C44	
C2		C-CH_3-25		C45	
C3		C-CH_3-25	17.8	C-CH_3-46	
C4		26C=CH_2		C-CH_3-46	17.0
C5		26C=CH_2		C47	72.6
C6		C27		C48	63.6
C7	77.5	C28		C49	
C8		C29		C50	74.7
C9	73.8	C30	76.9	C51	
C10	76.5	C-CH_3-31		C52	
C11	82.1	C-CH_3-31	14.7	C53	
C12	81.2	C32	77.3	C54	70.5
C13	48.2	C33	66.3	C55	71.6
C14		C34		C1'	
C15		C35		C2'	
C16		C36		C3'	
C17		C37		C4'	
C18		C38		C5'	
19C=CH_2		C39	42.2	$N(CH_3)_2$	45.3
19C=CH_2		C40	70.6	C6'	
C20	75.3	C41	79.3	C7'	
C21		C-CH_3-42		C8'	
C22		C-CH_3-42	17.0	C9'	
C23	73.3	C43		C10'	

a ^{13}C NMR spectral data assigned from an HMQC experiment, recorded at 23 °C in $CDCl_3$ at 300 MHz with chemical shifts in ppm.

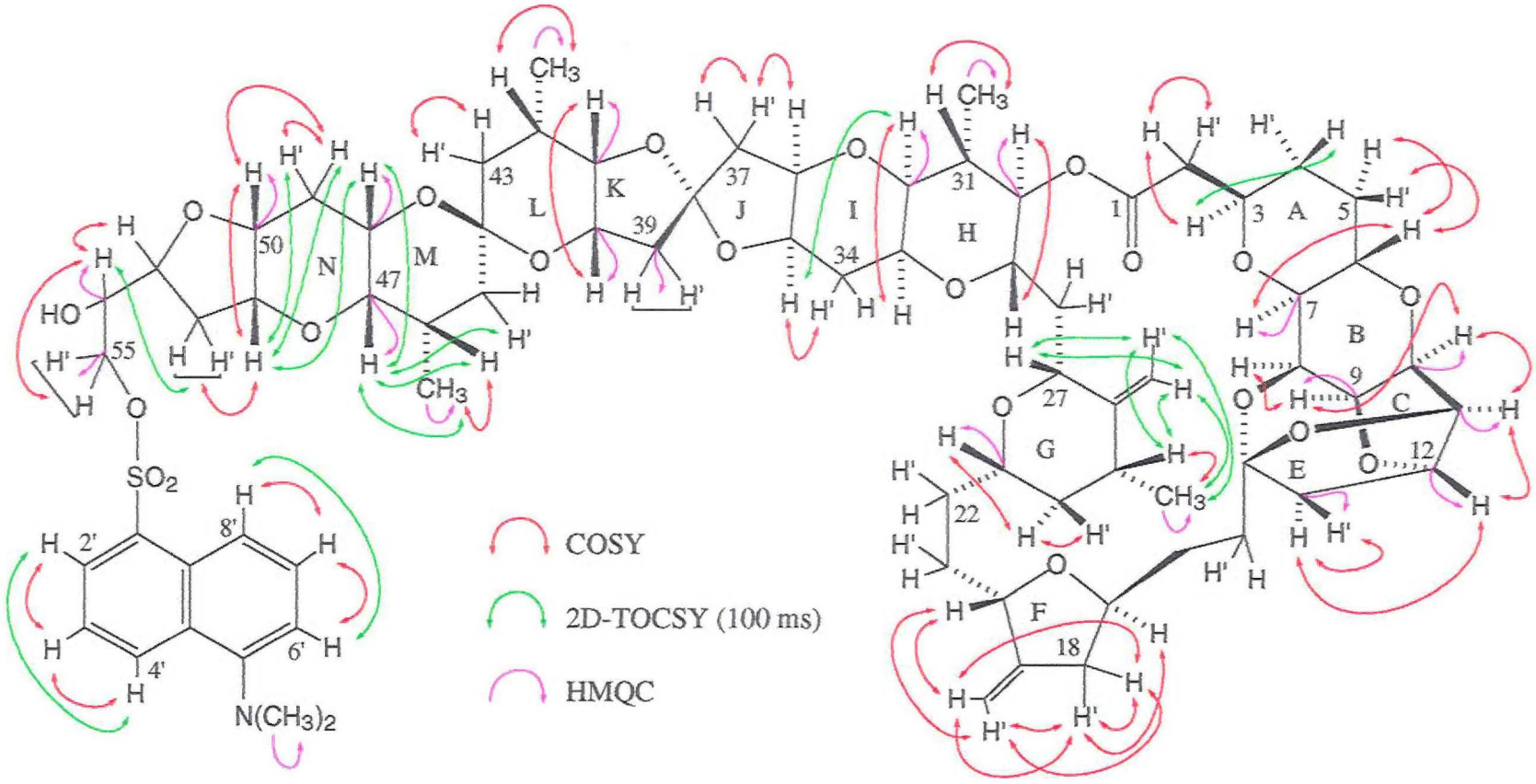

Figure 8.5.2 Dansyl Homohalichondrin B- Important NMR Correlations

NMR spectroscopic assignments of the ^{1}H and ^{13}C NMR spectra for resonances in the C1-C37 region were consistent with those of homohalichondrin B (**1.2.3**). As expected, interest was focused on changes in the terminal region of the molecule.

From the H47 proton resonance (at δ_H 3.02 ppm) correlations in the 2D-TOCSY spectrum were observed to a proton resonating at δ_H 3.47 ppm (H48), the CH_3-46 methyl protons at δ_H 0.89 ppm, a resonance at δ_H 2.10 ppm and another at δ_H 1.36 ppm. The CH_3-46 resonance was correlated to the δ_H 2.10ppm resonance in the COSY spectrum, identifying it as the H46 resonance. The δ_H 1.36 ppm resonance was therefore assigned as an H45 resonance. A COSY correlation observed between δ_H 2.10 ppm (H46) and δ_H 1.36 ppm (H45) supported this assignment. The H50 and H51 proton resonances were located from a COSY correlation between a resonance at δ_H 3.79 ppm (H50) and another at δ_H 3.96 ppm (H51). The H50 resonance was correlated to a signal at δ_H 1.70 ppm (H49'). The H49 resonance was located from a COSY correlation between the H49' resonance and its geminal partner at δ_H 2.07 ppm. The H51 resonance was correlated to a proton at δ_H 1.88 ppm which was attributed to the H52/H52' signal. Two COSY correlations were observed from a resonance at δ_H 3.67 ppm, to δ_H 4.02 ppm and to δ_H 4.12 ppm. The central proton resonance (δ_H 3.67 ppm) was assigned as H54. An HMQC correlation was observed for a carbon at δ_C 71.5 ppm to the proton resonance at δ_H 4.02 ppm. The carbon resonance was too shielded to be attributed to the C53 carbon resonance so was assigned as the C55 resonance. The δ_H 4.04 ppm proton signal was assigned as the H55/H55' resonance. The H55/H55' resonance in the ^{1}H NMR spectrum of homohalichondrin B (**1.2.3**) was observed at δ_H 3.69 ppm; a shift of δ_H 0.33 ppm to a more deshielded chemical shift for the corresponding protons in **8.5.2**. In the trial reaction to form the dansyl *n*-hexanol derivative (Section 8.5.1), a shift of δ_H 0.34

ppm, to a more deshielded position, was noted for the terminal hydroxy ^1H NMR resonances in the product.

Two spin systems were evident for the aromatic proton resonances from the COSY spectrum. One spin system was assigned from the COSY spectrum, from a central proton at δ_H 7.58 ppm resonance to protons correlated at δ_H 8.26 ppm and δ_H 7.25 ppm. The other spin system showed COSY correlation from a central resonance at δ_H 7.52 ppm to aromatic protons on either side at δ_H 8.60 ppm and δ_H 8.26 ppm. These represented the H2'-H3'-H4' and H6'-H7'-H8' spin systems. The most upfield resonance (δ_H 7.25 ppm) was assigned as the proton adjacent to the $N(CH_3)_2$ group *ie* the H6' resonance, thereby assigning the H7' (δ_H 7.58 ppm) and H8' (δ_H 8.26 ppm) resonances. The H2' resonance, adjacent to the sulfonyl functionality, was assigned as the most downfield proton resonance, δ_H 8.60 ppm, thereby assigning the chemical shifts of the H3' (δ_H 7.52 ppm) and H4' (δ_H 8.26 ppm) resonances.

These NMR data supported the formation of the dansyl derivative of homohalichondrin B (**8.5.2**).

Subsequent dansylation reactions were attempted on homohalichondrin B (**1.2.3**) in an attempt to increase the reaction yield. Reaction was attempted in a dry nitrogen atmosphere using the dichloromethane solvent method described previously. Reaction was then attempted using carbonate as the base in an aqueous acetone solvent system.

Homohalichondrin B (**1.2.3**) was dissolved in dichloromethane and dansyl chloride (15 mole equivalents), and pyridine were added to the solution. The resulting solution was stirred at 35°C for six and a half hours under an atmosphere of dry

nitrogen. Silica TLC performed on the reaction mixture indicated a minor amount of dansyl homohalichondrin B (**8.5.2**) had formed. More pyridine was added to the solution to ensure the pH remained high, and the solution was continued stirring overnight at 35°C. Silica TLC performed after this time indicated the major component was the dansyl homohalichondrin B derivative (**8.5.2**). A ^{1}H NMR spectrum performed on the product (in $CDCl_3$/ 0.1% pyridine-d_5) indicated the mixture was *ca* 65% dansyl homohalichondrin B (**8.5.2**) and 35% homohalichondrin B (**1.2.3**). This material was committed for the next reaction.

Dansyl chloride and sodium carbonate were added to the product from the previous reaction. Acetone and water were added and the resulting solution was stirred at 35°C for twenty-four hours. A ^{1}H NMR spectrum of the worked-up material, performed in $CDCl_3$/ 0.1% pyridine-d_5, indicated that the reaction had not gone to completion, with the H47 resonance of homohalichondrin B still visible at δ_H 3.06 ppm.

The dansylation reaction was attempted on isohomohalichondrin B (**1.2.9**) which has a primary hydroxyl group, rather than a terminal diol as in homohalichondrin B (**1.2.3**), to ascertain if the reaction would to completion in the absence of a terminal diol. The reaction was also attempted on halichondrin B (**1.2.1**).

8.5.3 Dansyl Chloride Reactions of Isomohalichondrin B

Isohomohalichondrin B (**1.2.9**) was dissolved in dichloromethane and dansyl chloride and pyridine were added to give a 15:1 ratio of dansyl chloride to **1.2.9**. The solution was stirred at 35°C for twenty-four hours. The reaction was carried out under an atmosphere of dry nitrogen and the reaction progress was monitored by silica TLC. TLC performed after twenty-four hours indicated the appearance of two components; a fluorescent yellow spot (under a visible lamp) at a higher R_f relative to isohomohalichondrin B (**1.2.9**) and a component with the same R_f as **1.2.9**. There appeared to be similar amounts of the two components in the reaction mixture. Additional pyridine was added to the reaction mixture to ensure the pH remained high and the reaction was continued for another six hours at 35°C. A ^{1}H NMR spectrum obtained from the product (in $CDCl_3$/ 0.1% pyridine-d_5) indicated the presence of a new H47 resonance at δ_H 3.08 ppm. An integration over this resonance indicated 59% of the dansylated isohomohalichondrin B product (**8.5.3**) was formed. Also apparent from this spectrum was the appearance of a new methyl doublet at δ_H 0.58 ppm, at a relatively shielded position. Several aromatic resonances were also apparent in the spectrum.

A COSY experiment was performed on the mixture. An analysis of this spectrum revealed the CH_3-46 resonance at δ_H 0.58 ppm was correlated to a proton resonance at δ_H 2.03 ppm. The δ_H 2.03 ppm resonance was correlated to the H47 resonance at δ_H 3.08 ppm. A COSY correlation was observed between the H47 resonance and the H48 resonance at δ_H 3.53 ppm. The H52 and H52' resonances were located from a COSY correlation observed between them at δ_H 2.40 ppm and δ_H 2.92 ppm. The H55/H55' and H54/H54' resonances were unable to be located in the COSY spectrum. The COSY spectrum revealed the two spin systems (H2'-H3'-H4' and H6'-

H7'-H8') for the aromatic protons of the dansyl derivative. COSY correlations were observed from a central triplet at δ_H 7.40 ppm to a resonance at δ_H 8.24 ppm and a resonance at δ_H 8.34 ppm. Another triplet at δ_H 7.44 ppm showed correlation to protons resonating at δ_H 8.70 ppm and δ_H 7.10 ppm.

These NMR data supported the TLC evidence that dansyl isohomohalichondrin B (**8.5.3**) had been formed in the reaction.

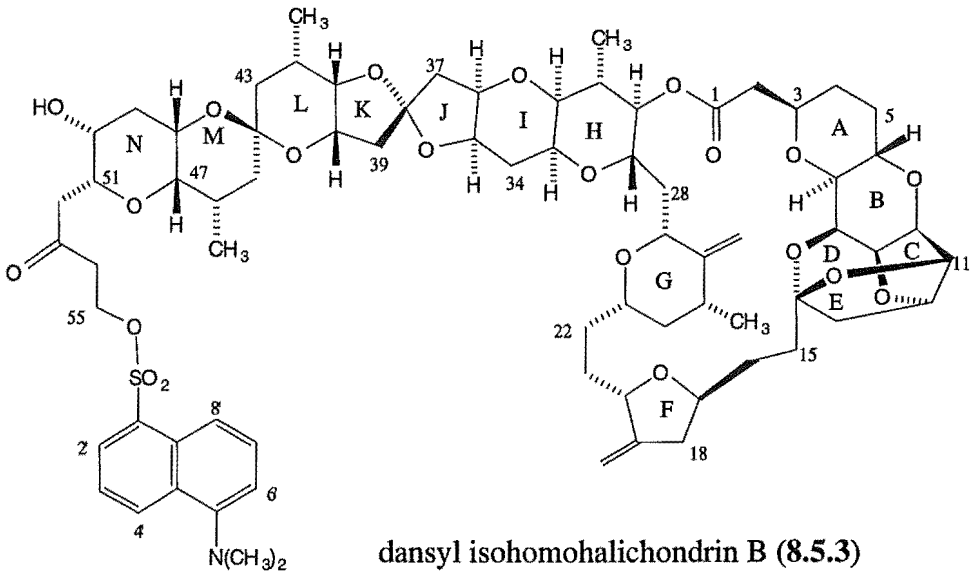

dansyl isohomohalichondrin B (**8.5.3**)

The product was re-reacted in pyridine with a *ninety-fold* excess of dansyl chloride. The reaction was stirred at 35°C, monitoring the reaction by silica TLC. After thirty hours reaction, silica TLC indicated the presence of a component with the same R_f as isohomohalichondrin B (**1.2.9**) and a less polar fluorescent yellow component. A ^1H NMR spectrum of the product ($CDCl_3$/ 0.1% pyridine-d_5) showed an increase in the complexity of the spectrum. The H47 resonance of isohomohalichondrin B (at δ_H 3.23 ppm) appeared to have reduced in intensity. The methyl region showed several new doublet resonances at *ca* δ_H 0.90 ppm and two new doublets at δ_H 0.69 ppm and δ_H 0.74 ppm. Also apparent from the spectrum was a decrease on the intensity of the

δ_H 0.58 ppm (CH_3-46) resonance of **8.5.3**. The distinctive H55/H55' triplet of isohomohalichondrin B (**1.2.9**) was no longer apparent at δ_H 3.69 ppm. Several aromatic resonances and the $N(CH_3)_2$ resonance were apparent in the spectrum. There appeared to be changes in the chemical shifts of other isohomohalichondrin B resonances, such as the H32 resonance (δ_H 3.20 ppm) and the CH_3-31 resonance (δ_H 1.00 ppm). This spectrum indicated that there were several components present in the product mixture, including minor amounts of isohomohalichondrin B (**1.2.9**) and dansyl isohomohalichondrin B (**8.5.3**). There also appeared to be at least one other, unidentified product present.

8.5.4 Dansyl Chloride Reaction of Halichondrin B

Halichondrin B (**1.2.1**) was dissolved in dichloromethane and dansyl chloride in dichloromethane, and pyridine, were added to give a 1:1 molar ratio of dansyl chloride to halichondrin B. The reaction was stirred at 35°C. Silica TLC performed on the reaction mixture after twenty minutes showed the formation of a less polar, fluorescent component relative to homohalichondrin B. The dansyl chloride: halichondrin B ratio was increased to 5:1 and the reaction mixture was stirred at 35°C. After a total of one hour reaction, silica TLC indicated an increased proportion of the less polar component. After a total of three hours reaction, silica TLC indicated no further change so the dansyl chloride to halichondrin B ratio was increased to 10:1. The reaction was continued stirring at 35°C for a further two and a half hours and the ratio was increased to 15:1 and the reaction was stirred overnight at 35°C. After this time the reaction was worked-up and a ^1H NMR spectrum was obtained from the product (in $CDCl_3$/ 0.1% pyridine-d_5) which indicated a mixture

of components was present. In the ^{1}H NMR spectrum of halichondrin B (**Figure 2.2.1**), the H47 resonance was obscured by other resonances at δ_H 3.61 ppm. This meant a quantification of the relative amounts of dansyl halichondrin B and halichondrin B was not possible directly from the ^{1}H NMR spectrum. Several proton resonances were apparent in the aromatic region and the $N(CH_3)_2$ singlet was also visible at *ca* δ_H 2.90 ppm, indicating that dansylation had occurred. TLC performed on the worked-up material indicated there were similar amounts of dansylated halichondrin B and halichondrin B present.

8.5.5 Conclusion

It was apparent, from the series of dansylation reactions that were performed on selected halichondrins, that a quantitative yield was not able to be achieved using the described methods. It was not possible to achieve greater than 60-65% dansylation, despite the variety of conditions attempted. The trial reactions with *n*-hexanol (Section 8.5.1) indicated that the reagent and methodology were suitable for the derivatisation of a simple alcohol. Failure to produce a quantitative yield for the dansylation reactions of the halichondrins appeared to be associated with the halichondrins themselves. If this problem was indeed a halichondrin-based problem it would not be a suitable analytical method.

Possible alternative fluorogenic reagents that may be more amenable to quantitative reaction at the primary alcohol of a halichondrin include AIC,[79] DMA-NN[80] or NIC.[81]

8.6 Biological Activity Data

The P388 cytotoxicity of the dansyl homohalichondrin B derivative (**8.5.2**) was tested to give additional structure-activity information. The activity of this derivative is cited in **Table 8.6.1** along with the P388 activity of the parent halichondrin, homohalichondrin B (**1.2.3**).

Table 8.6.1 *In Vitro* Cytotoxicities of Selected Halichondrins

Compound	P388 IC_{50} (ng/mL)
homohalichondrin B (1.2.3)	0.22
dansyl homohalichondrin B (8.5.2)	2.7

The P388 activity of the dansyl homohalichondrin B derivative (**8.5.2**) was *ca* twelve times less active than the parent halichondrin, homohalichondrin B (**1.2.3**). It is interesting to note that the addition of a relatively large substituent to the terminal hydroxyl group of homohalichondrin B did not result in a particularly large decrease in the P388 activity.

The biological activity of the dansyl homohalichondrin B derivative (**8.5.2**) is further discussed in relation to other halichondrin derivatives in Chapter 9.

CHAPTER 9

Summary of Structure-Activity Results

9.1 Introduction

The biological activities of the individual hemi-synthetic halichondrin derivatives were described in the previous Chapters. The activities of these derivatives are reviewed in this Chapter, in relation to each other and in relation to the biological activities of specific naturally-occurring halichondrins, to give an overall picture of structure-activity relationships in the halichondrin series.

The primary constraint placed upon the production of the hemi-synthetic halichondrin derivatives required to facilitate an investigation of the relationship between structure and activity in the halichondrin series, was the limited supply of halichondrin material available. The total amount of halichondrin material used for this project was less than 80 mg.

A second constraint placed on this aspect of the project was attributable to the complexity of the halichondrin molecule, placing relatively long time frames on the spectroscopic characterisation of the derivatives produced.

Another, less significant, limitation was the small number of functionalities that could be targeted for modification in the halichondrin molecule. Generally, this restricted the modifications to the terminal moiety, the lactone ring (C1-C30), the exocyclic methylenes (19=CH_2 and 26=CH_2) and the tricyclo system (C-E rings) of the halichondrin molecule.

Consequently, the derivatives produced were, for the most part, carefully selected to provide maximal structure-activity information. As such, these derivatives by no

means represented the complete range of "useful" semi-synthetic derivatives, in terms of structure-activity information.

9.1.1 Physical Properties and the Biological Assays

The antitumour activity observed for a compound is a function of several factors. In the case of mitotic inhibitors, the compound must first gain entry to the cell across the plasma membrane. There are several mechanisms by which compounds can cross the cell membrane: *via* simple diffusion, facilitated diffusion, active transport, through "pores" in the membrane or *via* pinocytosis or phagocytosis.[84] The process by which a molecule is transported across a membrane depends on the membrane type and the nature of the molecule. Generally, simple diffusion is governed by the partition coefficient; the higher the lipid/water ratio of the substance, the greater the proportion is found inside the cell after equilibration.[84] This relationship appears to fall off with increasing molecular weight (>150 g/mol) and increasing hydrophilicity.[84] This would tend to suggest that the physical size of the halichondrins reduces the likelihood of simple diffusion acting as the primary transport mechanism to enter the cell. There is evidence to suggest the entry to tumour cell types in the halichondrin series, and other antimitotic compounds, is receptor-mediated as tumour-specific activity is observed in the NCI primary screen (discussed in Section 1.1.3). Once inside the cell, the halichondrins arrest mitosis at metaphase by preventing tubulin polymerisation and other associated processes (discussed in Section 1.2.3).[24] The antitumour activity observed is therefore a complex interaction of several important factors.

The "structure" of the compound includes physical considerations such as the shape of the molecule (*ie* its conformation); its hydrophobicity and/or hydrophilicity and electronic effects. Any alteration to the nature of functional groups, chirality *etc* is likely to alter one, if not all of the above "structure" considerations and, as such, exert an influence on any one of the factors which determines antitumour activity in the halichondrin series.

It is important, in order to assess the significance of the biological activities observed, to have an appreciation of the kind of (statistical) errors and their relative importance in the generated results. These errors can be broadly classified into two groups: those arising from the submitted sample and those arising from the assay itself.

In terms of the sample, significant errors arise from the mass measurement of small samples and their corresponding dilutions for submission in the assay. Errors in volume measurements in the preparation of assay samples are also relatively significant. Another important consideration is the purity of the derivatives. Contamination arising from active compounds, such as the presence of small quantities of starting materials in the reaction product, would give misrepresentations in the activity observed and the possibility of synergistic or antagonistic effects in the assay.

In terms of the P388 assay, possible sources of error include the measurement of volumes for dilution series, the extrapolation of the $\log IC_{50}$ value from the dose-response curve and the inherent "biological nature" of the assay. To minimise the errors arising from these aspects of the biological activity measurements, samples were generally submitted at least twice, at two or more solution concentrations. Also included with each assay performed on a hemi-synthetic halichondrin derivative, was

a "control" halichondrin - either isohomohalichondrin B (**1.2.9**) or homohalichondrin B (**1.2.3**). Any control assay performed that gave an activity of greater than 0.4 ng/mL or less than 0.1 ng/mL was treated with suspicion and was subsequently re-assayed, along with the hemi-synthetic derivatives. Overall, examining the variability of the "control" halichondrins, the standard error averaged less than *ca* 20% of the mean, including the IC_{50} results >0.4 mg/mL and <0.1 ng/mL. This also accounts for errors in volume measurements in preparing samples for assay, but does not account for any possible errors in mass measurement.

The results for compounds submitted for assay in the NCI's primary *in vitro* antitumour screen were generally more reliable from a statistical sense. Each compound was tested in quadruplicate at three concentration ranges over sixty different cell lines. The standard errors for the GI_{50} results averaged less than 15% of the respective means.

Statistical errors arising from inaccuracies in mass measurement contributed up to ±20% to the actual activity results observed. Errors arising from sample impurities are addressed in the respective Chapters for the individual hemi-synthetic derivatives.

More emphasis is placed on the biological data results from the NCI primary screen, as these results represent an average activity over sixty different cell lines, and therefore represent the "average" cytotoxicity of the compound. However, it is likely that the most useful derivatives from a therapeutic sense will display a strong differential inter-panel (*ie* tumour-specific) activity. The following analysis does not take this aspect into account.

9.2 Summary of Biological Activity Data

9.2.1 P388 and NCI GI_{50} Data

Figures 9.2.1 to **9.2.6** summarise the P388 assay and NCI primary screen data, in graphical form. Included in these figures are the activities of selected derivatives produced in this work (discussed in Chapters 3-8), and the activities of selected, naturally-occurring halichondrins.

Figure 9.2.1 displays the absolute P388 *in vitro* assay results for selected halichondrins. Included in **Figure 9.2.1** are the naturally occurring halichondrins **1.2.1**, **1.2.3**, **1.2.9**, **1.2.10**, **1.2.11**, **1.2.12** and **1.2.13**. Also included are the terminal moiety-modified derivatives *viz* **3.2.1**, **3.4.1**, **3.4.2** and **8.5.2**; the olefinic moiety-modified derivatives, *viz* **4.3.1**, **4.3.2** and **4.5.1**; the lactone-modified derivatives, *viz* **5.2.1**, **5.2.2** and **5.3.1**; and the three acid products, *viz* **6.3.1**, **6.3.2** and **6.3.3**. Not included in **Figure 9.2.1** was the P388 activity of the oxidation product of isohomohalichondrin B monoacetate (**3.2.1**), as the structure was not able to be characterised with any degree of certainty (see Section 3.3).

It can be concluded that most of the derivatives produced were less active than the naturally occurring compounds (**Figure 9.2.1**). One exception to this generalisation was the naturally-occurring Me-isohomohalichondrin B-b (**1.2.12**), the C55 methyl derivative of isohomohalichondrin B (**1.2.9**), which recorded a reduced P388 activity relative to the other naturally-occurring halichondrins. The significance of this observation is discussed later.

In general terms, **Figure 9.2.1** indicates that changes in the terminal moiety resulted in less significant reductions in biological activity than alterations to other parts of the molecule. Large reductions in P388 activity were apparent when modifications involved the olefins and the lactone functionalities and the C38 stereochemistry. The isohomohalichondrin B di-osmate ester (**4.3.1**), was essentially inactive relative to the activities of the naturally occurring halichondrins.

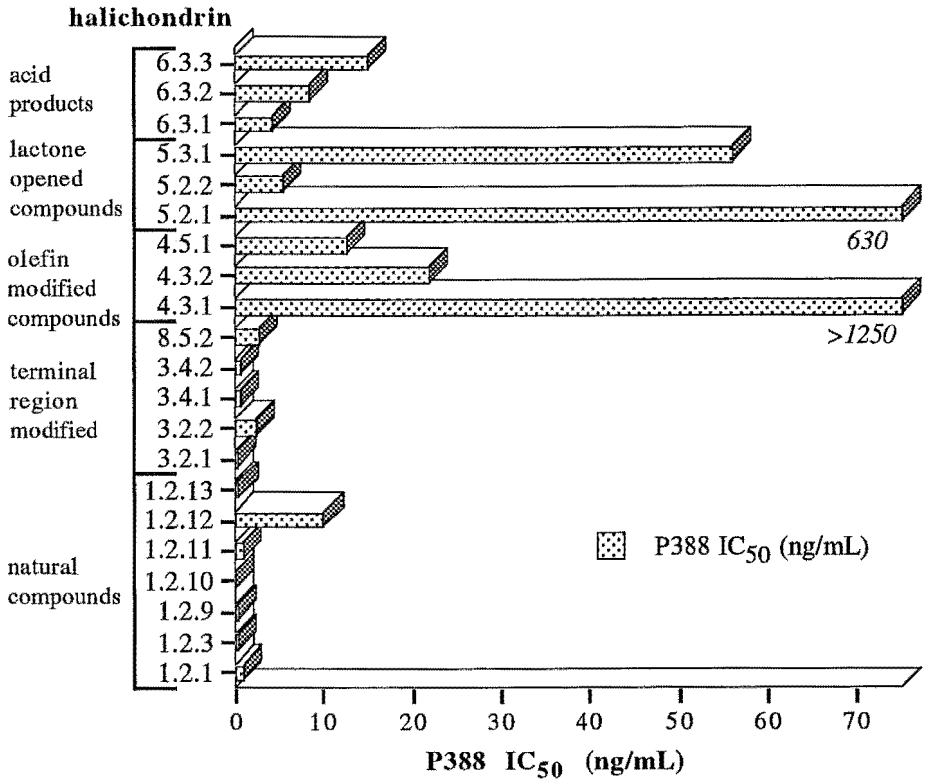

Figure 9.2.1 Graph of P388 Activities of Selected Halichondrins

In similar fashion, **Figure 9.2.2** displays the NCI *in vitro* primary screen assay GI_{50} results (over all sixty cell lines comprising the screen) for selected halichondrin

derivatives and naturally-occurring halichondrins. The hemi-synthetic derivatives **3.2.2** and **8.5.2** were not assessed in the NCI screen.

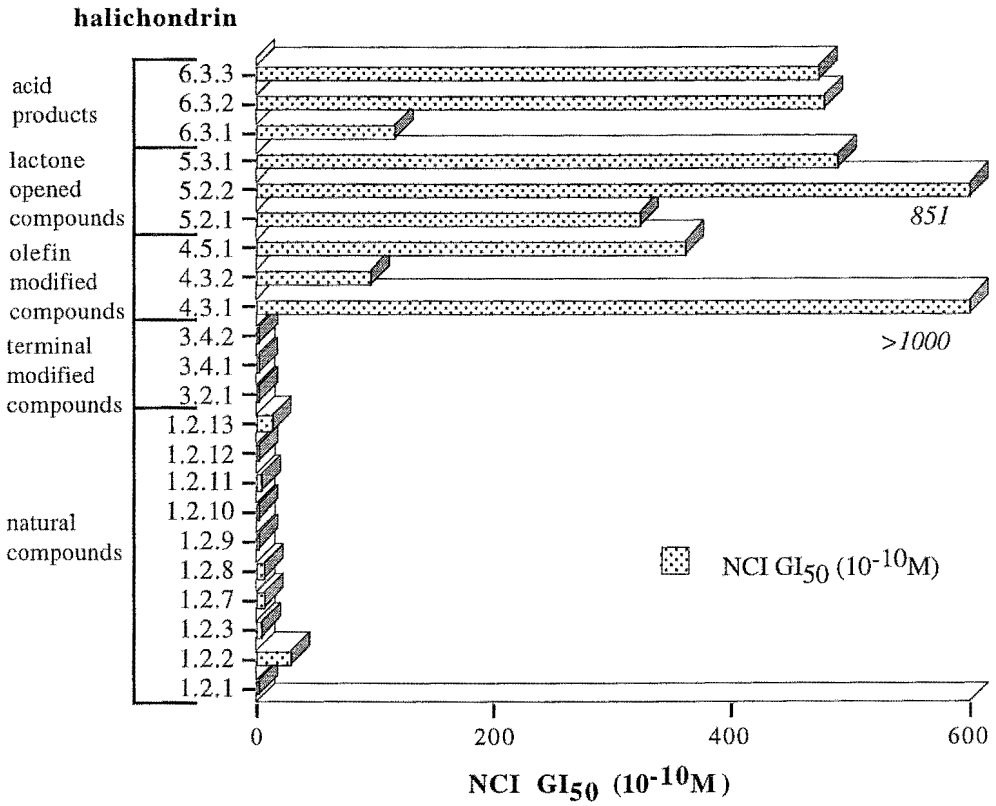

Figure 9.2.2 Graph of *In Vitro* Biological Activities of Selected Halichondrins in the NCI Primary Screen

Included with the naturally occurring compounds are norhalichondrin B (**1.2.2**) and the halistatins 1 and 2 (**1.2.7** and **1.2.8** respectively). Pettit *et al*,[20] reported the GI_{50}s of these halistatins in the NCI screen at 7.1×10^{-10}M (**1.2.7**) and 6.8×10^{-10}M (**1.2.8**) respectively. These compounds are 10α-hydroxy substituted halichondrin B (**1.2.7**) and 10α-hydroxy substituted homohalichondrin B (**1.2.8**) derivatives. The

activity observed for these 10α-hydroxy compounds is significantly reduced relative to the parent halichondrins, halichondrin B (**1.2.1**) at 1.38×10^{-10}M and homohalichondrin B (**1.2.3**) at 3.16×10^{-10}M. The presence of hydroxyl groups at C10 (in the tricyclo system) appears to reduce the cytotoxicity observed.

It is relevant to note that Hirata and Uemura[18] reported the B-16 (melanoma) *in vitro* activities of the "A-series" halichondrins norhalichondrin A and homohalichondrin A which have hydroxyl groups at the C12 and C13 positions of the molecule. These authors also included the B-16 activity of halichondrin C, the C12 hydroxyl derivative of halichondrin B. These naturally-occurring halichondrins were slightly less active than the corresponding "B series" halichondrins (*vide* **Table 1.2.1**). This result is consistent with the reduction in activity observed for the halistatin compounds.

Norhalichondrin B (**1.2.2**) and isonorhalichondrin B (**1.2.13**) with observed GI_{50}s of 29.5×10^{-10}M and 12.30×10^{-10}M also display significant reductions in cytotoxicity relative to the other naturally occurring halichondrins. This implies the presence of a carboxylate at the terminus of norhalichondrin B results in a reduction in cytotoxicity as do the unusual M and N rings of isonorhalichondrin B.

The activity of Me-isohomohalichondrin B-b (**1.2.12**) (2.00×10^{-10}M) appears to be comparable to halichondrin B (**1.2.3**) (1.38×10^{-10}M), homohalichondrin B (**1.2.3**) (3.16×10^{-10}M) and isohomohalichondrin B (**1.2.9**) (1.15×10^{-10}M). This was not the case in the P388 assay, suggesting that the P388 cell line is relatively more sensitive than the "average cell line" represented by the NCI overall GI_{50} result to the presence of a terminal methoxyl group.

In general terms, it was apparent that the hemi-synthetic derivatives produced which involved alteration to the terminal moiety (*viz* **3.2.1**, **3.4.1** and **3.4.2**) were of comparable activity to the naturally-occurring halichondrins. All of the other derivatives presented significantly reduced activities, with the di-osmate ester of isohomohalichondrin B (**4.3.1**) and the lactone-opened isohomohalichondrin B derivative (**5.2.1**) appearing inactive relative to the naturally-occurring halichondrins.

Next, the relative biological activities of the derivatives were examined. **Figure 9.2.3** shows the biological activities of the hemi-synthetic derivatives produced, relative to their parent halichondrins. The relative activity of the lactone-opened isohomohalichondrin B derivative (**5.2.1**) was expressed relative to Me-isohomohalichondrin B-b (**1.2.12**) to ascertain the effect of opening the lactone ring without the complication of the terminal methoxyl group. Implicit in this, was the assumption that the reduction in activity due to the presence of a terminal methoxyl group and an opened lactone ring in the same molecule produced effects that were mutually exclusive (*ie* there were no synergistic or antagonistic effects).

Generally, **Figure 9.2.3** shows that for the P388 assay results, the largest relative decreases in biological activity appeared to be associated with alterations to the olefins (**4.3.1**, **4.3.2** and **4.5.1**), the lactone ring (**5.2.1**, **5.2.2** and **5.3.1**) and the C38 stereochemistry (**6.3.2** and **6.3.3**). The furan acid product (**6.3.1**) appeared to show a significant, but lesser relative decrease in biological activity. The derivatives involving alteration of the terminal moiety (*viz* **3.2.1**, **3.2.2**, **3.4.1**, **3.4.2** and **8.5.2**) showed little change in the activity relative to the relative parent halichondrins.

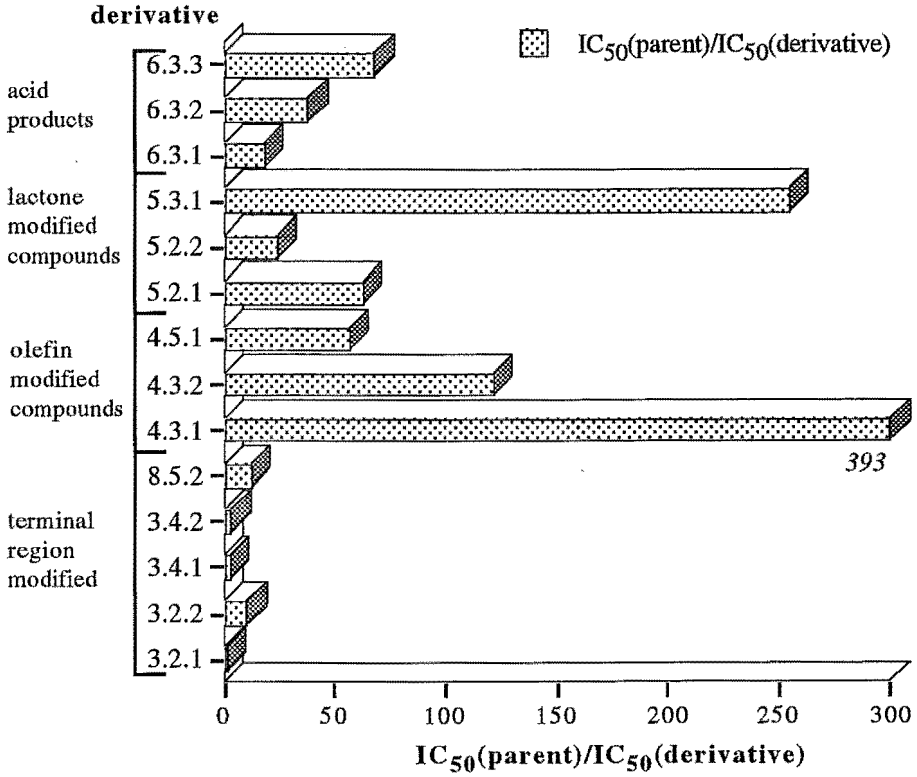

Figure 9.2.3 Graph of *In Vitro* Biological Activities of Derivative Halichondrins in the P388 Assay, Relative to the Relevant Parent Halichondrins

Figure 9.2.4 shows the NCI *in vitro* antitumour primary screen results (the GI_{50} averaged over all sixty cell lines) for the hemi-synthetic derivatives relative to the relevant parent halichondrins. From this graph, similar trends to **Figure 9.2.3** are observed; little change in activity of the derivatives involving terminal modifications, and large relative changes for alterations to the olefins (**4.3.1**, **4.3.2** and **4.5.1**), the lactone ring (**5.2.1**, **5.2.2** and **5.3.1**) and the C38 stereochemistry (**6.3.2** and **6.3.3**).

The furan acid product (**6.3.1**) also showed a significant, but lesser, relative decrease in biological activity.

It is interesting to note that the relative changes in activity overall were larger for the NCI primary screen results than the P388 assay results. This suggested that the murine leukemia cell line (P388) was less sensitive to changes in halichondrin structure than the NCI average over all of the sixty cell lines in the screen.

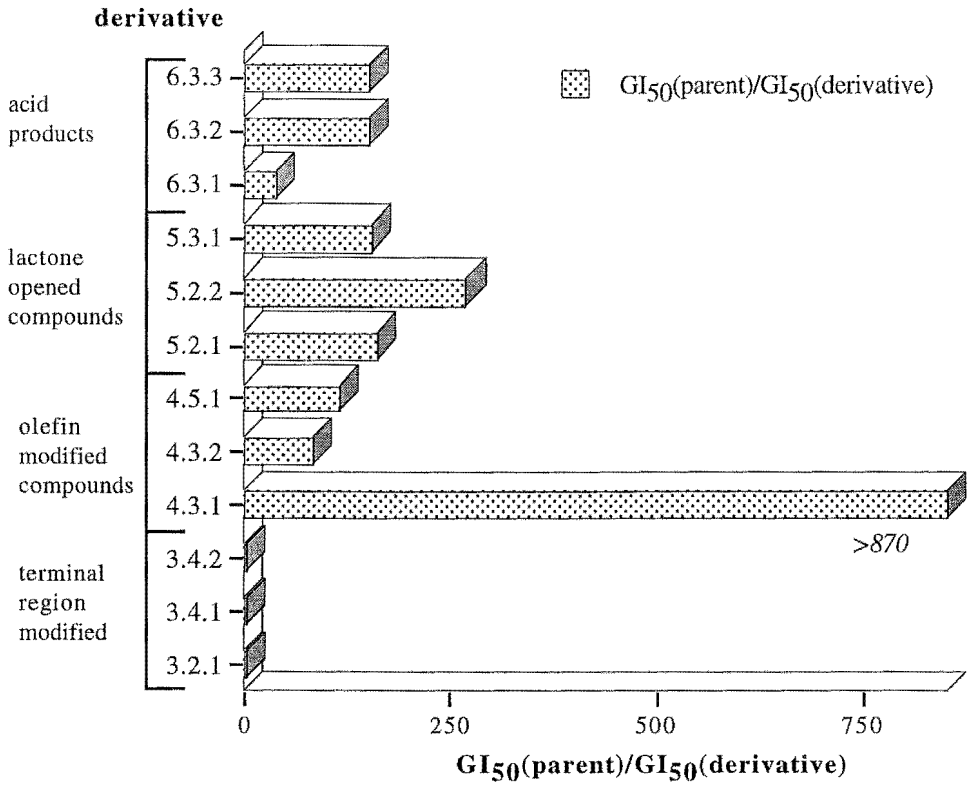

Figure 9.2.4 Graph of *In Vitro* Biological Activities of Derivative Halichondrins in the NCI Primary Screen, Relative to Relevant Parent Halichondrins

To ascertain if there was a relationship between the P388 assay results and the results obtained from testing in the NCI *in vitro* primary screen the results from the two assays were directly compared. Following discussions with Dr. David Newman of the NCI,[86] a comparison of one specific cell line from the NCI screen was undertaken, *viz* the CCRF CEM cell line (a human leukemia cell line) which was suggested to be the most comparable to the murine leukemia cell line (P388). Initially, the GI_{50} over all sixty cell lines was compared with the GI_{50}s extracted for the CEM cell line (**Figure 9.2.5**). From this graph, it is apparent that the GI_{50}s from the CEM cell line correlated well with the average GI_{50} over all sixty cell lines. One exception was the lactone-opened homohalichondrin B derivative (**5.2.2**) which appeared to be more sensitive to the CEM cell line than the "average" cell line.

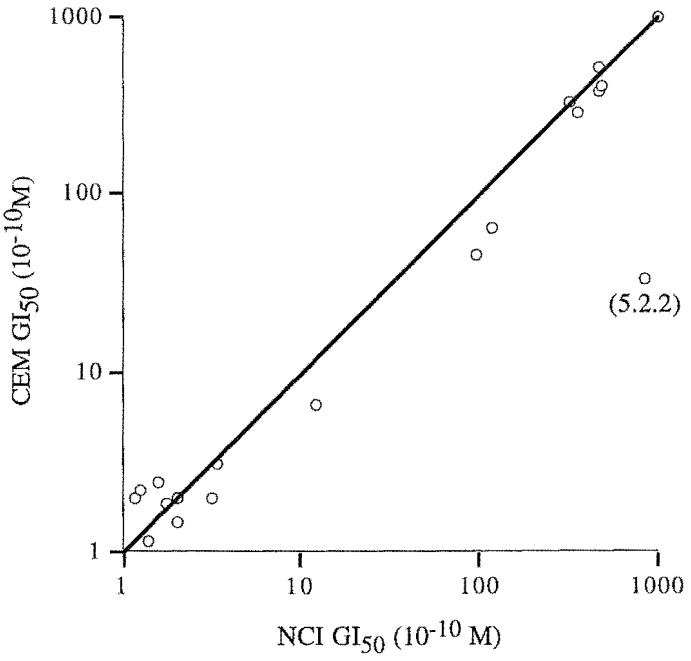

Figure 9.2.5 Graph of *In Vitro* Biological Activities of Selected Halichondrins Over All Cell Lines in the NCI Primary Screen, Relative to the CEM Cell Line

The CEM cell line therefore appeared to give a good representation of the "average" cell line in the NCI primary screen.

To facilitate the comparison of the P388 assay IC_{50}s to the GI_{50}s of the CEM cell line for the halichondrins tested in the NCI screen, the P388 assay results were converted to molar units. **Figure 9.2.6** displays the P388 assay results against the CEM cell line GI_{50} data for all of the halichondrins which underwent testing in the NCI screen.

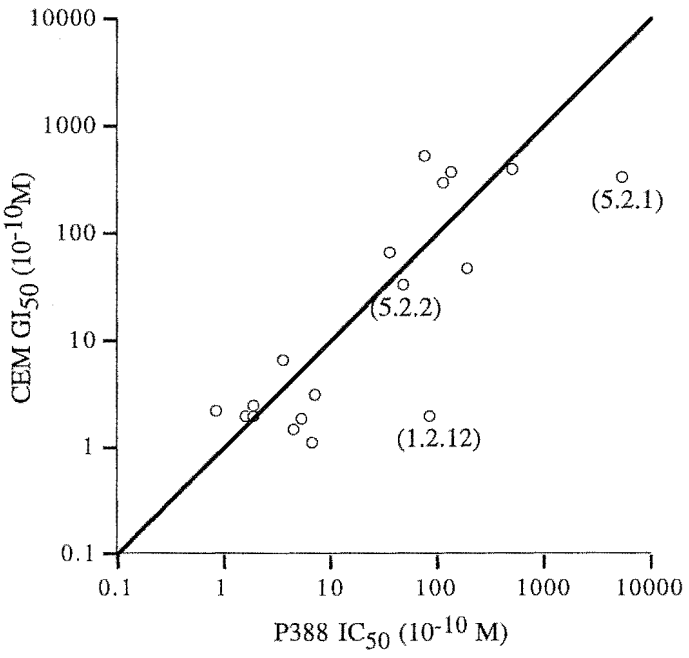

Figure 9.2.6 Graph of *In Vitro* Biological Activities of Selected Halichondrins Against the P388 Cell Line, Relative to the CEM Cell Line

From **Figure 9.2.6**, it is apparent that a correlation existed between the cytotoxicities observed in the P388 cell line and those observed in the NCI *in vitro* primary screen from one selected cell line from the screen (*ie* the CEM cell line). In general terms, those data appearing to the right of the bisecting line in the graph in **Figure 9.2.6** represent halichondrins which were more cytotoxic against the CEM cell line in the NCI screen, in terms of the GI_{50} results. Conversely, those data situated to the left of the bisecting line represent halichondrins which displayed greater cytotoxicities against the murine leukemia cell line (P388) than to the CEM cell line in the NCI screen. There appears to be a good correlation between the two sets of data. However, two halichondrins showed significant deviations from this trend; the lactone-opened isohomohalichondrin B derivative (**5.2.1**) and the naturally-occurring Me-isohomohalichondrin B-b (**1.2.12**). Interestingly, these two halichondrins showed a similar trend for the average GI_{50} (*ie* over all NCI cell lines) *versus* the P388 IC_{50} results and both halichondrins possess terminal methoxyl groups. This suggests that the P388 cell line is relatively insensitive to the presence of terminal methoxyl groups in the halichondrin series. The lactone-opened homohalichondrin B derivative (**5.2.2**) appeared to show a similar level of activity against the CEM cell line. This indicated that this derivative was significantly more cytotoxic against the two leukemia cell lines (CEM and P388) than the NCI "average" cell line.

9.2.2 NCI COMPARE Data

The COMPARE correlation coefficient, extracted from the NCI primary screen mean graph profiles, gives useful information as to the mechanism of action of a class of inhibitors (Section 1.1.3).[24,85]

Essentially, calculations of the COMPARE correlation coefficient involve comparison of a selected mean-graph profile, for example, a compound with a defined mechanism of action (denoted the "seed"), to the mean-graph profile of another compound. In practical terms, the delta values (the deviation relative to the average selected response *ie* GI_{50}, TGI or LC_{50}) are calculated for each of the sixty cell lines in the mean-graph of a selected compound. Default or otherwise unreliable delta values from individual cell lines are discarded and a comparison of the individual "seed" deltas to those of the corresponding partner cell lines of the selected compound is subsequently quantified using the SAS statistical program to generate a Pearson product correlation coefficient for the pairs of delta values.[85] The resulting COMPARE correlation coefficient value ranges from 0 (mean-graph profiles displaying no similarity) to 1 for compounds with identical mean-graph profiles relative to the "seed".

Figure 9.2.7 shows a comparison of the COMPARE correlation coefficients to the CEM cell line cytotoxicities (GI_{50}s) from the NCI primary screen. Compounds included in **Figure 9.2.7** are the hemi-synthetic derivatives and the naturally-occurring halichondrins tested in the NCI *in vitro* primary screen. The "seed" compound, against which comparisons of the GI_{50}-centred profiles were made, was halichondrin B (at the 10^{-7} M (upper limit) concentration) which was assigned a value of 1.00. Halichondrin B (**1.2.1**) and homohalichondrin B (**1.2.3**) are known to act as mitotic inhibitors, and as such display characteristic GI_{50}-centred profiles.[24] It was interesting to determine whether there was a correlation between the biological activity observed and the ability to display the characteristic mitotic inhibition features of the GI_{50}-centred profile.

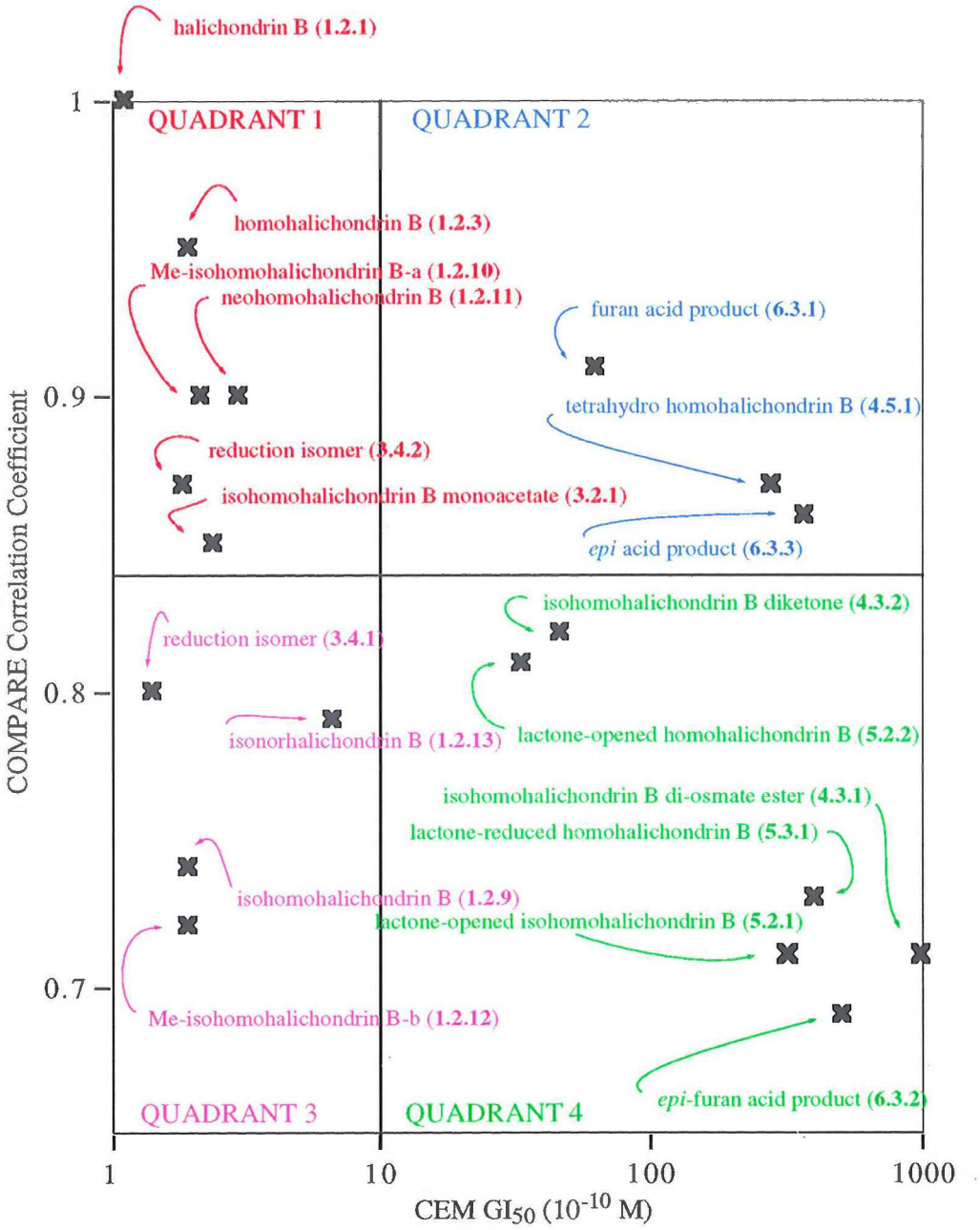

Figure 9.2.7 Graph of *In Vitro* Biological Activities of Derivative Halichondrins in the NCI Primary Screen *vs* the COMPARE Correlation Coefficients

Figure 9.2.7 has been arbitrarily divided into four quadrants to facilitate analysis of the data. The vertical line, placed at a GI_{50} of 10×10^{-10} M, divides those compounds which were relatively cytotoxic (appearing to the left of the line) from those displaying significantly reduced cytotoxicity relative to the parent halichondrins (appearing to the right of the line).

Some interesting points arise from an examination of **Figure 9.2.7**, such as those compounds lying in QUADRANT 2 which correspond to compounds with high COMPARE correlation coefficients relative to the naturally-occurring halichondrins but were relatively inactive; the furan acid product (**6.3.1**), the tetrahydro homohalichondrin B derivative (**4.5.1**) and the *epi* acid product (**6.3.3**). This indicates that these compounds were still mechanistically acting as mitotic inhibitors, but with significantly reduced potency. These derivatives may provide important lead compounds which are less cytotoxic, but which still display the characteristic mechanistic profiles of the more cytotoxic halichondrins such as halichondrin B (**1.2.1**). These derivatives may also provide important leads in the development of antibody-linked halichondrins for therapeutic use.

Also of interest are the six compounds in QUADRANT 4 which displayed reduced COMPARE correlation coefficients relative to the naturally-occurring halichondrins and correspondingly reduced cytotoxicities *viz* isohomohalichondrin B diketone (**4.3.2**), lactone-opened isohomohalichondrin B (**5.2.1**), lactone-reduced homohalichondrin B (**5.3.1**), the *epi*-furan acid product (**6.3.2**), the di-osmate ester (**4.3.1**) and the lactone-opened homohalichondrin B (**5.2.2**) derivative. The isohomohalichondrin B di-osmate ester (**4.3.1**) COMPARE correlation coefficient was calculated as <0.71, and as discussed previously, was essentially inactive in terms of cytotoxicity. This indicated that **4.3.1** had lost the ability to act as a mitotic inhibitor, resulting in the inactivity observed. These four compounds appeared to

follow the trend of displaying a loss in the characteristic halichondrin B antimitotic GI_{50}-centred profile with a concomitant loss in cytotoxicity. This is probably a reflection of the reduced ability of the compound to inhibit tubulin polymerisation and/or microtubule assembly giving rise to an observed decrease in cytotoxicity.

Four compounds situated in QUADRANT 3 displayed reduced COMPARE correlation coefficients with high cytotoxicities. These compounds appear to retain significantly high levels of cytotoxicity with a reduced ability to display the characteristic antimitotic mean-graph profile of halichondrin B (**1.2.1**).

QUADRANT 1 contains the "seed" halichondrin, halichondrin B (**1.2.1**) and five other halichondrins: three naturally-occurring halichondrins; Me-isohomohalichondrin B-a (**1.2.10**), neohomohalichondrin B (**1.2.11**) and homohalichondrin B (**1.2.3**), and two derivatives; reduction isomer (**3.4.2**) and isohomohalichondrin B monoacetate (**3.2.1**). These compounds presented high levels of cytotoxicity while displaying the characteristic mean-graph profile of halichondrin B (**1.2.1**).

For the less active derivatives displaying relatively low cytotoxicities (QUADRANTS 2 and 4), the compounds **5.2.1**, **5.2.2**, **5.3.1**, **6.3.2**, **6.3.1** and **6.3.3** appeared to display $CDCl_3$ conformations (as determined by NMR spectroscopy) which were unlike those of the active compounds halichondrin B (**1.2.1**) and homohalichondrin B (**1.2.3**). This implies that the reduction in biological activity observed, in a quantitative (GI_{50}) and qualitative sense (COMPARE),[85] was probably a function of the overall conformation of the molecule. In terms of the $CDCl_3$ conformations for the derivatives producing relatively high cytotoxicities (QUADRANTS 1 and 3), generally they appear to display $CDCl_3$ conformations similar to halichondrin B (**1.2.1**) such as homohalichondrin B (**1.2.3**) and

isohomohalichondrin B (**1.2.9**). This appeared to correlate with the GI_{50} results; those with $CDCl_3$ solution conformations corresponding more closely to those of the naturally-occurring halichondrins (*eg* halichondrin B and homohalichondrin B) presented correspondingly high cytotoxicities and *vice versa*.

9.3 Structure-Activity Conclusions

It is essential for the expression of potent antitumour activity (*ie* compounds in QUADRANTS 1 and 3 in **Figure 9.2.7**) that the halichondrin molecule retains the integrity of the lactone ring (C1-C30), the exocyclic methylenes (C19 and C26) and the natural stereochemistry of the C38 spiro centre. Of lesser importance is the nature of the tricyclo system; the presence of polar groups in this region resulted in a decrease in activity, although the presence of the E-ring furan reduced the activity significantly more. The nature of the terminal region of the molecule is less critical to the activity observed; this area was less sensitive to changes in structure, although the presence of an ionic terminal group (carboxylate) resulted in a significant decrease in activity. It would appear that the display of a high level cytotoxicity (QUADRANTS 1 and 3 in **Figure 9.2.7**) in the halichondrin series requires a $CDCl_3$ solution conformation similar to that of halichondrin B (**1.2.1**) and homohalichondrin B (**1.2.3**).

In a qualitative sense, it appears that some halichondrin derivatives may still act as inhibitors of tubulin polymerisation and microtubule assembly (as determined by the COMPARE correlation coefficient) while exhibiting a reduction in cytotoxicity. These halichondrins (*ie* those in QUADRANT 2 in **Figure 9.2.7**) appeared to exhibit different $CDCl_3$ solution conformations to those of halichondrin B (**1.2.1**) and homohalichondrin B (**1.2.3**).

It would be purely speculative, without knowing more about the detailed mechanisms by which the halichondrins enter cells *eg* interaction with a cell-specific receptor or simple diffusion, and the nature of the interactions of the active halichondrins with tubulin to inhibit its polymerisation and microtubule assembly, to

ascertain the essential *conformational* features of halichondrins under physiological conditions. However, it does appear that any change in the chemical structure of halichondrins which results in a conformational change (as observed by NMR spectroscopy in $CDCl_3$ solution) results in a large decrease in the cytotoxicity observed. As previously indicated, this conformational change does not necessarily reflect the ability of the compound to display the characteristic differential cytotoxicity patterns observed for more cytotoxic halichondrins.

It is important to note that the $CDCl_3$ solution conformation observed in the halichondrin series may not in fact represent the average solution conformation under physiological conditions or indeed the "active" conformation(s) which determine the high levels of cytotoxicity observed for selected members of the halichondrin series. However, it does appear that there is a correlation between the $CDCl_3$ solution conformation and the biological activities observed.

In terms of energetic considerations, the halichondrins, being relatively large molecules, have a high energetic cost associated with their synthesis relative to essential primary metabolites of similar size. The high energetic cost to the organism in producing such a large and apparently non-essential molecule indicates that it is producing a compound which has essential features for the display of cytotoxicity, with little or no structural redundancy, and this is reflected in the interpretation of the structure-activity results.

It is also likely that, in such a large structure, the overall folding conformation of the molecule is an important determinant of cytotoxicity rather than any one specific functional feature.

My interpretation of these results suggests that the synthesis of a model compound with only the essential features present which are required for the expression of antitumour activity would not be an efficient process from a total synthesis approach because such a large portion of the molecule appears to be essential for the display of cytotoxicity.

CHAPTER 10

Concluding Comment

The halichondrins, at the time of writing, represent exciting leads as anticancer compounds. Hopefully, the aspects of the chemistry and the biological activity of the compounds in the halichondrin series described in this thesis will improve the understanding of these compounds and will aid in the development of their future rôle as anticancer drugs.

EXPERIMENTAL

General Methods

All NMR spectra were recorded on a Varian Unity 300 spectrometer at 23°C, operating at 300 MHz for ^{1}H nuclei and at 75 MHz for ^{13}C nuclei. Other NMR experiments described in this thesis *viz* 1D and 2D-TOCSY, NOE, COSY, NOESY and the reverse-detected HMQC and HMBC experiments were recorded at 300 MHz. This instrument was fitted with a Nalorac Z.spec 5 mm Indirect Detection Probe, except that for work described in Chapters 6 and 8 the data were obtained from the Varian Unity 300 spectrometer fitted with a Nalorac Z.spec MID300 3 mm Indirect Detection Probe. Chemical shifts in this thesis were described in parts per million (ppm), on the δ scale, and were referenced to the appropriate solvent peaks: $CDCl_3$ referenced to $CHCl_3$ at δ_H 7.25 ppm (^{1}H) and $CHCl_3$ at δ_C 77.0 ppm (^{13}C); CD_3OD referenced to CHD_2OD at δ_H 3.30 ppm (^{1}H) and CD_3OD at δ_C 49.3 ppm (^{13}C). ^{1}H NMR spectra were recorded using an acquisition time (AT) of 2 s; ^{13}C NMR spectra were recorded using an AT= 0.5 s. All difference NOE experiments were recorded on undegassed solutions, with AT= 1 s and an irradiation time (D2) of 2 s and the decoupler offset 10,000 Hz for the control experiment. Percentage enhancements reported in this thesis represent the observed increase in the intensity of a specific resonance relative to the corresponding signal in the control spectrum. COSY experiments, including Phase-Sensitive and Double Quantum Filtered variants were recorded using an AT= 0.7 s, and a relaxation delay (D1) of 0.7 s. 1D and 2D-TOCSY spectra were recorded using an AT= 0.7 s, and D1= 1 s, with mixing times indicated in the discussion. An AT= 0.5 s and D1= 0.33 s with a mixing time of 0.3 s were used for the NOESY experiments discussed in this thesis. All HMQC spectra (including HSMQC) were recorded with an AT= 0.24 s, D1= 0.3 s, J (X-H spin coupling constant) = 130 Hz and null = 0.2 Hz. The acquisition parameters for

the HMBC experiments described in this thesis included: AT= 0.24 s, D1= 0.3 s, J = 130 Hz and JNXH = 6.0-8.0 Hz (average 2-3 bond coupling constant).

Mass Spectrometry was performed on a Kratos MS80 RFA Mass Spectrometer operated at 4000 V. FAB was performed with an Ion Tech ZNIIFN ion gun using Xe as the reagent gas, operating at 8 kV and 2 mA current with a *m*-nitrobenzyl alcohol (NOBA) matrix. Some samples (stated) were sent to Lewis Pannell (NIDDK, NIH) in the USA for HR FAB-MS analysis.

Infrared (IR) Spectra were recorded using a Perklin Elmer 1600 Series FTIR spectrometer equipped with a Hewlett Packard Color Pro plotter. Samples were recorded as films on a potassium bromide plate.

The HPLC work described in this thesis was performed on either one of two instruments. A Philips PU4100 Liquid Chromatograph equipped with a Philips PU4120 Diode Array Detector interfaced to a PC General 486 computer running Philips PU6003 Diode Array Detector System Software (V3.0), and a Philips PPG 3160/10 colour plotter was used for analytical and small-scale preparative HPLC. This instrument was equipped with a reverse-phase Brownlee Labs analytical C18 column (dimensions 220 mm (L) × 4.6 mm (ID), 5 μm particle size). Stated pre-mixed solvent mixtures of acetonitrile (filtered, HPLC grade) and water (deionised and filtered, with 0.05% trifluoroacetic acid (TFA) added as stated) were used with a solvent flow rate of 1 mL/ min. A Shimadzu LC-4A instrument equipped with a Shimadzu UV Spectrophotometric Detector SPD-2AS (wavelength λ= 199 nm) and a Hewlett Packard 3390A integrator was used for preparative reverse phase work using a Rainin Dynamax-60A C18 column (dimensions 250 mm (L) × 21.4 mm (ID), 8 μm average particle size (APD)), the stated acetonitrile (ACN)/ water (no TFA added) mixture with a flow rate of 5 mL/ min.

Diol column chromatography was performed using either *ca* 500 mg Bakerbond diol (40 μm APD) in a Pasteur pipette or using a 500 mg disposable diol Bakerbond spe extraction cartridge, typically eluting with increasing ACN/ dichloromethane (DCM) mixtures. Octadecyl (C18) column chromatography was performed using a C18 500 mg disposable Bakerbond spe cartridge, either gravity feed or vacuum-eluted using an Analytical International Vac-elut system, with stated solvent mixtures. Alternatively *ca* 500 mg C18 in a Pasteur pipette was used to perform gravity-feed C18 column chromatography using the stated solvent mixtures. "Florisil" column chromatography was performed using 100-200 US mesh "Florisil" in a Pasteur pipette, eluting with the stated solvents.

The analytical silica TLC described in this thesis was performed using Merck silica gel 60 F_{254} plastic-coated sheets, the silica 0.2 mm in thickness. Diol analytical TLC was performed using Merck F_{254} glass-backed plates of 0.2 mm thickness. Silica and diol plates were eluted with the stated methanol (MeOH)/ DCM mixtures, 100% ethyl acetate (EtOAc), or isopropyl alcohol (IPA)/ ACN mixtures. Whatman MKC_{18} F TLC plates of 0.2 mm thickness were used for the analytical C18 TLC performed in this thesis. Typically, the C18 TLC plates were eluted with the stated ACN/ H_2O mixtures. TLC plates containing halichondrins were visualised using a phosphomolybdic acid (PMA) in ethanol (EtOH) spray (10 % PMA in EtOH *w/v*), followed by heating at *ca* 80°C for 5 min to yield characteristic blue-brown spots. Some TLC plates (as stated) were initially visualised with iodine vapour or under short-wave (λ 254 nm) and/or visible lamps (λ 380-400 nm) before application of PMA spray. TLC results are described, where relevant, in Chapters 3-8.

Computer modelling described in this thesis was performed on an IBM RISC System /6000 computer using the program MacroModel V4.0 (in 2D graphics mode) and the associated computational program BatchMin V4.0. CSC ChemDraw 3D Plus V3.1.1

was used for manipulation, structure editing, structure display purposes and performing simple energy minimisations.

Microscale reactions were primarily performed in 1 mL, 3 mL or 5 mL reacti-vials, apparatus from an Ace microscale glassware kit and specially constructed glassware that was required for specific reactions, as described. The vials were silylated prior to use by filling with a 10% solution of dichlorodimethylsilane in toluene for 20 min. The vials were then washed with MeOH, and rinsed with water before use.

Technical grade solvents were distilled, dried and stored, where applicable, using standard procedures. Acetic anhydride was distilled immediately prior to use. Other reagents were either CP or AR grade, or were synthesised from CP or AR grade reagents and were used without further purification. "Ether" refers to specifically to diethylether. Methyltriphenylphosphonium iodide was obtained from Dr. Alan Happer in this Department. Hexane was prepared from petroleum ether (10 L, b.pt. 60-70°C), nitrating with a mixture of c. HNO_3 (1 L) and c. H_2SO_4 (1 L) for two days. After this time, the nitrating mixture was removed and the petroleum ether was washed with water (20 L), and dried over $CaCl_2$ overnight. The resulting solution was filtered through alumina and distilled.

The pure halichondrins used to undertake the investigations described in this thesis were obtained from a *Lissodendoryx* sp. extraction performed by Dr. Marc Litaudon; this extraction procedure is described in the paper in Appendix IV.

Work Described in Chapter Two

2.2 NMR Spectroscopic Assignment of Halichondrin B

Halichondrin B (**1.2.1**):

A pale yellow oil.

^{1}H and ^{13}C NMR data cited in **Tables 2.2.1** and **2.2.2** respectively.

2.4 NMR Spectroscopic Assignment of Homohalichondrin B

Homohalichondrin B (**1.2.3**):

A clear, colourless oil.

^{1}H and ^{13}C NMR data cited in **Tables 2.4.1** and **2.4.2** respectively.

2.5 Conformational and Stereochemical Studies on Isohomohalichondrin B

Optical rotation of isohomohalichondrin B (**1.2.3**, ($[\alpha]_D$ -21.6°)) determined in methanol solution at a concentration of 1.02 ng/mL using a Jasco J-20 recording spectropolarimeter.

Work Described in Chapter Three

3.2 Acetylations

Isohomohalichondrin B (**1.2.9**, 1.4 mg) was dissolved in dry pyridine (100 μL) and acetic anhydride (100 μL) was added. The reaction was stirred overnight at room temperature. The reaction was quenched by the addition of 0.5 mL water and the mixture was extracted with EtOAc (4 × 0.5 mL) and the solvent removed to give the products (1.4 mg). Silica TLC of the products was developed in 100% EtOAc and visualised.

Isohomohalichondrin B acetylation:

A pale yellow oil.

FAB-MS: *m/z* monoacetate: 1164 (MH^+), 1187 (MNa^+), 1129 (MNa^+-AcO•) and diacetate: 1206 (MH^+).

Isohomohalichondrin B (**1.2.9**, 2.3 mg) was dissolved in dry pyridine (100 μL) and placed in an ice-bath at -5°C, before acetic anhydride was added (100 μL). The reaction was stirred for 3 hrs at -5°C. The reaction was quenched with water (0.5 mL) after this time, and the mixture was extracted with EtOAc (5 × 0.5 mL). The solvent from the EtOAc extract was removed to give the product (**3.2.1**, 2.4 mg). Silica TLC of the product (**3.2.1**) was developed in 100% EtOAc and visualised.

Isohomohalichondrin B monoacetate (**3.2.1**):

A pale yellow oil.

Partial ^{1}H NMR data (H45/H45' - H55/H55') cited in **Table 3.2.1**.

To a solution of homohalichondrin B (**1.2.3**, 0.5 mg) in dry pyridine (75 μL), acetic anhydride (75 μL) was added, and the reaction was stirred at room temperature for 45 min. Silica TLC performed on a small aliquot (*ca* 2 μL) removed from the reaction mixture was developed in 100% EtOAc and visualised. After 5 hrs reaction, silica TLC was performed on a small aliquot removed from the reaction mixture, developed (in 100% EtOAc) and visualised. The reaction was quenched at this time with 0.5 mL water and extracted with EtOAc (5 × 1 mL). The solvent (EtOAc) was removed, to give 0.6 mg of the product (**3.2.1**).

Homohalichondrin B (**1.2.3**, 2.0 mg) was dissolved in dry pyridine (100 μL) and acetic anhydride (100 μL) was added to the solution. The reaction was stirred overnight at room temperature. Silica TLC was performed on a small aliquot removed from the reaction mixture, developed in 100% EtOAc, and then visualised. At this time the reaction was quenched (with 0.5 mL water), and the resulting solution was extracted with EtOAc (5 × 1 mL) and the solvent was removed to give 2.1 mg of the product (**3.2.2**).

Homohalichondrin B diacetate (**3.2.2**):

A pale yellow oil.

Partial ^{1}H NMR data cited in Chapter 3 (Section 3.2.1).

Homohalichondrin B (**1.2.3**, 1.5 mg) was dissolved in dry pyridine (75 μL) before acetic anhydride (75 μL) was added to the solution. The reaction was stirred overnight at room temperature. Silica TLC was performed on a small aliquot removed from the reaction mixture, developed in 100% EtOAc and visualised. At this time the reaction was quenched (with 0.2 mL water), and the resulting solution was extracted with EtOAc (10 × 0.2 mL) and the solvent was removed to give 1.5 mg of the product (**3.2.2**).

3.3 Oxidation

Isohomohalichondrin B monoacetate (**3.2.1**, 0.6 mg), dissolved in DCM (*ca* 100 μL), was added to freshly prepared pyridinium chlorochromate[48] (2.2 mg) and sodium acetate (0.4 mg) in DCM (50 μL). The resulting solution was stirred at room temperature. Silica TLC was performed on a small aliquot (*ca* 2 μL) removed from the reaction mixture after 60 hrs reaction, developed in 1% MeOH/ DCM and visualised initially with iodine vapour then PMA spray/heat. The reaction mixture was passed through a Florisil column equilibrated to 100% ether, and eluted with ether (6 mL) then 1% MeOH/ DCM (6 mL). These elutions were combined on the basis of silica TLC (developed and visualised as previously) and the solvent was removed to give 0.5 mg of material.

3.4 Sodium Borohydride Reduction

Sodium borohydride (2.2 mg) was added to isohomohalichondrin B (**1.2.9**, 0.9 mg) dissolved in 200 μL dry IPA. The resulting suspension was vigorously stirred at room temperature for 0.5 hr. At this time, silica TLC was performed on an aliquot (*ca* 2 μL) taken from the reaction mixture, developed in 5% MeOH/ DCM and visualised. After a further 0.5 hr the reaction was quenched by the addition of 2 mL aqueous ammonium chloride solution ($NH_4Cl_{(aq)}$, pH 3). This material was placed on a C18 cartridge (equilibrated with 100% H_2O) and washed with 6 mL 10% MeOH/ H_2O (2 column volumes) under vacuum. The column was eluted with 100% MeOH (2 × 6 mL, 4 column volumes) under vacuum and the solvent removed from the eluent to yield 0.9 mg of products (**3.4.1** and **3.4.2**).

To a solution of isohomohalichondrin B (**1.2.9**, 1.1 mg) in dry IPA (200 μL), sodium borohydride (2.5 mg) was added and the reaction was stirred vigorously at room temperature for 15 min. Silica TLC was performed at this time with a small aliquot of the reaction mixture, developed with 5% MeOH/ DCM and visualised. The reaction was quenched after a further 15 min by the addition of 2 mL $NH_4Cl_{(aq)}$ solution (pH 3) and placed on a C18 cartridge (equilibrated to 100% H_2O) under vacuum. The column was washed with 6 mL 10% MeOH/ H_2O and the products eluted with 100% MeOH (2 × 6 mL), under vacuum. The solvent was removed from the MeOH fractions to give 1.1 mg products (**3.4.1** and **3.4.2**).

The products from both sodium borohydride reactions were combined and preparative HPLC was performed on the combined material. The Shimadzu HPLC was equipped with the preparative C18 column and the column was equilibrated to 55% ACN/ H_2O prior to a single injection of the product mixture dissolved in a

mixture of 100 μL MeOH and 100 μL of the mobile phase. The two peaks containing the products were collected separately and the solvent was removed to give 0.6 mg of reduction isomer **3.4.1** and 0.4 mg of reduction isomer **3.4.2**.

To a solution of isohomohalichondrin B (**1.2.9**, 5.0 mg) in 1 mL dry IPA, 14.4 mg of sodium borohydride was added, and the reaction was stirred vigorously at room temperature for 0.5 hr. Silica TLC was performed at this time, on a small aliquot of the reaction mixture, with the TLC plate being developed in 5% MeOH/ H_2O and visualised. After a further 0.5 hr reaction, the reaction was quenched with 2 mL $NH_4Cl_{(aq)}$ solution (pH 3), and placed onto a cartridge C18 column equilibrated to 100% H_2O under vacuum. The cartridge was washed with 10% MeOH/ H_2O (14 mL) and the products were eluted off the column with 100% MeOH (2 × 6 mL). The solvent was removed from the MeOH fractions to give the products (**3.4.1** and **3.4.2**, 4.8 mg). Preparative HPLC using the Shimadzu HPLC equipped with the preparative C18 column and equilibrated to 55% ACN/ H_2O was performed in one injection of the products dissolved in 100 μL and 100 μL 55% ACN/ H_2O. Collection of the two respective product peaks, followed by solvent removal, yielded 1.6 mg of reduction isomer **3.4.1** and 1.2 mg of reduction isomer **3.4.2**. The respective reduction isomers were combined from both preparative HPLC separations and reweighed to yield a total 2.4 mg of reduction isomer **3.4.1** and 1.8 mg of reduction isomer **3.4.2**.

Reduction isomer (**3.4.1**):

A white powder.

^{1}H and ^{13}C NMR data cited in **Tables 3.4.1** and **3.4.2** respectively.

High Resolution FAB-MS *m/z* 1125.6016 (MH^+, +1.6 ppm for $C_{61}H_{89}O_{19}$). Performed at NIDDK, NIH (Lewis Pannell).

Reduction isomer (**3.4.2**):

A white powder.

^1H and ^{13}C NMR data cited in **Tables 3.4.3** and **3.4.4** respectively.

High Resolution FAB-MS *m/z* 1125.5952 (MH^+, -4.1 ppm for $C_{61}H_{89}O_{19}$). Performed at NIDDK, NIH (Lewis Pannell).

Work Described in Chapter Four

4.2 Trial Ozonolysis

β-Pinene (9.4 mg) dissolved in 1 mL DCM was placed in a reacti-vial which was then sealed with a teflon septum. The sharpened end of a 3 cm needlestock was inserted through the septum above the solvent level, with the other end inserted into a teflon tube which was placed into a solution of 10% potassium iodide and starch in 5% aqueous sulfuric acid. The ozoniser needle was inserted through the septum and lowered into the β-pinene solution with oxygen gas flowing through the needle. An energised Tesla coil vacuum tester was touched to the ozoniser needle stock above the reacti-vial to generate ozone, until the iodide/ starch solution turned blue/ black indicating complete O_3 absorption had occurred in the reacti-vial and the reaction was complete. Nitrogen gas was flushed through the system. A suspension of *ca* 20 mg zinc dust in a 50% aqueous acetic acid solution (200 μL) was added to the reacti-vial and the mixture was stirred overnight at room temperature. The mixture was extracted with ether (4 × 0.5 mL) and the solvent was removed.

4.3 Osmylation Reactions

An ether solution of osmium tetroxide (400 μL at 50 mg/ mL) was added to 10 mg of β-pinene in 500 μL ether and 280 μL pyridine and the reaction was stirred at room temperature. After 2 hrs, a solution of 18 mg sodium metabisulfite ($Na_2S_2O_5$) in 260 μL water and 175 μL pyridine was added to the reaction mixture and stirred at room

temperature for a further 15 min. The reaction was extracted with DCM (4 × 2 mL) and the solvent removed to give an oily product.

Benzoin (10 mg) was dissolved in an aqueous solution of freshly prepared 40 mM sodium periodate ($NaIO_4$, 600 μL) and two drops of MeOH. The reaction was stirred at room temperature, in the dark overnight. The reaction solution was extracted with DCM (3 × 1 mL) and the solvent was removed to give the products.

Isohomohalichondrin B (**1.2.3**, 0.4 mg) was dissolved in 20 μL $NaIO_{4\ (aq)}$ solution (40 mM) and two drops of MeOH. The resulting solution was stirred at room temperature in the dark overnight. After this time, the solution was extracted with DCM (3 × 1 mL). The solvent was removed to give 0.5 mg isohomohalichondrin B. Silica TLC was developed in 5% MeOH/ DCM and visualised.

A 100 mg/ mL solution of osmium tetroxide in ether (20 μL, 2.6 mol. equiv.) was added to isohomohalichondrin B (**1.2.9**, 3.3 mg) dissolved in pyridine (75 μL). After stirring the solution at room temperature for 4.5 hrs, a solution of $Na_2S_2O_5$ (6.0 mg) in water (90 μL) and pyridine (60 μL) was added to the reaction and stirred for a further 20 min at room temperature. The reaction mixture was extracted with DCM (4 × 2 mL) and the solvent removed to give 6.5 mg of material (**4.3.1**).

Isohomohalichondrin B di-osmate ester (**4.3.1**):

A black oil.

^1H and ^{13}C NMR data cited in **Tables 4.3.1** and **4.3.2** respectively.

A Pasteur pipette C18 column was equilibrated to 55% ACN/ H_2O and the isohomohalichondrin B di-osmate ester (**4.3.1**, 1.1 mg) dissolved in 100 μL MeOH and 100 μL 55% ACN/ H_2O was placed on the column bed, eluting with 55% ACN/ H_2O. Six fractions of *ca* 1 mL were collected before the column was stripped with 100% ACN (2 × 5 mL fractions). Fractions two through to five were combined on the basis of silica TLC results (developed in 10% MeOH/ DCM), and the solvent was removed to give 0.7 mg of **4.3.1** for bioassay analysis.

An aqueous 40 mM $NaIO_4$ solution (150 μL) was added to 5.4 mg of **4.3.1** with two drops of MeOH to solubilise the halichondrin material. The reaction was stirred in the dark at room temperature for 4 days. Silica TLCs of small aliquots from the reaction mixture (*ca* 2 μL) were developed in 10% MeOH/ DCM and visualised. The reaction mixture was extracted with DCM (8 × 1 mL) and the solvent removed to give 3.1 mg of the product (**4.3.2**).

After acquisition of the NMR data, this material was subjected to preparative HPLC using the Shimadzu instrument with the preparative C18 column equilibrated to 55% ACN/ H_2O. Fractions were collected from a single injection of the periodate cleavage product dissolved in a mixture of 100 μL MeOH and 100 μL mobile phase. The C18 column was subsequently stripped with 100% ACN. Silica TLC of the resulting fractions, developed in 10% MeOH/ DCM indicated that the halichondrin material was present in the 100% ACN column strip (2.8 mg). This material was placed on a C18 Pasteur pipette column equilibrated to 55% ACN/ H_2O. Fractions of 500 to 750 μL elutions of 55% ACN/ H_2O were analysed by silica TLC (developed in 10% MeOH/ DCM and visualised). Fractions nine through to fifteen which contained isohomohalichondrin B diketone (**4.3.2**), as determined by comparison to a reference TLC spot, were combined to give 0.8 mg of **4.3.2** for MS and bioassay analysis.

Isohomohalichondrin B diketone (**4.3.2**):

A yellow oil.

^{1}H and ^{13}C NMR data cited in **Tables 4.3.3** and **4.3.4** respectively.

High Resolution FAB-MS *m/z* 1165.49610 (MK^+, -2.1 ppm for $C_{59}H_{82}O_{21}K$). Average of 7 acquisitions.

A 40 mM aqueous $NaIO_4$ solution (20 μL) was added to homohalichondrin B diacetate (**3.2.2**, 0.6 mg) with two drops of MeOH. The resulting solution was stirred at room temperature for 55 hrs in the dark. Silica TLC of the reaction mixture was developed in 100% EtOAc and visualised. The solution was extracted with DCM (5 × 0.5 mL) and the solvent removed to give 0.5 mg unreacted homohalichondrin B diacetate (**3.2.2**).

Homohalichondrin B diacetate (**3.2.2**, 2.5 mg) was dissolved in pyridine (60 μL), 30 μL of osmium tetroxide solution in dry ether (50 mg/ mL, 2.8 mol. equiv.) was added, and the reaction was stirred at room temperature for 4.5 hrs. After this time a solution of $Na_2S_2O_5$ (4.8 mg) in water (75 μL) and pyridine (50 μL) was added and stirred for a further 20 min at room temperature. The reaction mixture was extracted with DCM (4 × 1 mL) and the solvent removed to give 2.8 mg of product. Silica TLC of the product was performed in 100% EtOAc and visualised.

A freshly prepared aqueous 40 mM $NaIO_4$ solution (110 μL) was added to the homohalichondrin B diacetate osmylation product with two drops of MeOH. The reaction was stirred in the dark at room temperature. Silica TLC was developed in 10% MeOH/ DCM and visualised. After 45 hrs reaction the reaction mixture was extracted with DCM (5 × 1 mL) and the solvent removed to give 2.5 mg of **4.3.3**.

Homohalichondrin B diacetate diketone (**4.3.3**):

A yellow oil.

^{1}H and ^{13}C NMR data cited in **Tables 4.3.5** and **4.3.6** respectively.

Homohalichondrin B diacetate (**3.2.2**, 1.5 mg) was dissolved in 30 μL pyridine, then 15 μL (nominally) of osmium tetroxide in ether (50 mg/ mL, 2.4 mol. equiv.) was added and the resulting solution was stirred at room temperature for 4.5 hrs. After this time a solution of $Na_2S_2O_5$ (2.7 mg) in water (45 μL) and pyridine (30 μL) was added to the reaction mixture and stirred at room temperature for a further 20 min. The mixture was extracted with DCM (10 × 0.5 mL) and the solvent removed to give 1.9 mg of products. After reaction was determined to be incomplete by ^{1}H NMR spectroscopy, the mixture of starting material and products were re-reacted under identical conditions to yield 1.7 mg of products. This material was subsequently dissolved in two drops of MeOH and 70 μL of freshly prepared 40 mM aqueous $NaIO_4$ solution was added. The reaction was stirred at room temperature for 47 hrs in the dark. Silica TLC was developed in 10% MeOH/ DCM prior to visualisation. The reaction mixture was extracted with DCM (5 × 0.5 mL) and the solvent was removed to give 1.0 mg of product (**4.3.3**).

4.4 Homohalichondrin B Diacetate Diketone Reduction

Homohalichondrin B diacetate diketone (**4.3.3**, 1.0 mg) was dissolved in 60 μL of 20% DCM/ IPA and a suspension of 2.1 mg $NaBH_4$ in 150 μL dry IPA was added. The reaction was stirred at room temperature and the reaction was monitored by silica TLC. Silica TLC was developed in 10% MeOH/ DCM and visualised. The

reaction was quenched after 18 hrs by the addition of 2 mL $NH_4Cl_{(aq)}$ solution (pH 3). This material was placed on a C18 cartridge equilibrated to 100% H_2O and washed with 6 mL 10% MeOH/ H_2O under vacuum. The column was eluted with 100% MeOH under vacuum and the solvent removed from the eluent to yield 0.7 mg of products. Silica TLC performed on the products was developed with 10% MeOH/ DCM and visualised. Diol TLC was developed in 1% IPA/ ACN and visualised. The reduction products were dissolved in DCM and placed on a cartridge diol column equilibrated to 100% DCM. Nineteen fractions of 0.5 mL 100% DCM elutions (fractions 1-19) were collected. A further five fractions (fractions 20-24) were eluted with 10% ACN/ DCM. One 2 mL fraction eluting with 50% ACN/ DCM (fraction 25) was followed by a 2 mL elution of 100% ACN (fraction 26). The column was stripped with 100% MeOH (fraction 27). All fractions were analysed by silica TLC (developed in 10% MeOH/ DCM and visualised). Fractions 11 to 20, containing the less polar component(s) of the reaction mixture were combined on the basis of silica TLC to give 0.2 mg of material. Fractions 22 to 25 were combined to give 0.2 mg of the more polar component(s).

4.5 Hydrogenation

A suspension of 5% Pd/C catalyst in 200 µL EtOH was added to homohalichondrin B (**1.2.3**, 2.3 mg) in a silylated 3 mL reacti-vial. The reacti-vial was attached to a 3-way tap and a hydrogen-filled balloon and a vacuum supply. The reacti-vial was evacuated then hydrogen was admitted; this procedure was repeated. The reaction was stirred vigorously under hydrogen overnight at room temperature before the vial was evacuated. The vial contents were filtered through celite in a Pasteur pipette

with EtOH and the solvent was removed to give 2.1 mg of unreacted homohalichondrin B (**1.2.3**).

A suspension of 2.0 mg PtO_2 (Adams' catalyst) in 200 μL EtOAc was placed in a 10 mL round bottom two-neck flask. On one neck, a three-way tap with a hydrogen-filled balloon was attached together with a vacuum supply. On the other neck of the flask a rubber seal was attached. The flask was evacuated and then filled with hydrogen three times and the catalyst was stirred at room temperature under hydrogen for 30 min. Homohalichondrin B (**1.2.3**, 2.1 mg) dissolved in 200 μL EtOAc was then injected through the septum into the flask. The reaction was stirred at room temperature for 4 hrs before the flask was evacuated. The flask contents were filtered through celite in a Pasteur pipette with EtOAc and the solvent was removed to give 2.1 mg of tetrahydro homohalichondrin B (**4.5.1**).

Tetrahydro homohalichondrin B (**4.5.1**):

A yellow oil.

^{1}H and ^{13}C NMR data cited in **Tables 4.5.1** and **4.5.2** respectively.

High Resolution FAB-MS *m/z* 1149.59430 (MNa^+, -2.7 ppm for $C_{61}H_{90}O_{19}Na$).

Work Described in Chapter Five

5.2 Methanolysis

Sodium methoxide (NaOMe) solution was freshly prepared by dropping sodium (Na) wire into dry methanol. A solution of NaOMe (10 mM, 200 μL) in dry methanol was added to isohomohalichondrin B (**1.2.9**, 1.1 mg). The resulting solution was stirred overnight at room temperature. After this time, Na wire was added to the reaction whilst cooling the reaction vessel to give a sodium methoxide concentration of *ca* 0.5 M. The resulting solution was stirred at room temperature overnight. Silica TLCs were developed in 5% MeOH/ DCM and visualised. The reaction was quenched by the addition of 2 mL acidified water (aqueous ammonium chloride $(NH_4Cl)_{aq}$, pH 3) and placed on a cartridge C18 column. The column was washed with 10% MeOH/ H_2O (2 × 5 mL) before eluting the halichondrin material off the column with 100% MeOH (2 × 5 mL). The MeOH fractions were combined and the solvent removed to give 1.3 mg of material (**5.2.1**). Some of this material (0.4 mg) was submitted for MS analysis and P388 assay.

Isohomohalichondrin B (**1.2.9**, 2.2 mg) was stirred in a solution of sodium methoxide in dry MeOH (*ca* 0.5 M, 200 μL) at room temperature overnight. After this time, Na wire was added to the reaction mixture to give a NaOMe concentration of *ca* 1 M, and the reaction was stirred overnight. Silica TLCs were developed in 5% MeOH/ DCM and visualised. The reaction was quenched with 2 mL acidified water ($(NH_4Cl)_{aq}$, pH 3) and placed on a cartridge C18 column. The column was washed with 10% MeOH/ H_2O (2 × 8 mL) and the halichondrin material was eluted in 100% MeOH (2 × 8 mL). The MeOH fractions were combined and the solvent

removed to give 2.2 mg of material (**5.2.1**). After comparison of their ^{1}H NMR spectra, the products from both reactions were combined to give 2.8 mg of **5.2.1**.

Lactone-opened isohomohalichondrin B (**5.2.1**):

A clear, pale yellow oil.

^{1}H and ^{13}C NMR data cited in **Tables 5.2.1** and **5.2.2** respectively.

IR (film) υ_{max} 3444, 1574 cm^{-1}.

High Resolution FAB-MS *m/z* 1193.56600 (MK^{+}, -0.2 ppm for $C_{62}H_{90}O_{20}K$).

Homohalichondrin B (**1.2.3**, 2.1 mg) was reacted with NaOMe in dry MeOH (*ca* 0.5 mM, 200 μL) stirring the reaction overnight at room temperature. Silica TLCs were developed in 10% MeOH/ DCM and visualised. The reaction was quenched with *ca* 2 mL acidified water ($(NH_4Cl)_{aq}$, pH 3) and placed onto a cartridge C18 column. The column was washed with 10% MeOH/ H_2O (2 × 8 mL), eluting the halichondrin material in 100% MeOH (2 × 8 mL). The MeOH fractions were combined and dried down to give 2.1 mg of a 50:50 mixture of starting material and product. The mixture was committed for re-reaction with NaOMe in dry MeOH (*ca* 0.5 mM, 200 μL), stirring the reaction at room temperature overnight. The reaction was quenched after this time and worked-up as previously described to give 1.9 mg of **5.2.2**.

Lactone-opened homohalichondrin B (**5.2.2**):

A white powder.

^{1}H and ^{13}C NMR data cited in **Tables 5.2.3** and **5.2.4** respectively.

High Resolution FAB-MS *m/z* 1179.55005 (MK^+, -0.4 ppm for $C_{61}H_{88}O_{20}K$).

5.3 Lithium Aluminium Hydride Reduction

Homohalichondrin B (**1.2.3**, 1.1 mg) was dissolved in 2 mL dry tetrahydrofuran (THF) before the addition of fresh lithium aluminium hydride (2.5 mg). The resulting suspension was stirred vigorously for 4 hrs at room temperature. After this time, the reaction was quenched with 2 mL acidified water ($(NH_4Cl)_{aq}$, pH 3), and placed on a C18 cartridge column. The column was washed with 10% MeOH/ H_2O (2 × 5 mL) and eluted with 100% MeOH (2 × 5 mL) to obtain 1.4 mg of **5.3.1**. Silica TLC was developed in 10% MeOH/ DCM and visualised.

Lactone-reduced homohalichondrin B (**5.3.1**):

A white powder.

^1H and ^{13}C NMR data cited in **Tables 5.3.1** and **5.3.2** respectively.

High Resolution FAB-MS *m/z* 1165.56800 (MK^+, -2.8 ppm for $C_{61}H_{90}O_{19}K$).

Work Described in Chapter Six

6.2 Acid Stability Studies

$CDCl_3$ was stored over K_2CO_3 overnight to remove residual HCl from the solvent. Homohalichondrin B (**1.2.3**, 0.3 mg) was dissolved in *ca* 600 μL of the supernatant $CDCl_3$ and the solution was transferred to an NMR tube. After a reference ^1H NMR spectrum was acquired, then 9 μL of a solution of pyridinium *p*-toluene sulfonate (PPTS) in the carbonate-treated $CDCl_3$ solvent (2.5 mg/mL, 0.33 mole equivalent) was added to the NMR tube. The solution in the NMR tube was thoroughly mixed and ^1H NMR spectra were acquired on the resulting solution after 0.5 and 0.75 hr. After this time, another 18 μL of the PPTS solution was added to the NMR tube to give a 1:1 molar ratio of PPTS: **1.2.3**. ^1H NMR spectra were acquired on this solution immediately after addition of PPTS (to give a 1:1 ratio), and at the following times subsequently: 2.5 hrs, 3.5 hrs , 4.5 hrs , 24.5 hrs , 50 hrs , 77 hrs, 4 days, 6 days, 7 days, 8 days, 9 days, 10 days, 12 days, 15 days, 19 days and 22 days. After this time, the solvent was removed and 1 mL of H_2O was added and 0.1 M sodium hydroxide (NaOH) was added to give a pH 7.5-8.0. The resulting solution was extracted with DCM (5 × 0.5 mL) and the solvent was removed to give 0.3 mg of worked-up material. Silica TLC performed was developed in 5% MeOH/ DCM and visualised. Analytical HPLC was performed using an analytical C18 column with 50% ACN/ H_2O as the mobile phase. Four injections (20 μL) were made of the worked-up material dissolved in the mobile phase (at 3.75 mg/ mL), and the peaks eluting before 400 s, the peak eluting at *ca* 400 s and the peak eluting at *ca* 550 s were collected as separate fractions.

Homohalichondrin B (**1.2.3**, 0.5 mg) was dissolved in 100 μL DCM. An aliquot (*ca* 2 μL) of this solution was taken and the solvent was removed. A solution of 50% ACN/ H_2O (10 μL) was added to the aliquot and an analytical HPLC injection (using an analytical C18 column equilibrated to 50% ACN/ H_2O) of the resulting solution was made. An aqueous solution (25 μM, 50 μL) of *p*-toluene sulfonic acid (PTSA) was added to the homohalichondrin B (**1.2.3**) in DCM solution to give a 360: 1 molar ratio of PTSA to **1.2.3**. The resulting mixture was stirred at room temperature, and 2 μL aliquots were removed from the DCM layer at regular intervals (*viz* after 1 hr, 3 hrs, 6 hrs, 23 hrs and 47 hrs reaction) for analytical HPLC analysis as described previously. After 47 hrs stirring at room temperature, 100 μL water was added to the reaction mixture. The pH of the aqueous layer was adjusted to pH 7.5-8.0 with 0.1 M NaOH solution before extracting with DCM (5 × 0.5 mL). The solvent (DCM) was removed to give homohalichondrin B (**1.2.3**, 0.3 mg).

Homohalichondrin B (**1.2.3**, 0.3 mg) was dissolved in DCM (50 μL) and 50 μL of an aqueous PTSA solution (5 mM) was added to give a 1:1 molar ratio of PTSA to **1.2.3**. The resulting mixture was stirred vigorously at room temperature. Aliquots (*ca* 2 μL) from the DCM layer were removed after 1.5 hrs and 27 hrs for analytical HPLC analysis. The solvent was removed from the aliquots and 10 μL of 50% ACN/ H_2O was added for HPLC injection (performed using an analytical C18 column with 50% ACN/ H_2O as the mobile phase). After 48 hrs stirring at room temperature, 100 μL water was added to the reaction mixture and the pH of the aqueous layer was adjusted to pH 7.0-7.5. The resulting mixture was extracted with DCM (5 × 0.5 mL). The solvent was removed to give unreacted homohalichondrin B (**1.2.3**, 0.3 mg).

Homohalichondrin B (**1.2.3**, 0.3 mg) was dissolved in a PTSA in DCM solution (1.1 mg/ mL, 100 μL) to give a molar ratio of *ca* 220: 1 PTSA to **1.2.3**. The resulting solution was stirred at room temperature for 48 hrs. After this time, 100 μL water was added and the pH of the aqueous layer was adjusted to pH 7.0-7.5 (with 0.1 M NaOH). The resulting mixture was extracted with DCM (5 × 0.5 mL) and the solvent was removed from this extract to give unreacted homohalichondrin B (**1.2.3**, 0.3 mg).

Homohalichondrin B (**1.2.3**, 0.8 mg) was dissolved in *ca* 500 μL CD_3OD and the resulting solution was transferred to an NMR tube. After the acquisition of a ^1H NMR spectrum from this solution, 25 μL of a solution of TFA in CD_3OD (5% *v/v* TFA in CD_3OD) was added to the NMR tube to give a *ca* 1:20 molar ratio of TFA: homohalichondrin B (**1.2.3**). The solution was thoroughly mixed and ^1H NMR spectra were acquired from the resulting solution immediately after TFA addition and after 3 hrs. After this time one drop of triethylamine (TEA) was added to give a pH of 8.0. The solvent was removed and 1 mL water was added and the resulting solution was extracted with DCM (5 × 1 mL). The solvent was removed from the DCM extract and the material was transferred to an NMR tube with $CDCl_3$/ 0.1% pyridine-d_5 and a ^1H NMR spectrum was re-acquired. Silica TLC performed was developed in 10% MeOH/ DCM and visualised. C18 in a Pasteur pipette was equilibrated to 55% ACN/ H_2O and the worked-up material was dissolved in the mobile phase and placed onto the column bed. Eight fractions of 1 mL were collected, followed by two fractions (1 mL) eluting with 100% ACN. Silica TLCs performed on the fractions were developed in 10% MeOH/ DCM and visualised. Fractions four through to nine were combined to give 0.6 mg of homohalichondrin B (**1.2.3**). Fraction ten contained 0.1 mg of material.

A *ca* 250 μL volume of TFA was made up to 100 mL with DCM in a volumetric flask. Two aliquots of this solution (10 mL) were titrated against standard aqueous NaOH solution (24.625 mM), using phenolphthalein indicator. The TFA concentration calculated from these titrations was 30.04 mM.

Homohalichondrin B (**1.2.3**, 0.3 mg) was dissolved in 100 μL of the standardised TFA solution to give an 11:1 molar ratio of TFA: **1.2.3**. The resulting solution was stirred at room temperature for 4 hrs. After this time, 200 μL water was added to the reaction mixture and the pH of the aqueous layer was adjusted to pH 7.5-8.0 with 0.1 M $NaOH_{(aq)}$. The water layer was removed and another 200 μL water was added to the reaction mixture. The resulting mixture was extracted with DCM (4 × 0.2 mL) and the solvent was removed to give 0.3 mg of worked-up material.

Homohalichondrin B (**1.2.3**, 2.2 mg) was dissolved in 100 μL of the standardised TFA in DCM solution to give a 1.5:1 molar ratio of TFA to **1.2.3**. The reaction was stirred at room temperature for 30 min. After this time, 1 mL water was added to the reaction mixture and the pH of the aqueous layer was adjusted to pH 7.5-8.0 with 0.1 M NaOH. The water layer was removed and the reaction mixture was washed with water (5 × 1 mL). Water was added to the reaction mixture (1 mL) and the resulting mixture was extracted with DCM (5 × 0.5 mL). The solvent was removed from the DCM extract to give 2.0 mg of worked-up material. Analytical HPLC was performed on the worked up material using an analytical C18 column with 50% ACN/ H_2O, 52.5% ACN/ H_2O and 60% ACN/ H_2O as the mobile phases. Analytical injections of 10 μL were made of the worked-up material dissolved in the mobile phase (2 mg/ mL).

Homohalichondrin B (**1.2.3**, 2.1 mg) was dissolved in 100 μL of the titrated TFA solution. The resulting solution was stirred at room temperature for 30 min. After this time, 1 mL water was added to the reaction mixture and the pH of the aqueous layer was adjusted to pH 7.5-8.0 with 0.1 M $NaOH_{(aq)}$. The water layer was removed and the reaction mixture was washed with water (5 × 1 mL). Water was added to the reaction mixture (1 mL) and the resulting mixture was extracted with DCM (5 × 0.5 mL). The solvent was removed from the DCM extract to give 2.1 mg of worked-up material. Preparative analytical HPLC was performed on the worked-up material using an analytical C18 column equilibrated to 60% ACN/ H_2O. The worked-up material was dissolved in 200 μL of mobile phase and injections of *ca* 20 μL were made, and the peaks eluting at 230 s (**1.2.3**) and 550 s (**6.3.1**) were collected. The solvent was removed from the 230 s eluting fraction to give 0.6 mg homohalichondrin B (**1.2.3**). The solvent was removed from the 550 s eluting fraction to give 0.5 mg of the furan acid product (**6.3.1**).

Homohalichondrin B (**1.2.3**, 4.4 mg) was dissolved in 200 μL of the titrated TFA in DCM solution. The resulting solution was stirred at room temperature for 30 min. After this time, 1 mL water was added to the reaction mixture and the pH of the aqueous layer was adjusted to pH 7.5-8.0 with 0.1 M $NaOH_{(aq)}$. The water layer was removed and the reaction mixture was washed with water (4 × 1 mL). Water was added to the reaction mixture (1 mL) and the resulting mixture was extracted with DCM (5 × 1 mL). The solvent was removed from the DCM extract to give 4.2 mg of worked-up material. Preparative analytical HPLC was performed on the worked-up material using an analytical C18 column with 60% ACN/ H_2O (0.05% TFA) as the mobile phase. Mobile phase (210 μL to give 20 mg/ mL) was added to the worked-up material and preparative injections of *ca* 20 μL were performed and the peaks eluting at *ca* 230 s (**1.2.3**) and *ca* 550 s (**6.3.1**) were collected. The solvent was

removed from the 230 s eluting fraction to give 2.4 mg of material. The solvent was removed from the 550 s eluting fraction to give 1.1 mg of material. These fractions were re-injected into the HPLC on an analytical scale (10 μL of 2 mg/ mL). The two fractions were re-combined and preparative HPLC using an analytical C18 column with 60% ACN/ H_2O (no TFA) was repeated, and the fractions were re-injected on an analytical scale indicating a good separation had been achieved.

Homohalichondrin B (**1.2.3**, 4.0 mg) was dissolved in 200 μL of the standardised TFA in DCM solution. The reaction was stirred at room temperature for 30 min. After this time, 1 mL water was added to the reaction mixture and the pH of the aqueous layer was adjusted to pH 7.5-8.0 with 0.1 M $NaOH_{(aq)}$. The water layer was removed and the reaction mixture was washed with water (4 × 1 mL). Water was added to the reaction mixture (1 mL) and the resulting mixture was extracted with DCM (5 × 1 mL). The solvent was removed from the DCM extract to give 4.4 mg of worked-up material. Preparative HPLC was performed on the worked-up material using an analytical C18 column with 60% ACN/ H_2O as the mobile phase. The worked-up material was dissolved in 220 μL and injections of 20 μL were performed, collecting the peaks eluting at *ca* 230 s (**1.2.3**) and *ca* 550 s (**6.3.1**) separately and the material eluting between injections. The solvent was removed from the three respective fractions to give 1.5 mg (**1.2.3**), 0.8 mg (**6.3.1**) and 1.6 mg (**6.3.2** and **6.3.3**). Each of the three respective fractions was re-analysed by HPLC on an analytical-scale using an analytical C18 column with 70% ACN/ H_2O as the mobile phase. The mixture of components (**6.3.2** and **6.3.3**) was subsequently separated on a preparative scale under the same HPLC conditions. The mixture was dissolved in 80 μL of the mobile phase and 20 μL injections were performed, collecting the peaks eluting at *ca* 800 s and *ca* 1000 s separately. These fractions were re-injected on an analytical scale to assess the quality of the separation. Diol

TLC performed on the four separated components (**1.2.3**, **6.3.1**, **6.3.2** and **6.3.3**) from the HPLC separation were developed in 1% MeOH/ DCM and visualised.

Homohalichondrin B (**1.2.3**, 4.0 mg) was dissolved in 200 μL of the titrated TFA in DCM solution. The reaction was stirred at room temperature for 30 min. After this time, 1 mL water was added to the reaction mixture and the pH of the aqueous layer was adjusted to pH 7.5-8.0 with 0.1 M $NaOH_{(aq)}$. The water layer was removed and the reaction mixture was washed with water (4 × 1 mL). Water was added to the reaction mixture (1 mL) and the resulting mixture was extracted with DCM (5 × 1 mL). The solvent was removed from the DCM extract to give 4.0 mg of worked-up material. Preparative HPLC was performed on the worked-up material using an analytical C18 column and 70% ACN/ H_2O as the mobile phase. The worked-up material was dissolved in 200 μL of the mobile phase and 40 μL HPLC injections were performed. The peaks eluting at *ca* 230 s, 300 s, 800 s and 1000 s were collected separately and the solvent was removed to give 0.9 mg (**1.2.3**), 0.8 mg (**6.3.1**), 1.0 mg (**6.3.2**) and 1.1 mg (**6.3.3**) of material respectively.

Homohalichondrin B (**1.2.3**, 4.8 mg) was dissolved in 200 μL of the standardised TFA in DCM solution. The reaction was stirred at room temperature for 30 min. After this time, 1 mL water was added to the reaction mixture and the pH of the aqueous layer was adjusted to pH 7.5-8.0 with 0.1 M NaOH. The water layer was removed and the reaction mixture was washed with water (4 × 1 mL). Water was added to the reaction mixture (1 mL) and the resulting mixture was extracted with DCM (5 × 1 mL). The solvent was removed from the DCM extract to give 4.6 mg of worked-up material. Preparative HPLC was performed on the worked-up material using an analytical C18 column and 70% ACN/ H_2O as the mobile phase. The worked-up material was dissolved in 200 μL of the mobile phase and 40 μL HPLC

injections were performed. The peaks eluting at *ca* 230 s, 300 s, 800 s and 1000 s were collected separately and the solvent was removed to give 0.9 mg (**1.2.3**), 0.8 mg (**6.3.1**), 0.9 mg (**6.3.2**) and 1.1 mg (**6.3.3**) of material respectively. This material was combined with the respective acid products from the previous reactions. This gave a total of 2.0 mg of the furan acid product (**6.3.1**), 1.8 mg of the *epi*-furan acid product (**6.3.2**) and 2.0 mg of the *epi* acid product (**6.3.3**) for subsequent structural identification.

6.3 Characterisation of TFA Reaction Products

A D_2O exchange experiment was performed on the furan acid product (**6.3.1**). A ^1H NMR spectrum and a selective 1D-TOCSY spectrum (irradiating at δ_H 4.90 ppm with an 80 ms mixing time) were acquired on the furan acid product (**6.3.1**) in $CDCl_3$/ 0.1% pyridine-d_5 solution. A single drop of D_2O was added to the NMR tube and the resulting mixture was vigorously mixed (vortexed). The mixture was left standing at room temperature for 5 min. After this time, a ^1H NMR spectrum and a selective 1D-TOCSY spectrum were acquired under identical NMR experimental conditions. The mixture was left standing at room temperature for another 1.5 hrs and the two NMR experiments were again repeated under identical NMR experimental conditions.

Furan acid product (**6.3.1**):

A clear, colourless oil.

^1H and ^{13}C NMR data cited in **Tables 6.3.1** and **6.3.2** respectively.

High Resolution FAB-MS *m/z* 1123.58689 (MH^+, +2.43 ppm for $C_{61}H_{87}O_{19}$).

Epi-furan acid product (**6.3.2**):

A clear, colourless oil.

^1H and ^{13}C NMR data cited in **Tables 6.3.3** and **6.3.4** respectively.

High Resolution FAB-MS *m/z* 1145.56413 (MNa^+, -1.75 ppm for $C_{61}H_{86}O_{19}Na$).

Epi acid product (**6.3.3**):

A clear, colourless oil.

^1H and ^{13}C NMR data cited in **Tables 6.3.5** and **6.3.6** respectively.

High Resolution FAB-MS *m/z* 1123.58589 (MH^+, +1.54 ppm for $C_{61}H_{87}O_{19}$).

6.4 Time-Scale Acid Reactions

A mixture of the three acid products (**6.3.1**, **6.3.2** and **6.3.3**) and homohalichondrin B (**1.2.3**) was prepared with nominally equal amounts (*ca* 0.04 mg) of each compound. A ^1H NMR spectrum was obtained on this sample in $CDCl_3$/ 0.1% pyridine-d_5. Integrals over the two furan resonances at δ_H 5.95 ppm and δ_H 6.18 ppm, and the H7 resonance at δ_H 3.06 ppm (common to the *epi* acid product (**6.3.3**) and homohalichondrin B (**1.2.3**)) were obtained. The actual amount of furans in the standard mixture was calculated as 24% and the non-furan components therefore contributed 76% to the ^1H NMR spectrum. The standard mixture was dissolved in 40 μL of 70% ACN/ H_2O and 10 μL of this solution was analysed by HPLC

(analytical C18 column with 70% ACN/ H_2O as the mobile phase). The four component peaks in the chromatogram were integrated at λ 199 nm. The sum of the furan components (**6.3.1** and **6.3.2**) contributed 65% to the total integral and the non-furan components (**1.2.3** and **6.3.3**) contributed 35% to the total integral. The ratio of the molar absorptivities of the furan products *vs* the non-furan components was calculated. This ratio was calculated as 5.9: 1 for ε_{furans}: $\varepsilon_{non\text{-}furans}$.

The furan acid product (**6.3.1**, 0.5 mg) was dissolved in 85 μL DCM. An aliquot (*ca* 2 μL) of this solution was taken and the solvent removed. This aliquot was dissolved in 70% ACN/ H_2O (10 μL) and this sample was analysed by HPLC (using an analytical C18 column and 70% ACN/ H_2O as the mobile phase). A 14.8 μL volume of diluted standardised TFA in DCM solution (a 1+1 DCM dilution of standardised TFA in DCM (30.04 mM)) was added to **6.3.1** in DCM to give a 1:2 molar ratio of TFA: **6.3.1**. The reaction was stirred at room temperature and monitored by analytical HPLC, with time. Aliquots (*ca* 2 μL) were removed after 10 min, 30 min, 1 hr, 2.5 hrs, 3.5 hrs, 4.5 hrs, 7 hrs, 11 hrs, 18 hrs, 35.5 hrs, 49 hrs and 73.3 hrs of reaction. The solvent was removed from each aliquot, immediately after removal from the reaction mixture, and 10 μL of the HPLC mobile phase (70% ACN/ H_2O) was added to each. Each 10 μL aliquot was immediately analysed by analytical HPLC using the same conditions as the first analysis. The identified component peaks (*viz* **6.3.1** and **6.3.2**) in the chromatogram (at λ 199 nm) were integrated. Each product was expressed as a relative percentage of the total identified components present at that point in time. Graph of results displayed in **Figure 6.4.1**.

The *epi*-furan acid product (**6.3.2**, 0.5 mg) was dissolved in 85 μL DCM. An aliquot (*ca* 2 μL) of this solution was taken and the solvent removed. This aliquot was dissolved in 70% ACN/ H_2O (10 μL) and this sample was analysed by HPLC (using an analytical C18 column and 70% ACN/ H_2O as the mobile phase). A 14.8 μL

volume of diluted standardised TFA in DCM solution (a 1+1 dilution of standardised TFA in DCM (30.04 mM) with DCM) was added to **6.3.2** in DCM to give a 1:2 molar ratio of TFA: **6.3.2**. The reaction was stirred at room temperature and monitored by analytical HPLC, with time. Aliquots (*ca* 2 μL) were removed after 15 min, 1 hr, 2 hrs, 3 hrs, 4 hrs, 7 hrs, 22 hrs, 48 hrs of reaction. The solvent was removed from each aliquot, immediately after removal from the reaction mixture, and 10 μL of the HPLC mobile phase (70% ACN/ H_2O) was added to each. Each 10 μL aliquot was immediately analysed by analytical HPLC using the same conditions as the first analysis. The identified component peaks (*viz* **6.3.1** and **6.3.2**) in the chromatogram (at λ 199 nm) were integrated. Each product was expressed as a relative percentage of the total identified components present at that point in time. Graph of results displayed in **Figure 6.4.2**.

The *epi* acid product (**6.3.3**, 0.5 mg) was dissolved in 85 μL DCM. An aliquot (*ca* 2 μL) of this solution was taken and the solvent removed. This aliquot was dissolved in 70% ACN/ H_2O (10 μL) and this sample was analysed by HPLC (using an analytical C18 column and 70% ACN/ H_2O as the mobile phase). A 14.8 μL volume of diluted standardised TFA in DCM solution (a 1+1 dilution of standardised TFA in DCM (30.04 mM) with DCM) was added to **6.3.3** in DCM to give a 1:2 molar ratio of TFA: **6.3.3**. The reaction was stirred at room temperature and monitored by analytical HPLC, with time. Aliquots (*ca* 2 μL) were removed after 15 min, 45 min, 1.17 hrs, 3 hrs, 3.5 hrs, 4.5 hrs, 7 hrs, 20.5 hrs, 47 hrs of reaction. The solvent was removed from each aliquot, immediately after removal from the reaction mixture, and 10 μL of the HPLC mobile phase (70% ACN/ H_2O) was added to each. Each 10 μL aliquot was immediately analysed by analytical HPLC using the same conditions as the first analysis. The identified components in the chromatogram (*viz* **1.2.3**, **6.3.1**, **6.3.2** and **6.3.3**) were integrated at λ 199 nm. The integrals were corrected to

account for the differences in the molar absorptivities (ε) of the furans (**6.3.1** and **6.3.2**) and the non-furan components (**1.2.3** and **6.3.3**). Each integrated component was expressed as relative percentage of the total of the integrated components. Results displayed in **Figure 6.4.3**.

Homohalichondrin B (**1.2.3**, 0.5 mg) was dissolved in 85 μL DCM. An aliquot (*ca* 2 μL) of this solution was taken and the solvent removed. This aliquot was dissolved in 70% ACN/ H_2O (10 μL) and this sample was analysed by HPLC (using an analytical C18 column and 70% ACN/ H_2O as the mobile phase). A 14.8 μL volume of diluted standardised TFA in DCM solution (a 1+1 dilution of standardised TFA in DCM (30.04 mM) with DCM) was added to **1.2.3** in DCM to give a 1:2 molar ratio of TFA: **1.2.3**. The reaction was stirred at room temperature and monitored by analytical HPLC, with time. Aliquots (*ca* 2 μL) were removed after 15 min, 1 hr, 1.5 hrs, 2.5 hrs, 3 hrs, 4 hrs, 5 hrs, 7 hrs, 8 hrs, 10 hrs, 18 hrs, 32 hrs and 44 hrs of reaction. The solvent was removed from each aliquot, immediately after removal from the reaction mixture, and 10 μL of the HPLC mobile phase (70% ACN/ H_2O) was added to each. Each 10 μL aliquot was immediately analysed by analytical HPLC using the same conditions as the first analysis. The identified components in the chromatogram (*viz* **1.2.3**, **6.3.1**, **6.3.2** and **6.3.3**) were integrated at λ 199 nm. The integrals were corrected to account for the differences in the molar absorptivities (ε) of the furans (**6.3.1** and **6.3.2**) and the non-furan components (**1.2.3** and **6.3.3**). Each integrated component was expressed as relative percentage of the total of the integrated components. Results displayed in **Figure 6.4.4**.

Homohalichondrin B (**1.2.3**, 0.5 mg) was dissolved in 48 μL DCM. A volume (2 μL) of camphor sulfonic acid (CSA, 30 mM) in DCM was added to the resulting solution to give a 10:1 molar ratio of **1.2.3**: CSA. An aliquot of this solution (*ca* 2

μL) was taken an the solvent was removed. This aliquot was dissolved in 70% ACN/ H_2O (10 μL) and this sample was analysed by HPLC (using an analytical C18 column and 70% ACN/ H_2O as the mobile phase). The reaction was stirred at room temperature and monitored by analytical HPLC, with time. Aliquots (*ca* 2 μL) were removed from the resulting solution after 30 min, 1 hr and 2.17 hrs. The solvent was removed from each aliquot, immediately after removal from the reaction mixture, and 10 μL of the HPLC mobile phase (70% ACN/ H_2O) was added to each. Each 10 μL aliquot was immediately analysed by analytical HPLC using the same conditions as the first analysis. After 2.17 hrs, an additional 3 μL of CSA in DCM solution (30 mM) was added to the reaction mixture to give a 3:1 molar ratio of **1.2.3**: CSA. The reaction was continued stirring at room temperature Aliquots (*ca* 2 μL) were removed from the resulting solution after 0.5 hr, 1 hr, 1.67 hrs, 3 hrs and 22 hrs at a molar ratio of 3:1. The solvent was removed from each aliquot, immediately after removal from the reaction mixture, and 10 μL of the HPLC mobile phase (70% ACN/ H_2O) was added to each. Each 10 μL aliquot was immediately analysed by analytical HPLC using the same conditions as the first analysis. The identified components in the chromatogram (*viz* **1.2.3**, **6.3.1**, **6.3.2** and **6.3.3**) were integrated at λ 199 nm. The integrals were corrected to account for the differences in the molar absorptivities (ε) of the furans (**6.3.1** and **6.3.2**) and the non-furan components (**1.2.3** and **6.3.3**). Each integrated component was expressed as relative percentage of the total of the integrated components. Results displayed in **Figure 6.4.5**.

Work Described in Chapter Seven

7.2 Base Stability Studies

A 0.1 M solution of sodium hydroxide (NaOH) in 10% MeOH/ H_2O (1 mL) was added to isohomohalichondrin B (**1.2.9**, 1.0 mg). Additional MeOH (600 μL) was added and the resulting solution was stirred overnight at room temperature. The reaction was quenched with 1 mL acidified water ($(NH_4Cl)_{aq}$, pH 3) and placed on a cartridge C18 column. The cartridge was eluted with the acidified water (1 × 3 mL), then 10% MeOH/ H_2O (1 × 3 mL). The halichondrin material was eluted in 100% MeOH (2 × 3 mL) and the solvent was removed from the MeOH fractions to give 1.4 mg isohomohalichondrin B (**1.2.9**).

7.3 Chelation Studies

Isohomohalichondrin B (**1.2.9**, 3.5 mg) was dissolved in 600 μL CD_3OD and two drops of D_2O, and the resulting solution was transferred to an NMR tube. A ^1H NMR spectrum was performed on this sample. An aqueous 0.16 M sodium perchlorate ($NaClO_4$) solution was added to the NMR tube (20 μL) to give a 1:1 molar ratio of isohomohalichondrin B to $NaClO_4$. The solution was mixed in the NMR tube and a ^1H NMR spectrum was acquired. Another 1 mole equivalent of the 0.16 M $NaClO_4$ solution was added (20 μL), mixed, and a ^1H NMR spectrum was acquired. Successive 20 μL additions of 0.16 M $NaClO_4$ solution were added to the NMR tube give a 3:1, 4:1 and 5:1 molar ratio of $NaClO_4$ to isohomohalichondrin B (**1.2.9**). After each addition of $NaClO_4$ the NMR tube was mixed carefully and a ^1H

NMR spectrum was acquired. Finally 100 μL of 0.16 M $NaClO_4$ was added to the NMR tube to give a 10:1 molar ratio of $NaClO_4$ to isohomohalichondrin B (**1.2.9**). The solution was mixed and a ^1H NMR spectrum was acquired from the resulting solution.

Work Described in Chapter Eight

8.2 Deuterium Exchange

A 2 M solution of NaOD was prepared by dropping Na wire (24 mg) into 520 μL D_2O. Isohomohalichondrin B (**1.2.9**, 0.4 mg) was dissolved in *ca* 600 μL CD_3OD and transferred to an NMR tube. Three drops of the NaOD solution was added to the NMR tube and mixed thoroughly. A ^1H NMR spectrum was acquired from this solution. The solvent was removed and a ^1H NMR spectrum was re-acquired in $CDCl_3$/ 0.1% pyridine-d_5.

Deuterated isohomohalichondrin B:

A pale yellow oil.

^1H NMR data (selected) described in Section 8.2.

FAB-MS *m/z* 1124, 1125, 1126, 1127 and 1128 (MH^+).

High Resolution FAB-MS *m/z* 1126.60358 (MH^+, +0.53 ppm for $C_{61}H_{84}D_3O_{19}$).

8.3 Sodium Borodeuteride Reduction

Isohomohalichondrin B (**1.2.9**, 0.5 mg) was dissolved in dry IPA (50 μL) and 1.0 mg sodium borodeuteride ($NaBD_4$ (98 atom % D)) in 150 μL dry ether was added. The resulting suspension was stirred vigorously at room temperature for 1 hr. Silica TLCs were developed in 10% MeOH/ DCM and visualised. After this time, 1 mL $NH_4Cl_{(aq)}$ (pH 3) solution was added to the reaction mixture and the resulting

solution was placed onto a 500 mg C18 cartridge. The column was washed with 10% MeOH/ H_2O (2 × 5 mL) and the halichondrin material was eluted with 100% MeOH (2 × 5 mL). The solvent was removed from the MeOH fractions to give 0.6 mg of **8.3.1** and **8.3.2.**

Isohomohalichondrin B sodium borodeuteride reduction isomers (**8.3.1** and **8.3.2**):

A white powder.

^1H NMR data (selected) described in Section 8.3.

High Resolution FAB-MS *m/z* 1126.60722 (MH^+, +1.01 ppm for $C_{61}H_{88}DO_{19}$).

8.4 Wittig Reaction

All Wittig reactions described in this Section were performed in a dry-box under an atmosphere of dry nitrogen.

Cholestane-3-one (2.0 mg) was dissolved in dry ether (50 μL) and added to a suspension containing the ylide (CH_2=PPh_3). The ylide was generated by addition of 1.6 M *n*-butyllithium solution (*n*-BuLi in hexane, 15 μL) to a stirred suspension of methyl triphenylphosphonium iodide ($MePh_3P^+I^-$, 7.4 mg) in 50 μL dry ether. The ylide suspension was stirred vigorously for *ca* 30 s before addition of cholestan-3-one in solution. The reaction was stirred overnight at room temperature. After this time, the ether was removed from the reaction mixture and the remaining material

was placed on a filter and washed with hexane. The solvent was removed to give 1.6 mg of 3-methylene cholestane.

Homohalichondrin B (**1.2.3**, 0.2 mg) was dissolved in water (170 μL) and 30 μL of an aqueous 1.6 M lithium hydroxide solution was added. The resulting solution was stirred overnight at room temperature. After this time, 1 mL acidified water ($(NH_4Cl)_{aq}$, pH 3) was added and the solution was extracted with DCM (4 × 2 mL). The solvent (DCM) was removed to give unreacted homohalichondrin B (**1.2.3**, 0.2 mg). Silica TLC was developed in 10% MeOH/ DCM and visualised.

Dry ether (100 μL) was added to homohalichondrin B diacetate diketone (**4.3.3**, 1.9 mg). The ylide was generated by the addition of *n*-BuLi in hexane (1.6 M, 8 μL) to $MePh_3P^+I^-$ (7.4 mg) in 100 μL dry ether while vigorously stirring. The **4.3.3** solution was added to the ylide, while stirring, and the resulting suspension was stirred overnight at room temperature. After this time, the ether was removed and the remaining material was placed on a filter and was washed with hexane. The hexane was removed to give 0.5 mg of material. The filter was washed with 20% DCM/ hexane and the solvent was removed from this extract to give 0.6 mg of material. Silica TLCs performed on both extracts were developed in 10% MeOH/ DCM prior to visualisation. The two extracts were recombined and re-reacted as described previously. The reaction was similarly worked-up except the hexane and 20% DCM/ hexane extracts were combined. The solvent was removed to give *ca* 0.5 mg of material.

8.5 Fluorescent Labelling

To a solution of *n*-hexanol (*ca* 2 mg) in pyridine (100 μL) at 0°C, a solution of dansyl chloride (5.8 mg, 1 mole equivalent) dissolved in 100 μL pyridine was added. The solution was stirred at room temperature for 4.5 hrs. After this time, 1 mL H_2O was added to the reaction mixture and the solution was extracted with DCM (4 × 1 mL). The solvent was removed to give pure dansyl *n*-hexanol.

To a solution of *n*-hexanol (2.2 mg) in EtOAc (100 μL), 11.8 mg (2 mole equivalents) dansyl chloride, and 13.6 mg Na_2CO_3 (6 mole equivalents) in EtOAc (100 μL) were added. The reaction was stirred overnight at 35°C. After this time, the solvent was removed and 100 μL H_2O was added and the resulting solution was extracted with DCM (4 × 1 mL). The solvent was removed from the DCM extract to give 70% dansyl *n*-hexanol. The worked-up material was re-reacted under identical reaction conditions to give 100% dansyl *n*-hexanol.

To a solution of *n*-hexanol (1.9 mg) in acetone (100 μL), 5.8 mg (1 mole equivalent) of dansyl chloride and 7.3 mg (3 mole equivalents) sodium carbonate (Na_2CO_3) and 100 μL H_2O were added. The reaction was stirred overnight at room temperature. After this time, the reaction mixture was extracted with DCM (4 × 1 mL) and the solvent was removed to give 78% dansyl *n*-hexanol.

Homohalichondrin B (**1.2.3**, 0.5 mg) was dissolved in 30 μL pyridine, and 20 μL (1 mole equivalent) of a solution of dansyl chloride (1.3 mg) in 200 μL pyridine was added at 0°C. The solution was stirred at room temperature for 4 hrs. Silica TLC

was developed in 5% MeOH/ DCM and visualised under a visible lamp before application of PMA spray. Water (50 μL) was added to the reaction mixture and the solution was extracted with DCM (4 × 0.5 mL) and then the solution was extracted with MeOH (4 × 1 mL) The solvent (DCM) was removed to give 0.5 mg of unreacted homohalichondrin B (**1.2.3**). The solvent was removed from the MeOH extract and this material was extracted with DCM (4 × 0.5 mL) and combined with the first DCM extract to give 0.6 mg of **1.2.3**.

Homohalichondrin B (**1.2.3**, 0.6 mg) was dissolved in 30 μL pyridine, and 20 μL (1 mole equivalent) of a solution of dansyl chloride (1.3 mg) in 200 μL pyridine was added at 0°C. The reaction was stirred at room temperature for 10 min and another 4 mole equivalents of dansyl chloride in pyridine were added to the reaction mixture. The resulting solution was stirred for 4 hrs at room temperature. Water (50 μL) was added to the reaction mixture and the solution was extracted with DCM (4 × 1 mL) and MeOH (4 × 1 mL). The solvent was removed from the DCM extract to give 1.0 mg unreacted homohalichondrin B (**1.2.3**).

Homohalichondrin B (**1.2.3**, 1.0 mg) was dissolved in 30 μL pyridine and 56.5 μL (15 mole equivalents) of a 58 mg/ mL dansyl chloride solution in pyridine, at 0°C, were added. The reaction was stirred at room temperature for 4 hrs. After this time water (50 μL) was added to the reaction mixture and the solution was extracted with DCM (4 × 1 mL) and MeOH (4 × 1 mL). The solvent was removed from the DCM extract to give 1.0 mg of unreacted homohalichondrin B (**1.2.3**). The silica TLC performed was developed in 10% MeOH/ DCM, visualised under a visible lamp before application of PMA spray.

Homohalichondrin B (**1.2.3**, 1.0 mg) was dissolved in 50 μL pyridine and a solution of dansyl chloride (2.6 mg, 10 mole equivalents) in pyridine (50 μL) was added at room temperature. The reaction was stirred at 35°C for 4 hrs. The silica TLCs performed were developed in 10% MeOH/ DCM, visualised under a visible lamp before application of PMA spray. Water (100 μL) was added to the reaction mixture and the solution was extracted with DCM (4 × 1 mL), then with MeOH (4 × 1 mL). The solvent was removed from the DCM extract to give 0.8 mg of product which was a mixture of 49% dansyl homohalichondrin B (**8.5.2**) and 51% homohalichondrin B (**1.2.3**).

The product was dissolved in 50 μL pyridine and a solution of dansyl chloride (2.6 mg, 13 mole equivalents) in pyridine (50 μL) was added at room temperature. The reaction was stirred at 35°C for 17 hrs. The silica TLC performed was developed in 10% MeOH/ DCM, visualised under a visible lamp before the application of PMA spray. Water (100 μL) was added to the reaction mixture and the solution was extracted with DCM (4 × 1 mL), then with MeOH (4 × 1 mL). The solvent was removed from the DCM extract to give 1.1 mg of product which was a mixture of 56% dansyl homohalichondrin B (**8.5.2**) and 44% homohalichondrin B (**1.2.3**).

HPLC was performed using an analytical C18 column with 50% ACN/ H_2O as the mobile phase. Analytical injections of 10 μL of 2 mg/ mL solutions were made, the samples were dissolved in the mobile phase.

A diol cartridge was equilibrated to 100% ACN. The mixture of **1.2.3** and **8.5.2** (1.1 mg) was dissolved in ACN and was placed onto the column bed. Three ACN fractions of 1 mL were collected. Three 1mL fractions of 0.5% IPA/ ACN were

collected followed by three 1 mL fractions eluting with 1% IPA/ ACN. Silica TLCs performed were developed in 10% MeOH/ DCM, visualised under a visible lamp before application of PMA spray.

The first three fractions were combined and placed onto a diol cartridge equilibrated to 100% DCM. Five 1 mL DCM fractions were collected before eluting with 10% ACN/ DCM (2 × 1 mL fractions). The column was eluted with 20% ACN/ DCM (2 × 2 mL fractions) and stripped with 100% ACN (2 × 2 mL fractions). The movement of the fluorescent material through the column was observed by shining a visible lamp on the column. The silica TLCs performed were developed in 10% MeOH/ DCM, visualised under a visible lamp before application of PMA spray. The solvent was removed from fraction one to give 0.1 mg of dansyl homohalichondrin (**8.5.2**). The solvent was removed from fraction two (containing a mixture of dansyl homohalichondrin B (**8.5.2**) and homohalichondrin B (**1.2.3**)) to give 0.4 mg of material. Fractions three through to eight were combined to give *ca* 0.1 mg homohalichondrin B (**1.2.3**).

Homohalichondrin B (**1.2.3**, 0.4 mg) was dissolved in 100 μL DCM, and 0.5 mg dansyl chloride (5 mole equivalents) and 5 μL pyridine (15 mole equivalents) were added to the solution. The solution was stirred overnight at room temperature. The silica TLCs performed were developed in 10% MeOH/ DCM, visualised under a visible lamp before application of PMA spray. After this time, 0.5 mg dansyl chloride (to give a total of 10 mole equivalents) in 50 μL DCM and 5 μL pyridine were added to the reaction mixture. The resulting solution was stirred at 35°C for 10 hrs before another 0.5 mg dansyl chloride (to give a total of 15 mole equivalents) in 50 μL DCM, and 5 μL pyridine were added to the reaction mixture. The resulting solution was stirred overnight at 35°C. The reaction was worked-up after this time.

Water (100 μL) was added to the reaction mixture and the solution was extracted with DCM (4 × 1 mL), then with MeOH (4 × 1 mL). The solvent was removed from the DCM extract to give 0.9 mg of worked-up material. This material was combined with fraction two from the previous diol column separation and the combined material was subjected to diol chromatography.

A diol cartridge was equilibrated to 10% hexane/ DCM and the combined material (1.3 mg) was dissolved in the mobile phase and placed onto the column. Fifteen 0.25 mL fractions were collected before eluting with 100% DCM (2 × 3 mL fractions). The column was stripped with 100% MeOH (2 × 3 mL fractions). The silica TLCs performed on the column fractions were developed in 10% MeOH/ DCM, visualised under a visible lamp before application of PMA spray. Fractions eleven through to twelve were combined to give 0.4 mg homohalichondrin B (**1.2.3**). Fractions three through to nine were combined to give 0.4 mg of dansyl homohalichondrin B (**8.5.2**).

Dansyl homohalichondrin B (**8.5.2**):

A yellow oil.

^{1}H and ^{13}C NMR data cited in **Tables 8.5.1** and **8.5.2** respectively.

The following reaction was performed in a dry-box under an atmosphere of dry nitrogen. Homohalichondrin B (**1.2.3**, 0.4 mg) was dissolved in dry DCM (100 μL) and 1.5 mg dansyl chloride (15 mole equivalents) in 100 μL DCM, and 5 μL dry pyridine were added. The resulting solution was stirred at 35°C for 6.5 hrs. The

silica TLCs performed were developed in 10% MeOH/ DCM, visualised under a visible lamp before the application of PMA spray. Additional pyridine was added (20 μL) and the reaction was stirred at 35°C overnight. After this time, water (100 μL) was added to the reaction mixture and the solution was extracted with DCM (4 × 1 mL), then with MeOH (4 × 1 mL). The solvent was removed from the DCM extract to give 0.6 mg of product which was a mixture of 65% dansyl homohalichondrin B (**8.5.2**) and 35% homohalichondrin B (**1.2.3**). This material was used in the next reaction.

Dansyl chloride (1.8 mg, 15 mole equivalents) and Na_2CO_3 (2.0 mg) were added to the product (0.6 mg) from the previous reaction. Acetone (25 μL) and water (25 μL) were added and the reaction was stirred at 35°C for 24 hrs. After this time, the solvent was removed and 100 μL H_2O was added and the resulting solution was extracted with DCM (4 × 1 mL). The solvent (DCM) was removed to give 0.6 mg of product.

The following reaction was performed in a dry-box under an atmosphere of dry nitrogen. Isohomohalichondrin B (**1.2.9**, 0.5 mg) was dissolved in 50 μL dry DCM. To this solution 1.5 mg dansyl chloride (15 mole equivalents) and dry pyridine (20 μL) were added. The reaction was stirred at 35°C for 24 hrs. The silica TLCs performed were developed in 10% MeOH/ DCM, visualised under the visible lamp before application of PMA spray. Additional dry pyridine (20 μL) was added to the reaction mixture. The solution was stirred for another 6 hrs at 35°C. After this time, water (100 μL) was added to the reaction mixture and the solution was extracted with DCM (4 × 1 mL), then with MeOH (4 × 1 mL). The solvent was removed from the DCM extract to give 0.8 mg of product which was a mixture of 59% dansyl

isohomohalichondrin B (**8.5.3**) and 31% isohomohalichondrin B (**1.2.9**). This material was used in the next reaction.

The product from the previous reaction (0.8 mg) was dissolved in dry pyridine and 11.5 mg of dansyl chloride (90 mole equivalents) in 150 μL dry pyridine were added. The reaction was performed in a dry-box under a dry-nitrogen atmosphere. The reaction was stirred for 30 hrs at 35°C. The silica TLC performed was developed in 10% MeOH/ DCM, visualised under a visible lamp before application of PMA spray. Water (200 μL) was added to the reaction mixture after this time and the solution was extracted with DCM (4 × 1 mL), then with MeOH (4 × 1 mL). The solvent was removed from the DCM extract to give the product which was a mixture of several components.

The following reaction was performed in a dry-box under a dry nitrogen atmosphere. Halichondrin B (**1.2.1**, 0.5 mg) was dissolved in 100 μL DCM. To this solution, 37 μL of a 3.5 mg/mL dansyl chloride in DCM solution (1 mole equivalent), and 5 μL dry pyridine were added. The resulting solution was stirred at room temperature for 20 min then an additional 148 μL (4 mole equivalents) dansyl chloride in DCM solution (3.5 mg/mL) was added. The reaction was stirred at 35°C for 3 hrs. After this time 0.5 mg dansyl chloride in 50 μL DCM (to give 10 mole equivalents total) was added and the reaction was stirred at 35°C for another 2.5 hrs. After this time a further 0.5 mg dansyl chloride and 5 μL pyridine were added to the reaction mixture, and the reaction was stirred at 35°C overnight. Water (100 μL) was added to the reaction mixture and the solution was extracted with DCM (4 × 1 mL), then with MeOH (4 × 1 mL). The solvent was removed from the DCM extract to give 0.6 mg of product.

ACKNOWLEDGMENTS

Sincere thanks are due to my supervisors, Dr. John W. Blunt and Dr. Murray H.G. Munro for the time and enthusiasm they have directed towards this research over the last three years.

I would like to express my gratitude to the technical staff in the Department of Chemistry, without whose expertise this project could not have been undertaken. Special thanks must go to Gill Barns for performing the P388 assays and to Bruce Clark for mass spectrometric analysis. I would also like to thank Lewis Pannell (NIDDK, NIH, USA) for additional mass spectroscopic analysis, Dr. M.R. Boyd (NCI, NIH, USA) for obtaining biological assays, Ron Thow and NIWA (Wellington) for sponge collection and Dr. Marc Litaudon for the halichondrin extraction.

Thanks must also go to PharmaMar (Spain), the NCI and FRST for their financial contributions towards this project, and to the New Zealand Lottery Grants Board for funds for equipment purchase. On a personal level, I would like to thank the New Zealand Vice Chancellors' Committee, the New Zealand Federation of University Women, and FRST for keeping me fed, clothed and housed.

I would like to express my gratitude to my fellow lab. mates for their support and continual amusement over the years; especially Gillian Nicholas, David Stirling, Kevin Mitchell, Rachel Lill, Shane Blincoe, Sarah Hickford and Michael Stewart. I would also like to thank my parents and family for their encouragement. Last, but not least, I would like to thank my husband Geoff. Thomas for his supporting role.

REFERENCES

1 Williams, D.H.; Stone, M.J.; Hauck, P.R. and Rahman, S.K. *J. Nat. Prod*, **1989**, *52(6)*, 1189.

2 Dr. Hank Cutler, Natural Products Workshop, Hort. Research, Lincoln, New Zealand, 9th February 1994.

3 Albert, A. *Selective Toxicity*, 7th ed.; Chapman and Hall Ltd.: London, 1985; p236.

4 Guyton, A.C. *Textbook of Medical Physiology*, 8th ed.; W.B. Saunders Company: Philadelphia, 1991; pp34-35.

5 der Marderosian, A.J. *J. Pharm. Sci.*, **1969**, *58*, 1.

6 Dr. Peter Murphy, Australian Institute of Marine Sciences, pers. comm. with Dr. Murray Munro.

7 Bergquist, P.R. *Sponges*, 1st ed.; Hutchinson & Co. Ltd.: London, 1978; p9.

8 Curtis, H. and Barnes, N.S. *Biology*, 5th ed.; Worth Publishers, Inc.: New York, 1989; pp522-523.

9 Boyd, M.R. *Principles and Practice of Oncology*, **1989**, *3(10)*, 1.

10 Marston, A; Décosterd, L.A. and Hostettmann, K. In: *Bioactive Natural Products: Detection, Isolation and Structural Determination*, Colegate, S.M. and Molyneux, R.J. (ed.s), 1st ed.; CRC Press Ltd.: Boca Raton, 1993; p222.

11 Perry, N.B.; Blunt, J.W.; Munro, M.H.G. and Pannell, L.K. *J. Am. Chem. Soc.*, **1988**, *110*, 4850.

12 Perry, N.B.; Blunt, J.W.; Munro, M.H.G. and Thompson, A.M. *J. Org. Chem.*, **1990**, *55*, 223.

13 Perry, N.B.; Blunt, J.W.; McCombs, J.D. and Munro, M.H.G. *J. Org. Chem.*, **1986**, *51*, 5476.

14 Litaudon, M.; Hart, J.B.; Blunt, J.W. and Munro, M.H.G. *Tet. Lett.*, **1994**, *35*, 9435.

15 Boyd, M.R. In: *Current Therapy in Oncology*, J.E. Neiderhuber (ed.), B.C. Decker: Philidelphia, 1992; p11.

16 Cordell, G.A.; Kinghorn, A.D. and Pezzuto, J.M. In: *Bioactive Natural Products: Detection, Isolation and Structural Determination*, Colegate, S.M. and Molyneux, R.J. (ed.s), 1st ed.; CRC Press Ltd.: Boca Raton, 1993; p200.

17 Uemura, D.; Takahashi, K.; Yamamoto, T.; Katayama, C.; Tanaka, J.; Okumura, Y. and Hirata, Y. *J. Am. Chem. Soc.*, **1985**, *107*, 4796.

18 Hirata, Y. and Uemura, D. *Pure & Appl. Chem.*, **1986**, *58(5)*, 701.

19 Pettit, G.R.; Tan, R.; Gao, F.; Williams, M.D.; Doubek, D.L.; Boyd, M.R.; Schmidt, J.M.; Chapius, J-C; Hamel, E.; Bai, R.; Hooper, J.N.A. and Tackett, L.O. *J. Org. Chem.*, **1993**, *58*, 2538.

20 Pettit, G.R.; Gao, F.; Doubek, D.L.; Boyd, M.R.; Hamel, E.; Bai, R.; Schmidt, J.M.; Tackett, L.P. and Rützler, K. *Gazetta Chimica Italiana*, **1993**, *123*, 371.

21 Bergquist, P.R. *Sponges*, 1st ed.; Hutchinson & Co. Ltd.: London, 1978; p14.

22 Lake, R.J., Internal Report, dated 26/2/88.

23 Litaudon, M., Internal Report, dated 25/2/93.

24 Bai, R.; Paull, K.D.; Herald, C.L.; Malspeis, L.; Pettit, G.R. and Hamel, E. *J. Biol. Chem.*, **1991**, *266(24)*, 15882.

25 Albert, A. *Selective Toxicity*, 7th ed.; Chapman and Hall Ltd.: London, 1985; p201.

26 Munro, M.H.G.; Blunt, J.W.; Lake, R.J.; Litaudon, M.; Battershill, C.N. and Page, M.J. In: *Sponges in Time and Space*, van Soest, R.W.M.; van Kempen, T.M.G. and Braekman, J.C. (ed.s), Balkema, A.A.: Rotterdam, 1994; p473.

27 Garson, M.J. In: *Sponges in Time and Space*, van Soest, R.W.M.; van Kempen, T.M.G. and Braekman, J.C. (ed.s), Balkema, A.A.: Rotterdam, 1994; p427.

28 Garson, M.J. *Unpublished Results*.

29 Aicher, T.D.; Buszek, K.R.; Fang, F.G.; Forsyth, C.J.; Jung, S.H.; Kishi, Y.; Scola, P.M.; Spero, D.M. and Yoon, S.K. *J. Am. Chem. Soc.*, **1992**, *114*, 3162.

30 Albert, A. *Selective Toxicity*, 7th ed.; Chapman and Hall Ltd.: London, 1985; p109.

31 Cooper, A.J.; Pan, W. and Salomon, R.G. *Tet. Lett.*, **1993**, *34(51)*, 8193.

32 Geen, H. and Freeman, R.J. *J. Magn. Res.*, **1991**, *93*, 93.

33 Karplus, M., *J. Chem. Phys.*, **1959**, *30*, 11.

34 Haasnoot, C.A.G.; de Leeuw, F.A.A.M. and Altona, C. *Tetrahedron*, **1980**, *36*, 2783.

35 Marshall, J.L.; Walter, S.R.; Barfield, M.; Marchand, A.P.; Marchand, N.W. and Segre, A.L. *Tetrahedron*, **1976**, *32*, 537.

36 MacroModel V3.5X User Manual, Department of Chemistry, Columbia University, 1992; p35.

37 Mohamadi, F.; Richards, N.G.J.; Guida, W.C.; Liskamp, R.; Lipton, M.; Caufield, C.; Chang, G.; Hendrickson, T. and Still, W. C. *J. Comput. Chem.*, **1990**, *11(4)*, 440.

38 Still, W.C.; Tempezyk, A.; Hawley, R.C.; and Hendrickson, T. *J. Am. Chem. Soc.*, **1990**, *112*, 6127.

39 Chang, G.; Guida, W.C. and Still, W.C. *J. Am. Chem. Soc.*, **1989**, *111*, 4379.

40 Saunders, M.; Houk, K,N.; Wu, Y-D.; Still, W.C., Lipton, M.; Chang, G. and Guida, W.C. *J. Am. Chem. Soc.*, **1990**, *112*, 1419.

41 Polak, E. and Ribiere, G. *Revue Francaise Inf. Rech. Oper.*, **1969**, *16*, 35.

42 MacroModel V3.5X User Manual, Department of Chemistry, Columbia University, 1992; p47.

43 Marion, D. and Wüthrich, K. *Biochem. Biophys. Res. Comm.*, **1983**, *117*, 479.

44 Dr. Quentin McDonald, Columbia University, U.S.A., pers. comm.

45 Greene, T.W. and Wuts, P.M. *Protective Groups in Organic Synthesis*, 2nd ed.; Wiley: New York, 1991; p88.

46 Pretsch, E.; Seibl, J.; Simon, W. and Clerc, T. *Tables of Spectral Data for Structure Determination of Organic Compounds*, 2nd ed.; Springer-Verlag: Berlin, 1983; pH5.

47 Stork, G.; Takahashi, T.; Kawamoto, I. and Suzuki, T. *J. Am. Chem. Soc.*, **1978**, *100*, 8272.

48 Corey, E.J. and Sugges, J.W. *Tet. Lett.*, **1975**, *31*, 2647.

49 Pryde, E.H.; Anders, D.E.; Teeter, H.M. and Cowan, J.C. *J. Org. Chem.*, **1960**, *25*, 618.

50 Cornforth, J.W.; Hunter, G.D. and Popják, G. *Biochem. J.*, **1953**, *54*, 590.

51 Beroza, M. and Bierl, B.A. *Anal. Chem.*, **1966**, *38(13)*, 1977.

52 Schröder, M. *Chem. Rev.*, **1980**, *80*, 187.

53 Criegee, R., *Ann.*, **1936**, *522*, 75.

54 Weisner, K.; Chan, K.K. and Demerson, C. *Tet. Lett.*, **1965**, 2893.

55 Cross, B.E. *J. Chem. Soc.*, (C), **1966**, 501.

56 Baran, J.S. *J. Org. Chem.*, **1960**, *25*, 257.

57 Criegee, R.; Marchand, B. and Wannowius, H. *Ann.*, **1942**, *550*, 99.

58 Pretsch, E.; Seibl, J.; Simon, W. and Clerc, T. *Tables of Spectral Data for Structure Determination of Organic Compounds*, 2nd ed.; Springer-Verlag: Berlin, 1983; pH120.

59 Fieser, L.F. and Fieser, M. *Reagents for Organic Synthesis*, 1st ed.; John Wiley and Sons, Inc.: New York, 1967; p759.

60 Augustine, R.L. *Oxidation. Techniques and Applications in Organic Synthesis*, 1st ed.; Marcel Dekker, Inc.: New York, 1969; p202.

61 Augustine, R.L. *Oxidation. Techniques and Applications in Organic Synthesis*, 1st ed.; Marcel Dekker, Inc.: New York, 1969; p203.

62 Greene, T.W. and Wuts, G.M. *Protective Groups in Organic Synthesis*, 2nd ed.; Wiley: New York, 1991; pp417-420.

63 Augustine, R.L. *Catalytic Hydrogenation*, 1st ed.; Marcel Dekker Inc.: New York, 1965; p36.

64 Augustine, R.L. *Catalytic Hydrogenation*, 1st ed.; Marcel Dekker Inc.: New York, 1965; p34.

65 Litaudon, M., Internal Report, dated 11/1/93.

66 Pretsch, E.; Seibl, J.; Simon, W. and Clerc, T. *Tables of Spectral Data for Structure Determination of Organic Compounds*, 2nd ed.; Springer-Verlag: Berlin, 1983, pI170.

67 Aicher, T.D.; Buszek, K.R.; Fang, F.G.; Forsyth, C.J.; Jung, S.H.; Kishi, Y. and Scola, P.M.; Spero, D.M. and Yoon, S.K. *J. Am. Chem. Soc.*, **1992**, *114*, 3162.

68 Pretsch, E.; Seibl, J.; Simon, W. and Clerc, T. *Tables of Spectral Data for Structure Determination of Organic Compounds*, 2nd ed.; Springer-Verlag: Berlin, 1983;pH265.

69 Pretsch, E.; Seibl, J.; Simon, W. and Clerc, T. *Tables of Spectral Data for Structure Determination of Organic Compounds*, 2nd ed.; Springer-Verlag: Berlin, 1983; pH65.

70 Pretsch, E.; Seibl, J.; Simon, W. and Clerc, T. *Tables of Spectral Data for Structure Determination of Organic Compounds*, 2nd ed.; Springer-Verlag: Berlin, 1983; pU135.

71 Pretsch, E.; Seibl, J.; Simon, W. and Clerc, T. *Tables of Spectral Data for Structure Determination of Organic Compounds*, 2nd ed.; Springer-Verlag: Berlin, 1983; pC135.

72 Pedersen, C.J. and Frensdorff, H.K. *Agnew. Chem.*, **1972**, *11*, 16.

73 Pedersen, C.J. *J. Am. Chem. Soc.*, **1967**, *89*, 2495.

74 Prestegard, J.H. and Chan, S.I. *J. Am. Chem. Soc.*, **1970**, *92*, 4440.

75 James, D.M.; Wintner, E.; Faulkner, D.J. and Siegel, J.S. *Heterocycles*, **1993**, *35 (2)*, 675.

76 Samuel, S.P.; Niu, T and Erikson, K.L. *J. Am. Chem. Soc.*, **1989**, *111*, 1429.

77 Büchi, G.; Hofheinz, W. and Paukstelis *J. Am. Chem. Soc.*, **1969**, *91*, 6473.

78 Schulman, S.G. In: *Molecular Luminescence Spectroscopy,* Elving, P.J.; Winefordner, J.P. and Kolthoff, I.M. (ed.s), 1st ed.; John Wiley & Sons, Inc.: New York, 1985; p653.

79 Wintersteiger, R. *J. Liquid Chromatography*, **1982**, *5 (5)*, 897.

80 Goto, J.; Komatsu, S.; Goto, N. and Nambara, T. *Chem. Pharm. Bull.*, **1981**, *29(3)*, 899.

81 Wintersteiger, R. and Wenninger-Weinzierl, G. *Fresenius Z. Anal. Chem.*, **1981**, *309*, 201.

82 Seiler, N. and Demisch, L. In: *Handbook of Derivatives for Chromatography,* Blau, K. and King, G.S. (ed.s), 1st ed.; Heyden & Son, Ltd.: London, 1978; p350.

83 Seiler, N. and Demisch, L. In: *Handbook of Derivatives for Chromatography,* Blau, K. and King, G.S. (ed.s), 1st ed.; Heyden & Son, Ltd.: London, 1978; p355.

84 Albert, A. *Selective Toxicity*, 7th ed.; Chapman and Hall Ltd.: London, 1985; p66-71.

85 Boyd, M.R. and Paull, K.D. *Drug Development Research*, **1995**, *34*, 91.

86 Pers. comm. with Dr. Murray Munro.

APPENDICES

APPENDIX I

Antimicrobial and Antiviral Assays

The antimicrobial assay currently screens against six bacterial and fungal organisms of interest: *Escherichia coli*, *Bacillus subtilis*, *Pseudomonas aeruginosa*, *Candida albicans*, *Trichophyton mentagrophytes* and *Cladosporium resinae*. The bacteria or fungi are grown over agar in a petri dish and the extract or compound of interest is impregnated on a paper disk and placed on the agar surface. The plate is then incubated with the appropriate positive controls. Samples exhibiting antimicrobial activity display a zone of inhibition outside the disk.

The antiviral *in vitro* assay uses the BSC-1 cell line (African Green Monkey kidney cells) infected with either Herpes simplex type 1 virus (a DVA virus) or Polio virus type 1 (an RNA virus). These cells are grown on the surface of plastic cells, infected with a test virus and the sample-impregnated paper disk is placed into the well. After incubation the well is examined for the size of the antiviral and/or cytotoxicity zones and the type of cytotoxicity present. An interpretation of the cytotoxicity observed by morphological evaluation of the cells relative to control cells can provide valuable information as to the specific mode of action of the test compound.

APPENDIX II

Halichondrin B mean graph profiles from NCI primary *in vitro* antitumour screen.

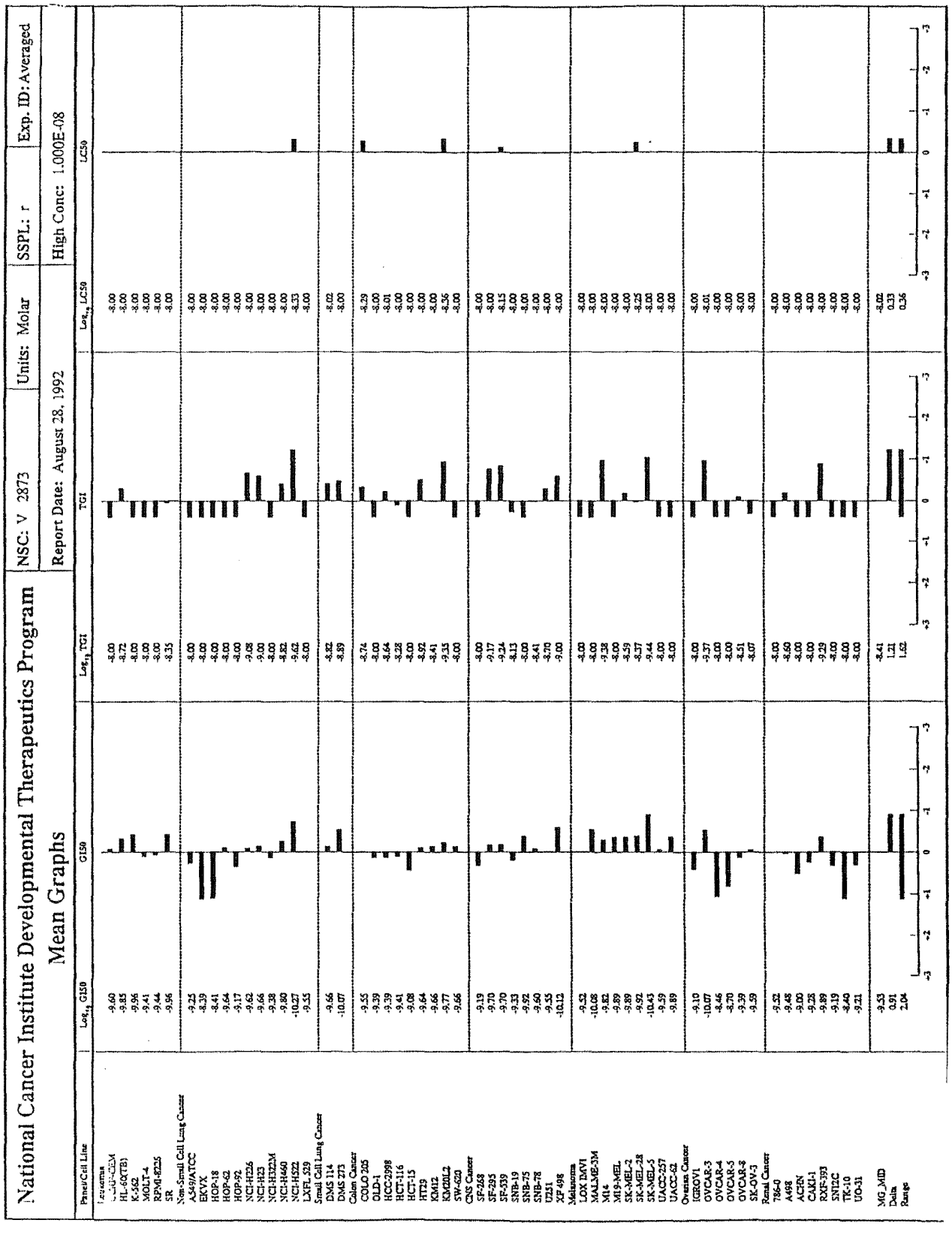

APPENDIX III

Total Synthesis of the Halichondrins

A summary of the synthetic strategy undertaken in the total synthesis of halichondrin B, achieved by Kishi and co-workers[1-5] in 1992, is illustrated in **Scheme 1**. A brief summary and discussion of this synthesis follows. Particular reference is given to the chemistry involved, the emphasis being in the final stages of the synthesis where the fragments resemble large fragments of the halichondrins. It was envisaged that a knowledge of the chemistry involved in these syntheses would provide further insight into the general chemistry of the halichondrins.

Synthetic work towards the halichondrins has also been undertaken in other laboratories.[6-15] A paper by Cooper *et al*[6] is given special reference as the authors comment on possible acid decomposition pathways for the tricyclo fragment C1-C14. Their observations have important implications in this project.

The total synthesis of halichondrin B (**1**) centred around the synthesis of the "left" (C39-C54) and "right half" (C1-C38) fragments of the structure and the coupling of the two "halves" to form the spiro centre at C38. The "left" hand side of the molecule from C39 furnished the desired halichondrin family fragment *viz* norhalichondrin, homohalichondrin or halichondrin (**2**). The "right" half of the molecule from C1 to C38 was synthesised (**3**) to furnish the B series fragment of the halichondrins.

Generally, the starting points for the synthesis of the fragments began with inexpensive, commercially available compounds of known absolute stereochemistry such as simple sugars.

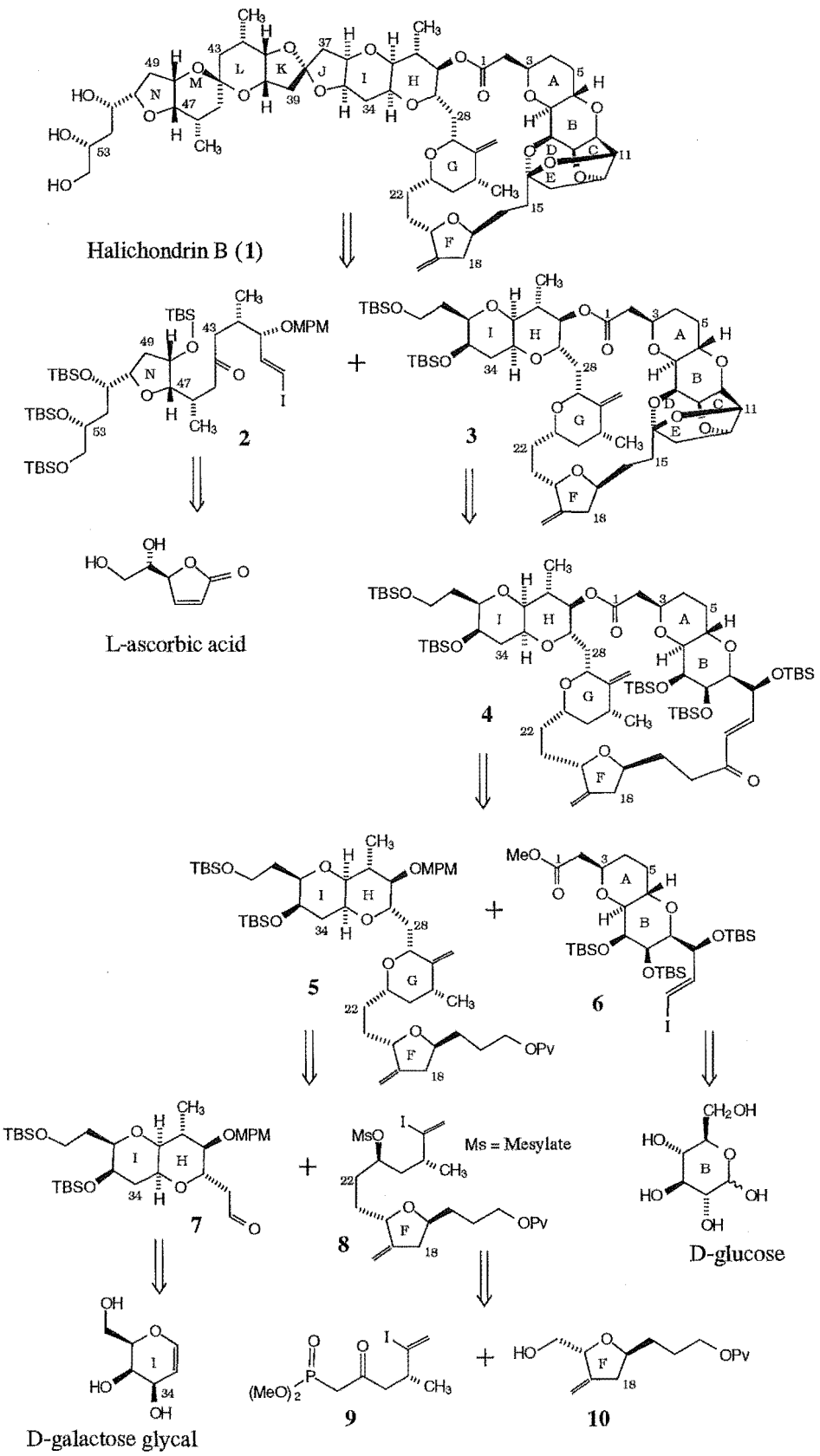

Scheme 1 Kishi Synthesis: Strategic Summary

C1-C13 Subunit and C14-C38 Coupling

The C1-C14 subunit was originally synthesised from 1,6-anhydro-D-galactose 3,4-acetonide and converted to 1,6-anhydro-D-talose 3,4-acetonide with antipodal stereochemistry around the B ring.[16] The C1-C14 subunit synthesised was therefore the antipode of the B series of halichondrins.

In the total synthesis, the construction of the C1-C13 subunit **6** involved starting with the diacetonide of D-glucose and conversion to the L-talofuranoside derivative[17] with the correct absolute stereochemistry.

The closure of the C, D and E rings of the tricyclo system was not carried out until coupling of the C1-C13 and C14-C38 fragments had been completed. Initially, the C14 aldehyde of **5** was coupled with **6** to form the new C13-C14 bond mediated by Ni(II)/Cr(II).[18] This reaction was carried out in THF (tetrahydrofuran) with DMF (*N,N*-dimethylformamide) as the base. This was then oxidised to the ketone at C14 to give the desired *trans*-enone in 77% overall yield. The Dess Martin reagent (periodinane) was used at room temperature as the oxidising agent. The C30 MPM ((*p*-methoxyphenyl) methyl) group was cleaved with DDQ (2,3-dichloro-5,6-dicyano-1,4-benzoquinone) at pH 7.0 in ^{t}BuOH. After the C1 methyl ester was hydrolysed with LiOH/H_2O in THF, a Yamaguchi lactonisation[19] furnished the lactone **4**. A Yamaguchi lactonisation involves initial formation of a mixed anhydride at the C1 carboxylic acid with 2,4,6-trichlorobenzoyl chloride with triethylamine in THF. Alcoholysis of the anhydride by the C30 alcohol in the presence of the acylation catalyst DMAP (dimethylamino pyridine) in toluene then forms the lactone ring. After cleavage of the TBS (*tert*-butyldimethylsilyl) protecting groups with TBAF ((n-Bu)$_4$NF) the *trans*-enone (**4**) underwent a Michael

addition to form the desired 5-membered C ring with a stereoselectivity of 5-6:1 at C12. Acid treatment with PPTS (pyridinium *p*-toluene sulfonate) in dichloromethane (DCM) resulted in intramolecular ketalisation and completion of the D and E rings to give **3**.

Formation of C14-C38

This subunit (**5**) was coupled to the C1-C13 subunit **6** to form the new "C1-C30" and C13-C14 bonds. The synthesis began with the pivaloyl (Pv; trimethylacetyl) ester **10** derived from 2-deoxy-L-arabinose diethyl thioacetal 4,5-acetonide in 13 steps (47% overall yield). The primary alcohol at C21 (halichondrin numbering) was then oxidised to give the aldehyde and coupling to **9** *via* a Horner-Emmons reaction resulted in formation of the new C21-C22 bond, and was followed by the conjugate reduction of the enone produced. Hydride reduction of the resulting saturated ketone produced a 1:1 ratio of the possible diastereoisomeric alcohols at C23. Kishi states that the two diastereoisomers were readily interconvertible *via* the Mitsunobu reaction[20] to form **8**. The next step was to add the C27-C38 subunit **7**.

The C27-C38 fragment was synthesised from D-galactose glycal using the C34 stereochemistry (halichondrin numbering) to dictate the C32 and C31 stereochemistry. This was achieved by way of an Ireland-Claisen rearrangement[21] of the C35 protected dipropionate of D-galactose glycal to give **11** initially, trapped as the silyl enol ether. This was carried out under HMPA (hexamethylphosphoramide)-THF solvent conditions with a stereoselectivity of 8:1 in favour of the desired stereoisomer.

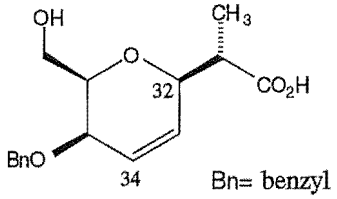

11

The mixture was iodolactonised, and the iodine reductively removed to give the γ–lactone **12.**

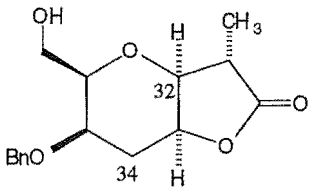

12

This was then converted to the aldehyde at C30 and coupled to acrylate to form the C29-C30 bond as a 2:1 diastereoisomeric mixture of the alcohol favouring the desired stereoisomer. A Michael reaction from the C33 deprotected alcohol gave the cyclised product with a 20:1 stereoselectivity at the new chiral centre formed at C29. The alcohol produced was then oxidised to form the aldehyde **7**.

Coupling of the two fragments **7** and **8** mediated by Ni(II)/Cr(II) with DMF in THF gave a 6:1 ratio of the two allylic alcohols at C27 which was then cyclised under basic conditions (KH/DME (1,2-dimethoxyethane)) to produce the desired tetrahydropyran ring "G" (**5**) in 50-60% overall yield.

That completed the synthesis of the C14-C38 subunit (**5**) which was subsequently coupled to C1-C13 (**6**) by the formation of the C13-C14 and "C1-C30" bonds and cyclisation of the tricyclo system as described previously.

C39-C54 halichondrin B

Coupling of this fragment (**2**) to the right hand side of halichondrin B (C1-C38). Kishi synthesised the "left hand" portions corresponding to norhalichondrin (derived from the C27-C38 synthesis; Ireland-Claisen rearrangement of the D-galactose glycal dipropionate in the *absence* of HMPA), and homohalichondrin and halichondrin families.[3,4]

The synthesis of the halichondrin subclass started from L-ascorbic acid. Protection of the diol as an acetonide followed by conversion of the α,β–unsaturated γ-lactone to **13** by methylcuprate (Me_2CuLi). This was converted to the epoxide **14** by routine functional group interconversions and coupled to the acetylene **15** derived from D-malic acid. Lindlar reduction of the product gave the expected *cis*-olefin **16** (86% yield from the epoxide).

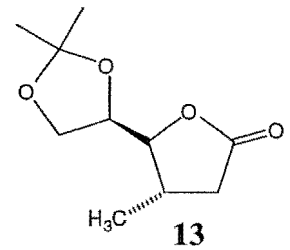

13

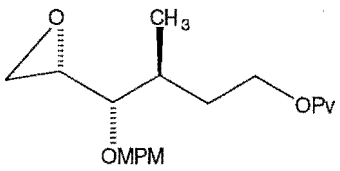

14

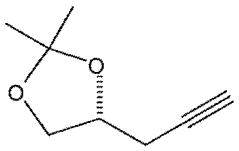

15

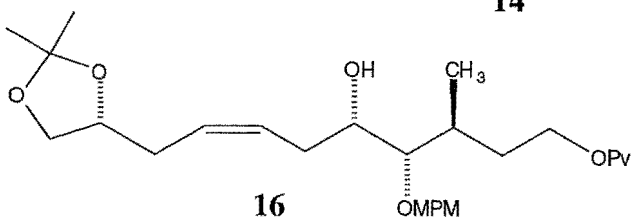

16

The epoxide was formed across the olefin by the Sharpless method,[22] and acid treatment gave the desired tetrahydofuran **17** with a 7-8:1 stereoselectivity.

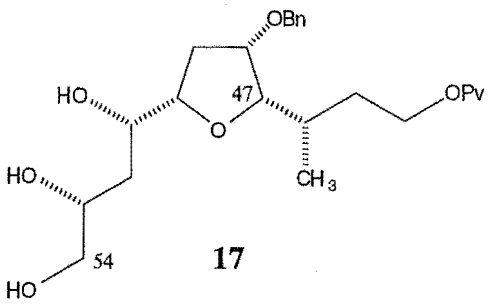

17

The free hydroxyl groups were protected and the pivaloyl ester group removed and oxidised to the aldehyde before coupling to **18.**

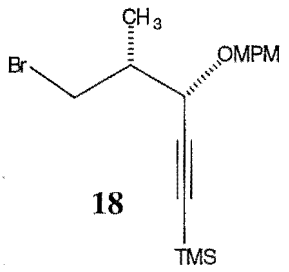

18

Fragment **18** was synthesised from S-(+)-methyl 3-hydroxy-2-methylpropionate in 8 steps (40% overall yield). After coupling of **18** to the oxidised **17** fragment the selective reduction of the acetylene to the *trans*-olefin, iodination and Dess-Martin oxidation[23] of the alcohol at C42 gave **2.**

Coupling of the left and right hand fragments

Deprotection and oxidation of the C1-C38 primary alcohol **3** at C38 under Dess-Martin conditions and coupling was achieved with the left "half" C39-C54 subunit **2** by a Ni(II)/Cr(II)/DMF mediated reaction. Dess-Martin oxidation of the C38 alcohol formed furnished the *trans*-enone. Three steps transformed this into halichondrin B with a high degree of stereoselectivity. Removal of the C48 TBS group with TBAF in DMF resulted in hemiketal formation at C44 gave the "M" ring. Michael addition from the hemiketal hydroxyl group furnished the "L" ring and the 6,6 spiro centre. Deprotection of the C41 MPM ((*p*-methoxyphenyl)methyl) group by DDQ (2,3-dichloro-5,6-dicyano-1,4-benzoquinone) at pH 7.0 followed by CSA (camphor sulfonic acid) treatment in DCM resulted in ketalisation and completion of the final 5,5 spiro centre at C38. Kishi comments that the stereoselectivity of the three steps was "very high".

Kishi reports that the product formed was assigned as halichondrin B on the basis of ^{1}H NMR spectroscopy, MS, IR, $[\alpha]_D$ and chromatography, relative to a sample of natural halichondrin B.

The Cooper Paper[6]

As part of an overview of the work in the synthetic area, an interesting observation was noted in a paper by Cooper *et al*[6]. They observed the formation of a furan derivative (**20**) after the synthetic fragment **19** was placed in $CDCl_3$ for 8 hours at room temperature, "presumably due to traces of HCl in the solvent". They comment

that a specific mode of acid decomposition for the halichondrins has not previously been reported and that this reactivity may have biological "significance".

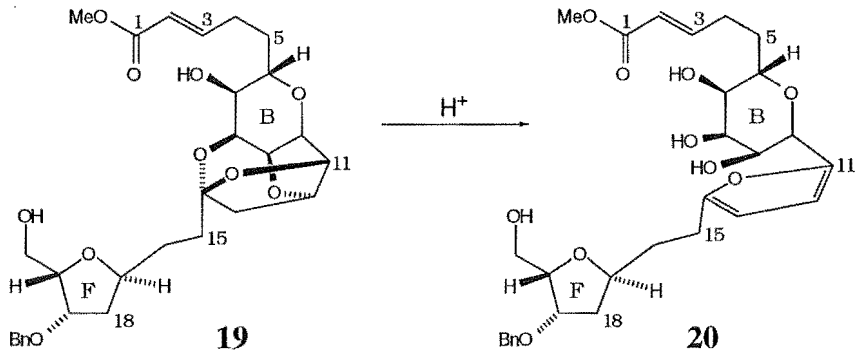

References

1 Aicher, T.D.; Buszek, K.R.; Fang, F.G.; Forsyth, C.J.; Jung, S.H.; Kishi, Y. and Scola, P.M.; Spero, D.M. and Yoon, S.K. *J. Am. Chem. Soc.*, **1992**, *114*, 3162.

2 Aicher, T.D.; Buszek, K.R.; Fang, F.G.; Forsyth, C.J.; Jung, S.H.; Kishi, Y. and Scola, P.M. *Tet. Lett.*, **1992**, *33(12)*, 1549.

3 Buszek, K.R.; Fang, F.G.; Forsyth, C.J.; Jung, S.H.; Kishi, Y.; Scola, P.M. and Yoon, S.K. *Tet. Lett.*, **1992**, *33(12)*, 1553.

4 Fang, F.G.; Kishi, Y.; Matelich, M.C. and Scola, P.M. *Tet. Lett.*, **1992**, *33(12)*, 1557.

5 Aicher, T.D.; and Kishi, Y. *Tet. Lett.*, **1987**, *28(30)*, 3463.

6 Cooper, A.J.; Pan, W. and Salomon, R.G. *Tet. Lett.*, **1993**, *34(51)*, 8193.

7 Duan, J.J.-W. and Kishi, Y. *Tet. Lett.*, **1993**, *34(47)*, 7541.

8 DiFranco, E.; Ravikumar, V.T. and Salomon, R.G. *Tet. Lett.*, **1993**, *34(20)*, 3247.

8 Cooper, A.J. and Salomon, R.G. *Tet. Lett.*, **1990**, *31(27)*, 3813.

9 Kim, S. and Salomon, R.G. *Tet. Lett.*, **1989**, *30(46)*, 6279.

10 Burke, S.D.; Buchanan, J.L. and Rovin, J.D. *Tet. Lett.*, **1991**, *32(32)*, 3961.

11 Horita, K.; Hachiya, S.; Nagasawa, M.; Hikota, M. and Yonemitsu, O. *SynLett*, **1994**, 38.

12 Horita, K.; Nagasawa, M.; Hachiya, S. and Yonemitsu, O. *SynLett*, **1994**, 41.

13 Hachiya, S.; Sakuri, Y.; Nagasawa, M.; Hachiya, S. and Yonemitsu, O. *SynLett*, **1994**, 43.

14 Hachiya, S.; Sakuri, Y.; Nagasawa, M.; Maeno, K; Hachiya, S. and Yonemitsu, O. *SynLett*, **1994**, 47.

15 Burke, S.D.; Jung, K.W.; Phillips, J.R. and Perri, R.E. *Tet. Lett.*, **1994**, *35(5)*, 703.

16 Jin, H.; Uenishi, J. and Kishi, Y. *J. Am. Chem. Soc.*, **1986**, *108*, 5644.

17 Takai, K.; Tagashira, M.; Kurod, T.; Oshima, K.; Utimoto, K. and Nozaki, H., *J. Am. Chem. Soc.*, **1986**, *108*, 6048.

18 Jin, H.; Uenishi, J.; Christ, W.J. and Kishi, Y. *J. Am. Chem. Soc.*, **1986**, *108*, 6048.

19 Inanaga, J.; Hirata, K.; Saeki, H. and Yamaguchi, M. *Bull. Chem. Soc. Jpn.*, **1979**, *52*, 1989.

20 Mitsunobu, O. *Synthesis*, **1981**, 1.

21 Ireland, R.E.; Mueller, R.H. and Willard, A.K. *J. Am. Chem. Soc.*, **1976**, *98*, 2868.

22 Sharpless, K.B. and Michaelson, R.C. *J. Am. Chem. Soc.*, **1973**, *95*, 6136.

23 Dess, D.B. and Martin, J.C. *J. Org. Chem.*, **1983**, *48*, 4155.

APPENDIX IV

Reproduction of paper published in *Tetrahedron Letters* Journal.

Pergamon

Tetrahedron Letters, Vol. 35, No. 50, pp. 9435-9438, 1994
Elsevier Science Ltd
Printed in Great Britain
0040-4039/94 $7.00+0.00

0040-4039(94)02039-6

Isohomohalichondrin B, a New Antitumour Polyether Macrolide from the New Zealand Deep-Water Sponge *Lissodendoryx* sp.

Marc Litaudon, Joanne B Hart, John W Blunt,* Robin J Lake & Murray H G Munro.*

Department of Chemistry, University of Canterbury, Christchurch, NEW ZEALAND.

Abstract: Isohomohalichondrin B, a new structural type in the halichondrin group, has been isolated from the deep-water New Zealand sponge *Lissodendoryx* sp. Like some other members of the halichondrin family isohomohalichondrin B exhibited remarkable cytotoxicity against the P388 (murine leukaemia) cell line and selective cytotoxicity in the NCI's primary screen.

During our investigation of the biological potential of the New Zealand marine biota,[1] attention was drawn to a bright yellow sponge *Lissodendoryx* sp. (family Myxillidae, order Poecilosclerida) collected by dredging from deep water (100 m) off the Kaikoura Peninsula. Trial extracts from this sponge were strongly inhibitory against the murine leukemia cell line P388, a DNA virus (*Herpes simplex* Type I) and an RNA virus (*Polio* vaccine virus). Initial studies on the sponge established that the active components were stable, and furthermore, crude extracts of this sponge offered significant extensions of life-span in an *in vivo* murine P388 model (T/C ~250%). Extraction of the sponge (5 kg) with CH_3OH/CH_2Cl_2 (3:1) was followed by partitioning of the crude extract between CH_2Cl_2 and water. Further partitioning of the organic soluble portion between aqueous CH_3OH (80%) and hexane yielded a crude organic extract (3.8 g). This was subjected to bioassay-directed C-18 reverse phase flash chromatography, LH-20 gel permeation chromatography (2x) using CH_3OH/CH_2Cl_2 (6:4) as eluent, and preparative C-18 reverse phase high pressure liquid chromatography with CH_3CN/H_2O (1:1) as eluent to yield three biologically active components **1** (2 mg; $4x10^{-5}$%), **2** (3.5 mg; $7x10^{-5}$%) and **3** (4.5 mg; $9x10^{-5}$%) and several (>6) minor components. Based on HRFAB mass spectroscopy and extensive 1-D and 2-D nmr analysis **1** and **2** were identified as halichondrin B and homohalichondrin B respectively, while **3** was recognised as a new class of halichondrin.[2]

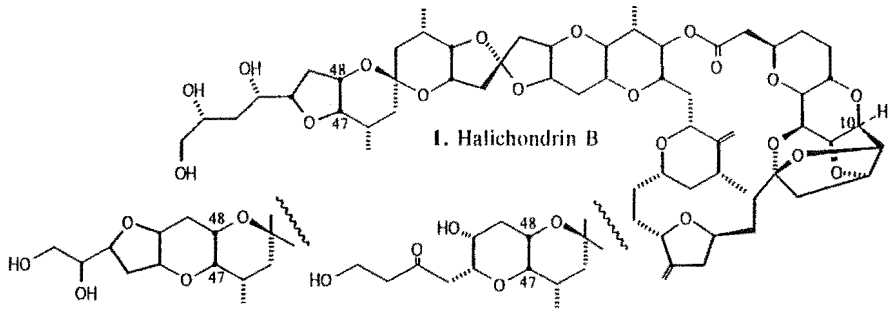

1. Halichondrin B

2. Homohalichondrin B

3. Isohomohalichondrin B

The halichondrins are a series of polyether macrolides originally isolated from the sponge *Halichondria okadai* Kadota.[3] Some of these, in particular halichondrin B, have shown potent *in vitro* and *in vivo* antitumor activity.[3-5] Subsequently, halichondrin B **1** and homohalichondrin B **2** have been isolated from two other Southern Hemisphere sponges,[4,5] along with halistatin 1 **4**, (10α-hydroxyhalichondrin B).[5] Halichondrin B **1** and halistatin 1 **4** have been determined to be noncompetitive inhibitors of the binding of vincristine to tubulin

9436

and to inhibit nucleotide exchange on tubulin.[5,6] In 1992 halichondrin B **1** was selected by the NCI Decision Network Decision Committee for development as an anticancer drug,[7] indicating the importance of this family of compounds as potential anticancer agents. The finding of a new halichondrin therefore is of significance for structure-activity relationships.

HRFABMS on **3** (as MK^+) corresponded to $C_{61}H_{86}O_{19}$, isobaric with homohalichondrin B. Consequently, the new halichondrin was named isohomohalichondrin B. The structure of **3** was established using ^1H-^1H COSY (two different solvents, CD_3OD and $CDCl_3$/pyridine-d_5 (1 drop)), 1D and 2D TOCSY, HMQC and HMBC experiments. Proton connectivities from C1 to C48 were identical with those already defined for halichondrin B **1** and homohalichondrin B **2**.[2,3-5] This region constitutes the unchanged section of the halichondrin system found through the norhalichondrin,[3] halichondrin **1** and homohalichondrin **2** series of compounds and their associated A, B and C families.[3,8] This unifying aspect of the halichondrin structure has been annunciated as the *halipyran* system by Pettit *et al.*[5] For isohomohalichondrin B **3** the "unique" region encompassing H48 to H55 was identified as three additional proton spin systems.[2] In the ^{13}C NMR spectrum at 125 MHz all 61 carbons were observed, but the ketone resonance for C53 was absent from a spectrum obtained at 75 MHz. The HMQC experiment confirmed the presence of 4 methines and 4 methylenes in the unique "left hand" end (from C47 to C55), while HMBC supported the unique sequence C51 to C55 by the observation of long-range correlations between the protons at positions 51, 52, 54 and 55 and the carbon at 209.5 ppm as shown in Figure 1. The sequence from H46 through to H51 was established by COSY and TOCSY correlations.

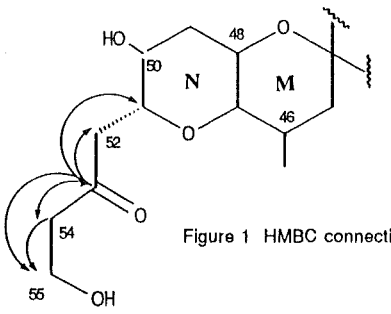

Figure 1 HMBC connectivities

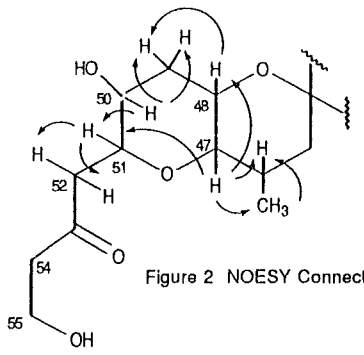

Figure 2 NOESY Connectivities

Figure 3

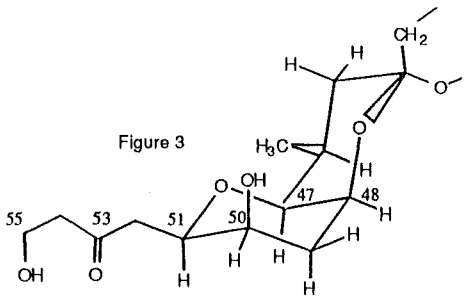

The relative stereochemistry of isohomohalichondrin **3** was established by NOESY experiments (see Figure 2). This confirmed the *cis* fusion of the M/N ring junction (H47 and H48 *cis*) as in all other halichondrins isolated to date. A strong correlation between H50 and H51, which was also correlated with H47, established the *cis* relationship of all 3 hydrogens. These NOESY results, supported by the derived coupling constants for the spin systems, are best interpreted in terms of a chair/chair conformation for this 1,5-bisoxadecalin system (Figure 3).

The absolute stereochemistry of isohomohalichondrin B, as depicted in **3** and Figure 3, is based on the defined stereochemistry of a norhalichondrin derivative by X-ray crystallography[3a] and the similarity in sign and magnitude of the optical rotation of **3**[2] with that of homohalichondrin B **2**, and other members of the halichondrin family of compounds.[3b]

9437

The side-chain (C52-C55) of **3** has more degrees of motional freedom than the central core. This is shown by the low intensity resonance for C53 (δ_C 209.5 ppm), which can be attributed to a longer relaxation time in comparison to the other carbons present and supported by the measurement of the relaxation times for the C54 and C55 protons which were 2x the average of the T_1 values of the other methylene protons.

Testing of the halichondrins from *Lissodendoryx* sp. in our in-house murine leukaemia (P388 cell line) assay confirmed the exceedingly potent nature of this group of compounds. [Isohomohalichondrin B **3**, halichondrin B **1** and homohalichondrin B **2** (IC_{50} 0.18, 0.78 and 0.22 ng/mL respectively)]. These results were confirmed when the New Zealand samples of the halichondrins (**1**, **2** and **3**) were tested against the >60 cell lines in the US NCI's human tumour cell line *in vitro* screen.[9] The pattern of inhibition demonstrated by the isohomohalichondrin B **3** was highly characteristic and use of the COMPARE algorithm[10] showed that it was highly correlated with the other known halichondrins (see Table below). As noted previously for halichondrin B **1** and homohalichondrin B **2**,[11] isohomohalichondrin B **3** was also highly correlated with tubulin-binding agents such as vincristine, maytansine and taxol. When tested in a tubulin binding assay[11] isohomohalichondrin B **3** was found to be an effective inhibitor of tubulin polymerisation.

Compound[a]	Mean Panel GI_{50} ($x10^{-10}M$)[b]	COMPARE Correlation Coeff.[c]
Halichondrin B **1**	1.38	1.00
Homohalichondrin B **2**	1.58	0.91
Isohomohalichondrin B **3**	1.15	0.80

[a] Compounds **1**, **2**, **3** were tested in quadruplicate at each of 3 different concentration ranges.
[b] Standard errors averaged < 15% of the respective means.
[c] Coefficients were calculated using the TGI-centered mean graph profiles from the highest test concentration. The TGI mean graph profile of halichondrin B **1** was used as the "seed" for all comparisons.

The halichondrins have now been isolated from three quite diverse sponge sources and detected in a fourth. The first reported isolation was from a Halichondrid sponge, *Halichondria okadai* Kadota, found on the Pacific coast of Japan.[3] The next reported findings were from the Axinellid sponges, *Axinella* sp and *Phakellia carteri*, found in the Western Pacific Island of Palau[4] and in the Republic of Comoros in the Eastern Indian Ocean,[5] respectively. This most recent finding has been from the New Zealand Poecilosclerid sponge *Lissodendoryx* sp. We have also detected the halichondrins in yet another New Zealand sponge, the black shallow-water Axinellid, *Raspalia agminata*.[12] The finding of the same compounds in such geographically and biologically diverse series strongly suggests that these compounds are less likely to be biosynthesised *de novo* by the sponge cells and more likely to originate from a sponge symbiont. Considerable attention has been focused recently on sponge symbionts and the role they play in the production of many of the so-called sponge metabolites.[13] We are currently examining samples of the *Lissodendoryx* sp. for symbionts and have undertaken a series of cellular dissociation experiments in an attempt to determine the possible origin of the halichondrins.[14]

One notable difference between the other halichondrin-containing sponges and the *Lissodendoryx* sp. is the relative yield of the halichondrins. The yield from the New Zealand sponge is >10x more than that noted for the other sponges. Notwithstanding, the halichondrins are another example of a rare resource with potential as an anticancer agent. Despite the successful synthesis[15] and partial syntheses[16] of the halichondrin skeleton the most obvious source of the compound in the near future is from natural sources. *Lissodendoryx* sp. is found in a challenging environment at only one site in New Zealand. To protect this resource and establish an alternative source of supply, intensive studies on the aquaculture of this sponge have been initiated.[17]

9438

Acknowledgments: Especial thanks to Dr M.R. Boyd, National Cancer Institute (NCI/DTP/LDDRD). To PharmaMar SA, Harbor Branch Oceanographic Institution/SeaPharm Project, University of Canterbury, New Zealand Universities Grants Committee, Canterbury Medical Research Foundation, New Zealand Lotteries Board (Scientific), Cancer Society of New Zealand our very grateful thanks for funding, past and present. We also wish to thank the following: Ms G. Barns & Mr R. Thow, Chemistry Department, University of Canterbury, Mr M.J. Page, NIWA, Wellington, Mr C. Spiers, Captain of the RV "Munida" & Dr D.J. Newman, Natural Products Branch, NCI, Frederick, USA.

References and Notes

1. Munro, M.H.G.; Blunt, J.W.; Barns, G.; Battershill, C.N.; Lake, R.J.; Perry, N.B. *Pure Appl. Chem.*, **1989**, *61*, 529-34.
2. Isohomohalichondrin B obtained as a white amorphous powder; no UV maximum above 210 nm ; IR (NaCl pellet) 3450, 1732, 1695 (sh), 1648 cm^{-1} (hydroxyls, a lactone and an aliphatic ketone). LRFABMS showed MNa^+ and MK^+ at m/z 1145 and 1161. HREIMS; observed m/z 1161.5395. (MK^+, calc: 1161.53999; error - 0.4 ppm). $[\alpha]_D$ -21.6° (c = 1.02, MeOH). Nmr spectra obtained on a Varian VXR 500 spectrometer operating at 500 MHz for ^1H and 126 MHz for ^{13}C. ^{13}C nmr (CDCl3) δ C1, 171.1; C2, 40.4; C3, 73.6; C4, 30.6; C5, 30.0; C6, 68.2; C7, 77.6; C8, 74.3; C9, 73.8; C10, 76.5; C11, 82.1; C12, 81.0; C13, 48.3; C14, 110.0; C15, 34.4; C16, 28.1; C17, 75.3; C18, 38.7; C19, 151.7; C19=CH_2, 104.4; C20, 75.3; C21, 29.3; C22, 32.0; C23, 74.8; C24, 43.3; C25, 35.9; C25-CH_3, 18.0; C26, 151.5; C26=CH_2, 104.1; C27, 73.5; C28, 36.9; C29, 71.1; C30, 77.2; C31, 36.5; C31-CH_3, 15.0; C32, 77.5; C33, 66.4; C34, 29.0; C35, 75.1; C36, 76.2; C37, 43.3; C38, 112.4; C39, 42.5; C40, 71.2; C41, 79.0; C42, 25.6; C42-CH_3, 17.5; C43, 36.9; C44, 97.2; C45, 37.2; C46, 28.6; C46-CH_3, 16.9; C47, 75.9; C48, 66.4; C49, 34.4; C50, 66.4; C51, 76.4; C52, 45.2; C53, 209.5; C54, 46.1; C55, 57.8 ppm. ^1H nmr (CDCl3) δ (position, mult) H2, 2.36, (*J*=16.8); H2, 2.61 (dd, *J*=16.8, 8.1); H3, 3.89 (*J*=8.1); H4, 1.75 (m); H4, 1.38 (m); H5, 1.41 (m); H5, 2.12 (m); H6, 4.35 (bm); H7, 2.95 (*J*=10.6); H8, 4.33 (*J*=3.9); H9, 4.06 (dd, *J*=6.4, 3.9); H10, 4.22 (dd, *J*=6.4, 4.5); H11, 4.60 (t, *J*=4.5, 4.5); H12, 4.70 (dd, *J*=4.5, 4.75); H13, 1.95 (dd, *J*=13.1, 4.75); H13, 2.16 (*J*=13.1); H15, 2.18* (m); H15, 1.62* (m); H16, 2.16* (m); H16, 1.42* (m); H17, 4.10 (m); H18, 2.27 (m); H18, 2.80 (m); C19=CH_2, 5.01 (brs, *J*=1.7); C19=CH_2, 4.93 (brs, *J*=1.7); H20, 4.39 (m); H21, 1.42 (m); H21, 1.90 (m); H22, 1.62 (m); H22, 1.62 (m); H23, 3.55 (m); H24, 1.05 (m); H24, 1.72 (m); H25, 2.23 (m); C25-CH_3, 1.07 (d, *J*=6.4); C26=CH_2, 4.83 (brs; C26=CH_2, 4.78 (brs); H27, 3.56 (m); H28, 2.01 (m); H28, 1.95 (m); H29, 4.22 (m); H30, 4.66 (m); H31, 2.03 (m); C31-CH_3, 1.00 (d, *J*=6.7); H32, 3.20 (dd, *J*=8.1, 6.15); H33, 3.84 (m); H34, 1.81 (m); H34, 2.16 (m); H35, 4.12 (m); H36, 4.12 (m); H37, 2.37 (m); H37, 1.92 (m); H39, 2.22 (m); H39, 2.22 (m); H40, 3.94 (m); H41, 3.64 (m); H42, 2.29 (m); C42-CH_3, 0.95 (d, *J*=7.0); H43, 1.52* (m); H43, 1.33* (m); H45, 1.49 (m); H45, 1.52 (t, *J*=12.7, 12.7); H46, 2.18 (m); C46-CH_3, 0.90 (d, *J*=6.9); H47, 3.23 (d, *J*=2.3); H48, 3.75 (brs); H49, 1.84 (d, *J*=3.2); H49, 2.13 (d, *J*=13.2); H50, 3.52 (s); H51, 3.82 (dd, *J*=5.0, 8.0); H52, 2.62 (dd, *J*=5.0, 15.7); H52, 2.93 (dd, *J*=8.0, 15.7; H54/H54, 2.73 (t, *J*=5.4, 5.4); H55/H55, 3.86 (t, *J*=5.4, 5.4) ppm (* Assignments are tentative)
3. (a) Uemura, D.; Takahashi, K.; Yamamoto, T.; Katayama, C.; Tanaka, J.; Okumura, Y.; Hirata, Y. *J. Amer. Chem. Soc.*, **1985**, *107*, 4796 -98. (b) Hirata, Y.; Uemura, D. *Pure Appl. Chem.*, **1986**, *58*, 701-710.
4. Pettit, G.R.; Herald, C.L.; Boyd, M.R.; Leet, J.E.; Dufresne, C.; Doubek, D.L.; Schmidt, J.M.; Cerny, R.L.; Hooper, J.N.A.; Rutzler, K.C. *J. Med. Chem.* **1991**, *34*, 3339-40.
5. Pettit, G.R.; Tan, R.; Gao, F.; Williams, M.D.; Doubek, D.L.; Boyd, M.R.; Schmidt, J.M.; Chapuis, J-C.; Hamel, E.; Bai, R.; Hooper, J.N.A.; Tackett, L.P. *J. Org. Chem.*, **1993**, *58*, 2538-43.
6. Bai, R.; Paull, K.D.; Herald, C.L.; Malspeis, L.; Pettit, G.R.; Hamel, E. *J. Biol. Chem.*, **1991**, *266*, 15882-89.
7. Minutes, NCI Decision Network Committee, March 23, 1992.
8. The A family of the halichondrins is characterised by a 12β, 13β diol sytem; the C family are 12β hydroxy only.
9. (a) Boyd, M.R. in: "Principles & Practise of Oncology." Ed. by DeVita,V.T. Jr.; Hellman, S.; Rosenberg, S.A. Lippincott Co: Philadelphia, PA, 1989, Vol. 3, No 10, pp 1-12. (b) Monks, A.; Scuderio, D.A.;. Skehan, P; Shoemaker, R.H.; Paull, K.D.; Vistica, D.; Hose, C.; Langley, J.; Cronise, P.; Vaigro-Wolff, A.; Grey-Goodrich, M.; Campbell, H.; Boyd, M.R. *J. Natl. Cancer Inst.*, **83**, 757 (1991). (c) Boyd M.R. in: "Current Therapy in Oncology." Ed. by Neiderhuber, J.E.; Decker, B.C. Philadelphia, 1992, pp 11-22.
10. Boyd, M.R.; Paul, K.D.; Rubenstein, L.R. in: "Antitumor Drug Discovery and Development." Ed. by Valeriote, F.A.; Corbett T.; Baker, L. Kluwer Academic Press, Amsterdam, 1992, pp 11-34.
11. Kellam, S.J.; Blunt, J.W.; Munro, M.H.G.; Perry, N.B. *J. Nat. Prod.* in press.
12. Internal research report, Dr R.J. Lake, Post-Doctoral Fellow, Marine Chemistry Group, University of Canterbury, 1988.
13. Garson, M.J.; Zimmermann, M.P.; Battershill, C.N.; Holden, J.L.; Murphy, P.T. *Lipids*, in press.
14. With Dr M.J. Garson, University of Queesland, Brisbane, Australia and Dr C.N. Battershill, NIWA, Wellington, New Zealand.
15. Aicher, T.D.; Buszek, K.R.; Fang, F.G. Forsyth, C.J.; Jung, S.H.; Kishi, Y.; Matelich, M.C.; Scola, P.M.; Spero, D.M.; Yoon, S.K. *J. Amer. Chem. Soc.* **1992**, *114* , 3162-3164.
16. (a) Burke, S.D.; Buchanan, J.L.; Rovin, J.D. *Tetrahedron Lett.* **1991**, *32*, 3961-3964. (b) Difranco, E.; Ravikumar, V.T.; Salomon, R.G. *Tetrahedron Lett.* **1993**, *34*, 3247-3250. (c) Duan, J.J-W.; Kishi, Y. *Tetrahedron Lett.* **1993**, *34*, 7541-7544. (d) Cooper, A.J.; Pan, W.X.; Salomon, R.G. *Tetrahedron Lett.* **1993**, *34*, 8193-8196. (e) Horita, K.; Hachiya, S.; Nagasawa, M.; Hikota, M.; Yonemitsu, O. *Synlett.* **1994**, 38-40. (f) Horita, K.; Hachiya, S.; Nagasawa, M.; Hikota, M.; Yonemitsu, O. *Synlett.* **1994**, 40-43. (g) Horita, K.; Sakurai, Y.; Nagasawa, M.; Hachiya, S.; Yonemitsu, O. *Synlett.* **1994**, 43-45. (h) Horita, K.; Sakurai, Y.; Nagasawa, M.; Maeno, K.; Hachiya, S.; Yonemitsu, O. *Synlett.* **1994**, 46-48. (i) Burke, S.D.; Jung, K.W.; Phillips, J.R.; Perri, R.E. *Tetrahedron Lett.* **1994**, *35*, 703-706.
17. Dr C.N.Battershill, NIWA, Wellington, NEW ZEALAND.

(*Received in UK* 22 *August* 1994; *accepted* 14 *October* 1994)

APPENDIX V

Two views of X-ray crystal structure of *p*-bromophenacyl ester of norhalichondrin A (*p*-bromophenacyl ester and C12 and C13 hydroxyls removed for simplicity).[17]